Naci Kocer

Giant Intracranial Aneurysms

A Case-Based Atlas of Imaging and Treatment

In collaboration with
Civan Islak
Osman Kizilkilic
Sedat Giray Kandemirli
Prabath Kumar Mondel

EXTRAS ONLINE

Springer

Giant Intracranial Aneurysms

Naci Kocer

Giant Intracranial Aneurysms

A Case-Based Atlas of Imaging and Treatment

In collaboration with

Civan Islak
Osman Kizilkilic
Sedat Giray Kandemirli
Prabath Kumar Mondel

Springer

Naci Kocer
Department of Neuroradiology
Istanbul University Cerrahpasa
Medical School
Istanbul
Turkey

Collaborators

Civan Islak
Department of Neuroradiology
Istanbul University Cerrahpasa
Medical School
Istanbul
Turkey

Sedat Giray Kandemirli
Department of Neuroradiology
Istanbul University Cerrahpasa
Medical School
Istanbul
Turkey

Osman Kizilkilic
Department of Neuroradiology
Istanbul University Cerrahpasa
Medical School
Istanbul
Turkey

Prabath Kumar Mondel
Consultant in Interventional
Neuroradiology
Fortis Hospital
Mumbai
India

ISBN 978-3-319-41786-8 ISBN 978-3-319-41788-2 (eBook)
DOI 10.1007/978-3-319-41788-2

Library of Congress Control Number: 2016954637

Printed on acid-free paper

This Springer imprint is published by Springer Nature
The registered company is Springer International Publishing AG Switzerland
The registered company address is Gewerbestrasse 11, 6330 Cham, Switzerland

To my wife Oya,
my children, Batuhan and Defne,
and my parents

Foreword

Giant Intracranial Aneurysms. A Case-Based Atlas of Imaging and Treatment is a superb atlas on the state of the art in the treatment of giant intracranial aneurysms in general and the endovascular treatment in particular. The author and his collaborators are well recognized as experts and pioneers in the field of endovascular surgery, with a long-term experience in the ever-expanding technical improvements in the minimally invasive treatment of giant intracranial aneurysms, where we have evolved from endovascular coiling, which was seen as ineffective, with a very high index of recanalization and compaction, difficult surgical techniques including bypass techniques, or the requirement of cardiac standstill that presently belongs to the history of the treatment of giant intracranial aneurysms, thanks to innovation and creativity so well illustrated in this atlas as case presentations, studying the clinical presentation, the imaging, and the potential techniques needed for management. In addition, each case is accompanied with pertinent bibliography, illustrations, relevant anatomy, and embryology.

The atlas is very well illustrated, permitting the reader to learn not only the techniques but the proper analysis of the pathology, rationale of treatment, and with many cases the long-term results. The case presentations, illustration of technical detail, and the methods of dealing with some of the complications add to the use of this excellent work for individual practitioners.

I believe that this work will prove to be of tremendous value also to those that are in the early stage of their career, as those of us with experience, through its illustrations, discussions, and reviews of the complex approach to giant intracranial aneurysms.

I congratulate Dr. Kocer and his collaborators for an excellent book, written in a simple yet useful format, and for demonstrating their skill and dedication to the management of giant intracranial aneurysms.

Alejandro Berenstein, MD
Professor of Neurosurgery, Radiology and Pediatrics
Icahn School of Medicine at Mount Sinai Health Systems
New York, NY, USA

Preface

As a reference center in our institution – Istanbul University, Cerrahpasa Medical Faculty, Neuroradiology Section – we are regularly treating patients with large, giant, and complex aneurysms from the beginning of the modern endovascular era in the early 1990s.

At Symposium Neuroradiologicum 2014, Springer-Verlag approached us with the idea of writing a textbook on giant intracranial aneurysms. I decided to write a case-based atlas instead of a didactic textbook on the subject. The aim was to illustrate neuroendovascular techniques and their evolution over the last two decades in the management of this challenging disease.

We wanted to provoke the readers to deliberate on the individual cases and their management strategies in that period and compare them with the present-day treatment. The time line for the cases is given in individual figure legends and also in a pullout excel sheet.

The book reflects our experience for the past 25 years in treating giant aneurysms in a tertiary care center in Turkey and various other institutions throughout the world. The same group of authors treated all the cases selected in this book. The selection and arrangement of the cases follow a pattern that we believe will stimulate and engage the minds of our readers. Though we have tried to move away from a theoretically intensive textbook, readers looking for salient features and topics of interest related to giant aneurysms will find them in purposely built boxes. These boxes describe either our thought process on a particular aspect of the case under review sometimes supported by illustrations (blue background) or more frequently a synopsis of the current literature pertaining to the topic or a sprinkling of anatomy and relevant embryology (gray background).

The book is divided into two main sections:

Introduction—containing description, relevant history, diagnosis, classification, and management options for giant intracranial aneurysms.

Cases—arranged to reflect the changing management strategies based on the hemodynamic or morphological characteristics of the giant aneurysms. Additionally, a few relevant open surgical options are described. However, it is not our aim to discuss in detail the open neurosurgical techniques involved in giant aneurysms.

All the cases are described with their dates of treatment and their follow-up. Cases with relatively long follow-ups were given priority over those with short-duration follow-ups in their selection for the book. Furthermore, a selection of a variety of techniques and materials was done to invoke the interest of readers. Figure legends are intentionally kept long and detailed with description including dates, techniques, and our underlying reasoning. A few animations and illustrations have also been included in the boxes and figures to help the reader better understand the technical complexity of the cases. Additionally, a few videos are available online for inquisitive readers to better understand the 3D anatomy and pre- and postprocedural angiograms in selected cases.

I have tried to include and cover all the different aspects that are relevant to giant aneurysms and their management. However, the aim of an atlas is to illustrate by figures rather than words and stimulate thinking on the subject and individual cases among readers rather than a comprehensive textbook on the subject. Finally, though there have been a few technical innovations and breakthroughs in the field of giant aneurysms and their management, we still have a long way to go before we make the management of giant aneurysms completely safe for all our patients.

Naci Kocer
Istanbul, Turkey

Commonly Mentioned Endovascular Devices and Their Manufacturers

FRED®	Microvention, Tustin, CA, USA
LEO®	Balt Extrusion, Montmorency, France
Onyx® and Onyx HD-500 ®	Onyx Liquid Embolic System, MTI, Irvine, CA, USA
PED®	ev3, Plymouth, Minnesota, USA
SILK® and SILK + ®	SFD; Balt Extrusion, Montmorency, France
VasoCT®	Philips Healthcare, The Netherlands

Abbreviations

ACA	Anterior cerebral artery
ACoM	Anterior communicating artery
AICA	Anterior inferior cerebellar artery
BTO	Balloon test occlusion
CCA	Common carotid artery
CE MRA	Contrast-enhanced magnetic resonance angiogram
CECT	Contrast-enhanced computed tomography
CTA	Computed tomography angiography
DSA	Digital subtraction angiography
FD	Flow diverter
FDCT	Flat panel detector computed tomography
FDCTA	Flat panel detector computed tomography angiography
GFAs	Giant fusiform aneurysms
GIA	Giant intracranial aneurysm
GSaAs	Giant saccular aneurysms
GSeAs	Giant serpentine aneurysms
IAFDCTA	Intra-arterial flat panel detector computed tomography angiography
ICA	Internal carotid artery
IEL	Internal elastic lamina
ISS	In-stent stenosis
IVFDCTA	Intravenous flat panel detector computed tomography angiography
MCA	Middle cerebral artery
MDCT	Multi-detector computed tomography
MRA	Magnetic resonance angiography
MRI	Magnetic resonance imaging
NECT	Non-enhanced computed tomography
PCA	Posterior cerebral artery
PCoM	Posterior communicating artery
PICA	Posterior inferior cerebellar artery
PTA	Persistent trigeminal artery
PVO	Parent vessel occlusion
SAH	Subarachnoid hemorrhage
SCA	Superior cerebellar artery
TOF MRA	Time-of-flight magnetic resonance angiogram

Contents

Introduction

History, Evolution, Definition, and Epidemiology

Dandy in his paper entitled "Intracranial aneurysms" stated that Morgagni was probably the first to recognize intracranial aneurysms at necropsy in 1761. Virchow in 1851 was the first to describe the regular "berry" aneurysm [1]. Bonet and Wiseman are believed to be the first to suggest intracranial aneurysms as a cause of subarachnoid hemorrhage. In 1875, Hutchison diagnosed a giant internal carotid aneurysm in a patient with III and VI cranial nerve palsy and bruit. This is the first described instance of giant intracranial aneurysm (GIA) in a patient. In 1890, Keen stated that Horsley had diagnosed a GIA prior to craniotomy. Though the site was not specified, this is the first instance where therapy for GIA was considered. Prior to angiography, intracranial aneurysms were diagnosed by clinical signs and/or surgical or autopsy observation. When Egaz Moniz demonstrated cerebral vasculature by angiography, Jefferson had commented referring to aneurysm that "In no case can Moniz's method of angiography be of greater benefit" [2].

Fearnsides et al. published the first clinical description of GIAs in 1916. He described a 67-year-old lady who died due to a ruptured partially thrombosed left middle cerebral artery aneurysm. Sarwar et al., in 1976, suggested that in most angiograms a size of 2 cm or more should be used to define GIAs [1]. Gabor and Potondi also used 2 cm as a cut-off to describe GIAs. This was based on a hypothesis that the real diameter of these aneurysms would be larger due to nonvisualized clot within the aneurysms on cerebral angiography [2].

The international cooperative study of intracranial aneurysms and subarachnoid hemorrhage collected data from a central registry over a 7-year period from 1963 to 1970 and classified aneurysms into various groups and assigned 25 mm as a cut-off to define GIAs. This size criterion has since been adopted universally to define GIAs [3, 4]. However, as GIAs are a very heterogeneous group, this classification based wholly on size as a criterion is considered inadequate by many authors. This is because it does not adequately consider the heterogeneous and varied subtypes that have distinct clinical, morphological, angiographic, and pathological features such as saccular versus fusiform versus serpentine, thrombosed versus nonthrombosed, etc. Furthermore, it is recognized that intracranial aneurysms are a spectrum extending from small to large to very large to giant and complex aneurysms and hence cannot have fixed discriminating sizes [3, 5].

Intracranial aneurysms are localized pathological dilatation of cerebral arteries. The prevalence of intracranial aneurysms is estimated to be around 2 % [6]. GIAs represent 5 % of the total aneurysms and commonly become symptomatic between 40 and 70 years. Giant aneurysms are arbitrarily defined as intracranial aneurysms with a fundus diameter of 25 mm or more. There is a female predominance with a ratio of 3:1 to 1:1. Approximately 5 to 10 % of these giant aneurysms present in the pediatric population [7]. The proportion of giant aneurysms in the pediatric population is higher and ranges from 7 to 14 % although there is some recruitment bias in the studies [6].

What's Different About Giant Intracranial Aneurysms?

The clinical presentation, natural history, location, therapeutic challenges, and treatment strategy are considerably different from routine intracranial aneurysms to warrant special attention to this subgroup. GIAs have three common clinical presentations. The commonest presentation is with mass effect and is seen in 50–75 % of all reported series. The other common presentations include subarachnoid hemorrhage and ischemic symptoms. Mass effect may result in optic tract and hypothalamic, hemispheric, or posterior fossa compression [6, 7]. In addition, cavernous GIAs with their particular compression syndromes are sufficiently unique so as to warrant a separate category. "True" cavernous GIAs constitute a larger proportion of GIAs, approximately 13–23 %, have a benign natural history in comparison to other GIAs and rarely rupture. They are also more common in women (up to 80 %) and

their natural history is characterized by a very low mortality rate [8–10].

Giant aneurysms have a very poor natural history with a mortality rate around 68–100 % at 2 years that is much worse than regular aneurysms. More than 50 % of untreated giant aneurysms rupture [11]. According to the International Study of Unruptured Intracranial Aneurysms (ISUIA), giant aneurysms have an 8 % annual risk of rupture in anterior circulation and 10 % annual rupture risk in posterior circulation. In contrast, small aneurysms have a 0–3 % annual rupture risk in anterior circulation and 0.5–3.7 % annual rupture risk in posterior circulation [12].

Around two-thirds of GIAs are located in the anterior circulation and one-third in posterior circulation [6]. Giant anterior circulation aneurysms have increased involvement of the cavernous and ophthalmic segments followed by the middle cerebral artery (MCA). In the posterior circulation, there is a predominant involvement of the BA bifurcation, P1 segment of posterior cerebral arteries (PCAs) and the superior cerebellar arteries (SCAs) [11].

Therapeutic management of GIAs is challenging. Patients with GIAs are generally older and have multiple medical comorbidities and a higher risk of general anesthesia complications. Additionally, GIAs have very wide necks, intraluminal thrombus, higher rate of wall thickening, calcifications, and atherosclerotic plaque with a higher frequency of multiple perforating arteries and major branches arising from the aneurysm [6, 7].

Therapeutic Options

The therapeutic options for the management of GIAs are both open surgical and endovascular. The various treatment options are summarized in Table 1.

Contemporary surgical series of GIAs have mortality rates of 5–30 %, morbidity rates of approximately 30 %, and good outcomes in only 60–90 % of patients [14]. In contrast, contemporary endovascular series discussing GIAs exclusively treated by flow modification techniques is not available. The authors of the pipeline for uncoilable or failed aneurysms (PUFS) trial, opined that compared to deconstructive techniques, flow diversion techniques may offer a similar safety profile with the advantage of parent vessel preservation. Furthermore, this trial has the largest mean diameter of intracranial aneurysms treated by flow diverters compared to other trials (mean diameter of 18.2 mm) and probably is the most representative of results of endovascular flow diversion techniques in the treatment of GIAs. In this study, 87.9 % of the treated 107 patients had good outcome while 9.3 % of patients had deterioration in their mRS scores. There were a total of 3 deaths and 2 patients with neurological deficit due to stroke [15]. The treatment of large and giant aneurysms using flow diverters (FDs) is associated with higher rates of stroke (3.8-fold) and subarachnoid hemorrhage (tenfold) compared to small aneurysms. The complete occlusion rate for GIAs vary between 76 and 100 % at 6 months [16]. The occlusion rate following flow diversion has been shown to improve further with increased duration after treatment [17, 18].

Table 1 Endovascular and open surgical treatment options in the management of giant intracranial aneurysms [13]

	Unruptured/ruptured aneurysms
Microsurgical options	Clip reconstruction
	Deep hypothermic circulatory arrest
	Bypass with proximal occlusion/trapping/distal occlusion
Endovascular options	Proximal occlusion/trapping after test occlusion
	Primary endosaccular occlusion with or without stent placement
	Flow modification (flow diversion and flow reversal)

Genetics

Genome wide linkage studies have revealed a strong linkage of aneurysms with chromosome regions 7q11.2, 19q13.3, 2p13 and 1p34.3-36-13. Familial aneurysms account for 5.1 % of patients with GIAs. There is a higher frequency of aneurysms in a familial aggregation and in hereditary diseases like polycystic kidney disease [6].

Types of Giant Intracranial Aneurysms

Giant aneurysms are classified into three morphological types namely: saccular, fusiform, and serpentine.

Giant Saccular Aneurysms (GSaAs)

These aneurysms have a demonstrable neck with a sac-like dilatation arising from the parent artery [6, 7].

Giant Fusiform Aneurysms (GFAs)

These aneurysms are characterized by circumferential dilatation of the parent artery [6, 7].

Giant Serpentine Aneurysms (GSeAs)

These aneurysms are partially thrombosed with residual serpiginous channel on angiography. GSeAs have an irregular eccentric channel through intraluminal thrombus with a wavy sinusoidal course [6, 7, 19].

Pathophysiology of Giant Intracranial Aneurysms

Giant Saccular Aneurysm

These aneurysms are believed to be the giant counterparts of small "berry" aneurysms at the circle of Willis. As the diameter of small berry aneurysm increases the transmural pressure increases as per the law of Laplace that favors further aneurysmal expansion [7].

There are two subtypes of saccular aneurysms namely: partially thrombosed and those without any thrombosis. Aneurysmal location (side-wall or bifurcation), 3D geometry, and intra-aneurysmal flow pattern are believed to influence the presence or absence of intra-aneurysmal thrombus.

Gradual growth of saccular aneurysms due to cyclical periods of endothelial damage by turbulent flow followed by periodic aberrant healing contributes to aneurysmal growth. Fresh hemorrhages have been demonstrated within the aneurysmal wall or between an existing thrombus and aneurysmal wall. This has been demonstrated in the majority of giant aneurysms (90–100 %) both on cross-sectional imaging and histopathological studies [20, 21].

Partially thrombosed aneurysms have laminated organized thrombus in their periphery. It is believed that an increase in the number and size of vasa vasorum coupled with fresh hemorrhage and thrombus formation in the inflow zone contribute to their growth over a period of time [6, 7].

It is believed that hemorrhagic enlargement of GIAs occur due to subadventitial rupture of this vasa vasorum. There are an increased number of vessels in the vasa vasorum in the proximal part of the aneurysm and in its wall that may contribute to its angiogenic potential. These aneurysms undergo continuous remodeling with weakening of wall in the zone of smooth muscle cell proliferation due to proteolysis. This mechanism can explain growth and expansion of completely thrombosed giant aneurysms either following treatment or spontaneously [20].

However, the second subgroup does not contain any thrombus. These remain stable for long periods of time but may exhibit sudden growth spurt with rapid increase in size to reach giant proportions and may also rupture [6, 7].

Thus saccular GIAs adapt well to prolonged periods of increasing wall tension and local hemodynamic factors and do not rupture initially. They continue to undergo progressive remodeling; however this does not prevent progressive aneurysmal growth or subsequent rupture [6, 7].

However, cavernous GIAs do not follow this well-established pattern. They appear the least likely to rupture amongst the GIAs and are able to adapt well to local hemodynamic changes by progressive increase in size [10].

Giant Fusiform Aneurysms

Fusiform aneurysms commonly occur following atherosclerotic and rarely nonatherosclerotic degeneration of vessel wall connective tissue.

Fusiform GIAs are seen in patients with connective tissue diseases like Marfan's syndrome, Ehlers Danlos syndrome, and pseudoxanthoma elasticum. Fragmentation of the internal elastic lamina and thickening of the intima are seen on histopathology. There are extensive defects in both the muscularis and internal elastic lamina in GFAs in contrast to focal defects of saccular aneurysms. Irregular thickness of tunica media, thickened fibrous tissue, hypertrophic and swollen connective tissue, and absence of intima have been described in GFAs [22].

It is believed that initially there is lipid deposition within and below the intima that disrupts the internal elastic lamina (IEL) and subsequently infiltrates the muscularis. This results in atrophy of both the elastic and muscular layers leading to tortuosity of the blood vessels. The blood flow becomes sluggish in certain portions of the tortuous artery and leads to thrombosis. There is usually an associated patent peripherally located vascular channel through the thrombosed region. The other proposed alternative mechanisms for GFA formation include congenital anomaly, proximal stenosis leading to "jet phenomenon" causing mechanical injury, initial intimal disruption due to dissection, and severe reticular fiber deficiency [23, 24]. These events are followed by intramural hemorrhage from the newly formed vessels within the thrombus and progressive aneurysmal growth or rupture [6, 7, 25].

Giant Serpentine Aneurysms

Giant serpentine aneurysms (GSeAs) grow when the main blood flow is diverted away from aneurysmal wall resulting in intraluminal thrombosis. There is progressive increase in the thrombosed portion with subsequent intramural hemorrhage and further development of new vascular channels within the thrombus that becomes cyclical. The eccentric vascular channel forms due to Coanda effect. Fodstad et al. first described this effect in a patient. As per this hemodynamic principle, there is a tendency of a jet of flowing blood to be deflected and preferentially flow towards one wall of the blood vessel rather than flow through its central portion. Subsequently, pressure changes along the jet stream reinforce its eccentric path.

On histopathology of GSeAs, a laminated clot is seen in the thrombosed portion. In addition to the irregular serpentine portion, multiple small irregular channels that end in blind pouches are seen in the wall. Arterial vessels similar to vasa vasorum along with hemosiderin deposits and calcification have been demonstrated in the aneurysmal wall. The aneurysmal wall is thicker compared to other aneurysms, around 1–3 mm and is primarily composed of fibrous tissue with no internal elastic lamina or endothelial lining [6, 7, 19].

Imaging Features of Giant Intracranial Aneurysms

Cross Sectional Imaging

Nonenhanced CT (NECT)

GIAs are well-circumscribed, mass lesions in the region of circle of Willis that are mild to moderately hyperdense on NECT [3]. Thin-walled aneurysms appear slightly hyperdense on NECT [26]. They are seen in close association with the circle of Willis. Partially thrombosed GIAs on NECT show the following components:

(a) A dense region composed of acutely thrombosed portion
(b) A lower density region containing the circulating channel
(c) A lowest density composed of chronically thrombosed portion

There is mass effect with frequent vasogenic edema in the adjacent cerebral parenchyma. Mass effect may cause parenchymal displacement across the midline, gyral, and sulcal effacement and acute/chronic obstructive hydrocephalus [27].

In patients with recent acute symptoms with partially thrombosed GIAs, a peripheral cresentic or convex-shaped region of hyperdensity in a laminated (variegated) thrombus is suggestive of recent hemorrhage [5, 28]. A peripheral rim of calcification may also be seen. The rim calcification is fine, linear, or crescentic. Rim calcification longer than 3 cm is almost invariably due to GIAs.

In long standing cases with GIA, NECT on bone window may show erosion and scalloping of adjacent osseous structures [27].

In ruptured GIAs, NECT may show hemorrhage as subarachnoid hemorrhage (sulci/ cisternal hyperdensity), intraventricular hemorrhage or intra-parenchymal hematoma [27].

Contrast Enhanced CT (CECT)

On CECT, non-thrombosed GIAs generally show homogenous enhancement.

Partially thrombosed GIAs show homogenous intense enhancement of the central circulating channel that is brighter than the acutely thrombosed portion in the periphery of the aneurysm. Although the thrombus does not enhance, there is enhancement of the aneurysmal wall. This combination of densities is known to produce the "Target sign" [26]. This sign was first described by Kricheff as a central hyperdensity of circulating channel, intermediate hypodensity of thrombus and peripheral hyperdensity of the wall [27].

In completely thrombosed GIAs there is absence of luminal enhancement [26]. A rim enhancement may be seen along the aneurysmal wall that is suggestive of vasa vasorum [29].

CT Angiography (CTA)

CTA is useful in analyzing the circulating channel of giant aneurysm. When the flow is fast and homogenous, there is complete opacification of the circulating channel and it is easier to analyze its size and relationship to the parent artery, adjacent vessels, and parenchyma. However, when the flow is slow and the channel is wide, there is partial filling of the circulating channel and problems in assessing the above-mentioned parameters [27].

Magnetic Resonance Imaging (MRI)

On T1W and T2W images, the fast flowing portions of the aneurysm are seen as flow voids. The "flow void" sign has a sensitivity of 88 % on both T1W and T2W sequences. The persistence of "flow void" on postcontrast T1W images is highly specific for the diagnosis of GIA. The combination of "flow void" sign and postcontrast T1W luminal enhancement of GIA has increased sensitivity, specificity, and higher positive and negative predictive value in the diagnosis of GIAs. Flow artifacts and ghost images extending on either side of the aneurysmal lumen along the phase encoding direction are motion artifacts. Their presence indicates patent aneurysmal lumen [30].

The slow flowing and thrombosed portions of aneurysms are heterogeneous due to varying signal characteristics of blood products. Gradient recalled echo (GRE) and susceptibility weighted imaging (SWI) (T2*W images) are very sensitive to blood products and calcifications. This appears as a strong hypointense signal that spills over to adjacent normal parenchyma. This is artifactual and causes overestimation of lesion size [27]. Additionally, the aneurysmal wall shows hemorrhage of different ages and postcontrast T1W enhancement of the aneurysmal wall suggestive of neovascularization due to vasa vasorum [30].

Circulating high blood flow can be demonstrated by three sequences namely:

1. Time-of-flight (TOF) MR angiogram (MRA): 3D preferred over 2D techniques
2. Contrast enhanced MR angiogram (CE MRA): 3D sequence

3D TOF MRA: The flow through GIAs is often heterogeneous because of a wide circulating channel. Therefore, it underestimates the circulating portion of the GIA and may miss some arterial efferent branches.

3D CE MRA: Provides reliable information about the size of the circulating portion of the aneurysm and patency of collateral branches. It also depicts aneurysmal enhancement [27].

The brain parenchyma may show edema (hypointense on T1W and hyperintense on T2W). It is, however, difficult to differentiate the inflammatory component from the component that is due to aneurysmal mass effect only. Edema that is seen distal to the aneurysmal location is commonly cytotoxic in nature and is due to ischemia. Subarachnoid hemorrhage (SAH) appears hyperintense on FLAIR and hypointense on T2*W images. Intraparenchymal hemorrhage is heterogeneous on T1W and T2W images and strongly hypointense on T2*W images. It also shows mass effect, compression and trophy of cranial nerves [27].

Partially thrombosed GIAs show an onionskin appearance of the thrombosed portion of aneurysm. This is due to the different ages of the hemorrhages. Postcontrast T1W images do not show enhancement of the thrombosed portion (sensitivity 100 %) [30].

Flat Panel Detector Computed Tomography (FDCT)

FDCT combines 2D radiography/fluoroscopy with 3D CT imaging. FDCT has a higher spatial resolution. The distinct advantage of FDCT is the immediate availability of CT imaging in the angiography suite. FDCT has a number of disadvantages, namely, lower dose efficiency, smaller field of view and lower temporal resolution [31]. The isotropic spatial resolution of FDCT potentially approaches 150x150x150 μm^3. This is superior in resolution in terms of both the voxel size and isotropic nature compared to multidetector computed tomography (MDCT). This allows manipulation of reconstructed images and interactive viewing of FDCT volumes more flexible and efficient [32].

Applications of FDCT [32]

(a) Evaluation of intracranial stents in the treatment of stenosis and aneurysms. It allows visualization of stent struts as small as 50–70 μm. The images can be rotated and reformatted in any plane, allowing superior stent visibility. It can also show kinking, prolapse, and flattening of stents.
(b) CT-like soft tissue imaging. Allows detection of intracerebral hemorrhage, SAH, assessment of ventricles, and immediate postprocedural patient management.
(c) FDCTA (FDCT angiography). Gives better depiction of vascular morphology compared to 3D DSA.
(d) Follow-up imaging. Detects in-stent stenosis (ISS). IVFDCTA is a less invasive option and safer compared to IAFDCTA.
(e) FDCT perfusion is still under development.

Digital Subtraction Angiography (DSA)

DSA remains the "gold standard" in the imaging of GIAs as it has excellent spatial and time resolution. Though dynamic, it cannot demonstrate noncirculating components of GIAs, namely, thrombosed portion, aneurysmal wall, and surrounding parenchyma. The size and morphology of aneurysms are assessed on 2D angiography and 3D rotational angiography. It enables dynamic study of arteries distal to aneurysm and collateral network. GIAs with slow flow may show recruitment of pial collaterals and transdural collaterals from meningeal arteries.

A balloon test occlusion (BTO) can be done to assess the adequacy of collaterals to enable a safe parent vessel occlusion (PVO) [27].

References

1. Sarwar M, Batnitzky S, Schechter MM Tumorous aneurysms. Neuroradiology 12(2):79–97. doi:10.1007/bf00333123
2. Fox JL (1983) Intracranial aneurysms, vol 1. Springer Science & Business Media
3. Pia HW, Zierski J (1982) Giant cerebral aneurysms. Neurosurg Rev 5(4):117–148
4. Sahs AL (1974) Cooperative study of intracranial aneurysms and subarachnoid hemorrhage. Report on a randomized treatment study. I. Introduction. Stroke 5(4):550–551
5. Krings T, Alvarez H, Reinacher P, Ozanne A, Baccin CE, Gandolfo C, Zhao WY, Reinges MH, Lasjaunias P (2007) Growth and rupture mechanism of partially thrombosed aneurysms. Intervent Neuroradiol 13(2):117–126
6. Lonjon M, Pennes F, Sedat J, Bataille B (2015) Epidemiology, genetic, natural history and clinical presentation of giant cerebral aneurysms. Neuro-Chirurgie 61(6):361–365. doi:10.1016/j.neuchi.2015.08.003
7. Parkinson RJ, Eddleman CS, Batjer HH, Bendok BR (2006) Giant intracranial aneurysms: endovascular challenges. Neurosurgery 59(5 Suppl 3):S103–S112; discussion S103–S113. doi:10.1227/01.neu.0000237410.32115.c9
8. Hahn CD, Nicolle DA, Lownie SP, Drake CG (2000) Giant cavernous carotid aneurysms: clinical presentation in fifty-seven cases. J Neuroophthalmol 20(4):253–258
9. Kupersmith MJ, Hurst R, Berenstein A, Choi IS, Jafar J, Ransohoff J (1992) The benign course of cavernous carotid artery aneurysms. J Neurosurg 7(5):690–693. doi:10.3171/jns.1992.77.5.0690
10. Penchet G, Mourier K (2015) Collaborative retrospective multicentre series of giant intracavernous carotid aneurysms. Neuro-Chirurgie 61(6):366–370. doi:10.1016/j.neuchi.2013.12.004
11. Choi IS, David C (2003) Giant intracranial aneurysms: development, clinical presentation and treatment. Eur J Radiol 46(3):178–194. doi:10.1016/s0720-048x(03)00090-1
12. White PM, Wardlaw JM (2003) Unruptured intracranial aneurysms. J Neuroradiol 30(5):336–350
13. Sekhar LN, Tariq F, Mai JC, Kim LJ, Ghodke B, Hallam DK, Bulsara KR (2012) Unyielding progress: treatment paradigms for giant aneurysms. Clin Neurosurg 59:6–21. doi:10.1227/NEU.0b013e3182698b75
14. Sughrue ME, Saloner D, Rayz VL, Lawton MT (2011) Giant Intracranial Aneurysms: Evolution of Management in a Contemporary Surgical Series. Neurosurgery 69(6):1261–1271. doi:10.1227/NEU.0b013e31822bb8a6
15. Becske T, Kallmes DF, Saatci I, McDougall CG, Szikora I, Lanzino G, Moran CJ, Woo HH, Lopes DK, Berez AL,

Cher DJ, Siddiqui AH, Levy EI, Albuquerque FC, Fiorella DJ, Berentei Z, Marosfoi M, Cekirge SH, Nelson PK (2013) Pipeline for uncoilable or failed aneurysms: results from a multicenter clinical trial. Radiology 267(3):858–868. doi:10.1148/radiol.13120099
16. Brinjikji W, Murad MH, Lanzino G, Cloft HJ, Kallmes DF (2013) Endovascular treatment of intracranial aneurysms with flow diverters: a meta-analysis. Stroke 44(2):442–447. doi:10.1161/strokeaha.112.678151
17. Lylyk P, Miranda C, Ceratto R, Ferrario A, Scrivano E, Luna HR, Berez AL, Tran Q, Nelson PK, Fiorella D (2009) Curative endovascular reconstruction of cerebral aneurysms with the pipeline embolization device: the Buenos Aires experience. Neurosurgery 64(4):632–642; discussion 642–633; quiz N636. doi:10.1227/01.neu.0000339109.98070.65
18. D'Urso PI, Lanzino G, Cloft HJ, Kallmes DF (2011) Flow diversion for intracranial aneurysms: a review. Stroke 42(8):2363–2368. doi:10.1161/strokeaha.111.620328
19. Christiano LD, Gupta G, Prestigiacomo CJ, Gandhi CD (2009) Giant serpentine aneurysms. Neurosurg Focus 26(5):E5. doi:10.3171/2009.2.focus0918
20. Krings T, Mandell DM, Kiehl TR, Geibprasert S, Tymianski M, Alvarez H, terBrugge KG, Hans FJ (2011) Intracranial aneurysms: from vessel wall pathology to therapeutic approach. Nat Rev Neurol 7(10):547–559. doi:10.1038/nrneurol.2011.136
21. Schubiger O, Valavanis A, Wichmann W (1987) Growth-mechanism of giant intracranial aneurysms; demonstration by CT and MR imaging. Neuroradiology 29(3):266–271
22. Little JR, St Louis P, Weinstein M, Dohn DF (1981) Giant fusiform aneurysm of the cerebral arteries. Stroke 12(2):183–188
23. Nakayama Y, Tanaka A, Kumate S, Tomonaga M, Takebayashi S (1999) Giant fusiform aneurysm of the basilar artery: consideration of its pathogenesis. Surg Neurol 51(2):140–145
24. Day AL, Gaposchkin CG, Yu CJ, Rivet DJ, Dacey RG, Jr. (2003) Spontaneous fusiform middle cerebral artery aneurysms: characteristics and a proposed mechanism of formation. J Neurosurg 99(2):228–240. doi:10.3171/jns.2003.99.2.0228
25. Shokunbi MT, Vinters HV, Kaufmann JC (1988) Fusiform intracranial aneurysms. Clinicopathologic features. Surg Neurol 29(4):263–270
26. Pinto RS, Kricheff, II, Butler AR, Murali R (1979) Correlation of computed tomographic, angiographic, and neuropathological changes in giant cerebral aneurysms. Radiology 132(1):85–92. doi:10.1148/132.1.85
27. Tollard E, Perot G, Clavier E, Gerardin E (2015) Imaging of giant cerebral aneurysms. Neuro-Chirurgie 61(6):378–384. doi:10.1016/j.neuchi.2013.10.124
28. Koyama S, Kotani A, Sasaki J (1996) Giant basilar artery aneurysm with intramural hemorrhage and then disastrous hemorrhage: case report. Neurosurgery 39(1):174–177; discussion 177–178
29. Golding R, Peatfield RC, Shawdon HH, Rice Edwards JM (1980) Computer tomographic features of giant intracranial aneurysms. Clin Radiol 31(1):41–48
30. Teng MM, Nasir Qadri SM, Luo CB, Lirng JF, Chen SS, Chang CY (2003) MR imaging of giant intracranial aneurysm. J Clin Neurosci 10(4):460–464
31. Kalender WA, Kyriakou Y (2007) Flat-detector computed tomography (FD-CT). Eur Radiol 17(11):2767–2779. doi:10.1007/s00330-007-0651-9
32. Kamran M, Nagaraja S, Byrne JV (2010) C-arm flat detector computed tomography: the technique and its applications in interventional neuro-radiology. Neuroradiology 52(4):319–327. doi:10.1007/s00234-009-0609-5

Case 1

N. Kocer, *Giant Intracranial Aneurysms*, DOI 10.1007/978-3-319-41788-2_1

1

Flow Computational Studies in Basilar Fusiform GIA Treated with Scaffolding Technique

Keywords: Cerebral aneurysm, Fusiform aneurysm, Telescopic covered stent, Hemodynamic principle, Flow computational study

Flow Computational Study

Pre- and postprocedural flow computational schematic studies demonstrate redirection of trajectory-dependent flow from unhealthy aneurysmal segment to the healthy arterial segment. The first illustration demonstrates flow within the aneurysm. The subsequent illustration shows flow redirection achieved by a combination of telescopic bare stent with a covered stent.

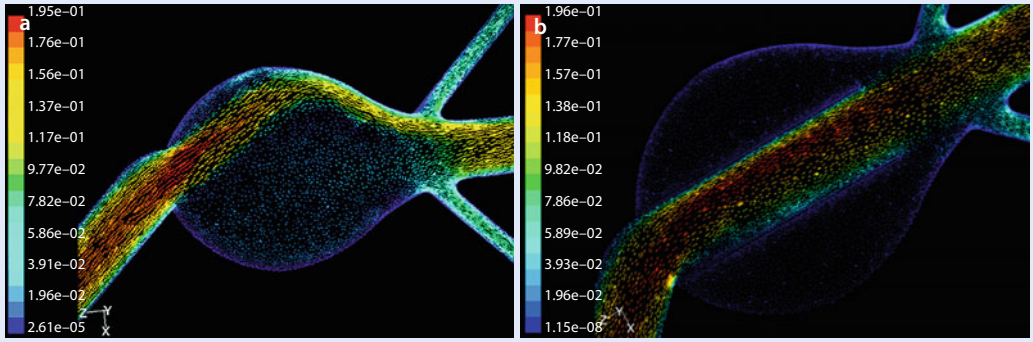

Principle of Flow Diversion in Aneurysmal Therapy

The hemodynamic principle described in this case was subsequently used to guide our management of GIAs using new-generation braided stent technology (scaffolding technique) [1] (Cases 3, 4, and 5).

Reference

1. Islak C, Kocer N, Albayram S, Kizilkilic O, Uzma O, Cokyuksel O (2002) Bare stent-graft technique: a new method of endoluminal vascular reconstruction for the treatment of giant and fusiform aneurysms. AJNR Am J Neuroradiol 23(9):1589–1595

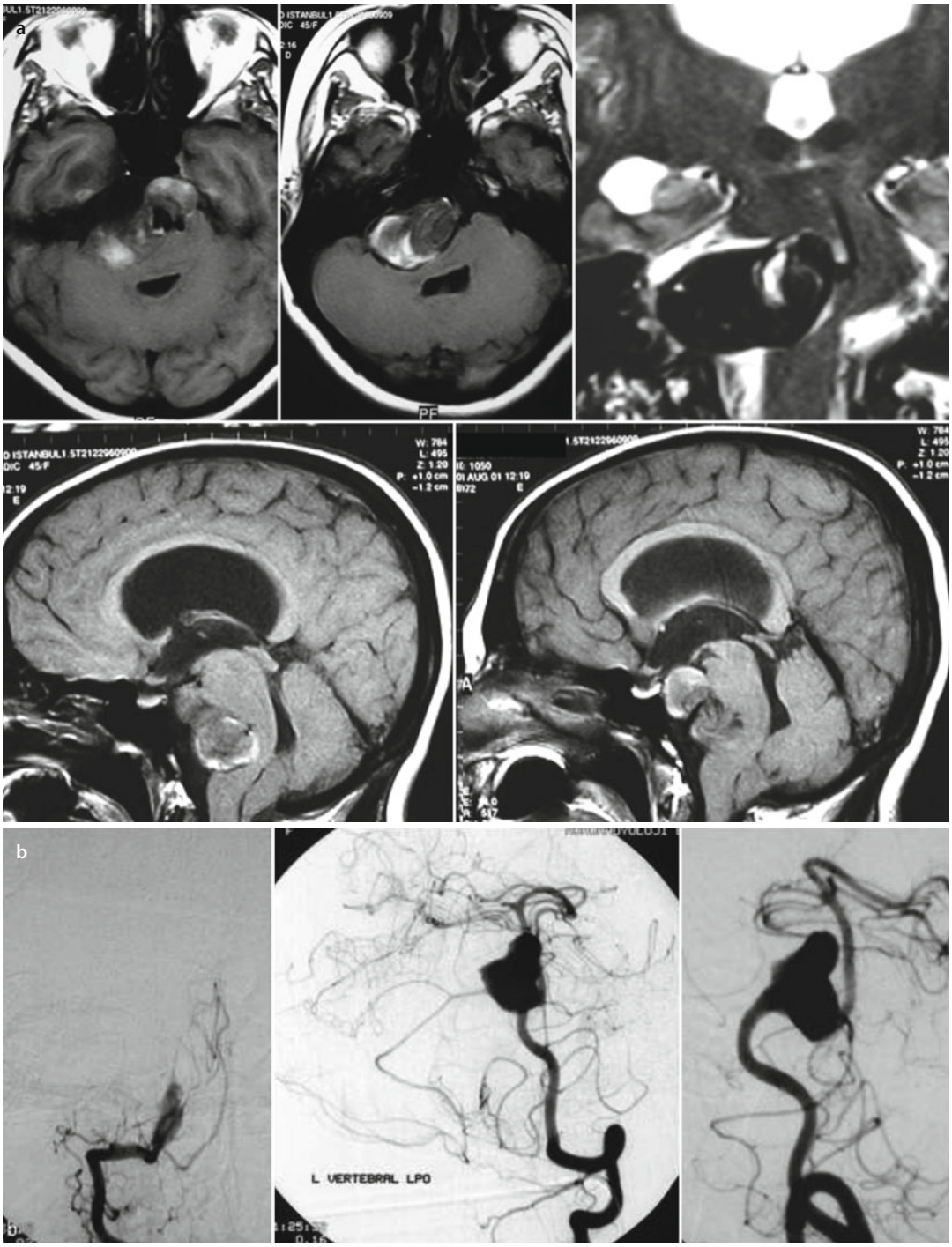

Fig. 1.1 A 44-year-old lady presented with acute onset headache, vomiting, and confusion. (**a**) MRI axial and sagittal images reveal a giant, partially thrombosed aneurysm involving the vertebrobasilar junction causing brain stem compression. (**b**) On August 2001, *right* vertebral angiogram reveals a fusiform luminal enlargement of the distal V4 vertebral artery and non-opacification of the basilar artery. *Left* vertebral angiograms reveal a 25 × 24 mm-sized, partially thrombosed fusiform vertebrobasilar junctional aneurysm. There was no collateral support to the posterior circulation from either PCoMs.

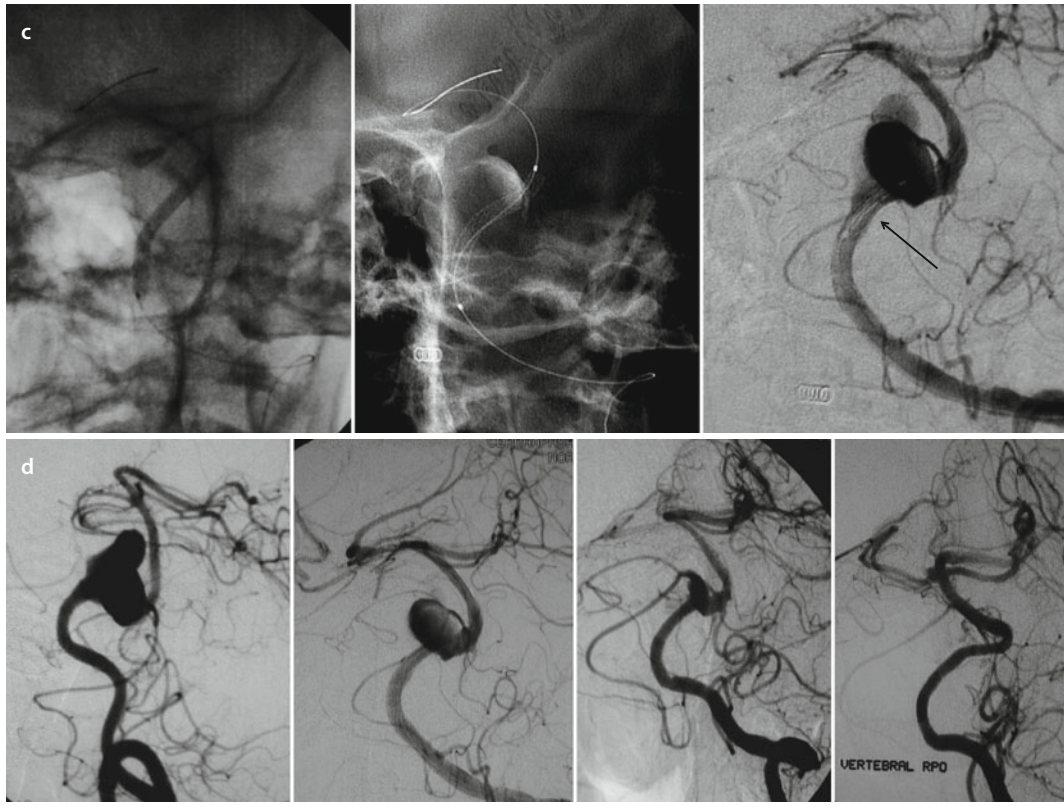

Fig. 1.1 (continued) (**c**) The authors believed that flow diversion would be the best treatment for this patient. However, in 2001, the only available tools for flow diversion were coronary stents. A 3 × 30 mm-sized balloon expandable stent (AVE S7®; Medtronics, Santa Rosa, CA, USA) was deployed across the aneurysmal segment from the proximal to distal healthy segment as a scaffold. This was followed by deployment of the shortest available stent graft (JO stent®; Jomed AB, Helsingborg, Sweden) (*arrow*) across the inflow zone measuring 3 × 12 mm telescopically within the scaffolding stent. The aim was to redirect the blood flow away from the aneurysmal segment to healthy arterial segment. (**d**) Cerebral DSA (pre, immediate post, 1 week and 7 months later, respectively) images show gradual hemodynamic decrease in aneurysmal filling with total occlusion 7 months later. This demonstrated that flow diversion alone, without aneurysmal luminal embolization, was sufficient to exclude the aneurysm from circulation.

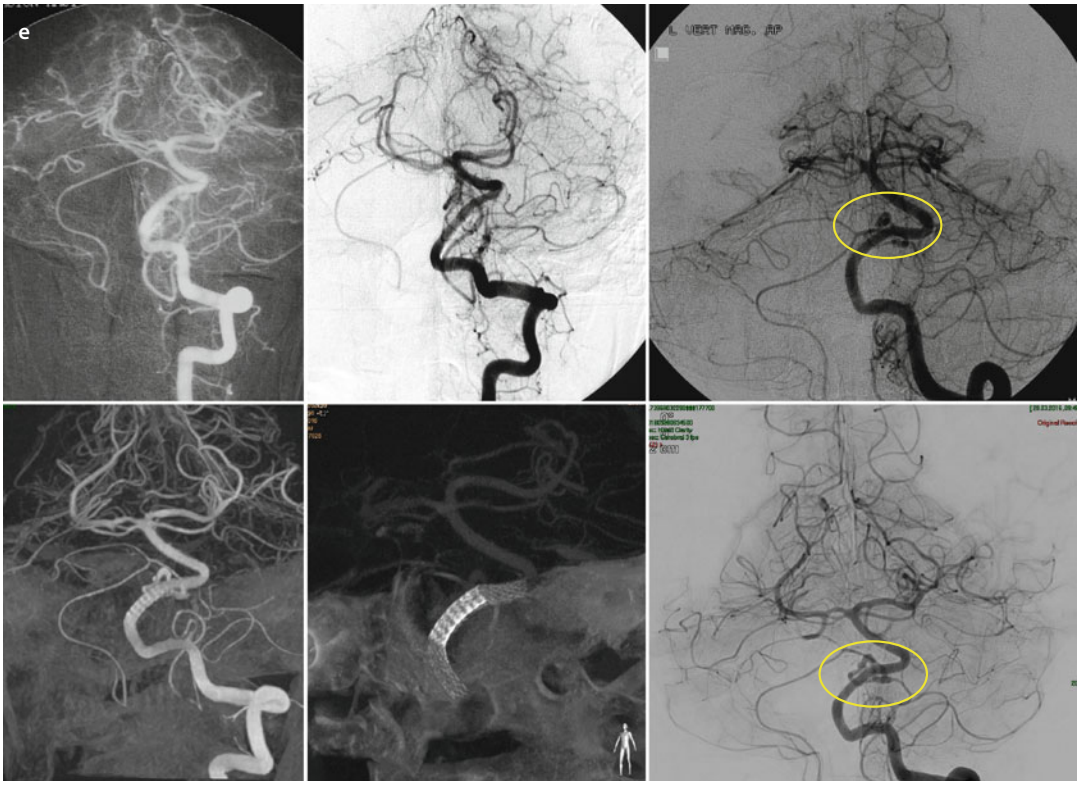

Fig. 1.1 (continued) (**e**) Follow-up cerebral DSAs after aneurysmal occlusion at 7 months, 2 years, and 5 years, respectively, show a remodeled vertebrobasilar segment with stable aneurysmal occlusion. Note that on a 5-year follow-up DSA, there is fusiform enlargement of the proximal segment of both the AICAs (*yellow circle*). This is suggestive of ongoing vessel wall pathology (probably dissecting in nature). Long-term follow-up after 15 years, 3D DSA, VASO CT®, and DSA images, shows stable aneurysmal occlusion with progressive enlargement of bilateral AICAs (*yellow circle*)

Case 2

N. Kocer, *Giant Intracranial Aneurysms*, DOI 10.1007/978-3-319-41788-2_2

In-Stent Stenosis (ISS)

Keywords: Cerebral aneurysm, Bare stent, In-stent stenosis

Etiology of ISS

Intracranial stents and flow diverters induce neo-endothelial reaction (intimal hyperplasia). This enables the complete exclusion of the aneurysm from circulation (healing reaction), but it is also responsible for ISS [1].

ISS in Intracranial Stenting

A literature search for ISS does not mention or differentiate any specific data related to GIAs. Hence the underlying data applies to aneurysms in general. It is well known in intracranial atherosclerotic disease treated with angioplasty and/or stenting. In the wingspan® (Boston Scientific, Fremont, CA) study, the rate of ISS was as high as 38 %. It was also more commonly seen in supraclinoid ICA particularly in young patients. Also supraclinoid ICA ISS was symptomatic in the majority of patients (up to 60 %) [2]. However, in patients with aneurysms treated using stent-assisted coiling, the rate of ISS was significantly less at 2.5 %. Both Enterprise® (Cordis, Miami Lakes, FL) and Neuroform® (Boston Scientific/Target, Fremont, CA) stents were used in the study. It was found that ISS was mild in most cases and did not require any intervention [1].

ISS in FD Therapy

Both self-expanding stents and FDs have a low radial force and cause minimal vessel injury and ISS. In a retrospective study from a single institution of 149 patients treated with PED® FD, ISS was relatively common occurring in around 16 % of patients. Previous studies have reported the incidence of PED® ISS to vary from 3.5 to 10 %. This is higher than in Neuroform® (Boston Scientific/Target, Fremont, CA) and Enterprise® (Cordis, Miami Lakes, FL) stents (2.5–5.8 %). Furthermore, ISS is an early manifestation in both, and most cases are found within 6 months of treatment. The PED® ISS was mild in nearly 50 % of cases and asymptomatic in all patients. The authors recommend continuation or re-institution of dual anti-platelet therapy with follow-up imaging in cases with ISS. The study also found ISS to be associated with anterior circulation FDs; all the affected patients were women (did not reach statistical significance) with a tenfold risk in patients not pretreated with aspirin [1].

A retrospective review of 47 patients treated at two institutions, with both SILK® and the newer SILK + ® FD, detected a midterm (mean follow-up 22 months) ISS of 57 %. Severe ISS (>50 % stenosis) was seen in 18.5 % of patients. Among these patients with ISS, 60 % improved or disappeared, 28 % were stable, and 12 % led to parent vessel occlusion. All ISS leading to PVO were seen in first-generation SILK® FD. However, the rate of ISS in SILK® FD was high in this series, as compared to previous series that were 7.8 % in Berge et al., 6 % in Byrne et al., and 5 % in Murthy et al. [3]. The lead author also published a retrospective study examining 20 patients with 27 aneurysms treated at the same two institutions with PED® FDs. He found a very low rate of ISS (10 %) at 3–6 month follow-up angiograms. All the ISS were mild (<50 % stenosis) and were asymptomatic [4].

A prospective study of 63 patients treated with PED® FD detected a total of 18.4 % ISS on a 3-month control angiogram. Of these, 8 % were mild (<50 %), 5 % were moderate (50–70 %), and 5 % were severe (>70 %). All stenoses were asymptomatic, and three cases showed regression by the 6-month control angiogram [5]. Another retrospective study examined intracranial ICA aneurysms less than 25 mm treated with both SILK® and PED® FDs and detected ISS in 38 and 39 % of patients treated with SILK® and PED®, respectively. Out of the total of six patients with ISS, a single patient with distal tapered severe ISS was symptomatic and treated with balloon angioplasty. All cases of ISS were detected early on 2-month control angiograms with no case of delayed ISS [6].

References

1. Chalouhi N, Polifka A, Daou B, Kung D, Barros G, Tjoumakaris S, Gonzalez LF, Starke RM, Hasan D, Judy B, Rosenwasser RH, Jabbour P (2015) In-pipeline stenosis: incidence, predictors, and clinical outcomes. Neurosurgery 77(6):875–879. doi:10.1227/neu.0000000000000908; discussion 879
2. Turk AS, Levy EI, Albuquerque FC, Pride GL, Jr., Woo H, Welch BG, Niemann DB, Purdy PD, Aagaard-Kienitz B, Rasmussen PA, Hopkins LN, Masaryk TJ, McDougall CG, Fiorella D (2008) Influence of patient age and stenosis location on wingspan in-stent restenosis. AJNR Am J Neuroradiol 29(1):23–27. doi:10.3174/ajnr.A0869
3. Lubicz B, Van der Elst O, Collignon L, Mine B, Alghamdi F (2015) Silk flow-diverter stent for the treatment of intracranial aneurysms: a series of 58 patients with emphasis on long-term results. AJNR Am J Neuroradiol 36(3):542–546. doi:10.3174/ajnr.A4143

4. Lubicz BB (2011) Pipeline flow-diverter stent for endovascular treatment of intracranial aneurysms: preliminary experience in 20 patients with 27 aneurysms. World Neurosurg 76(1–2):114–119
5. Lylyk P, Miranda C, Ceratto R, Ferrario A, Scrivano E, Luna HR, Berez AL, Tran Q, Nelson PK, Fiorella D (2009) Curative endovascular reconstruction of cerebral aneurysms with the pipeline embolization device: the Buenos Aires experience. Neurosurgery 64(4):632–642. doi:10.1227/01.neu.0000339109.98070.65; discussion 642–633; quiz N636
6. Cohen JE, Gomori JM, Moscovici S, Leker RR, Itshayek E (2014) Delayed complications after flow-diverter stenting: reactive in-stent stenosis and creeping stents. J Clin Neurosci : Off J Neurosurg Soc Aust 21(7):1116–1122. doi:10.1016/j.jocn.2013.11.010

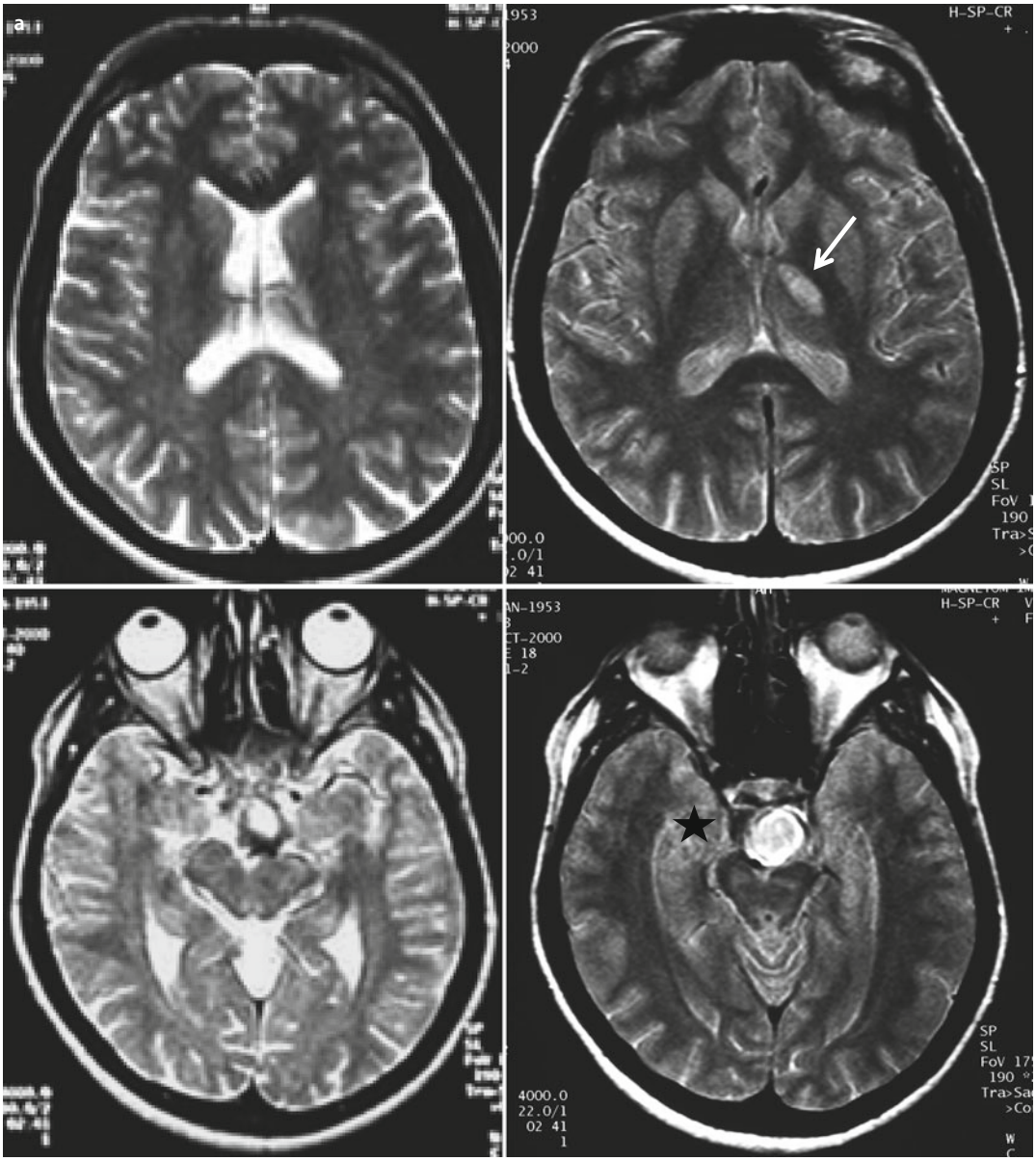

Fig. 2.1 A 47-year-old lady presented with intermittent headaches, memory loss, and left anisocoria. (**a**) MRI reveals left anterior thalamic infarct (*arrow*) with a large well-delineated heterogeneous signal intensity mass lesion with pulsation artifact (*star*) in the interpeduncular cistern compressing the left mesencephalon suggestive of an aneurysm.

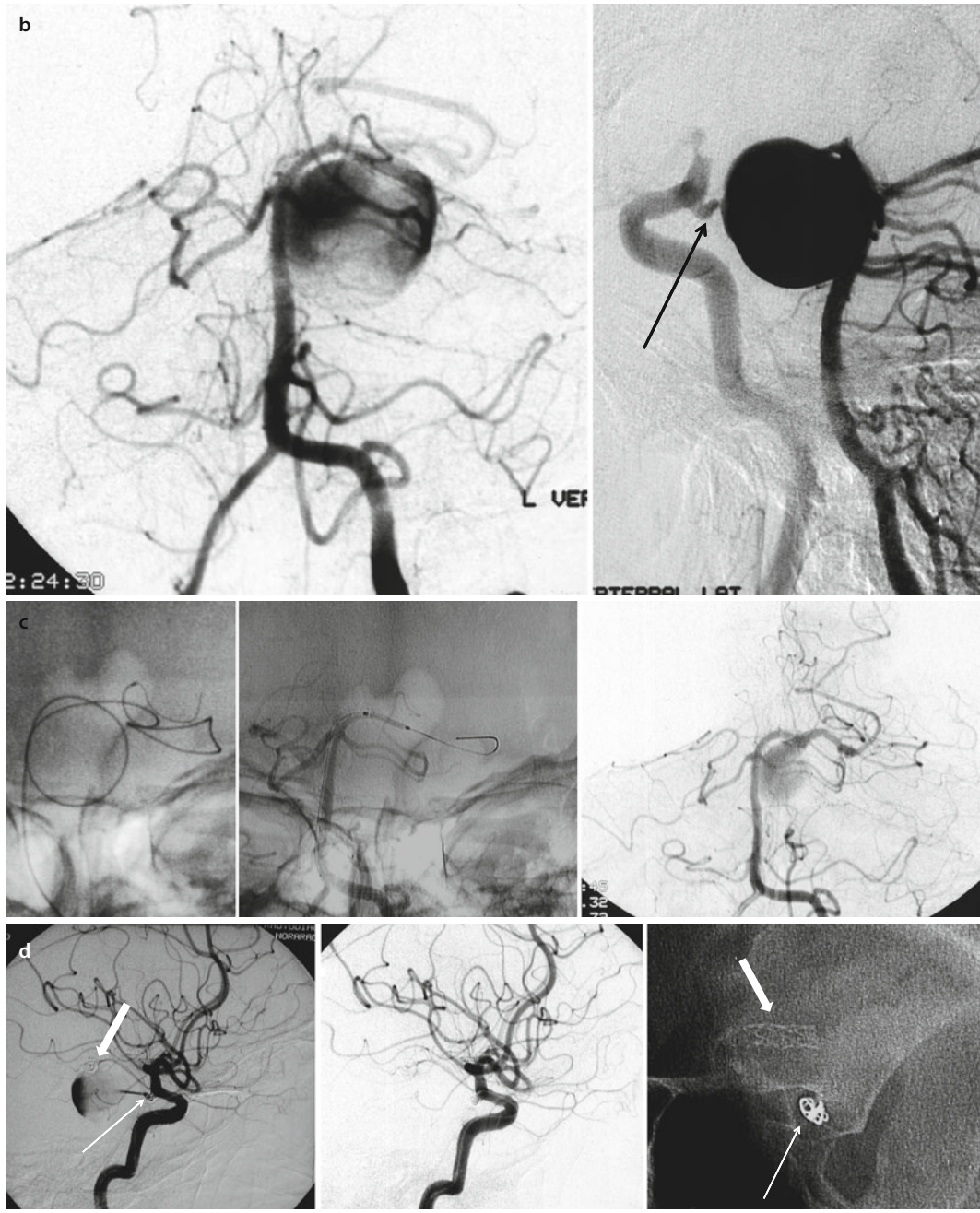

Fig. 2.1 (continued) (**b**) Cerebral DSA reveals a 25 × 22 mm-sized giant fusiform aneurysm in the middle and distal segments of the left PCoM. The aneurysm has a wide neck at its origin from PCA. The aneurysm had dominant filling from PCA with some flow from PCoM (*arrow*). The aneurysm had a slow luminal swirling flow with gradual opacification of the distal PCA branches. (**c**, **d**) On October 2000, the aneurysm neck was crossed using catheter-looping technique. A 2.5 × 9 mm-sized balloon-mounted coronary stent was deployed across the aneurysmal neck to create flow diversion. There was significant decrease in aneurysmal opacification with a small residual filling from PCoM. Hence, two coils were used to occlude the inflow zone from the PCoM infundibulum. Fluoroscopic AP image shows coils within the PCoM infundibulum (*arrow*) and coronary BMS (*block arrow*) within the PCA.

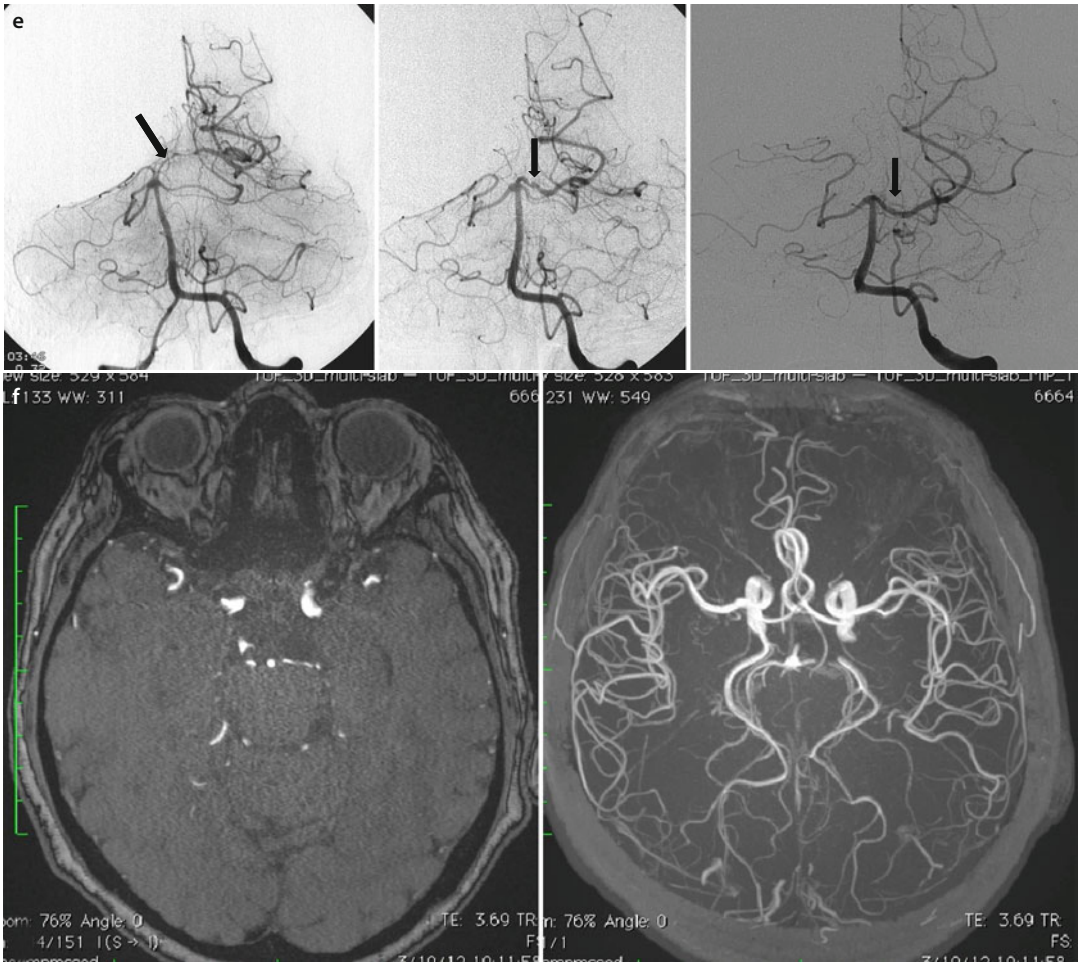

Fig. 2.1 (continued) (**e**) Control DSA at 6 months, 1 year, and 5 years, respectively, reveals complete exclusion of the aneurysm from circulation. There is moderate to severe in-stent stenosis in left PCA (*arrow*) at 6 months. Note the elevation of P1 and P2 segments due to mass effect of thrombosed aneurysm. Follow-up DSA at 1 year shows regression of the in-stent stenosis (*arrow*) with residual contour irregularity. The PCA has reverted to its original configuration following shrinkage of aneurysm. Subsequent DSA at 5 years shows complete resolution of left PCA in-stent stenosis (*arrow*) with a normal PCA configuration. (**f**) On a 13-year follow-up MRA, there is aneurysmal occlusion with normal appearance of intracranial arteries

Case 3

N. Kocer, *Giant Intracranial Aneurysms*, DOI 10.1007/978-3-319-41788-2_3

Side-Branch and Perforator Occlusion Post-FD Therapy

Keywords: Side branch occlusion, Flow diverter, Perforator occlusion

In Vitro Studies with FDs

A number of in vitro studies have shown blood flow across side branch, and perforators are preserved after deployment of a single flow diverter. It has also been shown that >90 % coverage of the perforator inlet area results in a flow reduction of <10 %. This is because blood flow into perforators is driven by "pressure gradient" unlike in aneurysms that is dependent on the trajectory of blood flow at the aneurysm-parent vessel interface. Thus, the flow into side branches and perforators can be envisaged as multiple small siphons at a lower pressure that drain blood from a high-pressure system, i.e., the parent artery [1]. However, despite these theoretical in vitro and animal studies, clinical cases of side branch and perforator occlusion have been described in literature [2, 3]. FD-covered side branches that have a robust collateral blood flow are more likely to occlude because the pressure gradient is not so steep in them [4]. A recent study found the rate of perforator infarction post-PED® FD treatment to be around 3 % with the majority of infarctions occurring in the posterior circulation [5]. The basilar artery appears to be at a higher risk of symptomatic perforator infarctions compared to ICA [6].

Side-Branch Occlusion in Diseased Arteries

*It is our observation (*Cases 5 *and* 7*) that side branches arising from diseased arterial segments like fusiform aneurysms or aneurysmal sac have a higher risk of occlusion post-FD therapy compared to side branches and perforators that arise from normal arterial segments that are merely covered by FD. The literature discussing this phenomenon is very sparse at this point of time* [7].

References

1. Fiorella D, Lylyk P, Szikora I, Kelly ME, Albuquerque FC, McDougall CG, Nelson PK (2009) Curative cerebrovascular reconstruction with the Pipeline embolization device: the emergence of definitive endovascular therapy for intracranial aneurysms. J Neurointerv Surg 1(1):56–65. doi:10.1136/jnis.2009.000083
2. D'Urso PI, Lanzino G, Cloft HJ, Kallmes DF (2011) Flow diversion for intracranial aneurysms: a review. Stroke J Cereb Circulation 42(8):2363–2368. doi:10.1161/strokeaha.111.620328
3. Dai D, Ding YH, Kadirvel R, Rad AE, Lewis DA, Kallmes DF (2012) Patency of branches after coverage with multiple telescoping flow-diverter devices: an in vivo study in rabbits. AJNR Am J Neuroradiol 33(1):171–174. doi:10.3174/ajnr.A2879
4. Saleme S, Iosif C, Ponomarjova S, Mendes G, Camilleri Y, Caire F, Boncoeur MP, Mounayer C (2014) Flow-diverting stents for intracranial bifurcation aneurysm treatment. Neurosurgery 75(6):623–631. doi:10.1227/neu.0000000000000522; quiz 631
5. Brinjikji W, Murad MH, Lanzino G, Cloft HJ, Kallmes DF (2013) Endovascular treatment of intracranial aneurysms with flow diverters: a meta-analysis. Stroke J Cereb Circulation 44(2):442–447. doi:10.1161/strokeaha.112.678151
6. Phillips TJ, Wenderoth JD, Phatouros CC, Rice H, Singh TP, Devilliers L, Wycoco V, Meckel S, McAuliffe W (2012) Safety of the pipeline embolization device in treatment of posterior circulation aneurysms. AJNR Am J Neuroradiol 33(7):1225–1231. doi:10.3174/ajnr.A3166
7. Tse MM, Yan B, Dowling RJ, Mitchell PJ (2013) Current status of pipeline embolization device in the treatment of intracranial aneurysms: a review. World Neurosurg 80(6):829–835. doi:10.1016/j.wneu.2012.09.023

Scaffolding Technique

Keywords: Scaffolding Technique, LEO with SILK FD

The idea behind using a LEO® stent scaffold for SILK® FD deployment began after we used a stent graft within a bare coronary stent to create flow diversion in early 2000 [1] (see Case 1).

Technique: (Cases 3, 4, and 5)

A delivery catheter (Vasco; Balt, Montmorency, France) is used to cross the aneurysm and safely position the catheter in a straight vessel portion distally, to prevent any damage to vessel wall by stent's distal wire tip. In cases with a challenging vascular morphology (very wide neck/difficult morphology GIAs) other possible microcatheter-microguidewire combinations were used to cross the aneurysm and then exchanged with the delivery microcatheter. First, a sufficiently long LEO® stent to scaffold the parent artery was loaded and positioned within the delivery microcatheter. The technique to deploy nitinol-braided stents is by maintaining a forward tension on the stent's pusher system to keep it in the desired position. The microcatheter is then simultaneously pulled back. This unsheaths the LEO® stent to cover the aneurysm from distal healthy to proximal arterial segment. Subsequently, the microcatheter was repositioned through the deployed LEO® stent. A shorter SILK® FD of sufficient length to cover inflow zone was deployed within LEO® stent. In cases with a discrepancy between the diameters of LEO® and SILK stents, a new microcatheter with an appropriate inner diameter for SILK® was navigated across the previously deployed LEO® stent.

Leo® stents were the longest available braided stents in this period. This prompted their use to scaffold the radially weak FDs like SILK® that were deployed within it for additional support.

Advantages of Scaffolding Technique

The advantages of using LEO® scaffold for SILK® FDs are:

1. The presence of a LEO® scaffold provides a stable mechanical platform that prevents the SILK® FD from excessive foreshortening especially in their deployment in fusiform/dolichoectatic arterial segments. Thus the Leo® scaffold prevents inadequate aneurysmal neck coverage and avoids the need for multiple overlapping FDs.
2. It increases the ease of SILK® delivery within the aneurysm by forming a stable construct for the FD (decreases friction between SILK® and native artery).
3. It provides a stable platform for SILK® and prevents unwieldy twisting, prolapsing or opening problems (commoner in tortuous anatomy).
4. The scaffolding technique enables use of a shorter SILK® FD that can be precisely placed across the inflow zone without compromising important side branches and perforator rich regions. The important side branches and perforator rich regions are covered by LEO® stent (scaffold) that provides the necessary mechanical support without significantly compromising them, e.g. Cases 3, 4, and 5.
5. It improves the stability of SILK® in a hostile vascular environment such as extreme tortuosity, acute angles and proximal and distal vessel size discrepancy (varying degrees of stenosis/ectasia at varying angles).

A search of the existing literature reveals that there are no strict guidelines that determine use of LEO® stent as a scaffold to deploy SILK® flow diverter. There are isolated case reports that describe the use of LEO® stent as a scaffold for SILK® FD deployment within it [2–5].

References

1. Islak C, Kocer N, Albayram S, Kizilkilic O, Uzma O, Cokyuksel O (2002) Bare stent-graft technique: a new method of endoluminal vascular reconstruction for the treatment of giant and fusiform aneurysms. AJNR Am J Neuroradiol 23(9):1589–1595
2. Shankar JJ, Vandorpe R, Pickett G, Maloney W (2013) SILK flow diverter for treatment of intracranial aneurysms: initial experience and cost analysis. J Neurointerv Surg 5(Suppl 3):iii11–15. doi:10.1136/neurintsurg-2012-010590
3. Binning MJ, Natarajan SK, Bulsara KR, Siddiqui AH, Hopkins LN, Levy EI (2011) SILK flow-diverting device for intracranial aneurysms. World Neurosurg 76(5):477.e471–476. doi:10.1016/j.wneu.2011.03.050
4. Siddiqui AH, Abla AA, Kan P, Dumont TM, Jahshan S, Britz GW, Hopkins LN, Levy EI (2012) Panacea or problem: flow diverters in the treatment of symptomatic large or giant fusiform vertebrobasilar aneurysms. J Neurosurg 116(6):1258–1266. doi:10.3171/2012.2.jns111942
5. van Oel LI, van Rooij WJ, Sluzewski M, Beute GN, Lohle PN, Peluso JP (2013) Reconstructive endovascular treatment of fusiform and dissecting basilar trunk aneurysms with flow diverters, stents, and coils. AJNR Am J Neuroradiol 34(3):589–595. doi:10.3174/ajnr.A3255

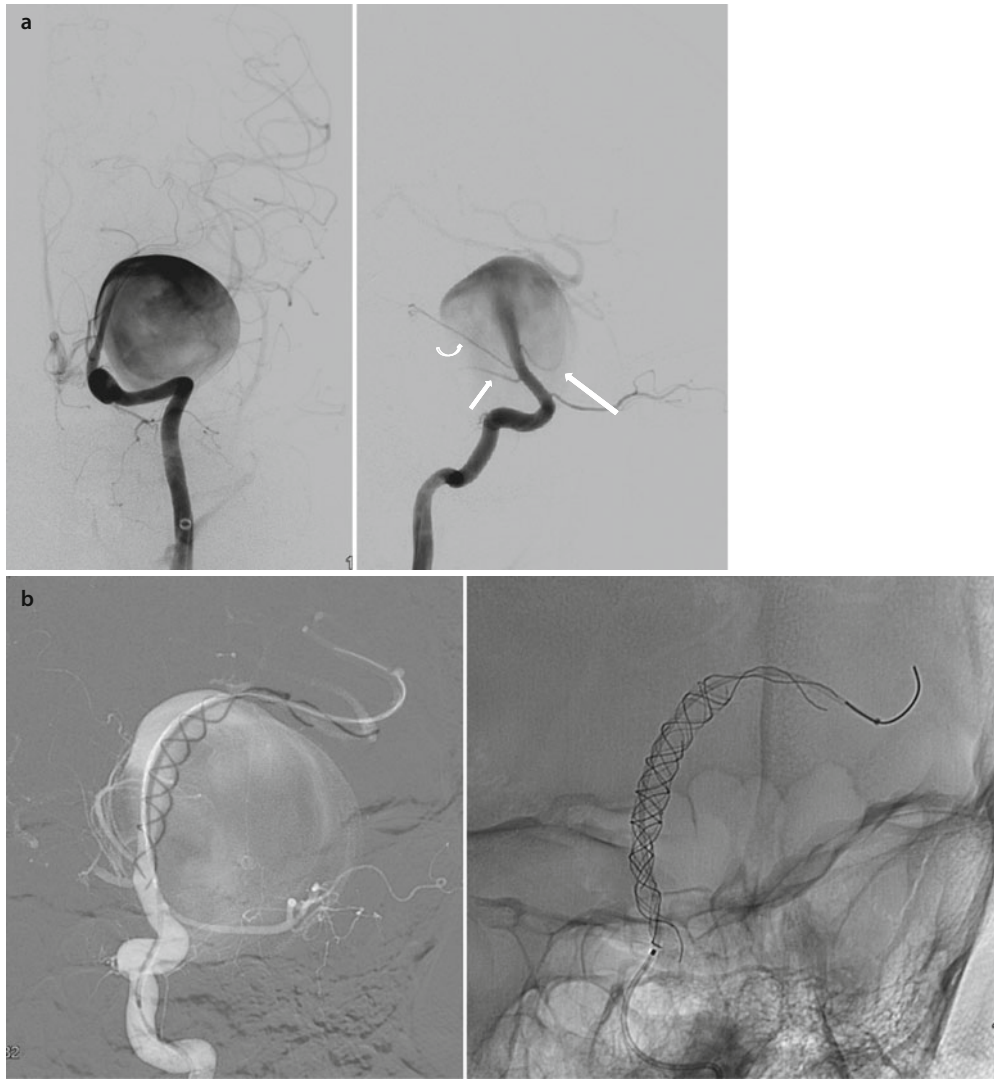

Fig. 3.1 A 12-year-old girl presented with absence seizures. The cross-sectional imaging revealed a giant aneurysm compression on the medial temporal lobe and diencephalon. (**a**) Cerebral DSA shows a 42 × 36 mm giant unruptured left supraclinoid ICA fusiform aneurysm with a wide neck extending to the proximal M1 segment of left MCA. The left ACA (*block arrow*) is incorporated into the aneurysm sac. The PCoM (*arrow*) and anterior choroidal arteries (*curved arrow*) arise in close proximity to the aneurysmal neck. (**b**) On December 2012, a LEO® stent was positioned across the aneurysm followed by a shorter SILK® FD that was telescopically deployed within it by using the *scaffolding technique.*

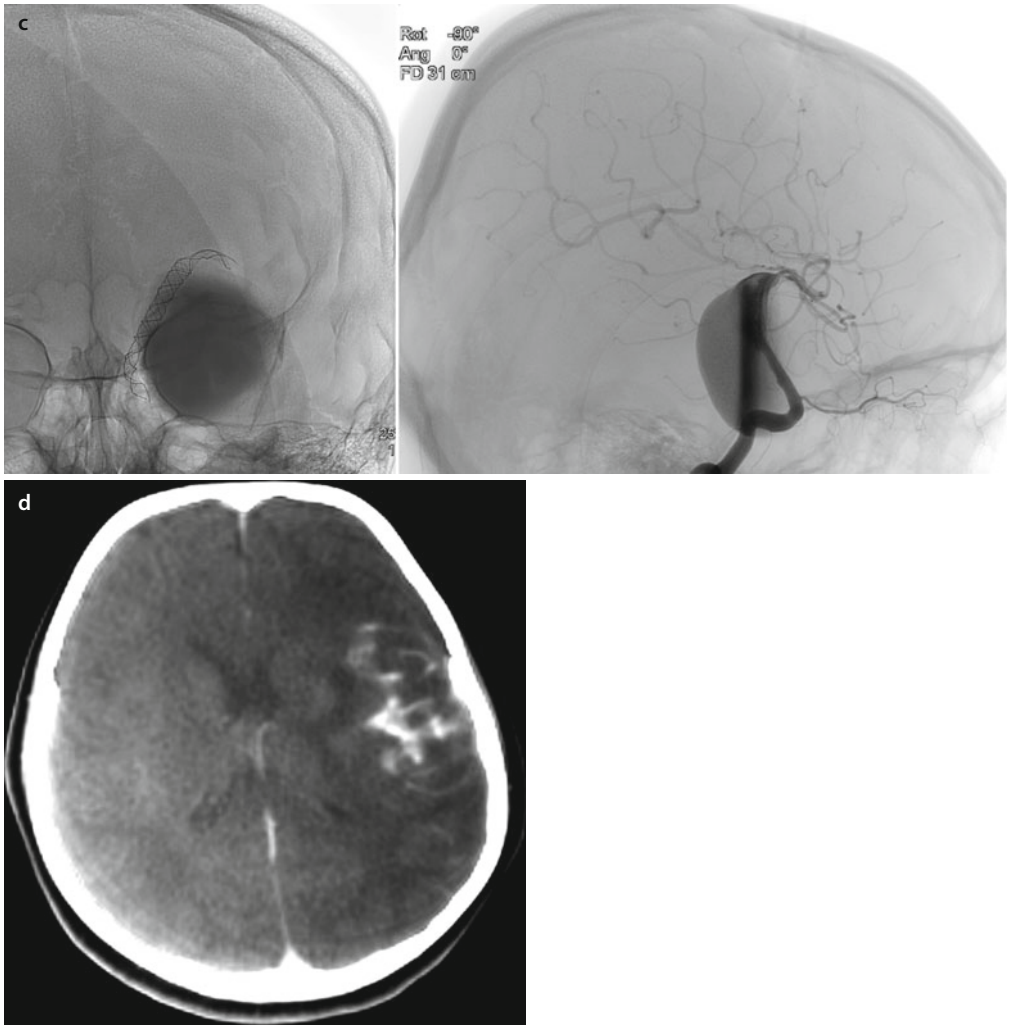

Fig. 3.1 (continued) (**c**) Fluoroscopic images reveal the final position of LEO® and SILK® FD across the aneurysm with "eclipse" sign suggestive of immediate intra-aneurysmal stagnation. The origins of ACA, anterior choroidal, and posterior communicating arteries were covered by the stents. Note: there is an increased flow into distal branches due to flow redirection. (**d**) Immediate postprocedural FDCT shows left Sylvian fissure subarachnoid hemorrhage. This was probably due to wire perforation as there was no contrast extravasation at any time during the procedure. The patient complained of mild headache but was otherwise normal.

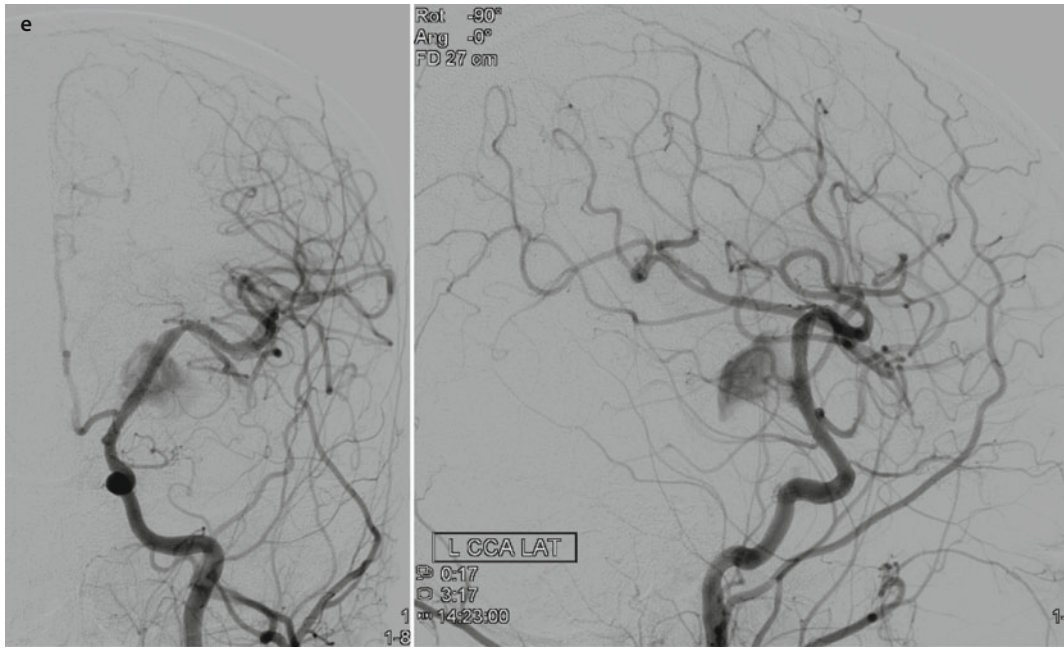

Fig. 3.1 (continued) (**e**) Cerebral DSA 24 h later reveals significant reduction in aneurysmal flow with an intact anterior cerebral, anterior choroidal, and PCoM arteries.

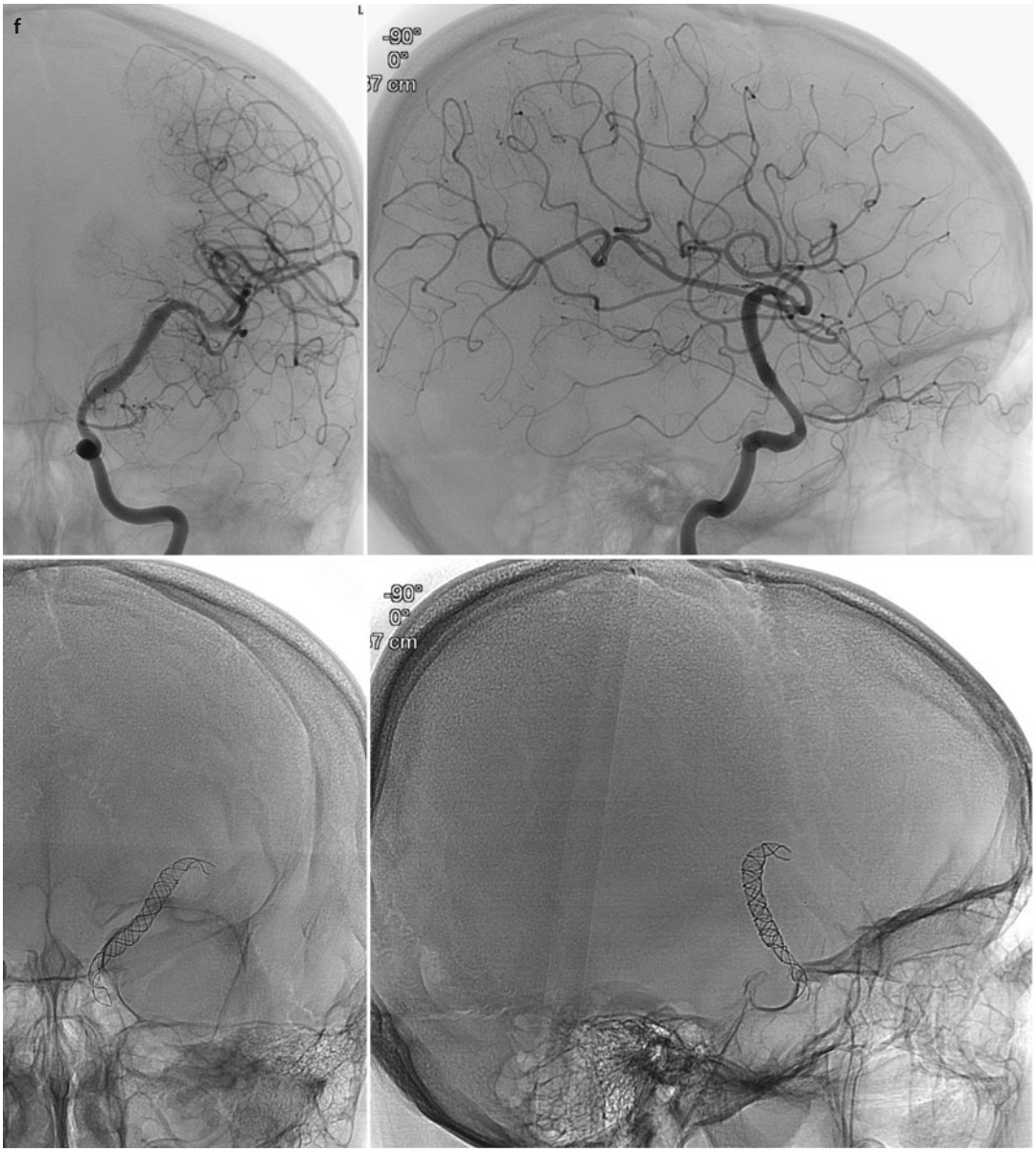

Fig. 3.1 (continued) (**f**) Control DSA at 3 months reveals remodeling of the supraclinoid ICA and MCA to a normal caliber and configuration. There is complete exclusion of the aneurysm from the circulation with patent anterior choroidal and PCoM arteries. The ACA was opacified from the right ICA.

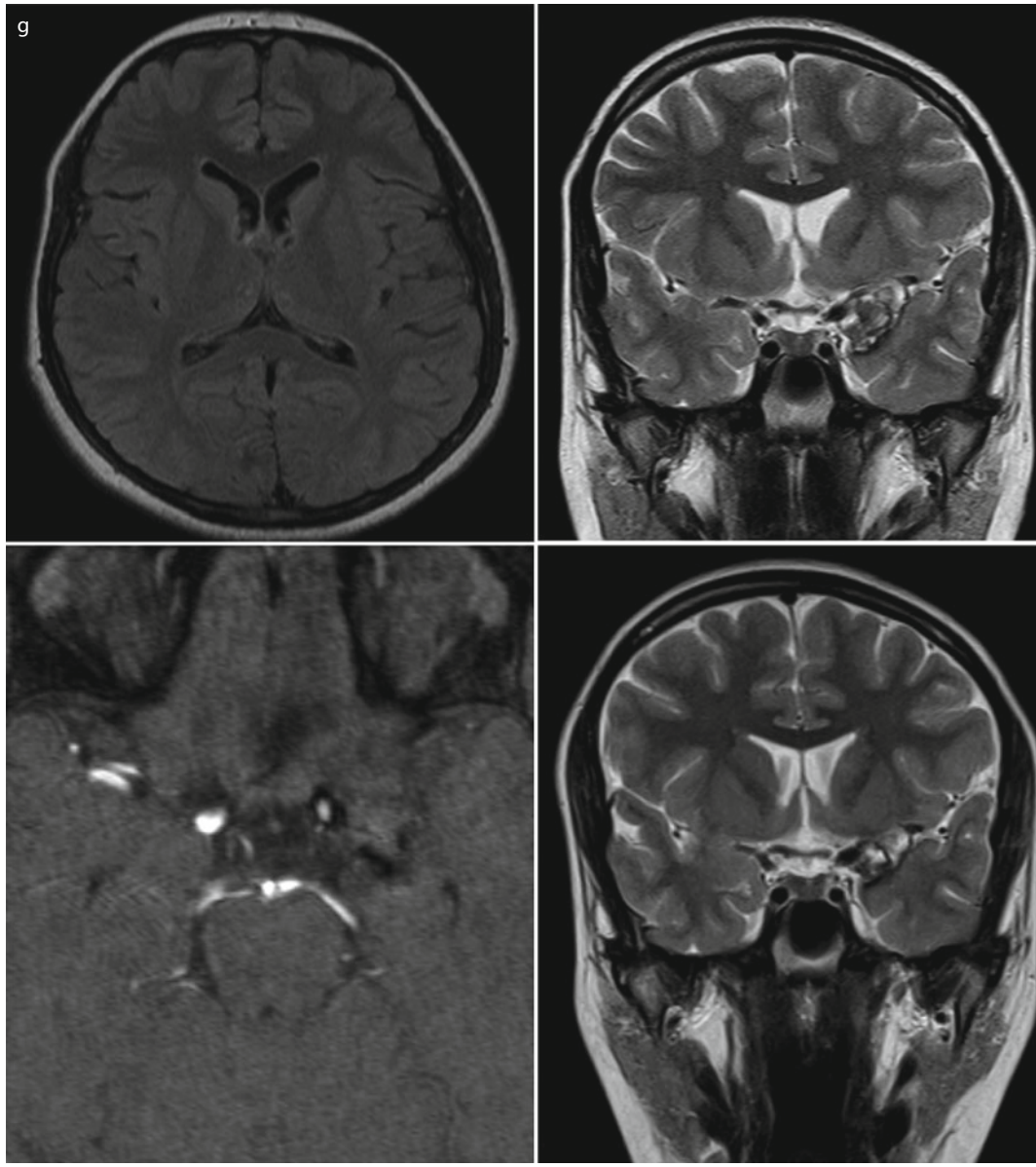

Fig. 3.1 (continued) (**g**) Follow-up MRI at 6 months after treatment shows no parenchymal pathology with a thrombosed and shrunken aneurysm. MRI with MRA at 18 months follow-up shows further shrinkage of the GIA with the remodeled parent artery

Case 4

N. Kocer, *Giant Intracranial Aneurysms*, DOI 10.1007/978-3-319-41788-2_4

Cavernous ICA GIAs

Keywords: Cavernous aneurysms, Giant aneurysms

Introduction and Anatomy

Cavernous ICA aneurysms account for 2–9 % of all intracranial aneurysms [1]. Large and giant cavernous aneurysms constitute approximately 60 % of all cavernous ICA aneurysms [2]. According to the ISUIA study, asymptomatic cavernous GIAs have a 6.4 % rupture risk within 5 years. The cavernous aneurysms usually rupture into the cavernous sinus that leads to the formation of carotid cavernous fistula. Rupture into the subarachnoid space of cavernous aneurysms is rare and is seen in aneurysms with an intradural component. However, current imaging techniques cannot distinguish between these aneurysms [3]. The presence of bilateral cavernous aneurysms and aneurysms that show growth is associated with increased risk of rupture [1]. Cavernous GIAs are considered in a separate category of their own. This is because the natural history, clinical presentation, and treatment of cavernous GIAs are different from GIAs in other locations [4].

The cavernous segment of ICA extends from the superior part of petrolingual ligament to the proximal dural ring. It is in close relationship with four cranial nerves, namely, the third cranial nerve, first part fifth cranial nerve, fourth cranial nerve, and sixth cranial nerve [1, 4]. The anterior aspect of the cavernous segment of ICA is in close contact with the posterior aspect of sphenoid sinus.

Transitional cavernous aneurysms are a separate subcategory in cavernous aneurysms. They have a neck in the cavernous segment while its body and fundus enter the subarachnoid space through the dural ring. It is associated with a risk of subarachnoid hemorrhage in case of rupture [4].

Cavernous ICA aneurysms arising from Debrun cavernous segment C1 are located in the epidural space and are small saccular aneurysms with a greater tendency to rupture into subarachnoid space. In contrast, cavernous aneurysms that arise from Debrun cavernous segments C5, C4, C3, and C2 tend to be large to giant and are often fusiform aneurysms. These present with symptoms secondary to mass effect like cranial nerve deficits and rarely present with life-threatening hemorrhage [2].

Clinical Presentation and Treatment Strategies

In a study of 57 patients over a 30-year period with cavernous ICA GIAs, 81 % were women and 19 % were men. The patients presented with symptomatic diplopia (89 %), retro-orbital pain (61 %), headaches (19 %), diminished or blurred vision (14 %), and photophobia (4 %). The commonest clinical sign was ophthalmoplegia seen in 93 % of patients. The ophthalmoplegia involved the third cranial nerve in 54 %, fourth cranial nerve in 25 %, and sixth cranial nerve in 81 % of patients. The fifth cranial nerve was involved in 37 %. The other common clinical signs at presentation include ptosis in 51 % and decreased visual acuity in 12 % [5]. By contrast in patients with transitional cavernous aneurysms, the commonest clinical presentation was subarachnoid hemorrhage (57 %), compressive symptoms in 39 %, and asymptomatic in 4 % of patients [6].

Current therapeutic strategies in the management of cavernous ICA aneurysms include flow diversion and carotid sacrifice with or without bypass. Carotid sacrifice has a 98.7 % rate of complete aneurysm occlusion, an 81 % resolution of diplopia, and a 5 % risk of procedure-related neurological deficits. However, carotid sacrifice in young patients has an additional estimated life-time incidence of 4–11 % formation and growth of aneurysms contralateral to the sacrificed carotid artery [7]. In contrast, reconstructive endovascular techniques using coils with or without stents achieved a complete occlusion rate of only 43 %. Flow diversion using flow diverters has achieved nearly 100 % complete occlusion rate and symptomatic resolution in 72 % of patients [7]. In a recent systematic review published in 2014, flow diversion using FDs for cavernous ICA aneurysms was associated with an overall morbidity of 4.1 % and a mortality of 0.7 % [3].

References

1. Eddleman CS, Hurley MC, Bendok BR, Batjer HH (2009) Cavernous carotid aneurysms: to treat or not to treat? Neurosurg Focus 26(5):E4. doi:10.3171/2009.2.focus0920
2. Bavinzski G, Killer M, Ferraz-Leite H, Gruber A, Gross CE, Richling B (1998) Endovascular therapy of idiopathic cavernous aneurysms over 11 years. AJNR Am J Neuroradiol 19(3):559–565
3. Tanweer O, Raz E, Brunswick A, Zumofen D, Shapiro M, Riina HA, Fouladvand M, Becske T, Nelson PK (2014) Cavernous carotid aneurysms in the era of flow diversion: a need to revisit treatment paradigms. AJNR Am J Neuroradiol 35(12):2334–2340. doi:10.3174/ajnr.A4081
4. Penchet G, Mourier K (2015) Collaborative retrospective multicentre series of giant intracavernous carotid aneurysms. Neuro-Chirurgie 61(6):366–370. doi:10.1016/j.neuchi.2013.12.004

5. Hahn CD, Nicolle DA, Lownie SP, Drake CG (2000) Giant cavernous carotid aneurysms: clinical presentation in fifty-seven cases. J Neuro-Ophthalmol 20(4):253–258
6. al-Rodhan NR, Piepgras DG, Sundt TM, Jr (1993) Transitional cavernous aneurysms of the internal carotid artery. Neurosurgery 33(6):993–996; discussion 997–998
7. Puffer RC, Piano M, Lanzino G, Valvassori L, Kallmes DF, Quilici L, Cloft HJ, Boccardi E (2014) Treatment of cavernous sinus aneurysms with flow diversion: results in 44 patients. AJNR Am J Neuroradiol 35(5):948–951. doi:10.3174/ajnr.A3826

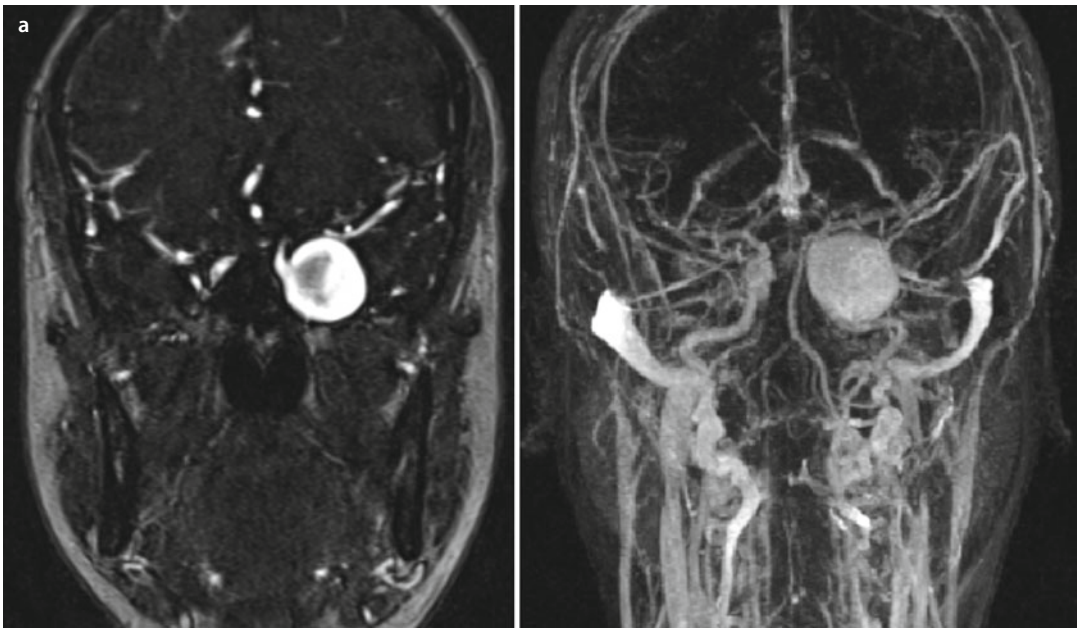

Fig. 4.1 A 30-year-old lady presented with headaches and ophthalmoplegia. (**a**) MR angiogram reveals 3D morphology of the giant cavernous ICA aneurysm.

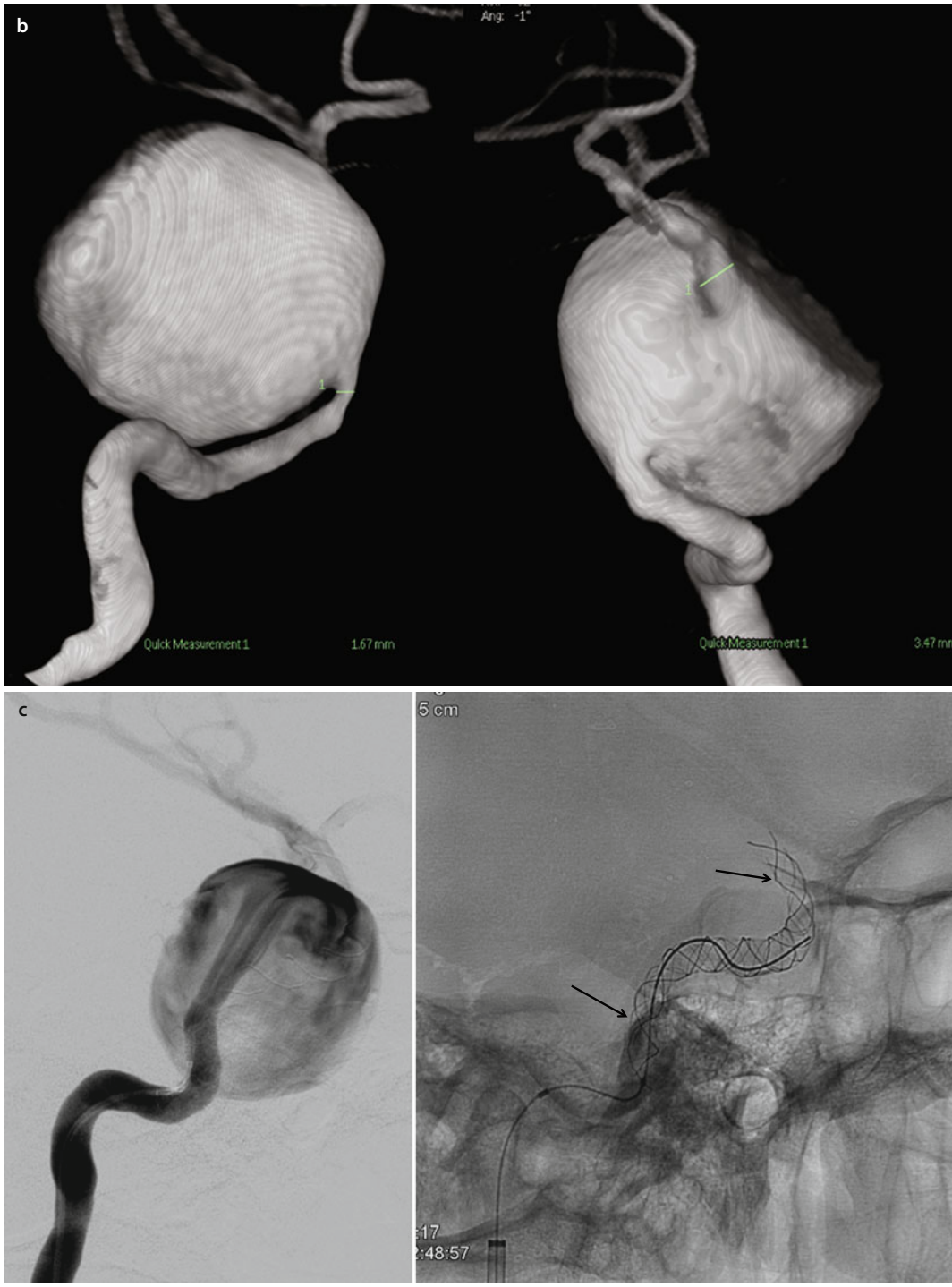

Fig. 4.1 (continued) (**b**) On May 2013, 3D DSA angiogram shows a 30 × 27 mm-sized ICA aneurysm with a clear depiction of the inflow and outflow segments. Note the significant discrepancy in the size of pre- and post-aneurysmal ICA segments that measure 1.7 mm proximally and 3.4 mm distally on the 3D DSA, whereas there was no such discrepancy seen on routine cerebral DSA images. This is due to 3D DSA artifact. (**c**) On May 2013, a LEO® stent followed by a shorter SILK® FD (*arrows depict the SILK® FD*) were deployed across the inflow zone of the aneurysmal neck.

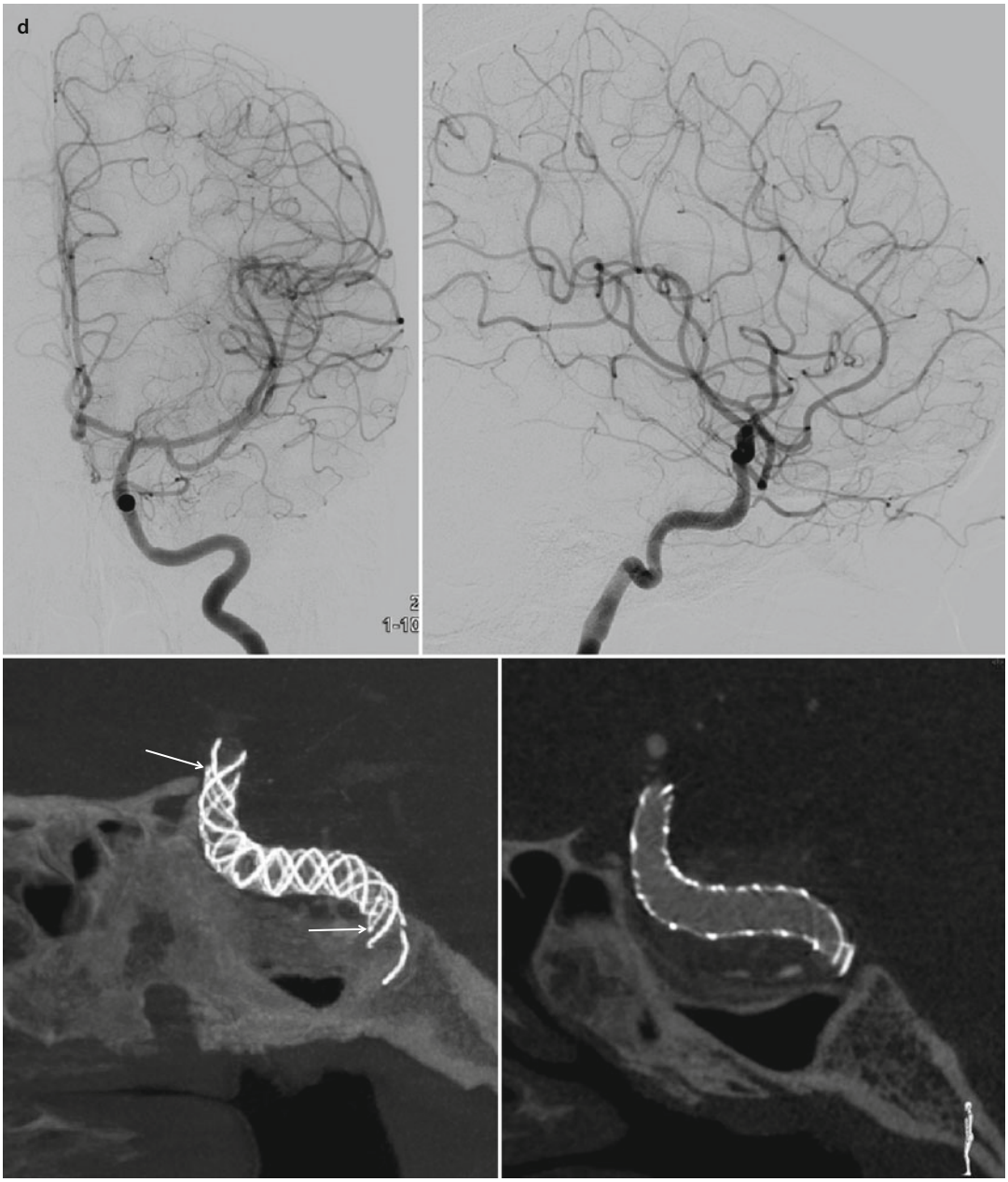

Fig. 4.1 (continued) (**d**) Control angiogram after 6 months reveals complete remodeling of the cavernous ICA with no aneurysmal opacification. I.V. FDCT (VASO CT®) after 1½ year reveals stable dual-stent configuration. There is no intimal hyperplasia seen (*arrows depict the SILK® FD*)

Case 5

Electronic supplementary material The online version of this chapter (doi:10.1007/978-3-319-41788-2_5) contains supplementary material, which is available to authorized users.

N. Kocer, *Giant Intracranial Aneurysms*, DOI 10.1007/978-3-319-41788-2_5

Antiplatelet Regimen for FD Therapy of Ruptured and Unruptured Aneurysms

Keywords: Cerebral aneurysm, Ruptured and unruptured aneurysms, Antiplatelet drug regimen, Flow diverter

Antiplatelet Regimen and Aneurysm Occlusion

There are no systematic studies that address the above concerns regarding antiplatelet regimens. This results in varied response to FD treatment. For example, residual filling of GIAs or even unchanged aneurysmal opacification is the commonest finding in the immediate post-FD treatment angiograms. Immediate aneurysm occlusion is an exception. Aneurysms less than 5 mm with immediate occlusion have been documented in 8–21 % of all cases [1]. However, another author had no documented cases of immediate occlusion though nearly 50 % of his cases comprised aneurysms less than 5 mm [1, 2]. This was attributed to a more aggressive antiplatelet regimen with 500 mg aspirin and 600 mg of clopidogrel at least one day before procedure as opposed to a standard antiplatelet therapy of 100–325 mg of aspirin and 75 mg of clopidogrel 48–72 h before the procedure. Furthermore dual antiplatelet therapy was prolonged for 1 year instead of the usual 6 weeks to 6 months [1, 2].

This was also reflected by the lowest aneurysm occlusion rate among the series of GIAs treated with FDs (74 % at 10 months) that is otherwise in the range of 84–95 % at 6 months. Thus both high dose and prolonged dual antiplatelet therapy may significantly delay aneurysmal occlusion post-FD therapy [1].

Antiplatelet Regimen in FDs: Unruptured and Ruptured Aneurysms

Currently, there are no standard guidelines on duration and dose of antiplatelet agents for FDs. Dual antiplatelet loading prior to the procedure followed by its continuation for a minimum of 3 months is essential (selected cases up to 1 year) to prevent in-stent thrombosis. Multiple PED® FDs appear to increase the risk of in-stent thrombosis, but the optimum antiplatelet dose and duration is as yet undetermined [1]. The antiplatelet drug regimen protocols balance prevention of thromboembolic complications against an iatrogenic increased risk of bleeding. The risk of serious non-neurological bleeding is as high as 4.5 %. Furthermore an ESMINT FD-related bleeding survey reported delayed thromboembolic events in 4.73 % of patients, and it was unclear if some of the patients were adequately anti-aggregated [3].

In ruptured cerebral aneurysms, FDs are deployed without any pretreatment, i.e., antiplatelet drugs are not loaded over a period of 48–72 h in standard doses. Thus, when FDs are used without pretreatment, e.g., recent SAH, 500 mg aspirin is given intravenously and is effective in minutes along with an oral dose of thienopyridine. Additional anticoagulation is given during FD deployment, which is discontinued postprocedure [3].

Antiplatelet Regimen Post FD

Posttreatment, antiplatelet drugs should be given for a total duration of 3–6 months. A typical maintenance regimen is 75–300 mg aspirin and 75 mg clopidogrel every day, though exact doses may vary. Because of individual variations in drug response and an expected 15 % of total individuals not responding to oral clopidogrel, testing platelet activity after a loading dose is an important precaution [3].

References

1. Tse MM, Yan B, Dowling RJ, Mitchell PJ (2013) Current status of pipeline embolization device in the treatment of intracranial aneurysms: a review. World Neurosurg 80(6):829–835. doi:10.1016/j.wneu.2012.09.023
2. Fischer S, Vajda Z, Aguilar Perez M, Schmid E, Hopf N, Bazner H, Henkes H (2012) Pipeline embolization device (PED) for neurovascular reconstruction: initial experience in the treatment of 101 intracranial aneurysms and dissections. Neuroradiology 54(4):369–382. doi:10.1007/s00234-011-0948-x
3. Byrne JV, Szikora I (2012) Flow diverters in the management of intracranial aneurysms: a review. EJMINT Original Article 1225000057

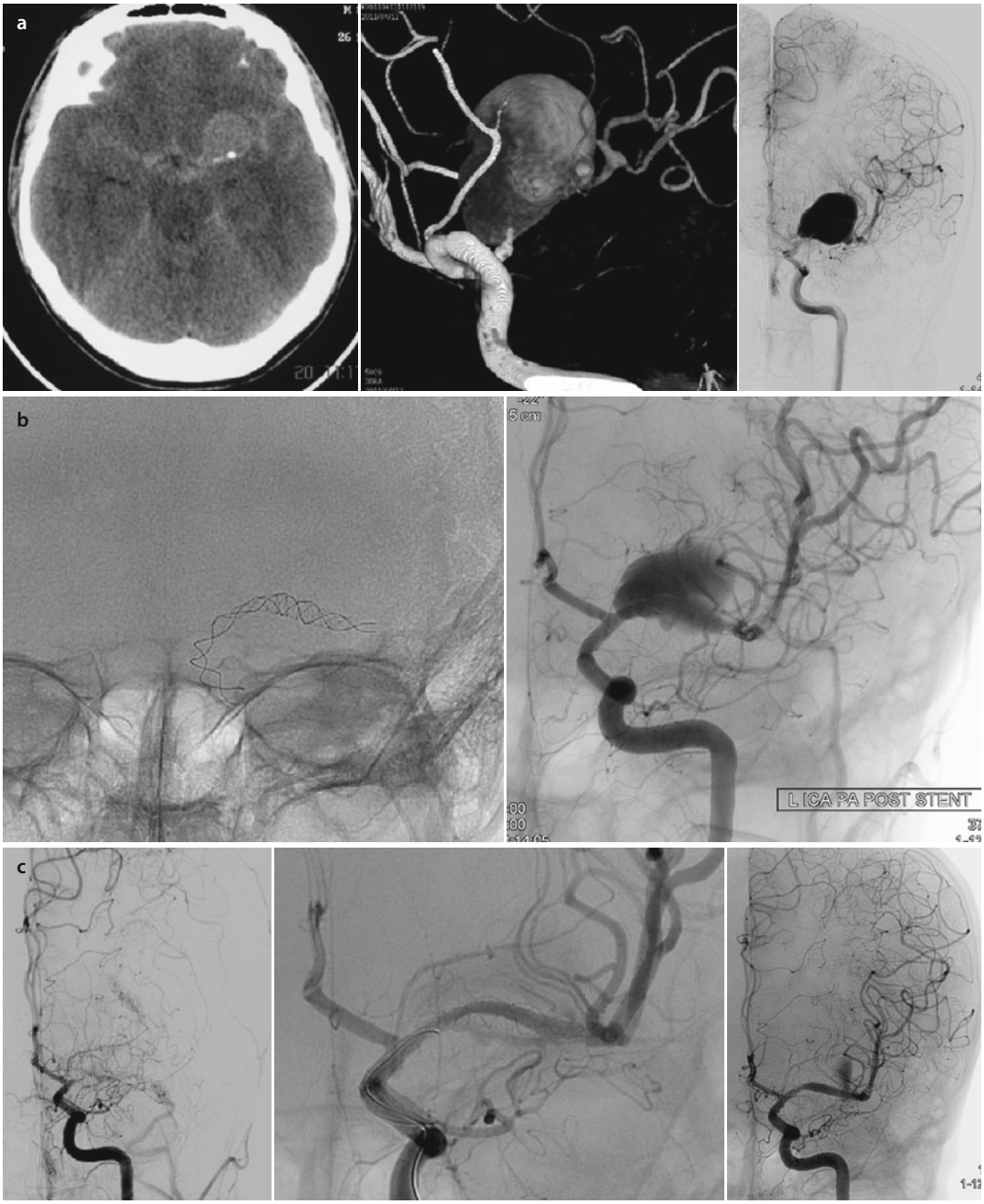

Fig. 5.1 A 38-year-old man with acute subarachnoid hemorrhage. (**a**) NECT shows a large 3.5 × 3.0 cm, well-defined, spherical hyperdensity in the left Sylvian fissure with extensive subarachnoid hemorrhage and focal calcification. Cerebral DSA and 3D images reveal a giant 3.5 cm-sized left M1 segment MCA fusiform aneurysm with proximal stenosis. (**b**) On April 2011, the patient underwent treatment with a LEO® scaffold and a SILK® flow diverter within. Note the persistent, approximately 40 % stenosis in the proximal M1 segment after deployment of flow diverter. In the immediate postprocedural angiogram, due to flow diversion, the lateral lenticulostriate branches are better opacified with flow stagnation in the aneurysmal sac. Note the SILK® FD does not intentionally cover the left ACA origin. (**c**) After 2 h, the patient developed sudden altered sensorium, and a control angiogram reveals acute in-stent thrombosis. A balloon angioplasty with Gateway® balloon (Boston Scientific, Fremont, California) was done across the stenosis with restoration of flow. On a 24-h postprocedural angiogram, there is significant decrease in the aneurysmal opacification with good distal flow

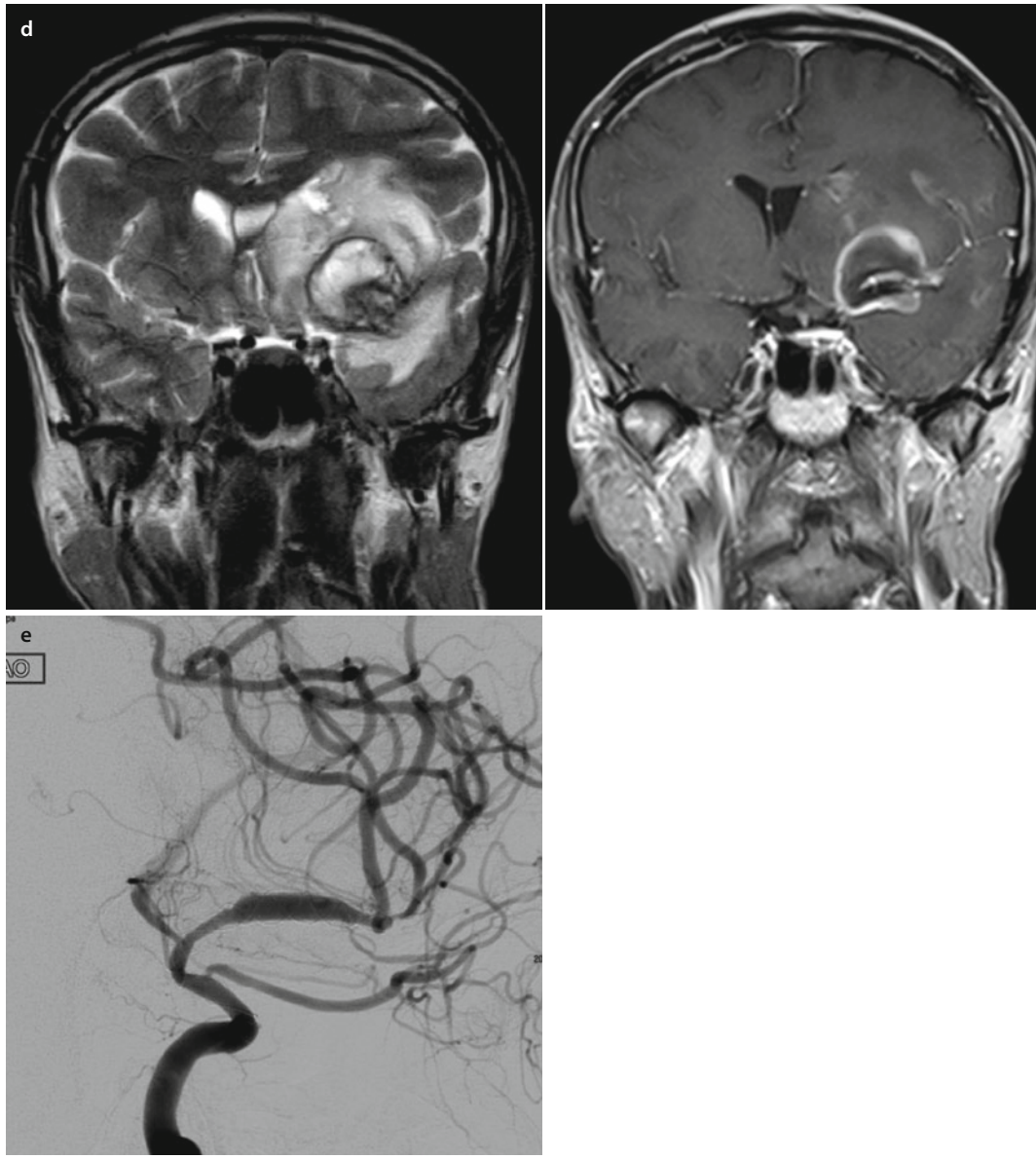

Fig. 5.1 (continued) (**d**) Follow-up MRI 1 month later reveals aneurysmal wall enhancement and extensive peri-aneurysmal vasogenic edema involving the frontal and temporal lobes, peri-insular region, and diencephalon. The aneurysm is thrombosed with infarctions in the lateral lenticulostriate territory and perisylvian region. (**e**) Control DSA at second month reveals total exclusion of the aneurysm from circulation. The aneurysm bearing M1 segment of left MCA shows focal enlargement

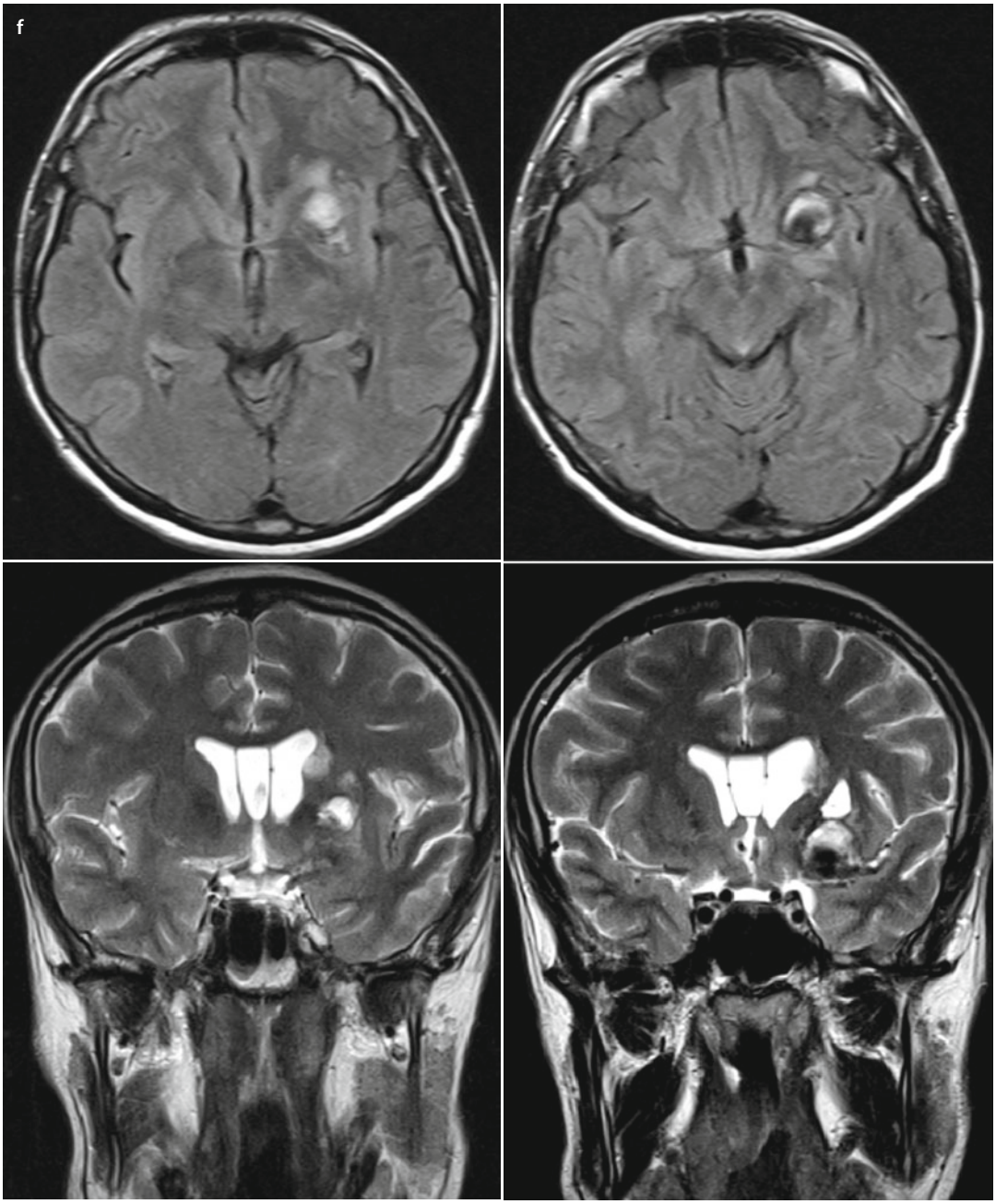

Fig. 5.1 (continued) (**f**) MRI images at third month reveal thrombosed and shrunken MCA GIA. There is complete resolution of the vasogenic edema with lenticulostriate and perisylvian regional infarction

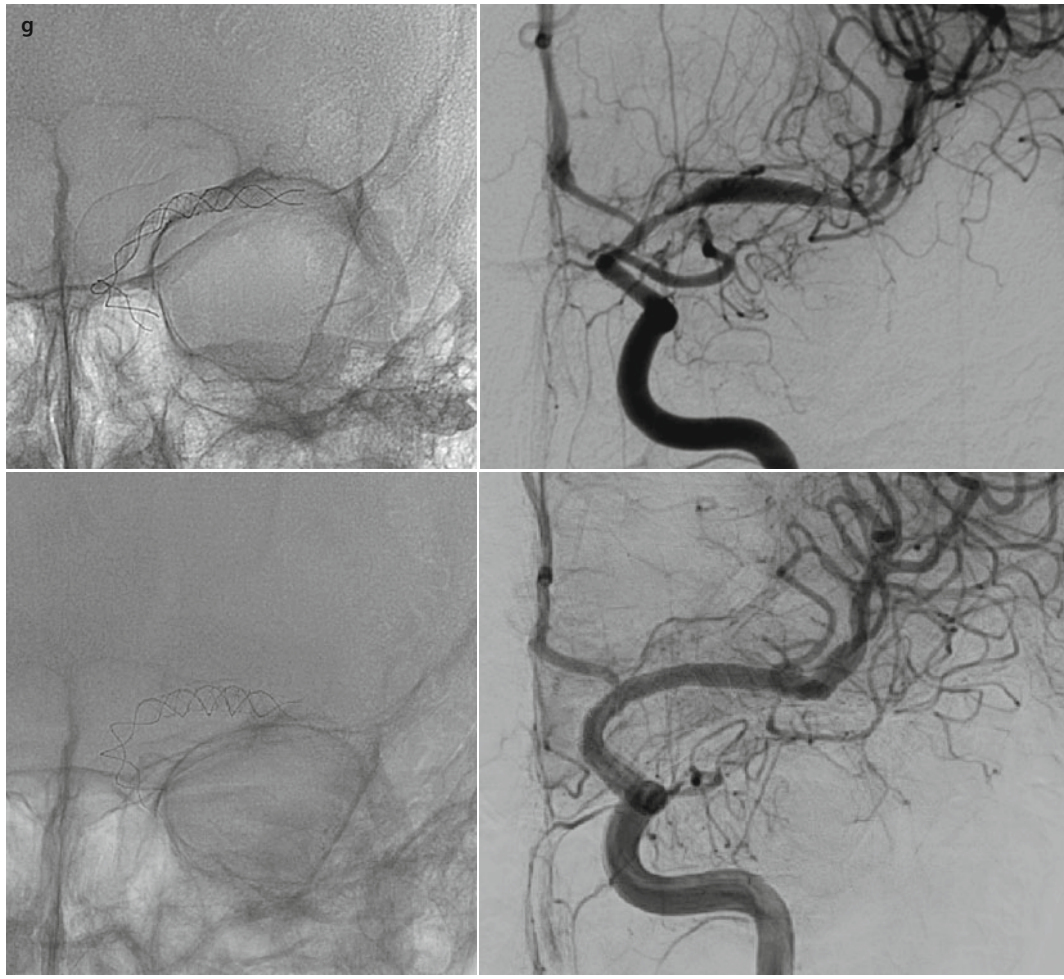

Fig. 5.1 (continued) (**g**) Comparison of follow-up DSAs at 2 months and 3 years posttreatment reveals a patent left MCA segment. There is progressive remodeling of the carotid siphon: aneurysmal segment and M1 segment of MCA to a normal caliber. The left ACA remains patent

Case 6

Electronic supplementary material The online version of this chapter (doi:10.1007/978-3-319-41788-2_6) contains supplementary material, which is available to authorized users.

N. Kocer, *Giant Intracranial Aneurysms*, DOI 10.1007/978-3-319-41788-2_6

Looping and Anchoring Technique

Keywords: Giant intracranial aneurysms, Looping and anchoring technique, FRED®

The majority of aneurysms do not require any special technique to cross the aneurysmal neck. However, in some GIAs with a very wide neck, fusiform/serpentine configuration and difficult anatomy due to tight angulation and separation of inflow and outflow zones special techniques like the "looping and anchoring" may be required.

Technique

In this case, a Headway 27 microcatheter with intra-aneurysmal looping enabled us to find the exit zone in this very wide neck aneurysm and cannulate the distal MCA (Fig. 1a). FRED® being a nitinol FD maintains the intra-aneurysmal loop (Fig. 1b). The design of the flared end of FRED® FD enables easy opening, immediate anchoring, and precise initial deployment in a short segment of the distal artery (Fig. 1c). The secure distal anchoring and adequate radial force of FRED® enable further manipulation within the aneurysm till we obtain a satisfactory position of the FD. This also includes straightening of intra-aneurysmal loop (Fig. 1d). The immediate anchoring of FRED® enables easy selection of appropriate FD length that further avoids the need for multiple telescopic Ds.

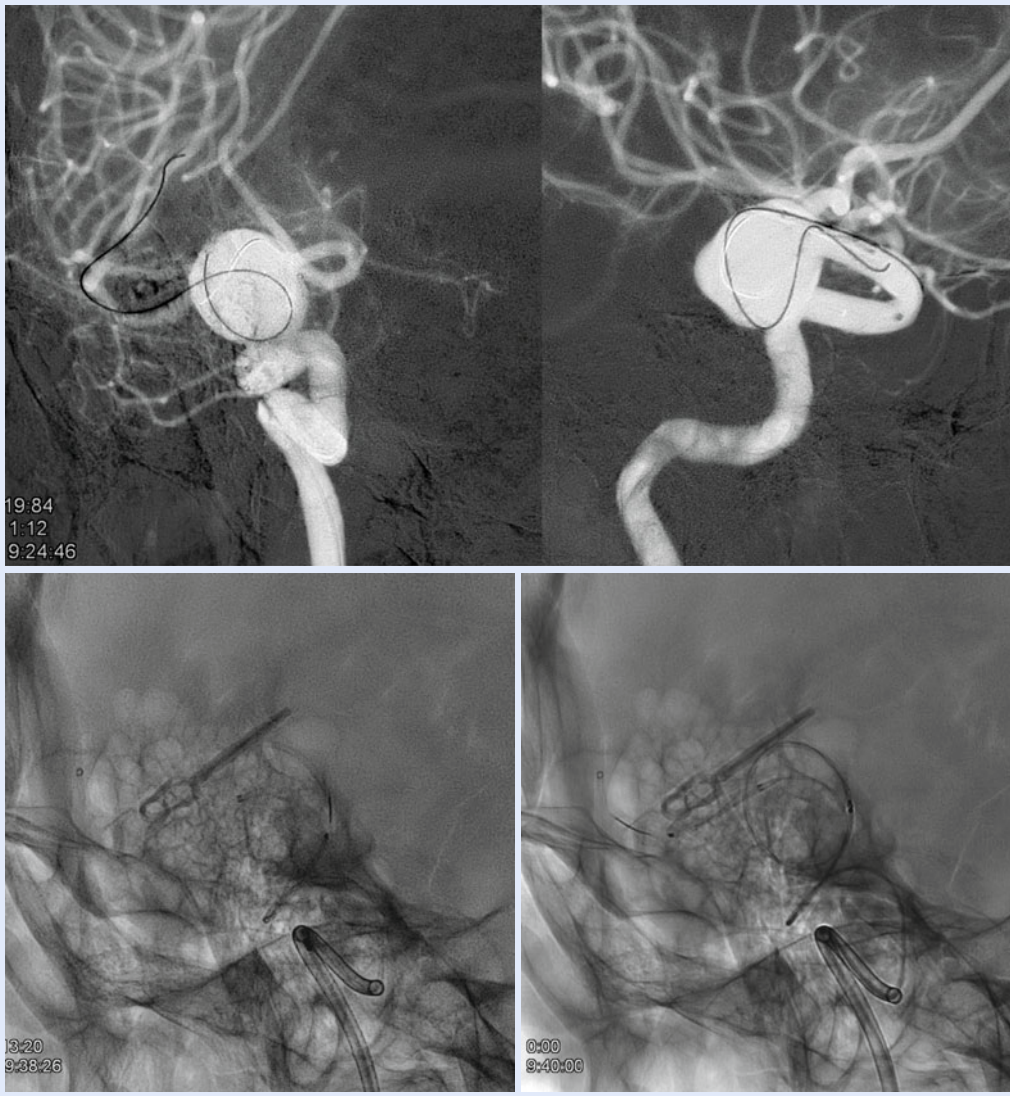

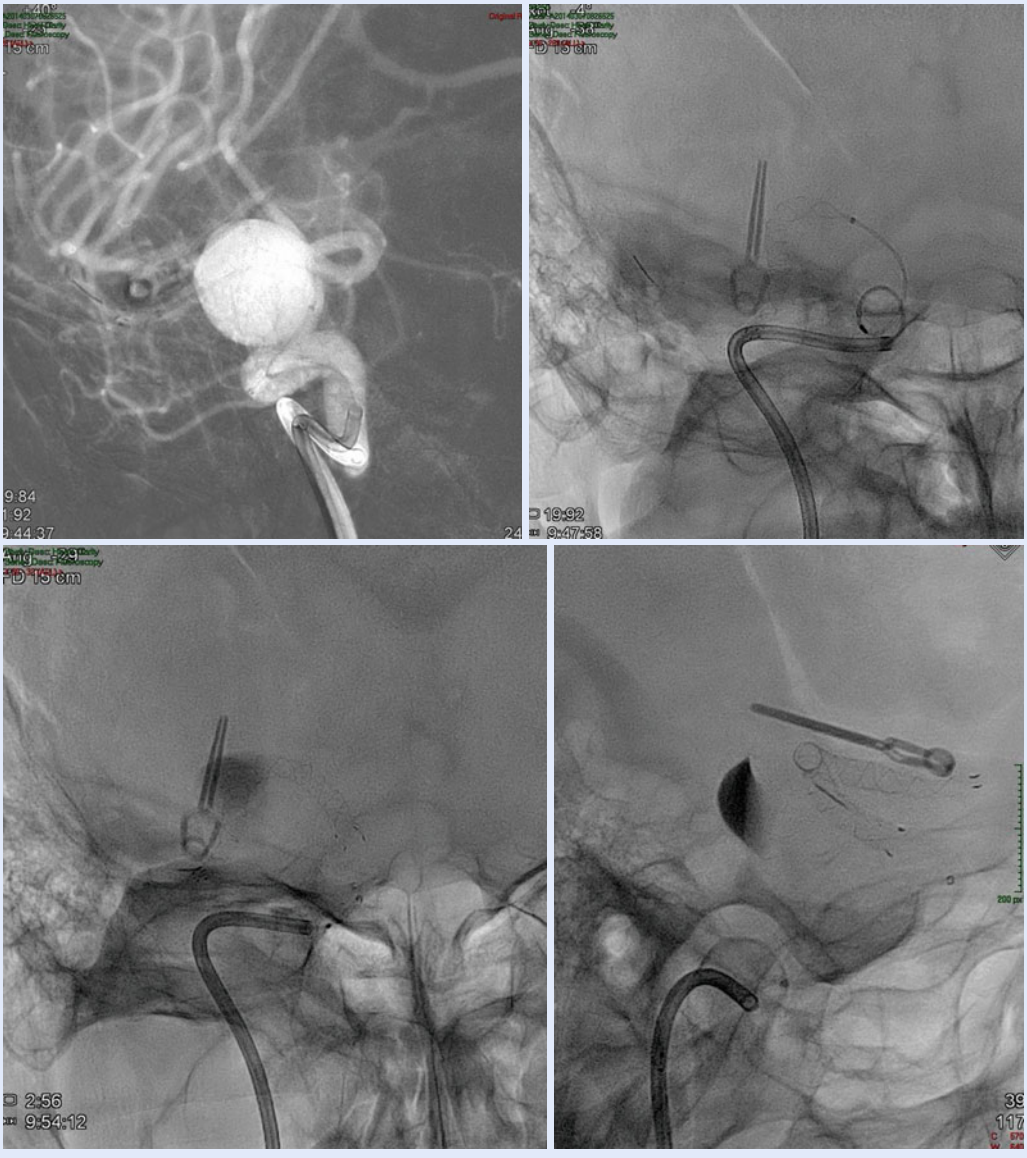

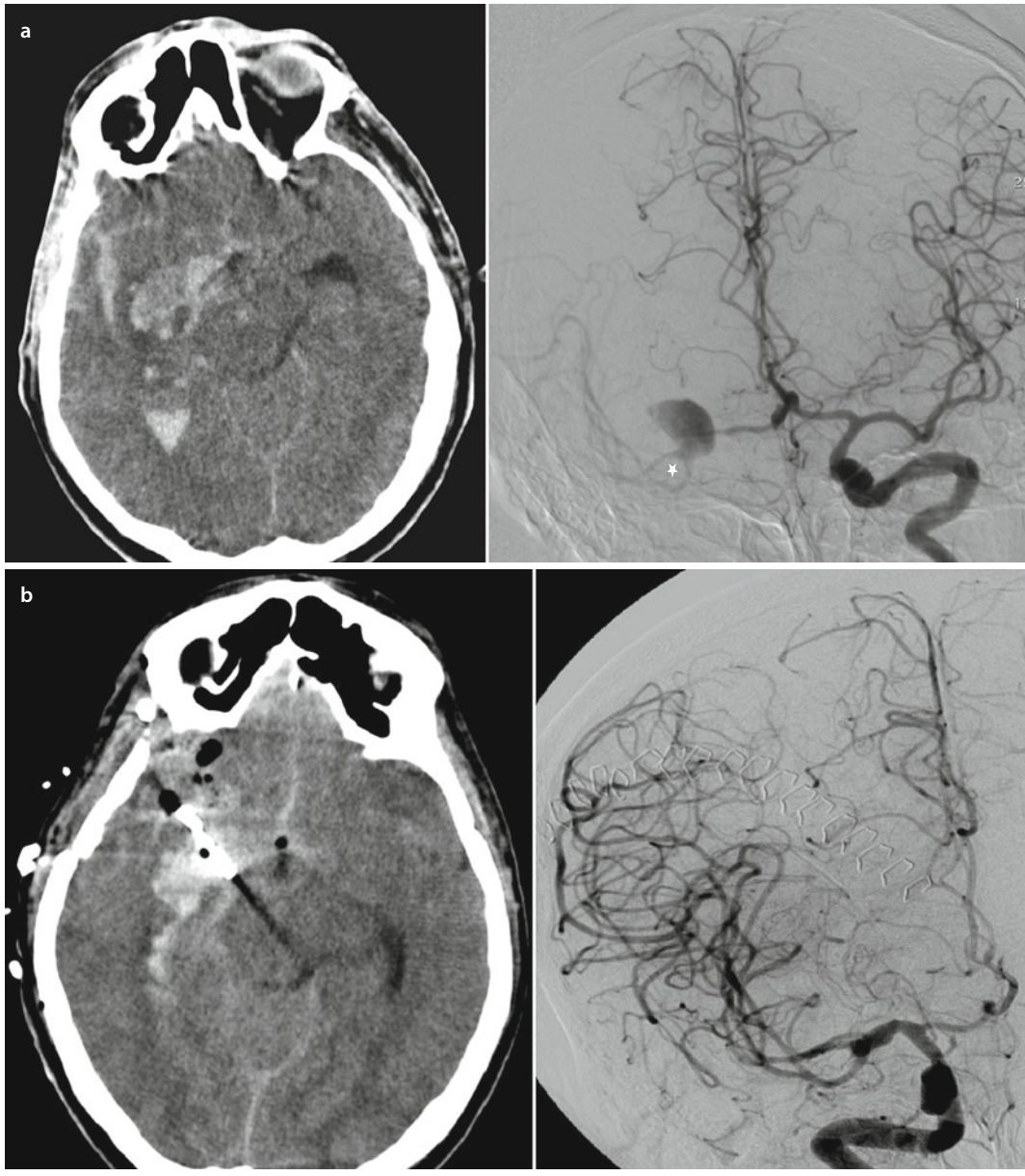

Fig. 6.1 A 66-year-old man initially admitted in 2004 with acutely ruptured right MCA giant aneurysm. (**a**) NECT shows acute subarachnoid hemorrhage with intraventricular and intraparenchymal extension. There is a well-defined heterogeneous mass lesion in the right Sylvian cistern suggestive of a GIA. Cerebral DSA shows a distal M1 segment GIA with patent bifurcation (*star*). The patient was initially treated by open surgical reconstruction with a clip. (**b**) Postsurgical, cross-sectional, and DSA images reveal exclusion of the aneurysm with an ectatic M1 segment. Note the residual hematoma and subarachnoid hemorrhage

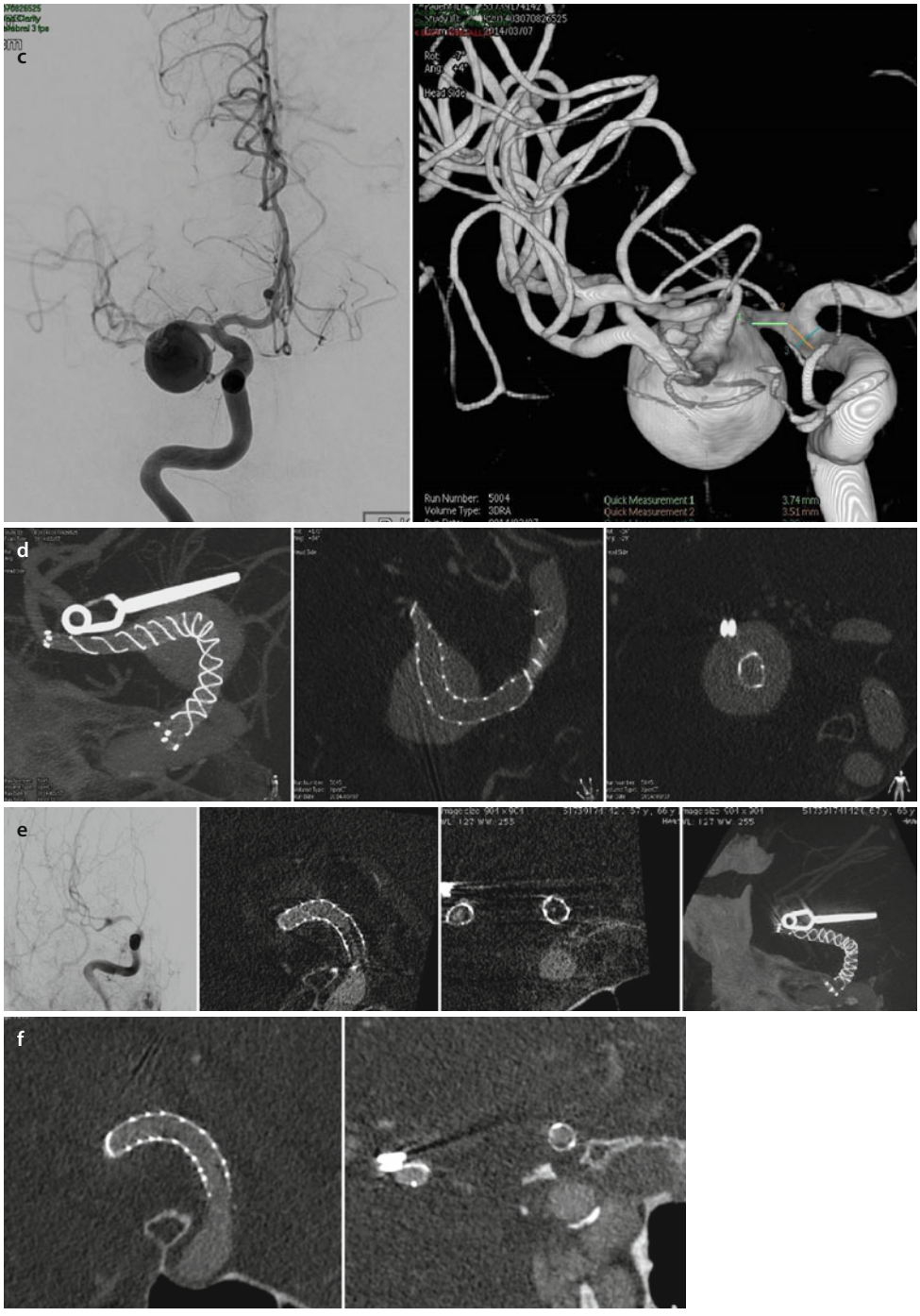

Fig. 6.1 (continued) (**c**) Patient presented 10 years later with headaches. Right ICA AP and 3D DSA images reveal right M1 segment fusiform regrowth measuring 23×18 mm. (**d**) On July 2014, the patient was treated using a long FRED® FD measuring 3.5×40×36 mm in size using *looping and anchoring technique*. IA VASO CT® depicts intra-aneurysmal FRED® location and displacement of the clip by aneurysmal regrowth. (**e**) After 3 months, the patient presented with diffuse right-sided headaches. Control DSA and IA VASO CT® reveals total exclusion of GIA from circulation with a stable stent configuration. There is intimal hyperplasia causing high-grade (approximately 95%) short-segment stenosis involving the stented segment. The patient was treated by balloon angioplasty of the in-stent stenosis. Post balloon angioplasty there was significant improvement in the caliber of the stenotic segment and improved perfusion of the distal territory. (**f**) After 1.5 years, IV VASO CT® reveals stable aneurysmal occlusion with no intimal hyperplasia

Case 7

N. Kocer, *Giant Intracranial Aneurysms*, DOI 10.1007/978-3-319-41788-2_7

Telescopic Multiple FD Technique

Keywords: Posterior circulation dissecting aneurysms, Telescopic FDs, FD porosity

Vertebrobasilar Dissecting Aneurysms and FDs

In a literature review for cases similar to the present case, we found two described instances. First, in a retrospective study of 88 consecutive patients treated with 101 PED® FDs, there was a single case of a dissecting basilar fusiform aneurysm that was initially treated with two PED®s 3 × 18 mm in size. After aneurysm shrinkage on 8-month follow-up angiogram, there was regrowth and reperfusion on 11-month angiogram. The authors believed that this was due to continued perfusion from right vertebral artery causing turbulent flow around the outer surface of PED®s and occluded the right V4 segment by coiling. No further follow-up of this patient was described in this paper [1]. Second, another case of a ruptured vertebrobasilar dissecting fusiform aneurysm, treated with coiling and a single FD with subsequent regrowth that healed only after 3 additional PED® FDs, was deployed [2].

Why Telescopic Multiple FDs?

A number of in vitro studies have suggested that stent porosity is the most important factor in reducing intra-aneurysmal flow, the optimal porosity being 60–76 % [3]. With telescopic multiple FD technique, an additional PED® FD increases the mesh density by approximately 5 % and increases the aneurysmal flow reduction from 37 to 55 %.

There are no guidelines to determine the use of telescopic multiple FDs. The reasons commonly ascribed by various authors to use telescopic multiple FDs include telescopic reconstruction of large neck aneurysms, when FD apposition proximally and/or distally was unfavorable, in 360° involvement of parent artery, to ensure adequate neck coverage; to eliminate inflow jet into the aneurysm, unchanged aneurysm blood flow; to decrease aneurysm emptying relative to parent artery, a deceleration of aneurysm contrast circulation without contrast stagnation into venous phase; and to increase the degree of flow diversion [1, 4–6]. Multiple telescopic FDs have also been used intentionally to enhance the flow-diverting effect and eventual healing in the treatment of fusiform and dissecting large and GIAs [7].

Drawbacks in Telescopic Multiple FD Technique

Their use in this manner is contentious, as telescoping causes randomly decreased pore size and increased pore density that increases chances of side-branch and perforator compromise [8]. Additionally, there is longer coverage of perforator-rich regions, increased mesh density that impairs perforator ostial patency, and delayed endothelialization due to increased circumferential metal luminal coverage [9]. Furthermore, telescopic FDs could theoretically unnecessarily compromise the luminal diameter and also increase the risk of thromboembolic events due to increased volume of foreign material within the parent artery [10]. Although animal studies have shown usage of up to 3 PED® FDs maintaining patency of perforating arteries, clinical reports of inadvertent occlusion are documented on using telescopic FDs [11–14]. In a retrospective study of 23 patients with intracranial dissecting aneurysms treated with single or multiple PED® FDs, none of the treated patients had recanalization or re-rupture over a mean of 6-month follow-up (1–18 months) [7].

Thus as seen in the present case, in an occasional dissecting aneurysm, coiling with stenting including a dual-layered FD may be insufficient to prevent aneurysmal regrowth.

References

1. Fischer S, Vajda Z, Aguilar Perez M, Schmid E, Hopf N, Bazner H, Henkes H (2012) Pipeline embolization device (PED) for neurovascular reconstruction: initial experience in the treatment of 101 intracranial aneurysms and dissections. Neuroradiology 54(4):369–382. doi:10.1007/s00234-011-0948-x
2. Kerolus M, Kasliwal MK, Lopes DK (2015) Persistent aneurysm growth following pipeline embolization device assisted coiling of a fusiform vertebral artery aneurysm: a word of caution! Neurointervention 10(1):28–33. doi:10.5469/neuroint.2015.10.1.28
3. Alderazi YJ, Shastri D, Kass-Hout T, Prestigiacomo CJ, Gandhi CD (2014) Flow diverters for intracranial aneurysms. Stroke Res Treatment 2014:415653. doi:10.1155/2014/415653
4. Saatci I, Yavuz K, Ozer C, Geyik S, Cekirge HS (2012) Treatment of intracranial aneurysms using the pipeline flow-diverter embolization device: a single-center experience with long-term follow-up results. AJNR Am J Neuroradiol 33(8):1436–1446. doi:10.3174/ajnr.A3246
5. Phillips TJ, Wenderoth JD, Phatouros CC, Rice H, Singh TP, Devilliers L, Wycoco V, Meckel S, McAuliffe W (2012) Safety of the pipeline embolization device in treatment of posterior circulation aneurysms. AJNR Am J Neuroradiol 33(7):1225–1231. doi:10.3174/ajnr.A3166
6. Kan P, Siddiqui AH, Veznedaroglu E, Liebman KM, Binning MJ, Dumont TM, Ogilvy CS, Gaughen JR, Jr., Mocco J, Velat GJ, Ringer AJ, Welch BG, Horowitz MB, Snyder KV, Hopkins LN, Levy EI (2012) Early postmarket results after treatment of intracranial aneurysms with the pipeline embolization device: a U.S. multicenter experience. Neurosurgery 71(6):1080–1087. doi:10.1227/NEU.0b013e31827060d9; discussion 1087–1088
7. de Barros Faria M, Castro RN, Lundquist J, Scrivano E, Ceratto R, Ferrario A, Lylyk P (2011) The role of the pipeline embolization device for the treatment of dissecting intracranial aneurysms. AJNR Am J Neuroradiology 32(11):2192–2195. doi:10.3174/ajnr.A2671
8. Siddiqui AH, Abla AA, Kan P, Dumont TM, Jahshan S, Britz GW, Hopkins LN, Levy EI (2012) Panacea or problem: flow diverters in the treatment of symptomatic large or giant fusiform vertebrobasilar aneurysms. J Neurosurg 116(6):1258–1266. doi:10.3171/2012.2.jns111942
9. Meckel S, McAuliffe W, Fiorella D, Taschner CA, Phatouros C, Phillips TJ, Vasak P, Schumacher M, Klisch J (2013) Endovascular treatment of complex aneurysms at the vertebrobasilar junction with flow-diverting stents: initial experience. Neurosurgery 73(3):386–394. doi:10.1227/01.neu.0000431472.71913.07
10. Lylyk P, Miranda C, Ceratto R, Ferrario A, Scrivano E, Luna HR, Berez AL, Tran Q, Nelson PK, Fiorella D (2009) Curative endovascular reconstruction of cerebral aneurysms with the pipeline embolization device: the Buenos Aires experience. Neurosurgery 64(4):632–642. doi:10.1227/01.neu.0000339109.98070.65; discussion 642–633; quiz N636
11. D'Urso PI, Lanzino G, Cloft HJ, Kallmes DF (2011) Flow diversion for intracranial aneurysms: a review. Stroke J Cereb Circulation 42(8):2363–2368. doi:10.1161/strokeaha.111.620328
12. De Vries J, Boogaarts J, Van Norden A, Wakhloo AK (2013) New generation of Flow Diverter (surpass) for unruptured intracranial aneurysms: a prospective single-center study in 37 patients. Stroke J Cereb Circulation 44(6):1567–1577. doi:10.1161/strokeaha.111.000434
13. Dai D, Ding YH, Kadirvel R, Rad AE, Lewis DA, Kallmes DF (2012) Patency of branches after coverage with multiple telescoping flow-diverter devices: an in vivo study in rabbits. AJNR Am J Neuroradiol 33(1):171–174. doi:10.3174/ajnr.A2879
14. Martin AR, Cruz JP, Matouk CC, Spears J, Marotta TR (2012) The pipeline flow-diverting stent for exclusion of ruptured intracranial aneurysms with difficult morphologies. Neurosurgery 70(1 Suppl Operative):21–28. doi:10.1227/NEU.0b013e3182315ee3; discussion 28

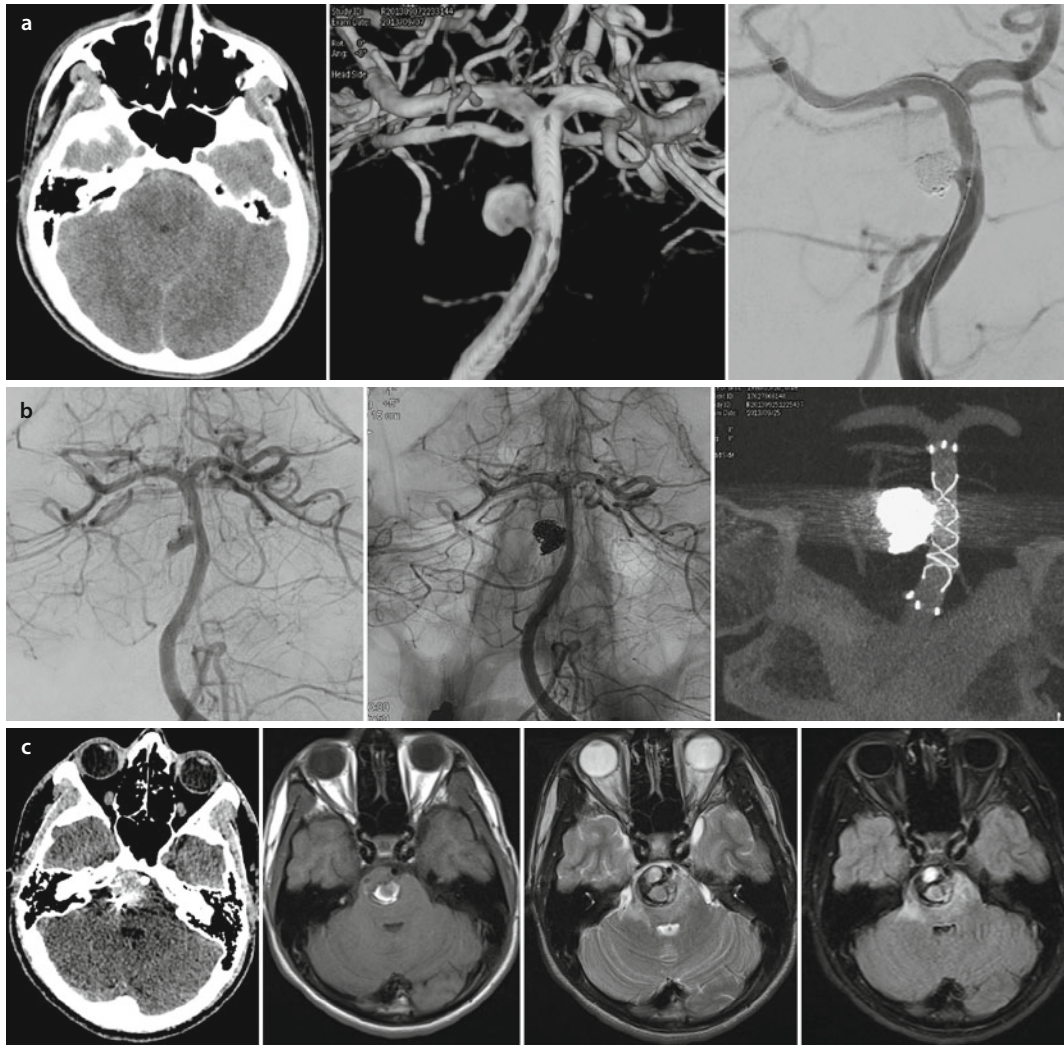

Fig. 7.1 A 17-year-old man presented with severe headache. (**a**) On September 2013, Fisher grade 1 acute SAH on NECT with a GCS 15. Cerebral DSA reveals a mid-basilar aneurysm suggestive of underlying dissection. The patient was treated with balloon-assisted coiling. As there was strong suspicion of an underlying dissection, the patient was planned for interval basilar stenting after 2 weeks. (**b**) The patient underwent a control DSA after 18 days. There was aneurysmal neck recanalization. The patient was re-treated with balloon-assisted coiling followed by FRED® FD deployment. (**c**) After 2 months, the patient presented with features of brain stem compression and edema. NECT and MRI images of the brain stem reveal a well-defined mixed intensity mass lesion compressing the pons. There is adjacent peri-aneurysmal vasogenic edema.

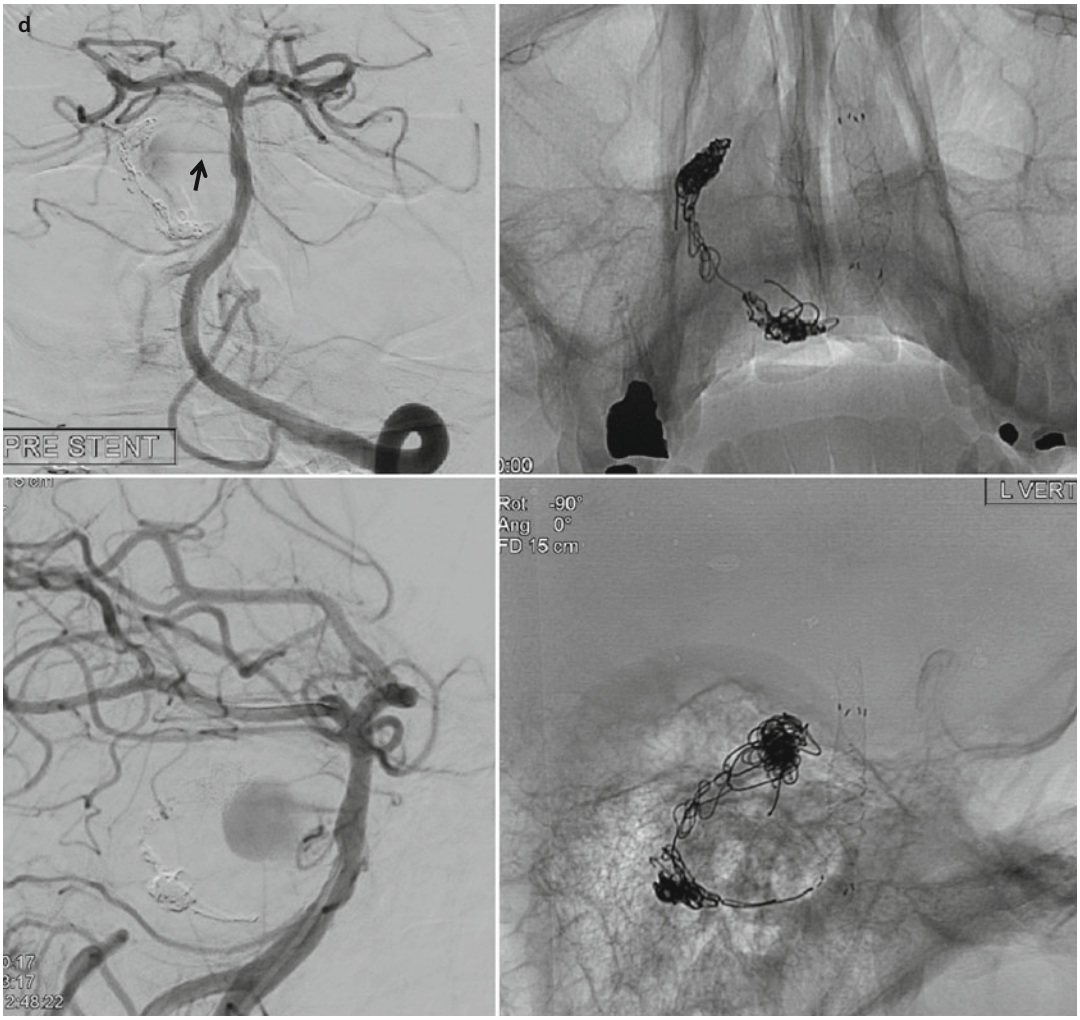

Fig. 7.1 (continued) (**d**) Cerebral DSA reveals dispersion of the coil mass with inflow jet phenomenon (*arrow*) into the now transformed GIA. Note this portion of the basilar artery was previously well covered by FD. There was no proximal endoleak. The patient was re-treated with a single-layer PED® FD that was deployed telescopically within the previous dual-layered FD (FRED®) (*Telescopic multiple flow-diverter technique*). We used a slightly oversized both FRED® and PED® to enhance the radial force of the stent complex.

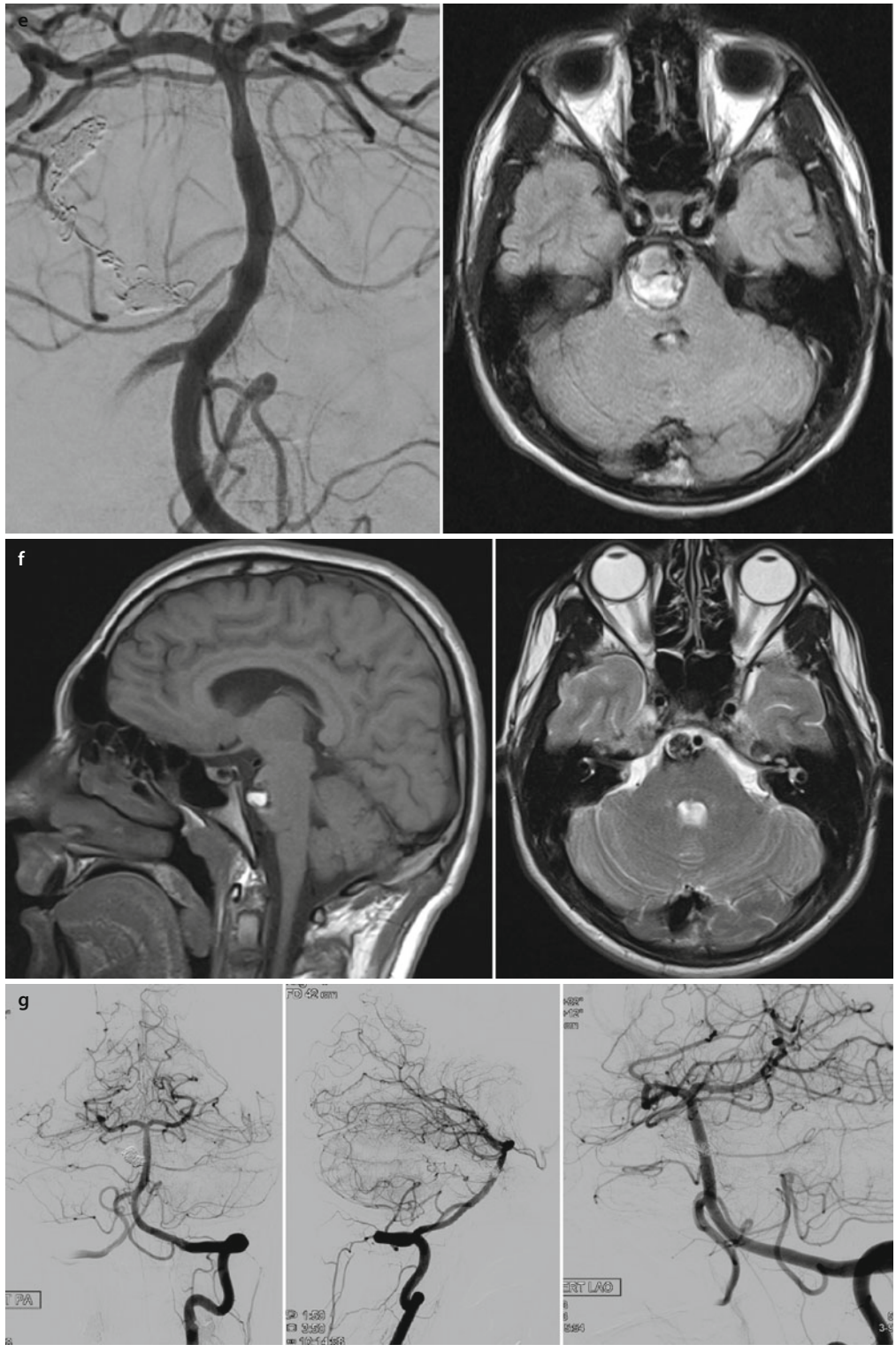

Fig. 7.1 (continued) (**e**) Cerebral DSA and MRI, 3 months post second treatment, reveal resolution of the brain stem vasogenic edema and exclusion of the aneurysm from circulation. (**f**) Follow-up MRI, 7 months post second treatment, reveals shrinkage of the treated basilar GIA and no further indentation on the pons. (**g**) On January 2015, 2-year follow-up DSA, there is stable aneurysmal exclusion from the circulation with a patent basilar lumen. Note the coil mass has reassembled to its initial position

Case 8

N. Kocer, *Giant Intracranial Aneurysms*, DOI 10.1007/978-3-319-41788-2_8

Troubleshooting FDs

Keywords: Flow diverter, Compressibility, Premature detachment

Troubleshooting Inadvertently Deployed FDs

(a) In cases with unopened twisted FD, it is better to retrieve the FD.
(b) In a similar position, it would be better to Snare® (Amplatz GooseNeck; Covidien Vascular Therapies, Mansfield, Massachusetts)/Lasso® (Lasso retriever; Balt, Montmorency, France) the device using the microcatheter as a railroad.

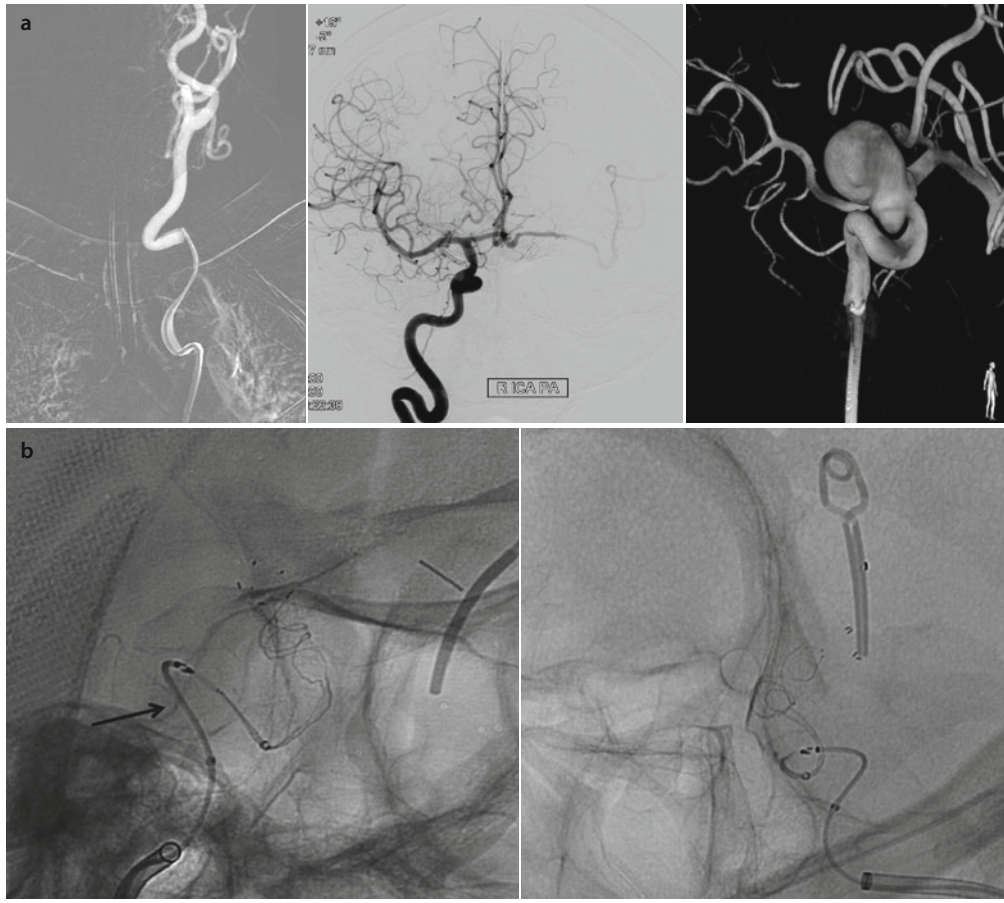

Fig. 8.1 A 64-year-old lady presented with headaches and visual problems. (**a**) Radiological investigations reveal an unruptured left supraclinoid ICA GIA with the fundus pointing medially, superiorly, and posteriorly. There was poor cross circulation to the left hemisphere. Cerebral DSA reveals severe tortuosity of the left CCA and ICA. Technical challenges: (1) Peri-aneurysmal proximal and distal size discrepancy of ICA. (2) Proximal and distal supraclinoid ICA has acute angulation around the aneurysmal neck. (3) Wide aneurysmal neck. Another aneurysm on the right has already been clipped. (**b**) The GIA neck was crossed with a Headway 27® (MicroVention, Tustin, California). A 4.5 × 26 × 20 mm-sized FRED® FD was used. However, due to extreme tortuosity and vessel size discrepancy, FRED® FD twisted around its axis and did not open at the anterior bend of ICA (Debrun cavernous C1 segment). During further attempts to open this portion of the FD, the proximal unopened portion of FRED® inadvertently detached within the microcatheter (*arrow*).

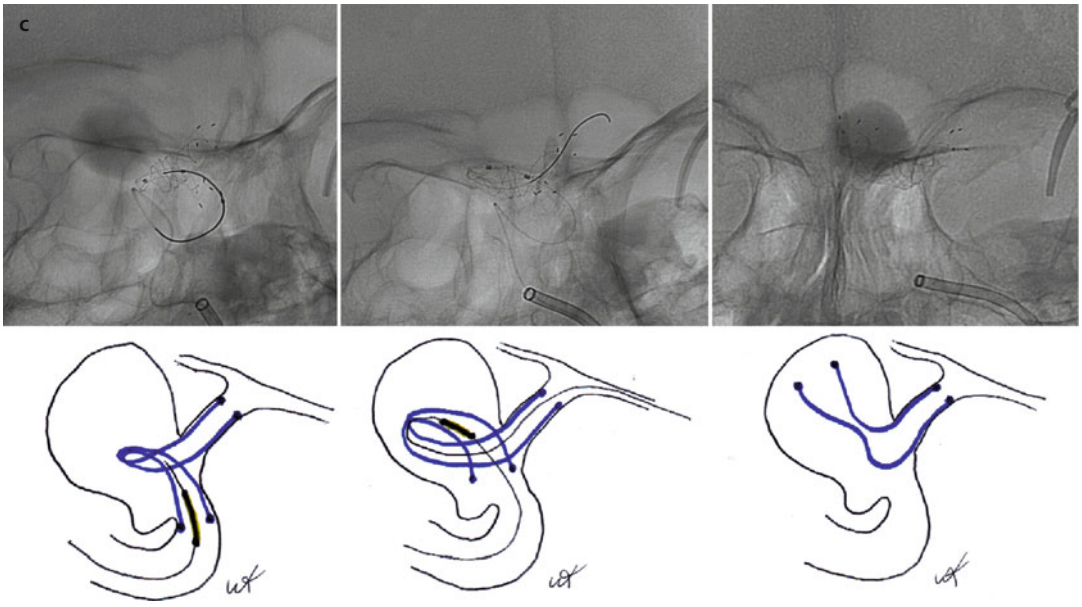

Fig. 8.1 (continued) (**c**) At this point of time, it was believed an in-stent balloon angioplasty could open the proximal FRED®. Although the microwire and balloon could be re-navigated through the deployed FRED®, a balloon angioplasty could not open the kink at the anterior ICA bend. At the same time, it was observed that the entire complex had a tendency to move distally. After noticing this, the author decided to take advantage of this phenomenon. He pushed the FRED® FD into the aneurysmal sac using the balloon.

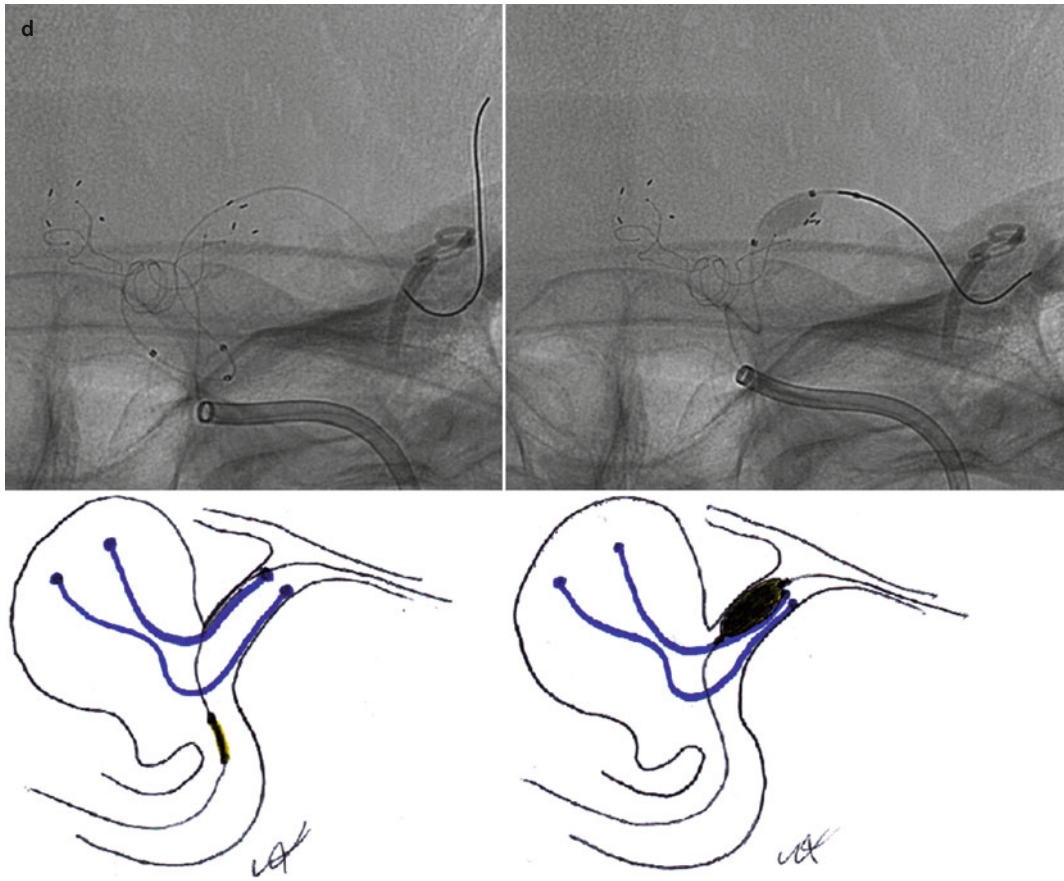

Fig. 8.1 (continued) (**d**) Subsequently, the balloon was manipulated around the deployed FRED® into the MCA. The balloon was used to check the compressibility of the deployed FRED® in distal ICA. On confirming adequate compressibility, the balloon was exchanged with a Headway 27® microcatheter (MicroVention, Tustin, California).

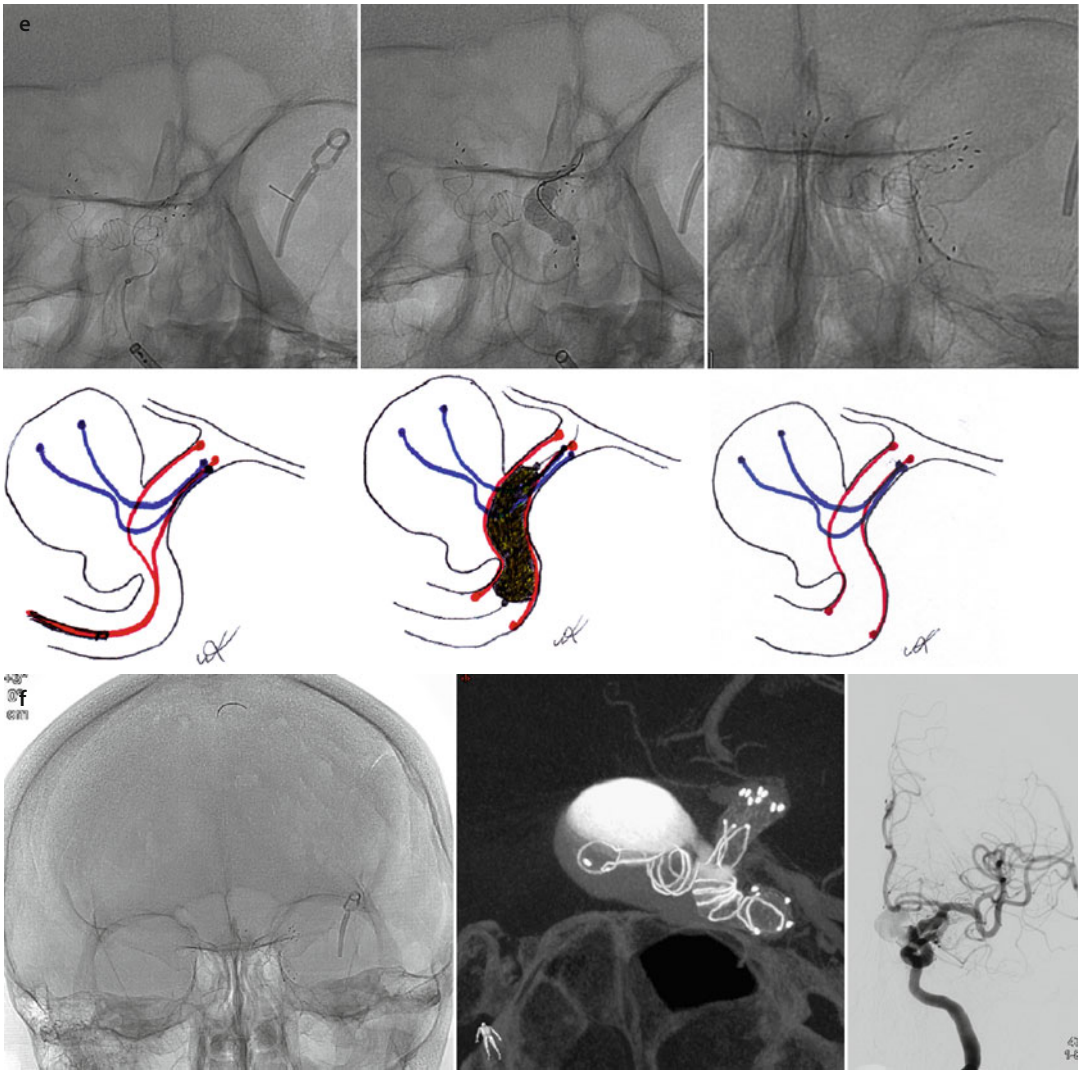

Fig. 8.1 (continued) (**e**) Another 4.5 × 25 × 18 mm-sized FRED® was then deployed adjacent to the previously deployed FRED® and the aneurysmal neck. This was done, as the author was confident about the high radial strength of FRED®. A 4 × 15 mm-sized hyperglide® (ev3, Irvine, CA) balloon was navigated into this second FRED®, and angioplasty was done to ensure stent apposition to the ICA wall. Post-balloon angioplasty, there is near-normal caliber of the stented ICA. (**f**) Immediate postprocedural angiograms and IA VASO CT® demonstrate decreased aneurysmal filling, good stent wall apposition, and the compressed first FRED® that is extending from distal ICA to aneurysm

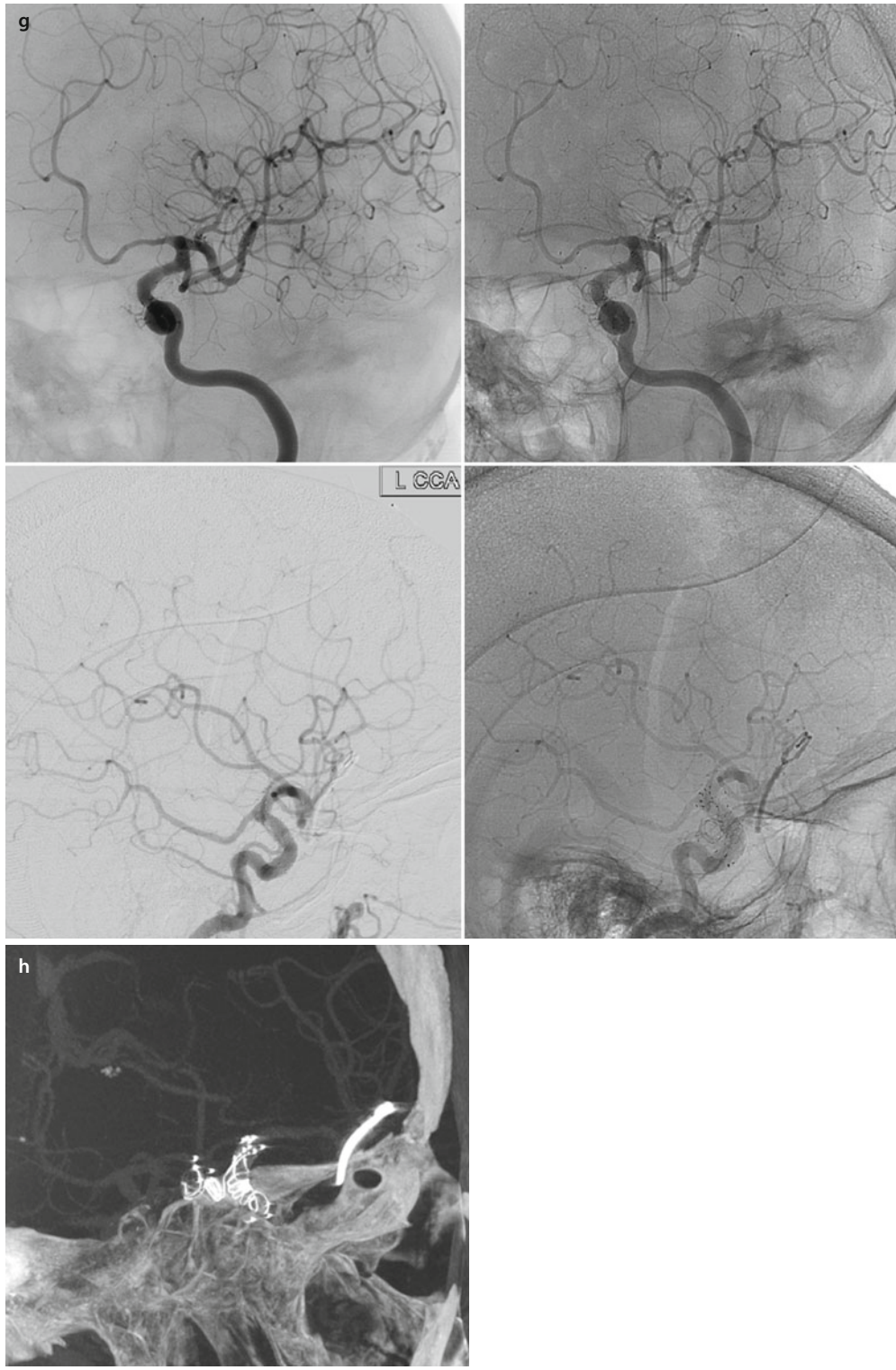

Fig. 8.1 (continued) (**g**, **h**). Follow-up 6-month DSA and 2-year IV VASO CT® reveals complete aneurysmal exclusion and remodeled ICA.

In schematic illustrations, *blue color* indicates the first stent, *red color* indicates the second stent, and *black/yellow color* indicates balloon

Case 9

N. Kocer, *Giant Intracranial Aneurysms*, DOI 10.1007/978-3-319-41788-2_9

Cerebral Edema in Cavernous GIAs

Keywords: Perianeurysmal edema, Vasogenic edema, Cavernous aneurysm

Perianeurysmal Edema in GIAs

A large multicenter study group on GIAs found the prevelance of perianeurysmal edema (PAE) in GIAs to be 33.3 %. The highest proportion of GIAs with PAE was located in MCA (66.7 %) followed by posterior circulation (46.7 %) and the supraclinoid ICA (33.3 %). Furthermore the authors observed that cavernous ICA GIAs did not show any PAE though they exerted mass effect on the adjacent cerebral parenchyma. They believed that the duramater acts as a barrier and prevents PAE in this location. It is believed that the mass effect from GIAs decreases perfusion of surrounding cerebral parenchyma and cause PAE. Furthermore, direct compression of adjacent cerebral veins and their branches are also thought to play an important role in the pathogenesis of PAE. In the study, the volume of GIAs and presence of partial thrombosis were associated with PAE [1]. This phenomenon is not known to occur with microsurgical techniques probably because most neurosurgeons puncture the aneurysmal sac after clipping to shrink the sac, thus limiting the degree of thrombosis and subsequent PAE [2].

PAE Post FD Therapy

GIA thrombosis (therapeutic/spontaneous) can cause vasogenic PAE and breakdown of blood brain barrier that usually presents, 3 to 15 days later with headaches and pseudostroke. On imaging, there is a statistically significant association between MRI inflammatory features and clinical aggravation in patients with PAE. The MRI features include peri-aneurysmal high signal intensity on FLAIR images, increased ADC values and circumferential post contrast enhancement. There was no significant increase in aneurysmal size in patients with PAE after FD placement. Approximately 41 % of neurological worsening in patients treated with FDs is due to PAE. It is more commonly seen in aneurysms that are larger (Mean Diameter: 22 mm versus 13.1 mm), aneurysms in close proximity to brain parenchyma and aneurysms with an occlusion of atleast 50 % of their volume [2].

Pathogenesis of PAE

It is believed that aneurysmal thrombosis causes endothelial damage and release of "stress signals" that activate inflammasome with production of IL -1β in surrounding tissues. PAE is commonly treated using steroids for atleast 2 weeks. Symptomatic resolution usually occurs within 30 days of onset. PAE may have a spectrum of severity with mild reaction in endosaccular coiling to severe reaction after FD placement [2]. The final phase could be an inflammation mediated aneurysmal rupture in patients with no obvious aneurysmal recanalization [3].

References

1. Dengler J, Maldaner N, Bijlenga P, Burkhardt JK, Graewe A, Guhl S, Hong B, Hohaus C, Kursumovic A, Mielke D, Schebesch KM, Wostrack M, Rufenacht D, Vajkoczy P, Schmidt NO (2015) Perianeurysmal edema in giant intracranial aneurysms in relation to aneurysm location, size, and partial thrombosis. Journal of neurosurgery 123 (2):446-452. doi:10.3171/2014.10.jns141560
2. Berge J, Tourdias T, Moreau JF, Barreau X, Dousset V (2011) Perianeurysmal brain inflammation after flow-diversion treatment. AJNR American journal of neuroradiology 32 (10):1930-1934. doi:10.3174/ajnr.A2710
3. Kulcsar Z, Houdart E, Bonafe A, Parker G, Millar J, Goddard AJ, Renowden S, Gal G, Turowski B, Mitchell K, Gray F, Rodriguez M, van den Berg R, Gruber A, Desal H, Wanke I, Rufenacht DA (2011) Intra-aneurysmal thrombosis as a possible cause of delayed aneurysm rupture after flow-diversion treatment. AJNR American journal of neuroradiology 32 (1):20-25. doi:10.3174/ajnr.A2370

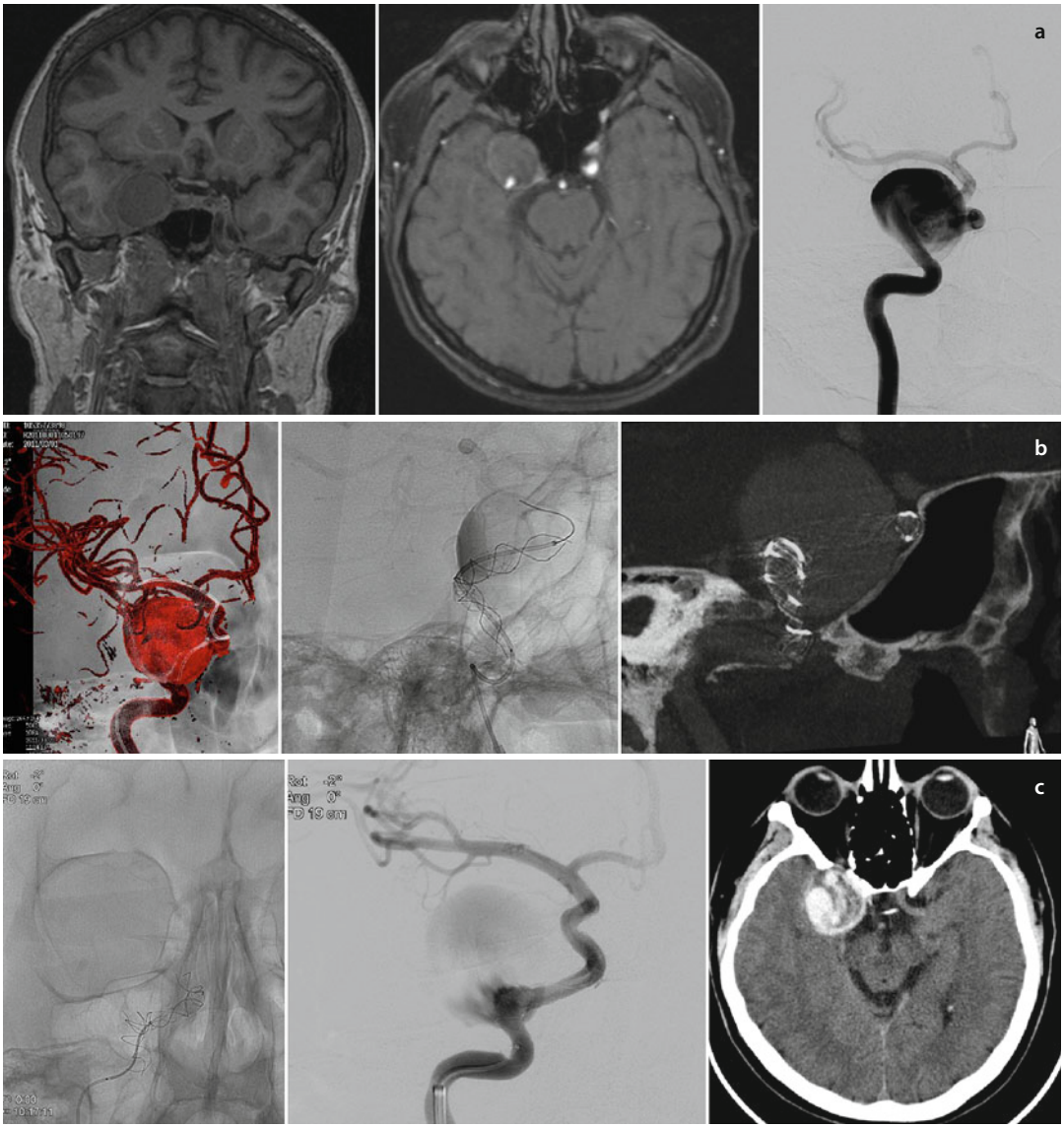

Fig. 9.1 A 30-year-old man presented with retroorbital pain and ophthalmoplegia in 2011. (**a**) Coronal T1 MRI and axial TOF source images reveal a cavernous ICA aneurysm with indirect temporal lobe compression. There is no aneurysmal thrombosis or cerebral edema. Cerebral DSA reveals a giant sacculo-fusiform unruptured petro-cavernous aneurysm with a very wide neck demonstrating inflow zone at petro-cavernous junction. (**b**) On March 2011, using 3D road map imaging, a microcatheter was negotiated across the aneurysmal neck to the right MCA, and telescopic LEO® and SILK® flow diverters were deployed. On the second month follow-up, IV VASO CT® shows no aneurysmal sac thrombosis with partial coverage of inflow zone with an inner flow diverter. (**c**) After second telescopic SILK® deployment with further coverage of inflow zone, there was immediate intra-aneurysmal stasis (eclipse sign). NECT at 1 month after second treatment shows substantial aneurysmal thrombosis.

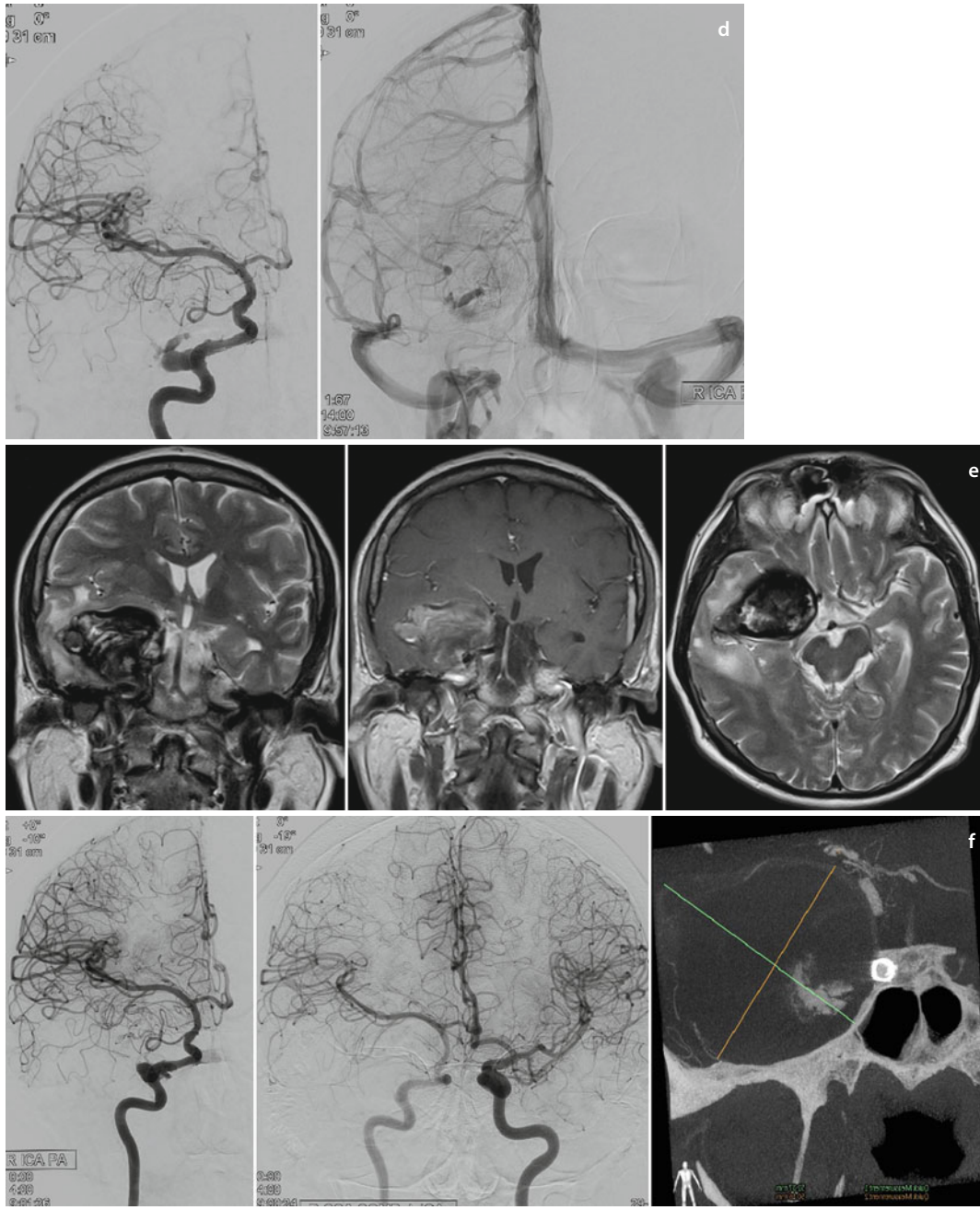

Fig. 9.1 (continued) (**d**) The patient has progressive improvement in his ophthalmoplegia. Control angiogram at 1 year reveals persistent residual filling in the vicinity of aneurysmal neck. (**e**) The patient presented after 2 ½ years of second treatment with headaches. T2W and postcontrast MRI images reveal onion skin appearance of thrombosed aneurysm with substantial increase in the aneurysmal size, peri-aneurysmal vasogenic edema, and mass effect on temporal lobe. (**f**) Cerebral DSA and IA VASO CT® at 2½ years of second treatment show persistent mild filling around aneurysmal neck and increased aneurysmal size measuring 52 × 50 mm. There was good cross flow across the anterior communicating artery from left cerebral circulation with no significant delay.

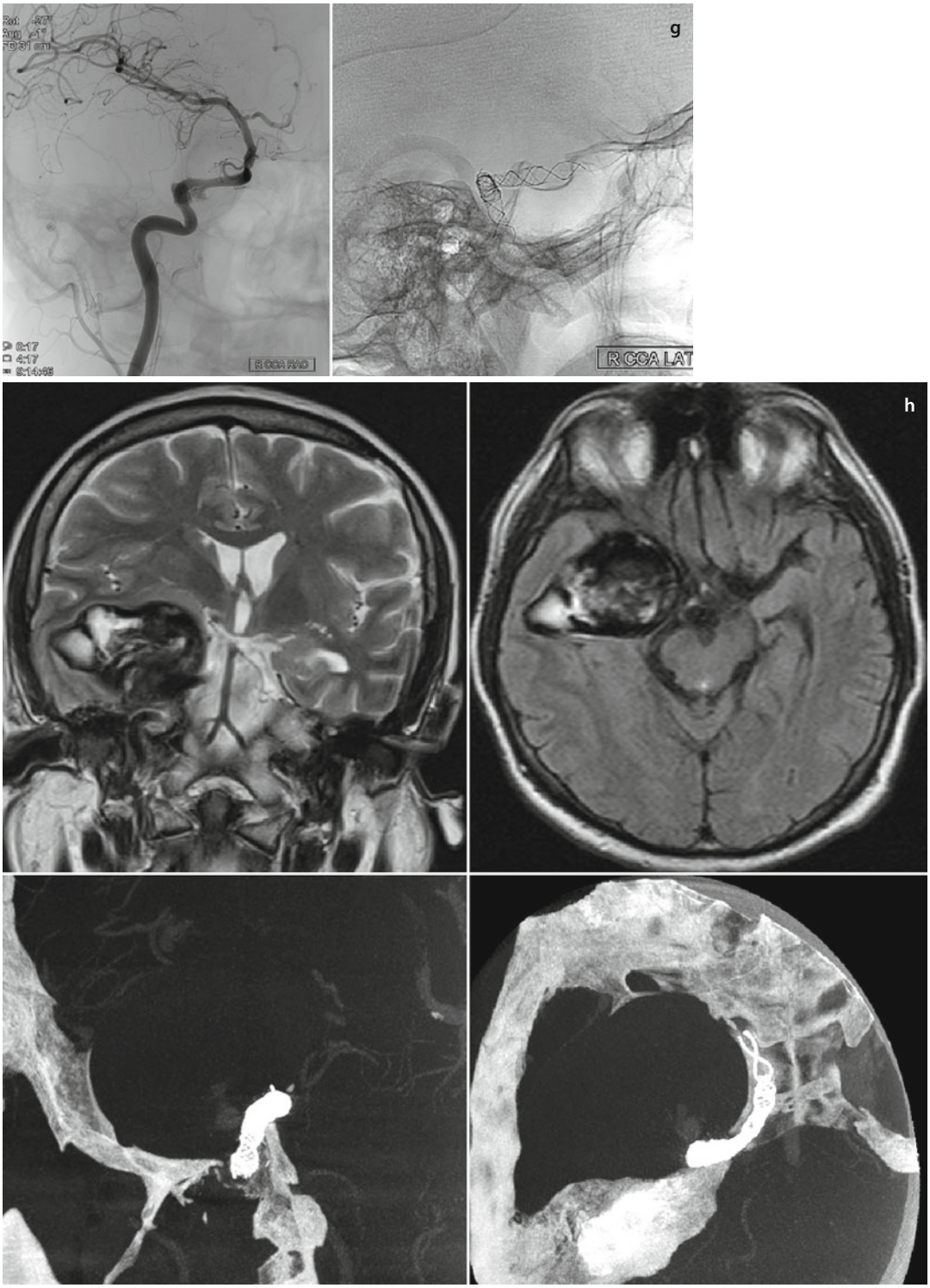

Fig. 9.1 (continued) (**g**) On May 2015, a third treatment session was planned. It was decided to preserve the ICA. A PED® FD was deployed across the previously deployed stents and flow diverter *as part of a telescopic multiple flow-diverter technique*. The patient received corticosteroids in the immediate postprocedural period to control peri-aneurysmal edema. (**h**) MRI and VASO CT® obtained 2 weeks and 3 months, respectively, after the third treatment, reveal progressive decrease in the aneurysmal size, mass effect, and no residual vasogenic edema despite mild aneurysmal neck filling as seen on VASO CT. The patient was asymptomatic at 3-month follow-up following the third treatment.

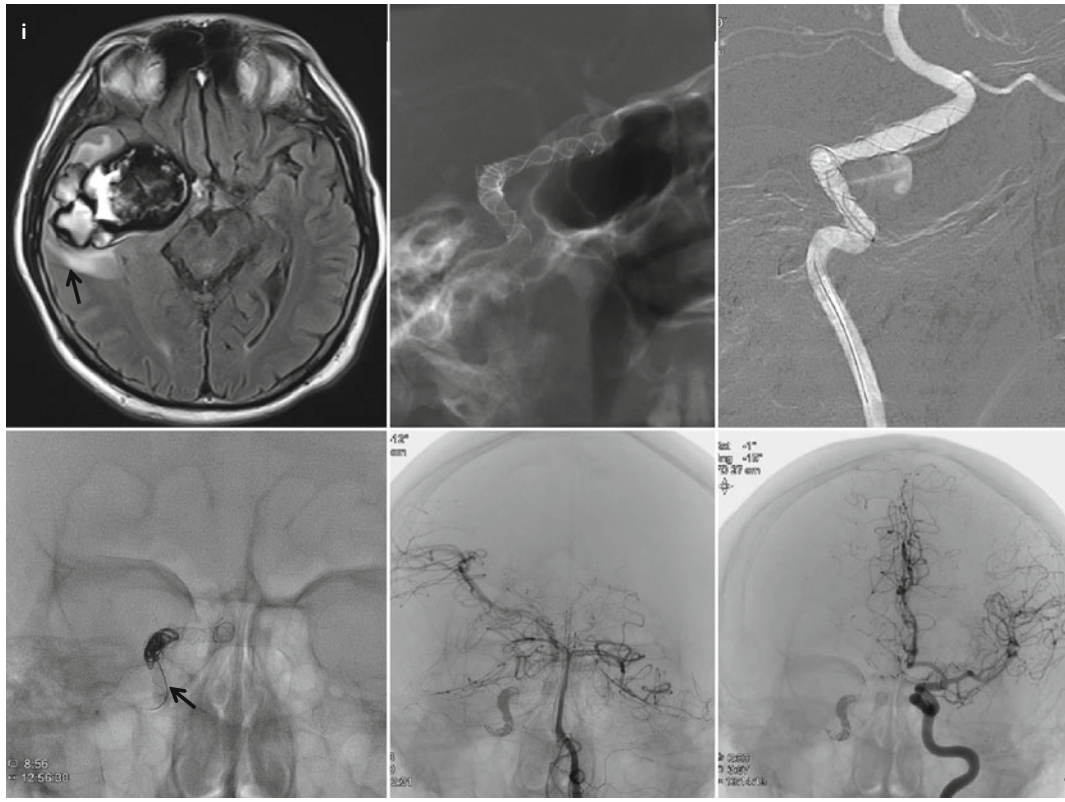

Fig. 9.1 (continued) (**i**) Twelve months after the third treatment, the patient presented with severe headaches. MRI reveals increased size of the thrombosed aneurysm with recurrent vasogenic edema (*arrow*) in the temporal lobe. VASO CT® and corresponding DSA shows persistent inflow jet phenomenon into the anterio-medial portion of the thrombosed aneurysm. The patient was treated by parent vessel occlusion of the ICA cavernous segment. This was accomplished using a dual-lumen balloon catheter (Scepter C®) (*arrow*) and subsequent coiling through its lumen. Postprocedural vertebral and internal carotid angiograms reveal adequate opacification and perfusion of the right cerebral hemisphere across the anterior and posterior communicating arteries. The patient had gradual relief of his headaches with complete relief after 1 week

Case 10

N. Kocer, *Giant Intracranial Aneurysms*, DOI 10.1007/978-3-319-41788-2_10

Late Rupture After FD Therapy

Keywords: Giant aneurysm, Flow diverter, Late rupture

Late Aneurysmal Rupture

In a review of patients with late aneurysmal rupture post-FD treatment, concomitant aneurysmal loose coiling is not protective in all cases. The majority of ruptures (80 %) occurred within 30 days of treatment [1]. A multicenter, worldwide, retrospective survey (the ESMINT Retrospective Analysis of Delayed Aneurysm Ruptures (RADAR) after Flow Diversion) on late rupture after FD treatment reported late ruptures in 2.1 % (14 patients) of treated large and giant aneurysms. All except one aneurysm were larger than 19 mm (Average size = 24 mm) [2].

The exact mechanism of late rupture is unknown. A few computational flow studies have shown an increase in intra-aneurysmal pressure post-FD deployment due to flow modification that may predispose to rupture. Studies have proposed that the intraluminal aneurysmal thrombus has proteases with high proteolytic activity that could degrade the aneurysmal wall [1]. The ruptured aneurysms showed organizing intraluminal thrombus with mural necrosis, loss of fibrous tissue, and smooth muscle cells with macrophage infiltration up to adventitia at the site of rupture [3].

Late rupture was associated with large or giant size (mean diameter 22 ± 6 mm), symptomatic aneurysms, dome height to neck ratio >1.6, and morphological inertia-driven aneurysmal blood flow.

Late Aneurysmal Rupture: Our Experience

Our own retrospective study analyzing late aneurysmal rupture post FD revealed five patients with delayed rupture (6.6 %). In this study, unlike other studies, we analyzed a study group of very large and giant (>20 mm) intracranial aneurysms. The mean aneurysmal diameter of ruptured aneurysms was 32.2 mm vs. a mean of 15.1 mm for the entire group. One of the ruptured aneurysms was treated with concomitant loose coil packing as well [4].

At present to prevent late (intradural) GIA rupture after FD treatment, our policy is to first occlude the aneurysm with coils except when the aneurysms are located in perforator rich arterial segments (tight packing) followed by FD deployment in the same session.

References

1. Rouchaud A, Brinjikji W, Lanzino G, Cloft HJ, Kadirvel R, Kallmes DF (2015) Delayed hemorrhagic complications after flow diversion for intracranial aneurysms: a literature overview. Neuroradiology. doi:10.1007/s00234-015-1615-4
2. Kulcsár Z, Szikora I (2012) The ESMINT retrospective analysis of delayed aneurysm ruptures after flow diversion (RADAR) study. EJMINT 2012:1244000088
3. Kulcsar Z, Houdart E, Bonafe A, Parker G, Millar J, Goddard AJ, Renowden S, Gal G, Turowski B, Mitchell K, Gray F, Rodriguez M, van den Berg R, Gruber A, Desal H, Wanke I, Rufenacht DA (2011) Intra-aneurysmal thrombosis as a possible cause of delayed aneurysm rupture after flow-diversion treatment. AJNR Am J Neuroradiol 32(1):20–25. doi:10.3174/ajnr.A2370
4. Velioglu M, Kizilkilic O, Selcuk H, Kocak B, Tureci E, Islak C, Kocer N (2012) Early and midterm results of complex cerebral aneurysms treated with Silk stent. Neuroradiology 54(12):1355–1365. doi:10.1007/s00234-012-1051-7

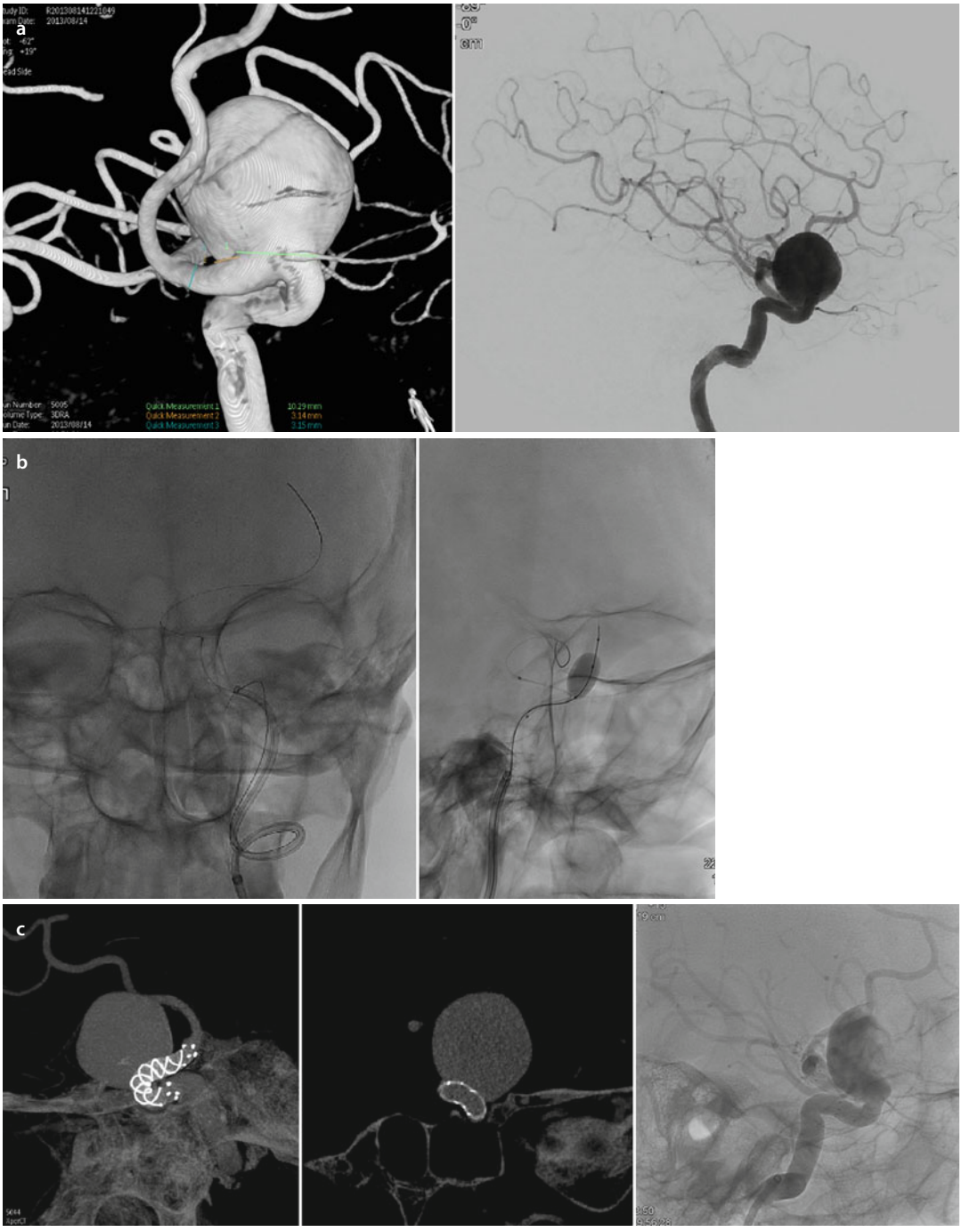

Fig. 10.1 A 63-year-old lady presented with headaches with visual disturbances. (**a**) On August 2013, cerebral DSA reveals a giant, very wide-neck paraophthalmic aneurysm. (**b**) The proximal ICA showed extreme tortuosity. On repeated attempts Headway 27® microcatheter (MicroVention, Tustin, California) could not be navigated across the aneurysmal neck. A balloon-tipped microcatheter was used, with the balloon inflated at the aneurysmal neck. The inflated balloon facilitated distal catheterization with microcatheter by narrowing the neck. (**c**) The patient was treated with a 4.5 × 25 × 18 mm-sized FRED® FD across the aneurysmal neck. IA VASO CT® with thin sections shows the FRED® FD at the aneurysmal segment with good wall apposition. Immediate postprocedural cerebral DSA reveals intra-aneurysmal contrast stagnation.

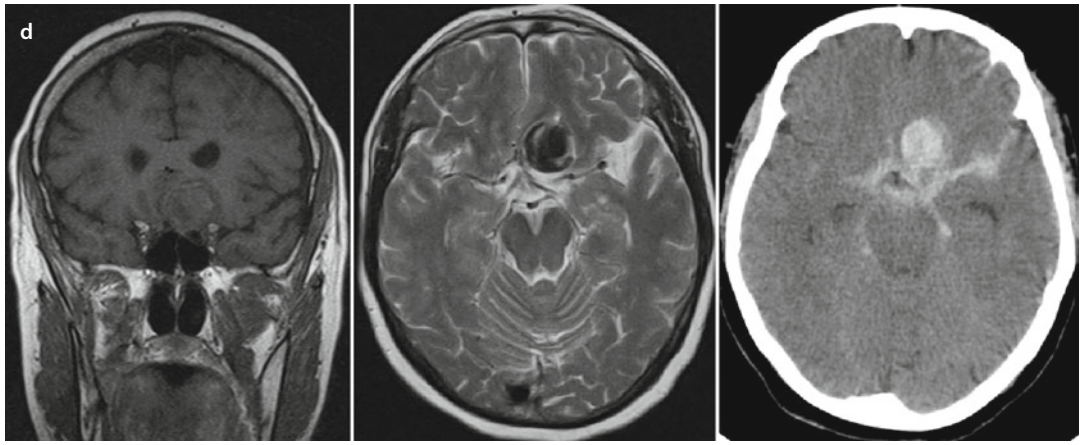

Fig. 10.1 (continued) (**d**) The patient presented 8 days later with severe headaches. The patient was already receiving steroids. Axial T2 W and coronal T1 W images show partial thrombosis within the aneurysm without visible subarachnoid hemorrhage or parenchymal abnormality. The patient was planned for a second FD treatment, but she had an acute seizure attack. The NECT showed acute aneurysmal rupture with SAH. The patient succumbed to it within 6 h of admission

Case 11

Electronic supplementary material The online version of this chapter (doi:10.1007/978-3-319-41788-2_11) contains supplementary material, which is available to authorized users.

N. Kocer, *Giant Intracranial Aneurysms*, DOI 10.1007/978-3-319-41788-2_11

Theories of Late Rupture and Flow Studies

Keywords: Flow diverter, Late rupture, Inflammatory theory, Hemodynamic theory

Introduction
A meta-analysis of 1654 aneurysms treated with FDs reported SAH from late aneurysm rupture in nearly 4 % all treated patients. This was significantly higher in large and giant aneurysms [1]. One of the earliest reported instances of late rupture after a successful FD deployment was in 2009. A 69-year-old lady with an incidentally detected large paraophthalmic aneurysm was treated with SILK® FD. After 20 days the patient had a rupture with extensive SAH and became comatose [2]. Since then various theories have been put forth and flow studies were done to explain this disastrous phenomenon. The two theories to the forefront are the "hemodynamic theory" and the "inflammatory theory" [3].

Hemodynamic Theory [4]
The hemodynamic theory has been substantiated by computational studies for late aneurysm rupture.
The computational fluid studies (CFDs) reveal two important contributors to post-FD aneurysm rupture, namely:

1. In some of the ruptured aneurysms, there was a proximal focal segmental moderate stenosis. This stenosis was opened by angioplasty or stenting. This was done to properly appose the FDs against the parent arterial wall. This decreases the proximal resistance and increases the flow in the aneurysmal segment and causes increased intra-aneurysmal pressure.
2. In aneurysms that accept most of the flow from their parent artery (usually associated with severe tortuosity), there is a rise in local resistance after FD deployment (particularly in large and GIAs). The rise in local resistance proximally coupled to a decrease in blood flow distally activates the cerebrovascular autoregulation. The autoregulation in-turn decreases the distal vascular resistance. This prompts the systemic blood pressure to increase to maintain cerebral blood flow. As the flow rate increases in the parent artery, it also increases in the still patent aneurysm. However, as the flow rate increases, the effect on intra-aneurysmal pressure is also correspondingly increased. Thus relatively small elevations in systemic blood pressure cause substantial increase in intra-aneurysmal pressure. For example, if the flow increased to pretreatment levels, the increase in intra-aneurysmal pressure can be as high as 25 mmHg. Therefore, in the intervening period between FD placement and the appearance of organized aneurysmal thrombus to reenforce the weak aneurysmal wall, there is increased aneurysmal wall tension with a tendency to rupture [4].

Additionally we believe that placement of an FD decreases the pulsatility of the aneurysmal segment making it more rigid and thereby decreasing its ability to withstand pretreatment stress and strain with resultant wall rupture.

Inflammatory Theory [5]
Following FD therapy, there is a hemodynamic change that leads to significant or complete aneurysmal thrombus formation. However, the reduced but persistent intra-aneurysmal flow causes continuous thrombus renewal. This favors aggressive autolytic thrombus formation. Gross examination of ruptured aneurysms reveals massive organizing intraluminal thrombus with mural thinning at site of rupture. It has been suggested that a large amount of rapidly developing red thrombus with its autolytic enzymes may overwhelm the aneurysmal defense mechanism that prevents aneurysmal rupture. On histopathological examination, there was thrombus without significant organization or cellular colonization in the ruptured aneurysms. Thus the balance of pro- and anti-autolytic enzymatic activity determines either rupture or reverse remodeling and cicatrization of the aneurysm, respectively [5].

References

1. Brinjikji W, Murad MH, Lanzino G, Cloft HJ, Kallmes DF (2013) Endovascular treatment of intracranial aneurysms with flow diverters: a meta-analysis. Stroke J Cereb Circulation 44(2):442–447. doi:10.1161/strokeaha.112.678151
2. Turowski B, Macht S, Kulcsar Z, Hanggi D, Stummer W (2011) Early fatal hemorrhage after endovascular cerebral aneurysm treatment with a flow diverter (SILK-Stent): do we need to rethink our concepts? Neuroradiology 53(1):37–41. doi:10.1007/s00234-010-0676-7
3. Tse MM, Yan B, Dowling RJ, Mitchell PJ (2013) Current status of pipeline embolization device in the treatment of intracranial aneurysms: a review. World Neurosurg 80(6):829–835. doi:10.1016/j.wneu.2012.09.023

4. Cebral JR, Mut F, Raschi M, Scrivano E, Ceratto R, Lylyk P, Putman CM (2011) Aneurysm rupture following treatment with flow-diverting stents: computational hemodynamics analysis of treatment. AJNR Am J Neuroradiol 32(1):27–33. doi:10.3174/ajnr.A2398
5. Kulcsar Z, Houdart E, Bonafe A, Parker G, Millar J, Goddard AJ, Renowden S, Gal G, Turowski B, Mitchell K, Gray F, Rodriguez M, van den Berg R, Gruber A, Desal H, Wanke I, Rufenacht DA (2011) Intra-aneurysmal thrombosis as a possible cause of delayed aneurysm rupture after flow-diversion treatment. AJNR Am J Neuroradiol 32(1):20–25. doi:10.3174/ajnr.A2370

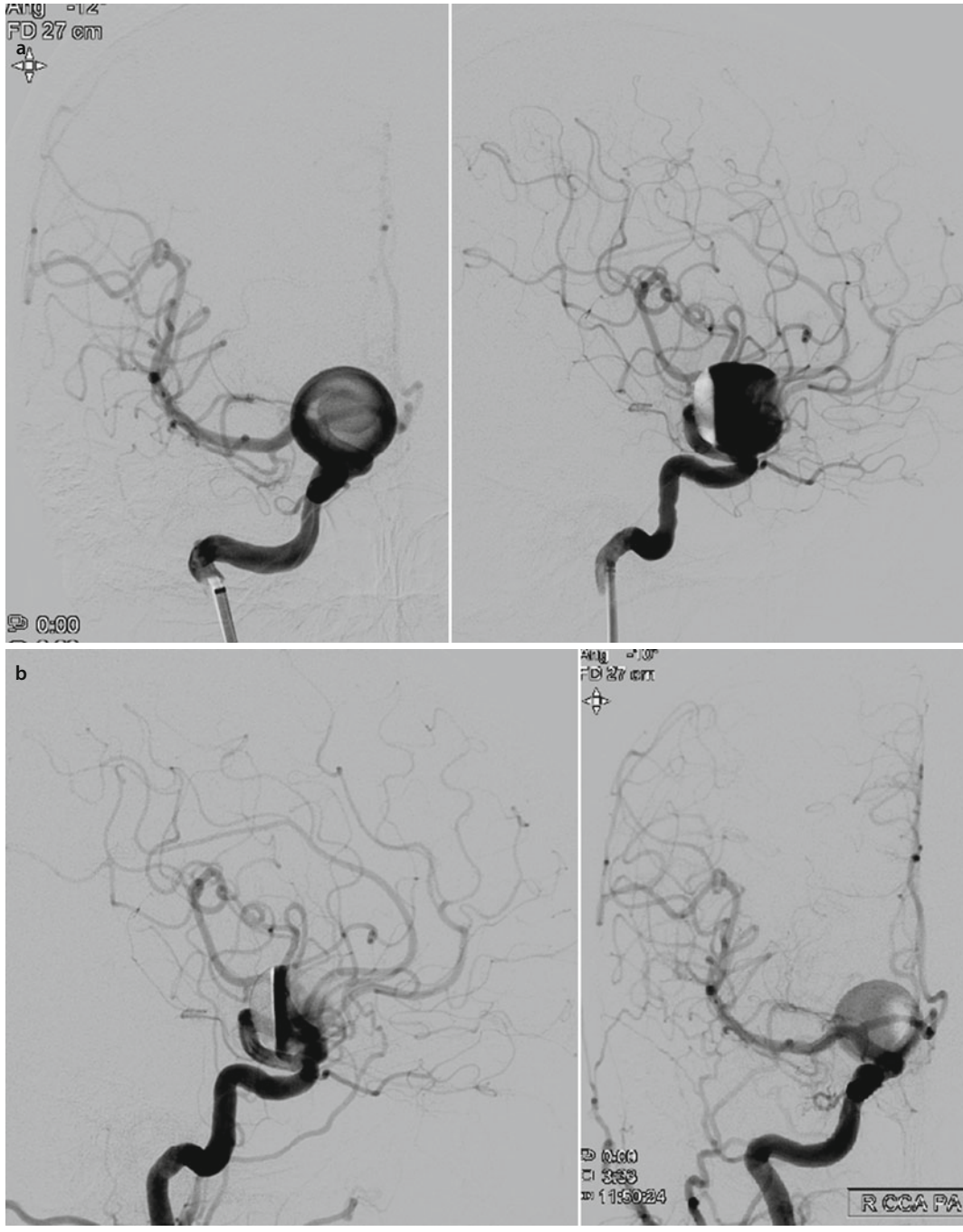

Fig. 11.1 A 47-year-old lady presented with headaches and visual disturbances. On cross-sectional imaging the patient was detected with a left paraophthalmic GIA. (**a**) Cerebral DSA reveals a giant, relatively narrow neck (6 mm) paraophthalmic aneurysm. (**b**) On April 2011, a SILK® FD was deployed across the aneurysm. Immediate postprocedural angiogram reveals intra-aneurysmal stasis with "eclipse" sign

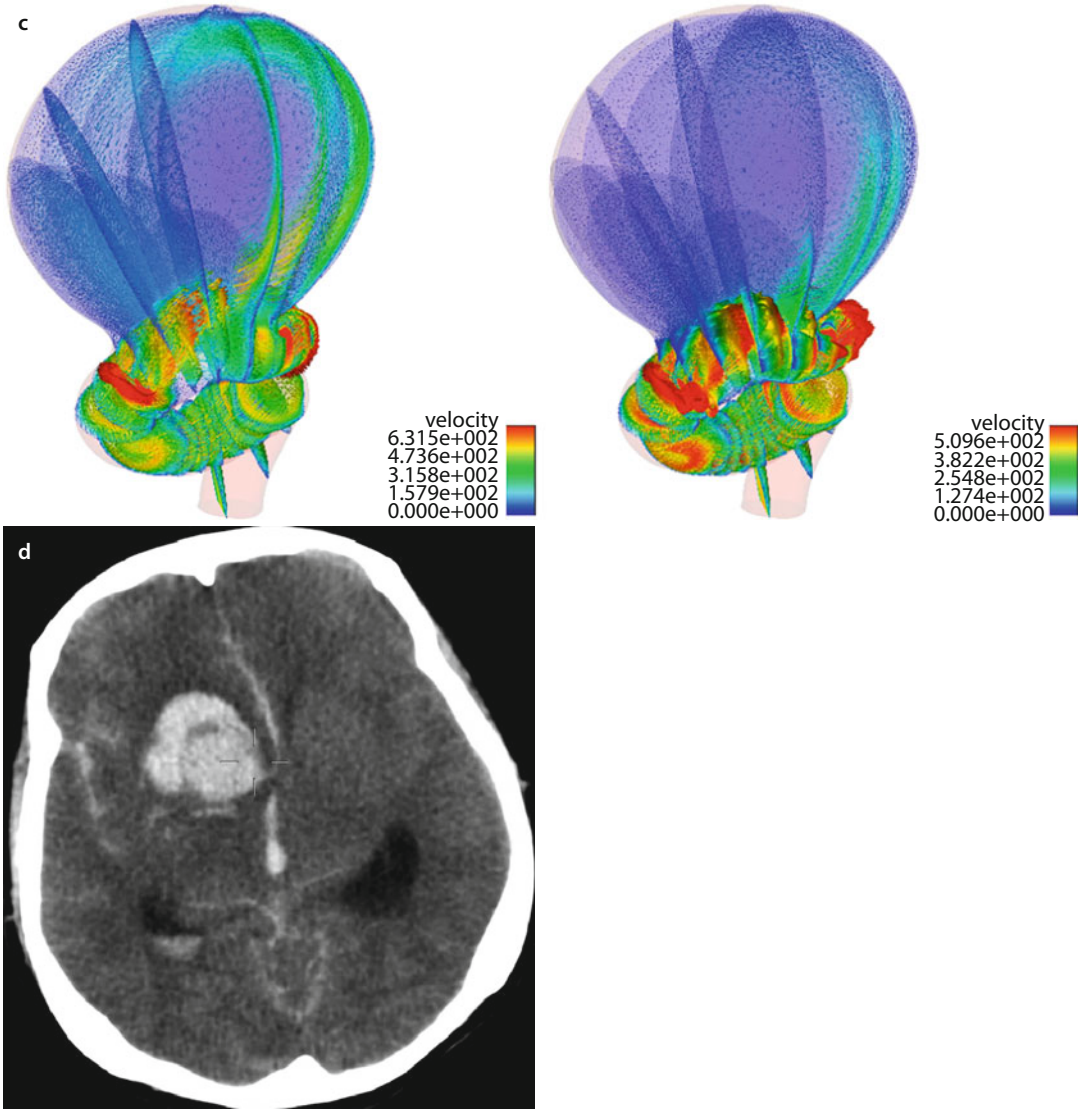

Fig.11. 1 (continued) (**c**) Computational flow studies pre- and post-FD deployment show decreased aneurysmal filling and altered pulsatility. (**d**) The patient presented 5 days later with increasing headaches and sudden onset seizures. NECT reveals a ruptured aneurysm with intraparenchymal hemorrhage with intraventricular extension and SAH

Case 12

N. Kocer, *Giant Intracranial Aneurysms*, DOI 10.1007/978-3-319-41788-2_12

Evolution in Serpentine Aneurysms (Cases 12 and 13)

Keywords: Giant aneurysm, Fusiform aneurysm, Serpentine aneurysm

Dynamic GSeAs: Start of Evolution

Giant serpentine aneurysms (GSeAs) are dynamic entities. Segal and Mc Laurin in 1977 first used the term "serpentine GIAs" [1]. Serpentine aneurysms are known to arise either from saccular aneurysms by continued expansion or from fusiform aneurysms [2]. There are multiple reports of saccular aneurysms that were related to a serpentine configuration [3]. It has been suggested that partially thrombosed dolichoectatic aneurysm could also evolve into serpentine aneurysm [4]. One of the earliest angiographic demonstrations of this evolution was in 1978, when Fodstad et al. showed the transformation of a left sacculo-fusiform cavernous aneurysm into a GSeA over a period of 2 months following proximal carotid ligation. The GSeA was excised. On histopathology, there was partial thrombosis of the aneurysm with thrombus organization in its periphery. The thrombus contained a large blood channel lined by granulation tissue and some endothelial cells. The wall was a thick fibrous tissue with fragmented elastic fibers, edema, and hemorrhage [5]. In 1979 another case report described the evolution of a small MCA fusiform aneurysm (posterior temporal branch) to a GSeA over a period of 5 years [2].

Coanda Effect in GSeAs

The development of GSeAs is attributed to the "Coanda effect" or "boundary wall effect." According to this principle, first described by Robinson and Roberts, the jet stream direction due to a stenosis is deflected toward one blood vessel wall and is stabilized by countercurrent changes in the relatively lower pressure zones along the wall immediately distal to the stenosis [2, 5]. Due to this effect, there is considerable decrease in blood flow through both the central and adjacent peripheral walls of the aneurysm distal to the stenosis leading to stagnation and thrombosis.

Dynamic GSeAs: Continuing Evolution

As the thrombus accumulates, there is continuous evolution in GSeAs. There are cases with rapid neurological decline and death due to ischemic infarcts in the territories supplied by GSEAs or even intracranial hemorrhage (in approximately 28 %) of patients [1, 2]. However, there is a documented case of a left MCA GSeA that spontaneously thrombosed and occluded in an interval of 13 days with stable occlusion over the next 3 years [6].Even complete thrombosis of GSEAs should not be considered as the final stage of this evolution. There is a described case of a young woman with an occluded and thrombosed PCA GSeA that was confirmed on DSA, MRI, and CT imaging. However, 3 weeks later, the patient returned with progressive headaches, and a repeat DSA and MRI showed a patent distal PCA GSeA [7].

It has also been shown that serpentine aneurysms are not a subgroup of fusiform aneurysms that have thrombosed. This is because they do not have a fusiform shape nor do they have the funnel-shaped appearance of feeding and draining arteries [3].

References

1. Christiano LD, Gupta G, Prestigiacomo CJ, Gandhi CD (2009) Giant serpentine aneurysms. Neurosurg Focus 26(5):E5. doi:10.3171/2009.2.focus0918
2. Aletich VA, Debrun GM, Monsein LH, Nauta HJ, Spetzler RF (1995) Giant serpentine aneurysms: a review and presentation of five cases. AJNR Am J Neuroradiol 16(5):1061–1072
3. Haddad GF, Haddad FS (1988) Cerebral giant serpentine aneurysm: case report and review of the literature. Neurosurgery 23(1):92–97
4. Vishteh AG, Spetzler RF (1999) Evolution of a dolichoectatic aneurysm into a giant serpentine aneurysm during long-term follow up. Case illustration. J Neurosurg 91(2):346. doi:10.3171/jns.1999.91.2.0346
5. Fodstad H, Liliequist B, Wirell S, Nilsson PE, Boquist L, Abdul-Rahman A (1978) Giant serpentine intracranial aneurysm after carotid ligation. Case report. J Neurosurg 49(6):903–909. doi:10.3171/jns.1978.49.6.0903
6. Sari A, Kandemir S, Kuzeyli K, Dinc H (2006) Giant serpentine aneurysm with acute spontaneous complete thrombosis. AJNR Am J Neuroradiol 27(4):766–768
7. Lee KC, Joo JY, Lee KS, Shin YS (1999) Recanalization of completely thrombosed giant aneurysm: case report. Surg Neurol 51(1):94–98

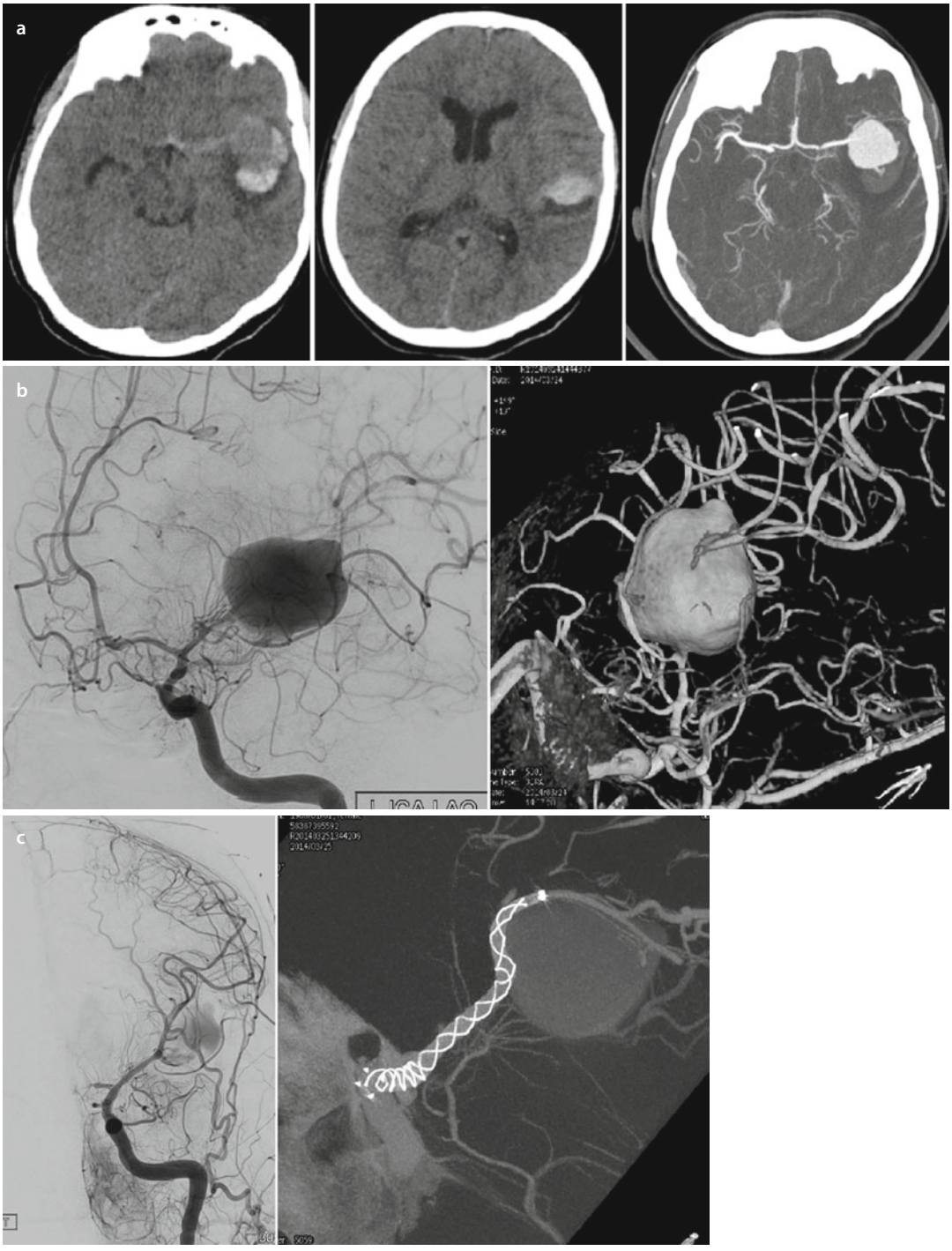

Fig. 12.1 A 34-year-old lady presented with sudden onset severe headache. (**a**) NECT with CTA reveals a 35 × 25 mm-sized acutely ruptured left MCA partially thrombosed GIA with acute SAH. (**b**) Cerebral DSA reveals a 27 × 25 mm-sized luminal filling of a MCA bifurcation GIA. The lower trunk of MCA is incorporated into the aneurysm. (**c**) On March 2014, the aneurysm was treated using FRED® FD across the aneurysm. Immediate postprocedural angiograms reveal significant decrease in aneurysmal filling with good antegrade flow in the upper trunk of MCA. IA VASO® CTA shows the relative position of FD and aneurysm.

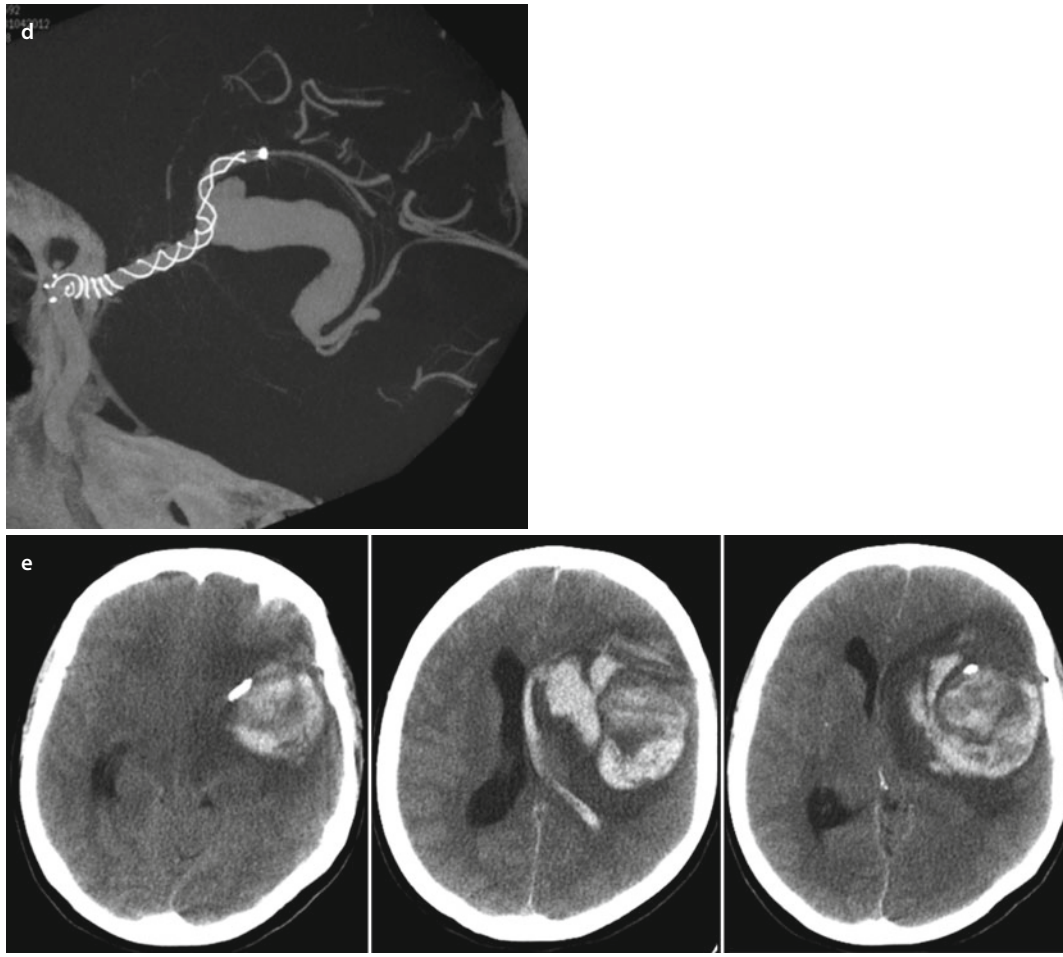

Fig. 12.1 (continued) (**d**) IV VASO® CTA at 1½ months reveals partially thrombosed GIA with serpentine configuration of the residual lumen extending to the MCA lower trunk with a patent upper trunk. The patient is asymptomatic. (**e**) Four months later, the patient had sudden headache, altered sensorium, and became comatose. NECT revealed parenchymal and intraventricular hemorrhage with adjacent mass effect and sub-falcine herniation. The patient succumbed to this episode

Case 13

Electronic supplementary material The online version of this chapter (doi:10.1007/978-3-319-41788-2_13) contains supplementary material, which is available to authorized users.

N. Kocer, *Giant Intracranial Aneurysms*, DOI 10.1007/978-3-319-41788-2_13

Posterior Cerebral Artery and Parent Vessel Occlusion

Keywords: Posterior cerebral aneurysm, Parent vessel occlusion, Serpentine aneurysm

Posterior Cerebral Artery Anatomy

The PCA is commonly divided into four anatomical segments [1]:

P1: From its origin to its junction with the posterior communicating artery (PCoA)
P2: From PCoA to the dorsal midbrain
P2A: From PCoA to edge of cerebral peduncle
P2B: From edge of cerebral peduncle to the dorsal midbrain
P3: From the dorsal midbrain to anterior calcarine fissure
P4: Terminal cortical branches of PCA

Unique Features of PCA Aneurysms

PCA aneurysms are rare and constitute around 1 % of all cerebral aneurysms [2]. They have several unique features, namely [3]:

1. Young age at presentation including higher occurrence in pediatric patients (average age: 38 years versus fifth to sixth decades at other locations).
2. High incidence of GIAs (23 % versus 3–5 % at other locations).
3. Aneurysmal size and surgical technique used to treat these aneurysms have no influence on patient outcomes (unlike any other location) [2,3].

Why Parent Vessel Occlusion in PCA Aneurysms?

Drake et al., in their historic series of 125 PCA aneurysms, reported excellent or good visual field outcomes in 87.9 % of patients. He found that the outcome P1 or P2 occlusion or trapping was associated with a mere 17 % rate of postoperative hemianopsia. He also questioned the benefits of bypass to P2, in cases that require P2 occlusion especially in GIAs [4].

This low incidence of visual field defects is due to a rich anastomotic network between [1]:

(a) Long circumflex (P1 branches) and superior cerebellar arteries at the level of quadrigeminal plate
(b) Lateral posterior choroidal (P2B branch) and anterior choroidal arteries
(c) Splenial (P3/P4 branch) and posterior pericallosal arteries and
(d) Inferior temporal (P4 branches) and superior temporal pial-pial collaterals

Open Surgical Treatment Strategies and Outcome

A direct transcranial approach to PCA aneurysms is difficult as varied approaches are required for different locations. Sometimes resection or retraction of part of temporal lobe is required to improve aneurysm access. When extensive, this causes swelling and venous injury with resultant neurological deficits. In a review of 63 patients published in 1996, it was found that 19 % of patients died, 13 % had poor recovery, and a mere 68 % had fair to good recovery. In a recent series of 28 patients, good recovery was seen in only 33 % of unruptured and 25 % of ruptured PCA aneurysms. Another study in 2005 reported their 15-year experience of surgery in 16 PCA aneurysms, with 69 % of patients having a good recovery [5].

Endovascular Treatment Strategies and Outcome

A review of the five major case series of PCA aneurysms treated by endovascular technique only reveals a mortality of 4 % (three patients) with 90 % good recovery. Although in half of these patients the PCA was occluded, only 11 % of patients had permanent morbidity (three had homonymous hemianopia and one had hemiparesis). Of the three patients who died, two were poor grade at presentation (HH grade 4 or 5) and one patient died from rupture of a coiled aneurysm [5]. *Our own series examined a group of seven patients with large/giant fusiform PCA aneurysms that was treated by endovascular PVO using coils. There was 100 % aneurysmal occlusion with 12.5 % permanent morbidity and no mortality on a 6-month to 1-year follow-up* [6]. Furthermore a recent series has shown that it is feasible to occlude the PCA proximally (P1 and P1–P2 junction) segment despite the presence of multiple brain stem perforators if the paramedian group of perforators (arising from P1 segment of PCA) could be spared [2].

Role of surgical revascularization (bypass) in PCA aneurysms:
In a large study of 34 distal PCA aneurysms, 14 (41 %) patients were treated with occipital to PCA bypass and PVO (surgical or endovascular). The study found that patients undergoing bypass had a significantly worse outcome compared to those without any bypass. Also, the addition of bypass to the treatment strategy did not significantly lower the incidence of acquired visual defects and death. The rate of bypass failures was very high (57 %) in this study spanning a 10-year period [4].

References

1. Ciceri EF, Klucznik RP, Grossman RG, Rose JE, Mawad ME (2001) Aneurysms of the posterior cerebral artery: classification and endovascular treatment. AJNR Am J Neuroradiol 22(1):27–34
2. Oishi H, Tanoue S, Teranishi K, Hasegawa H, Nonaka S, Magami S, Yamamoto M, Arai H (2015) Endovascular parent artery occlusion of proximal posterior cerebral artery aneurysms: a report of two cases. J Neurointervent Surg. doi:10.1136/neurintsurg-2015-011762
3. Ferrante L, Acqui M, Trillo G, Lunardi P, Fortuna A (1996) Aneurysms of the posterior cerebral artery: do they present specific characteristics? Acta neurochirur 138(7):840–852
4. Chang SW, Abla AA, Kakarla UK, Sauvageau E, Dashti SR, Nakaji P, Zabramski JM, Albuquerque FC, McDougall CG, Spetzler RF (2010) Treatment of distal posterior cerebral artery aneurysms: a critical appraisal of the occipital artery-to-posterior cerebral artery bypass. Neurosurgery 67(1):16–25. doi:10.1227/01.neu.0000370008.04869.bf; discussion 25–26.
5. Roh HG, Kim SS, Han H, Kang HS, Moon WJ, Byun HS (2008) Endovascular treatment of posterior cerebral artery aneurysms using detachable coils. Neuroradiology 50(3):237–242. doi:10.1007/s00234-007-0321-2
6. Arat A, Islak C, Saatci I, Kocer N, Cekirge S (2002) Endovascular parent artery occlusion in large-giant or fusiform distal posterior cerebral artery aneurysms. Neuroradiology 44(8):700–705. doi:10.1007/s00234-002-0747-5

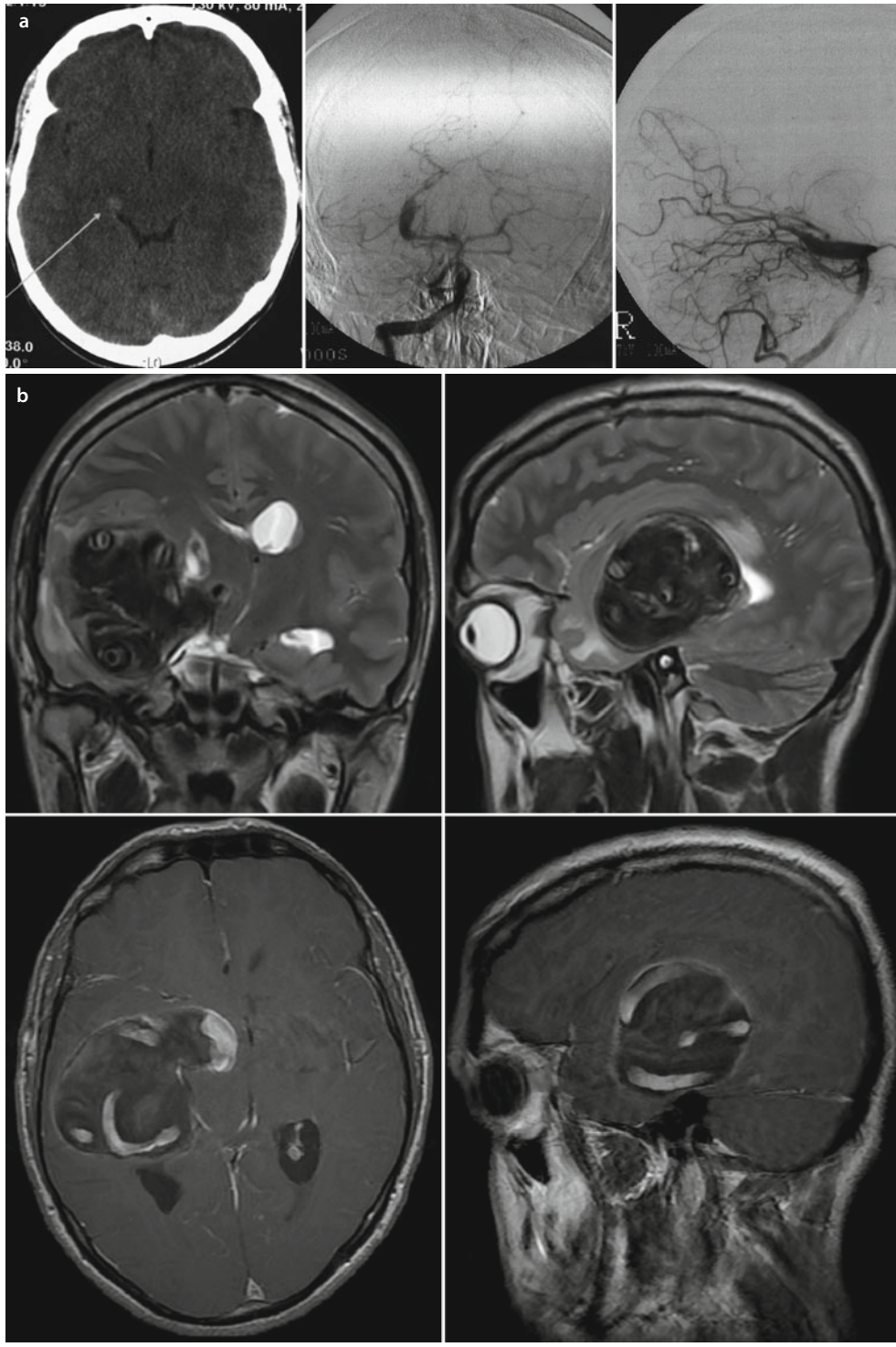

Fig. 13.1 A 32-year-old man presented with headache and diaphoresis. (**a**) NECT reveals a hyperdense mass in the right ambient cistern (*arrow*). In 2007, cerebral DSA shows a right PCA (P2 and P3 segments) dolichoectatic fusiform enlargement. (**b**) After a period of 6 years, the patient presented with worsening symptoms; a repeat MRI on 2013 reveals a heterogeneous predominantly hypointense mass with peri-lesional vasogenic edema in the right deep temporal region adjacent to the mesencephalon probably along the choroidal fissure. Postcontrast MRI images show serpentine enhancing vessels within the heterogeneous mass

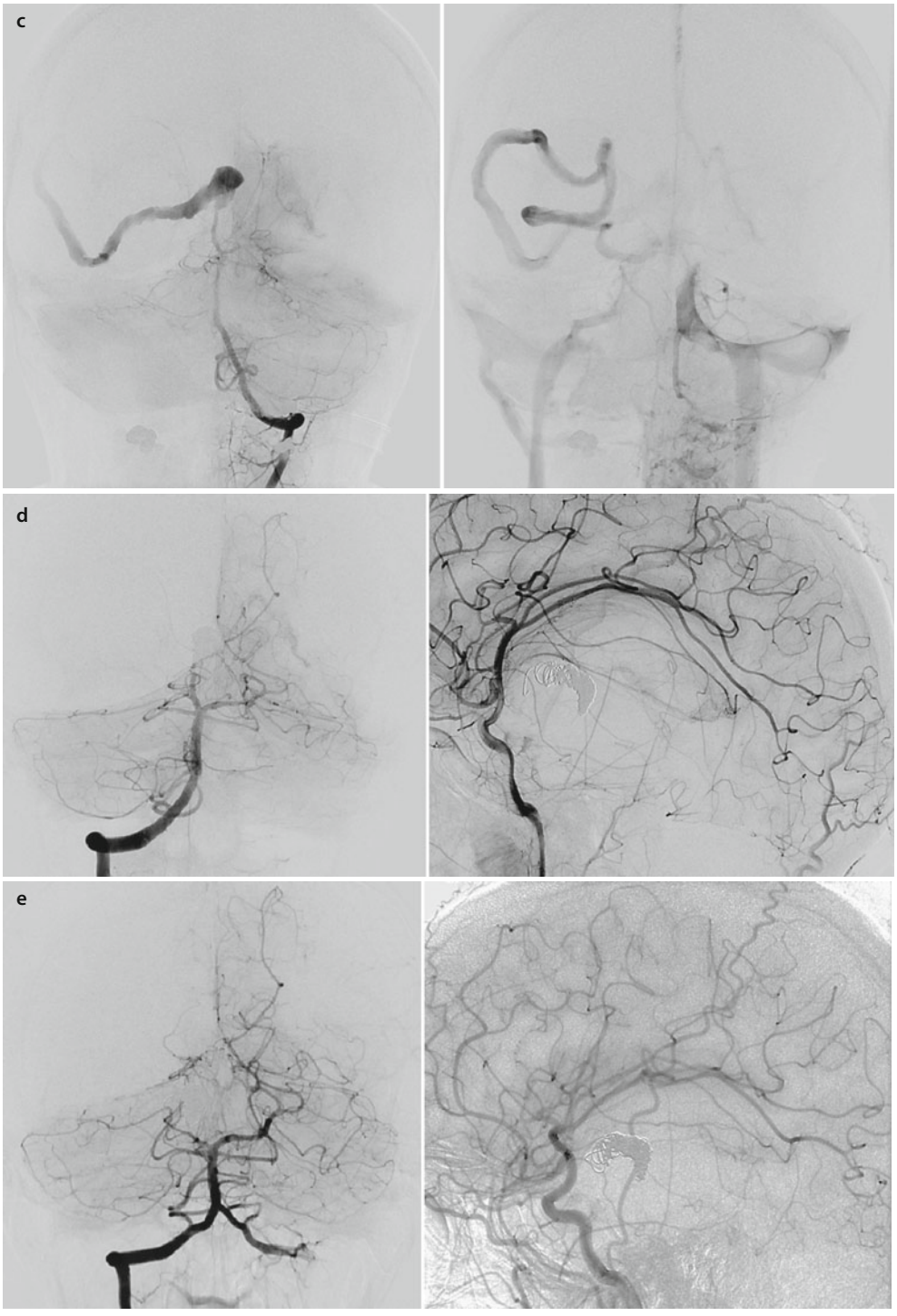

Fig. 13.1 (continued) (**c**) On March 2013, cerebral DSA shows a giant serpentine aneurysm of the right P2 and P3 segments. The serpentine aneurysm has evolved from the previously seen dolichoectatic fusiform enlargement of the same segment. There is normal caliber and perfusion of the distal PCA territory with prolonged circulation time. (**d**) On March 2013, the patient was treated by parent vessel occlusion of the PCA with detachable coils. The coiling involved occlusion of proximal segment of the serpentine fusiform enlargement. The distal PCA branches were opacified by pial-pial collaterals through MCA. (**e**) At a 1-year follow-up, cerebral DSA shows exclusion of the aneurysm from the circulation with stable collateral flow and perfusion into the distal PCA territory

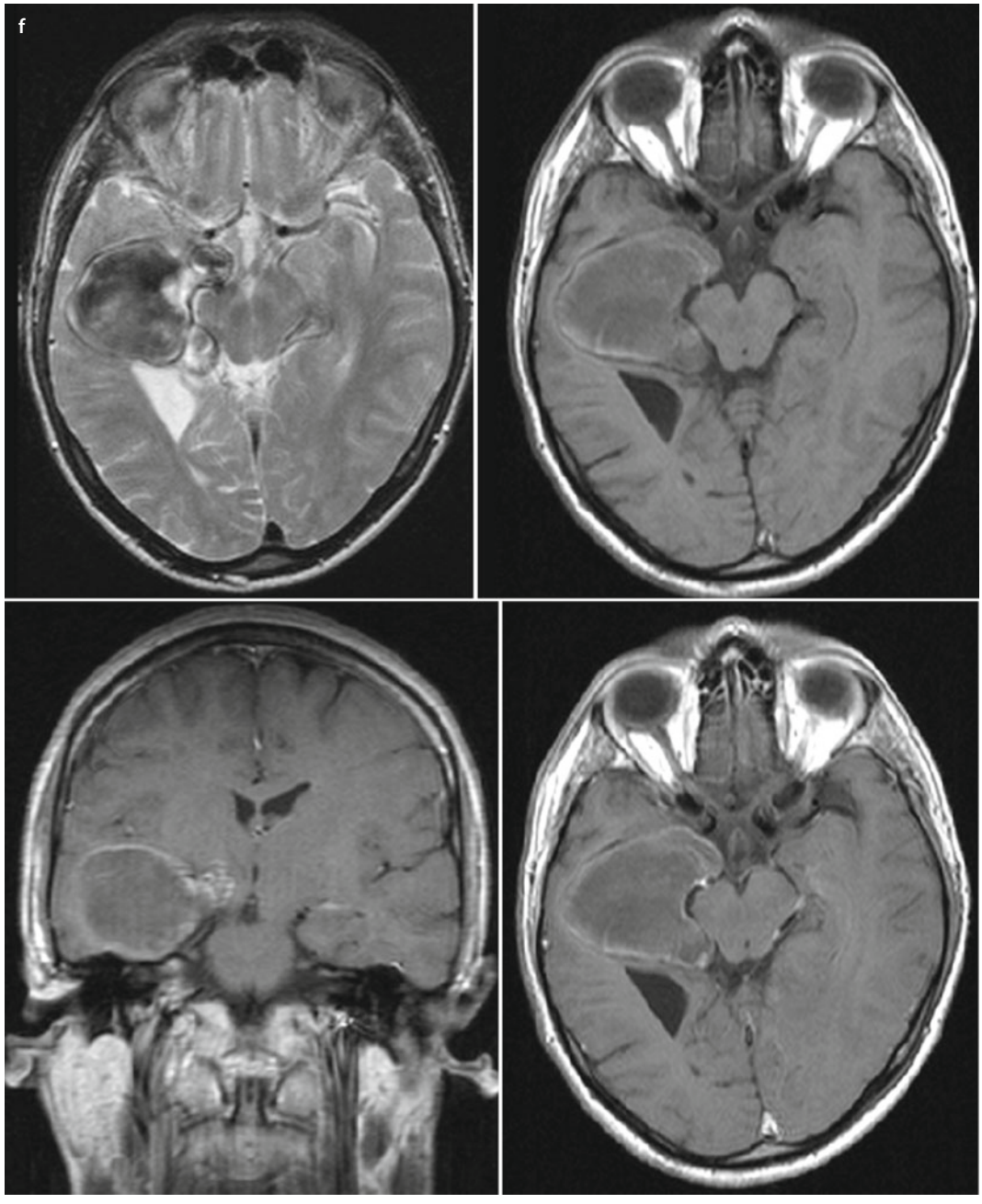

Fig. 13.1 (continued) (**f**) Follow-up cranial MRI 2 years after treatment reveals decreased mass effect on brain stem and adjacent brain parenchyma. Around the residual thrombosed mass, no edema was detected. There is no patent serpentine lumen within the mass (axial T2W, non-contrast T1W, postcontrast T1W, coronal postcontrast T1W)

Case 14

N. Kocer, *Giant Intracranial Aneurysms*, DOI 10.1007/978-3-319-41788-2_14

Onyx® (Liquid Embolic Agents) in Intracranial Aneurysms (Cases 14, 15, and 20)

Keywords: Onyx, Recanalization, Balloon assisted

Conditions Favoring Successful Endovascular Aneurysm Treatment

Three conditions are essential for a durable endosaccular occlusion of aneurysm, namely:

1. There must be effective hemostasis throughout the aneurysm that needs to be sustained over some critical period.
2. The intra-aneurysmal thrombus must mature during this critical period ideally healing by formation of a fibrointimal scar.
3. The endosaccular occlusion must support neointimal overgrowth over the aneurysm neck; the aneurysm base must be uniformly occluded by a stable biomechanical complex [1].

Balloon-Assisted Onyx Aneurysm Embolization

In the Cerebral Aneurysm Multicenter European Onyx (CAMEO) trial designed to treat aneurysms considered high risk for surgical and conventional endovascular therapy, the 1-year complete aneurysm occlusion rate was 78.9 %. There was an associated mortality of 4.1 % and permanent morbidity of 8.2 %. An additional 10 % of aneurysms required re-treatment within 3–12 months (5 % were GIAs). Furthermore, nine patients out of a total of 97 (9.3 %) had parent artery occlusion. All the parent artery occlusions occurred within 3 months of the procedure (two caused permanent deficit) [2].

Another study described treatment of 15 GIAs using Onyx 500HD® and balloon remodeling. There was recanalization in eight (53.3 %) aneurysms with three (20 %) requiring re-treatment [2]. In another study of large and giant aneurysms, it was found that Onyx with balloon remodeling had a recanalization rate of 36 % even on short-term follow-up (3–6 months) [3].

Endosaccular occlusion with Onyx® and balloon remodeling has a low initial complete occlusion rate (76–78 %) that decreased further to 65 % at 3–6 months follow-up with a 69 % recanalization rate. The procedural mortality and major morbidity were comparable to surgical series of 9 % and 12.5 %, respectively [3].

Technical Limitations of Balloon-Assisted Onyx® Embolization

The technique of balloon-assisted Onyx embolization has limited application as [3, 4]:

1. Prolonged balloon inflation is essential.
2. The artery arising from the aneurysm hinders Onyx® aneurysm occlusion.
3. Aneurysms located in perforator-rich regions such as posterior circulation, M1 segment of MCA have a high risk of ischemic complications.
4. A large parent artery cannot be sealed by balloon.

Recanalization and subsequent rupture of Onyx®-treated aneurysms is well known [5]. It is believed that the recanalization is because the polymer is nonadhesive and a channel may open between the Onyx® and aneurysm lumen [6]. Also, as the diseased parent artery is not healed, there is recurrence from an adjacent segment [7].

References

1. Nelson PK, Sahlein D, Shapiro M, Becske T, Fitzsimmons BF, Huang P, Jafar JJ, Levy DI (2006) Recent steps toward a reconstructive endovascular solution for the orphaned, complex-neck aneurysm. Neurosurgery 59(5 Suppl 3):S77–92. doi:10.1227/01.neu.0000240664.00611.bb; discussion S73–13
2. Wehman JC, Hanel RA, Levy EI, Hopkins LN (2006) Giant cerebral aneurysms: endovascular challenges. Neurosurgery 59(5 Suppl 3):S125–138. doi:10.1227/01.neu.0000237330.11482.90; discussion S123–113
3. Cekirge HS, Saatci I, Ozturk MH, Cil B, Arat A, Mawad M, Ergungor F, Belen D, Er U, Turk S, Bavbek M, Sekerci Z, Beskonakli E, Ozcan OE, Ozgen T (2006) Late angiographic and clinical follow-up results of 100 consecutive aneurysms treated with Onyx reconstruction: largest single-center experience. Neuroradiology 48(2):113–126. doi:10.1007/s00234-005-0007-6
4. van Rooij WJ, Sluzewski M (2009) Endovascular treatment of large and giant aneurysms. AJNR Am J Neuroradiol 30(1):12–18. doi:10.3174/ajnr.A1267
5. Molyneux AJ, Cekirge S, Saatci I, Gal G (2004) Cerebral Aneurysm Multicenter European Onyx (CAMEO) trial: results of a prospective observational study in 20 European centers. AJNR Am J Neuroradiol 25(1):39–51
6. Parkinson RJ, Eddleman CS, Batjer HH, Bendok BR (2006) Giant intracranial aneurysms: endovascular challenges. Neurosurgery 59(5 Suppl 3):S103–112. doi:10.1227/01.neu.0000237410.32115.c9; discussion S103–113
7. Fiorella D, Lylyk P, Szikora I, Kelly ME, Albuquerque FC, McDougall CG, Nelson PK (2009) Curative cerebrovascular reconstruction with the Pipeline embolization device: the emergence of definitive endovascular therapy for intracranial aneurysms. J Neurointervent Surg 1(1):56–65. doi:10.1136/jnis.2009.000083

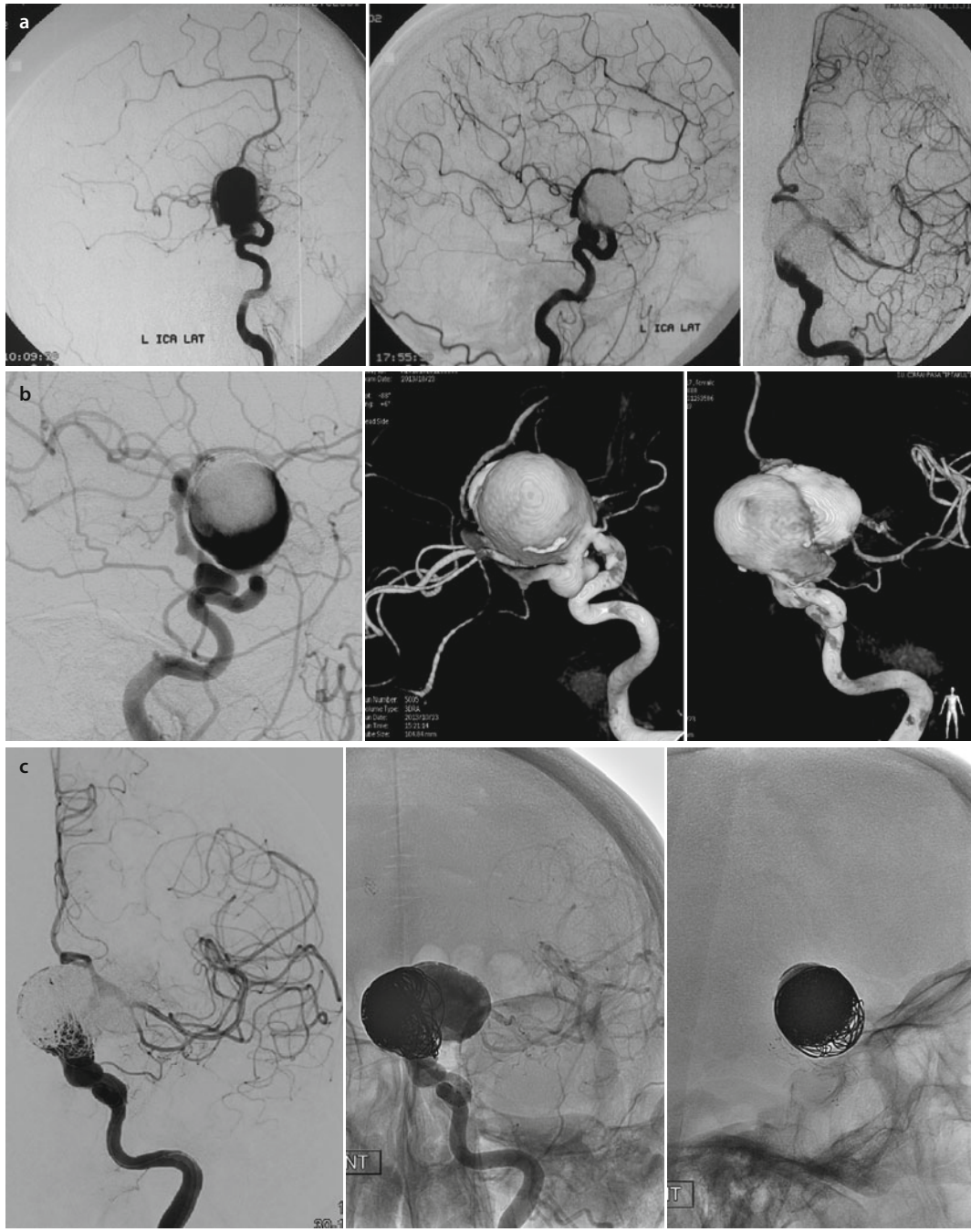

Fig. 14.1 A 37-year-old woman presented with headaches. (**a**) Cerebral DSA in 2002 reveals bilateral supraclinoid ICA aneurysms. The left ICA sacculo-fusiform aneurysm arising from the anterior wall measures 31 × 20 mm with a 12 × 9 mm-sized bilobed aneurysm arising from the posterior wall of the same segment. On May 2002, the patient was treated with Onyx 500 HD® embolization with balloon remodeling technique for the left supraclinoid GIA. Post-embolization angiogram reveals complete exclusion of the aneurysm from the circulation. However, during the treatment there was Onyx embolization into proximal MCA branch with acute ischemic infarction. (**b**) Follow-up angiogram in 2013 (after 11 years) showed recanalization with regrowth of left ICA giant aneurysm. There is no change in the bilobed posterior wall aneurysm. (**c**) In June 2014, the patient was re-treated with balloon-assisted coiling followed by deployment of a 3.5 × 40 × 36 mm FRED® in the supraclinoid ICA. The FD was deployed across aneurysmal necks of both the giant aneurysm and bilobed smaller aneurysm. There was a focal stenosis in ICA proximal to the aneurysmal neck causing approximately 50 % stenosis

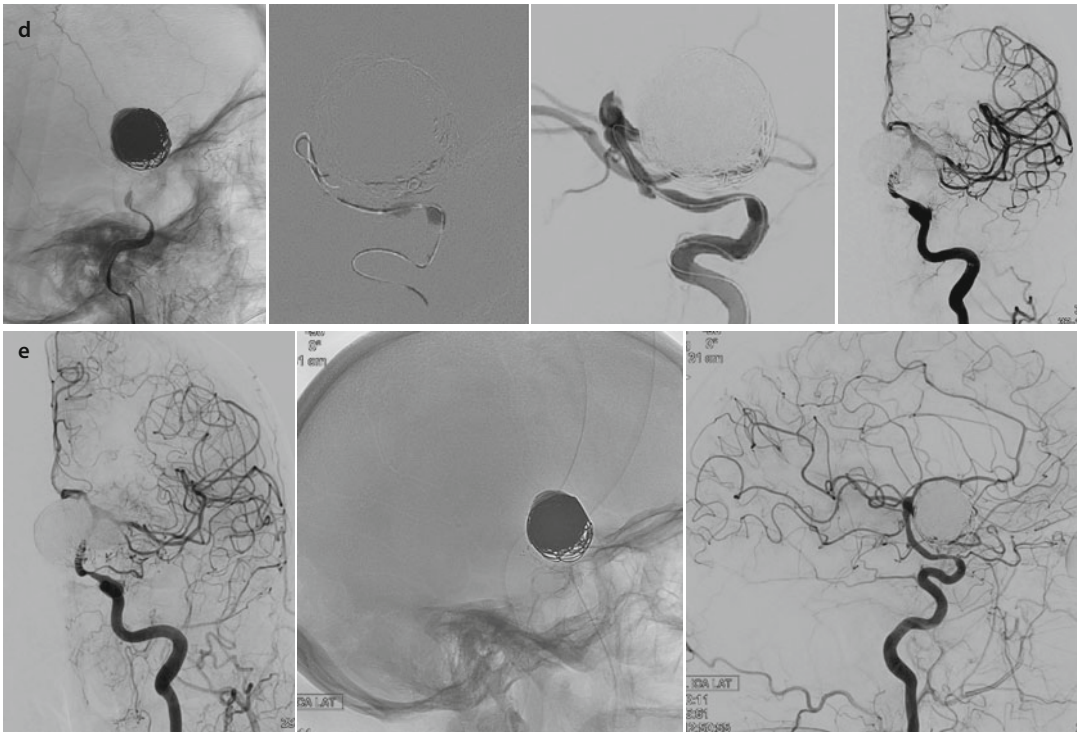

Fig. 14.1 (continued) (**d**) After 2 h, the patient had deterioration in the sensorium, and repeat angiogram revealed acute occlusion of the ICA in the flow-diverter segment. A balloon angioplasty was done with Gateway® balloon (Boston Scientific, Fremont, California) across the stenotic segment of ICA. Post angioplasty, there was restoration of flow with good caliber of the stenotic segment. A 3.5 × 20 mm-sized PED® was deployed telescopically within the FRED®. There was complete exclusion of both the giant and the smaller aneurysm post angioplasty and telescopic flow-diverter therapy. (**e**) Follow-up angiogram after 1 year reveals moderate intimal hyperplasia of the stented segment with complete exclusion of both the aneurysms

Case 15

N. Kocer, *Giant Intracranial Aneurysms*, DOI 10.1007/978-3-319-41788-2_15

GIAs Causing Compression Syndromes

Keywords: Giant aneurysms, Compression syndrome, Mass effect

Introduction: Role of Coiling, Clipping, and Flow Diversion

Giant aneurysms are associated with increased morbidity due to their high incidence of rupture and neurological deficits caused by compression of the adjacent neural structures [1]. Large and giant aneurysms of the cavernous, ophthalmic, and supraclinoid segments of ICA frequently present with compression syndrome on adjacent cranial nerves. Compression of the optic nerve results in decreased visual acuity and visual field deficits and is commonly associated with carotico-ophthalmic or hypophyseal (supraclinoid) aneurysms [2]. The treatment of giant aneurysms that present with compression syndrome is limited by high surgical morbidity and limited efficacy of endovascular techniques due to high rate of incomplete aneurysmal occlusion and recurrence [1]. Patients treated by clipping are at risk of cranial nerve injury during manipulation or temporary clipping or total arterial occlusion. Patients treated by endovascular coiling are at risk of subsequent recanalization [3]. Parent vessel occlusion is an effective strategy to decrease aneurysmal compression syndrome but is restricted to aneurysms with sufficient collateral circulation. The addition of "surgical bypass" compensates the lack of collaterals but increases the overall morbidity of therapy. Flow diversion has been shown to reduce intra-aneurysmal circulation and cause aneurysmal thrombosis. Furthermore, collapse of large and GIAs has also been observed following flow diversion [1].

Etiology of Compression Syndrome

The underlying etiology includes a direct "compressive mass" effect, the pulsatile aneurysmal "water-hammer effect," and the "irritant" effect of the adherent aneurysm/subarachnoid hemorrhage [3, 4]. The initial injury is in the form of neuropraxis and axonolysis (potentially reversible changes). However, with long-standing injury, there is axonal degeneration (irreversible change). The consensus is that the total duration and the initial degree of paresis affects cranial nerve recovery. Studies have demonstrated that the chances of complete recovery after cranial nerve palsy diminish in patients with persistent palsy for one month and those with a complete palsy at presentation [4].

Giant Aneurysmal Therapy in Compression Syndrome

It has also been claimed that neurosurgical clipping of aneurysms is better at reducing the mass effect on the cranial nerves compared to coiling [5]. Studies have also shown improvement in cranial nerve palsy following endovascular coiling. This has been attributed to the immediate cessation of the "pulsatile water-hammer effect" on the surrounding tissue after coiling [5–7]. However, this goal can be achieved only if the neck of the aneurysm can be completely sealed. Since the majority of aneurysms presenting with compression syndrome have wide necks, this sealing is difficult to achieve by coiling alone, and it decreases the efficacy of coiling in relieving compression syndromes. This also increases the tendency of coil compaction with increased chances of subsequent worsening of compression syndrome. Aneurysmal occlusion by liquid embolic agents may provide better stability by converting a soft aneurysmal mass into a hard mass that transmits arterial pulsation to adjacent cerebral parenchyma. Flow diversion has achieved a very high rate of complete and stable aneurysmal occlusion that was difficult or impossible to achieve by conventional endovascular techniques. A large single center study showed a 61 % rate of aneurysmal shrinkage following flow diversion. However, there are reported instances of temporary worsening of compression syndrome and delayed aneurysmal rupture following flow diversion [1].

Visual Loss Due to Compression Syndrome

Visual loss from compression syndrome has been described with carotico-ophthalmic, cavernous, and supraclinoid ICA aneurysms. Proximal supraclinoid aneurysms cause asymmetric visual loss with greater involvement of the ipsilateral optic nerve, while distal supraclinoid aneurysms may mimic suprasellar tumor causing bitemporal hemianopia. Posterior expansion of supraclinoid aneurysms may compress the optic tract [8]. In a recent study, all the patients with vision loss ($n = 6$) attributed to compression syndrome due to ICA aneurysms showed improvement following flow diversion. However, two patients also had a temporary worsening of their visual acuity. In the study aneurysm shrinkage was seen as early as three months and as late as eight months following flow diversion. The majority of these aneurysms were either large or giant [1].

References

1. Szikora I, Marosfoi M, Salomvary B, Berentei Z, Gubucz I (2013) Resolution of mass effect and compression symptoms following endoluminal flow diversion for the treatment of intracranial aneurysms. AJNR Am J Neuroradiol 34(5):935–939. doi:10.3174/ajnr.A3547
2. van Rooij WJ, Sluzewski M (2008) Unruptured large and giant carotid artery aneurysms presenting with cranial nerve palsy: comparison of clinical recovery after selective aneurysm coiling and therapeutic carotid artery occlusion. AJNR Am J Neuroradiol 29(5):997–1002. doi:10.3174/ajnr.A1023
3. Panagiotopoulos V, Ladd SC, Gizewski E, Asgari S, Sandalcioglu EI, Forsting M, Wanke I (2011) Recovery of ophthalmoplegia after endovascular treatment of intracranial aneurysms. AJNR Am J Neuroradiol 32(2):276–282. doi:10.3174/ajnr.A2281
4. Mansour N, Choudhari KA (2007) Outcome of oculomotor nerve palsy from posterior communicating artery aneurysms: comparison of clipping and coiling. Neurosurgery 60(3):E582. doi:10.1227/01.neu.0000255363.17442.25; author reply E582
5. Hassan T, Hamimi A (2013) Successful endovascular management of brain aneurysms presenting with mass effect and cranial nerve palsy. Neurosurg Rev 36(1):87–97. doi:10.1007/s10143-012-0404-3; discussion 97
6. Birchall D, Khangure MS, McAuliffe W (1999) Resolution of third nerve paresis after endovascular management of aneurysms of the posterior communicating artery. AJNR Am J Neuroradiol 20(3):411–413
7. Mansour N, Kamel MH, Kelleher M, Aquilina K, Thornton J, Brennan P, Bolger C (2007) Resolution of cranial nerve paresis after endovascular management of cerebral aneurysms. Surg Neurol 68(5):500–504. doi:10.1016/j.surneu.2006.12.061; discussion 504
8. Norwood EG, Kline LB, Chandra-Sekar B, Harsh GR, 3rd (1986) Aneurysmal compression of the anterior visual pathways. Neurology 36(8):1035–1041

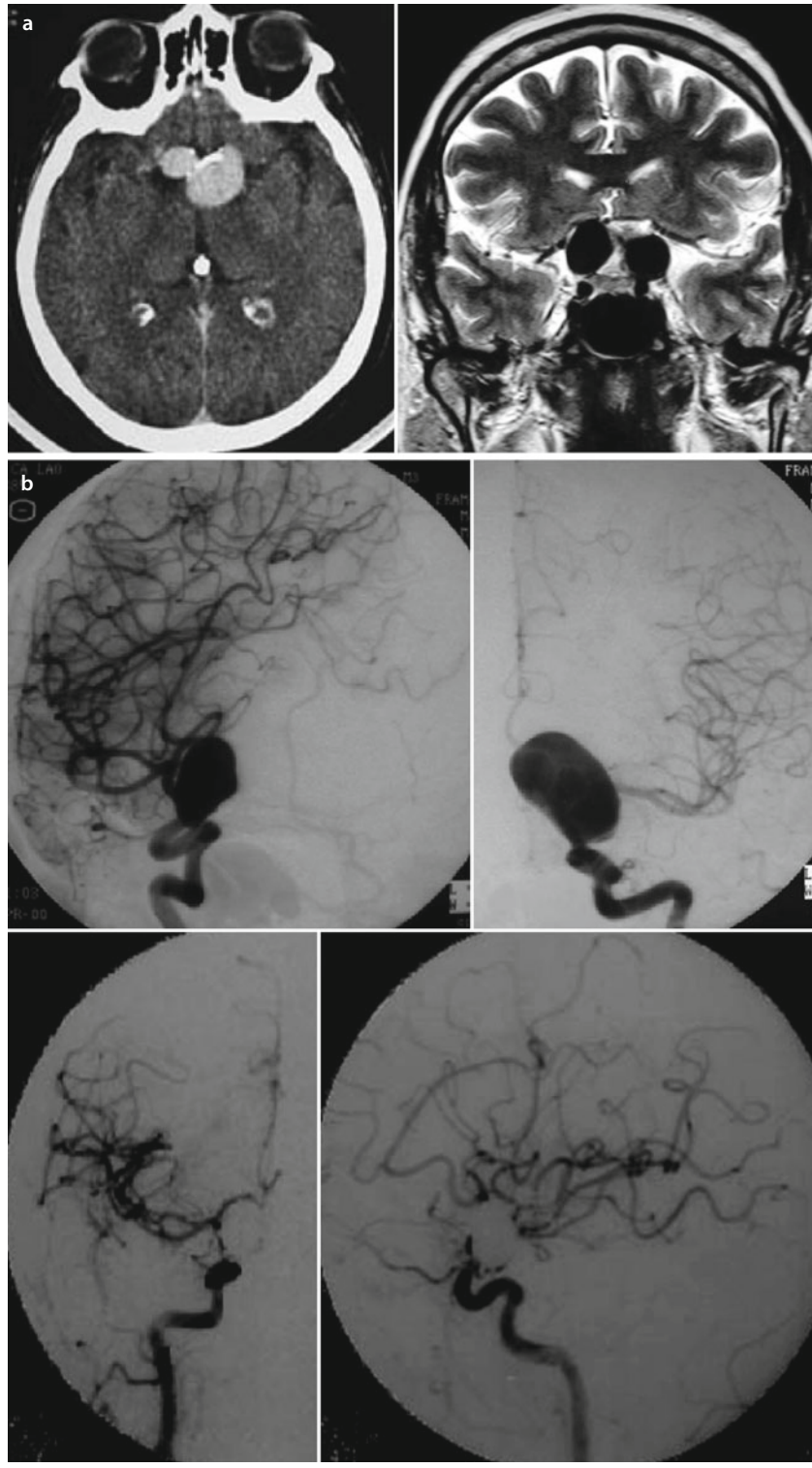

Fig. 15.1 A 55-year-old lady had progressive bilateral visual loss. (**a**) On March 2000, axial CECT and coronal T2W MRI images show bilateral supraclinoid ICA aneurysms, with the left GIA and right very large aneurysm extending into the suprasellar cistern and compressing on optic chiasma. (**b**) On April 2000, both the aneurysms were treated with coiling at an outside institution with a stretched coil in the right proximal ICA

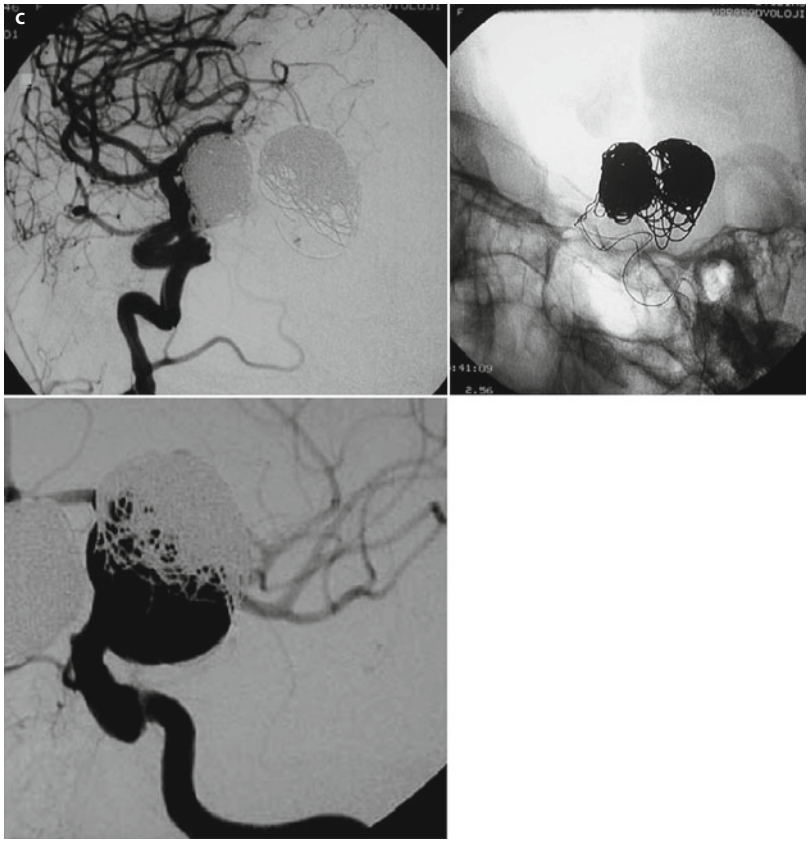

Fig. 15.1 (continued) (**c**) After 1 year, the patient presented with worsening visual symptoms and on examination had perception of light in both eyes. On December 2001, cerebral DSA reveals regrowth with coil compaction of bilateral supraclinoid ICA aneurysms. There is displacement of both the A1 segments of ACA by the aneurysms. On cross-compression study, there is cross-circulation to the left hemisphere across the ACoM

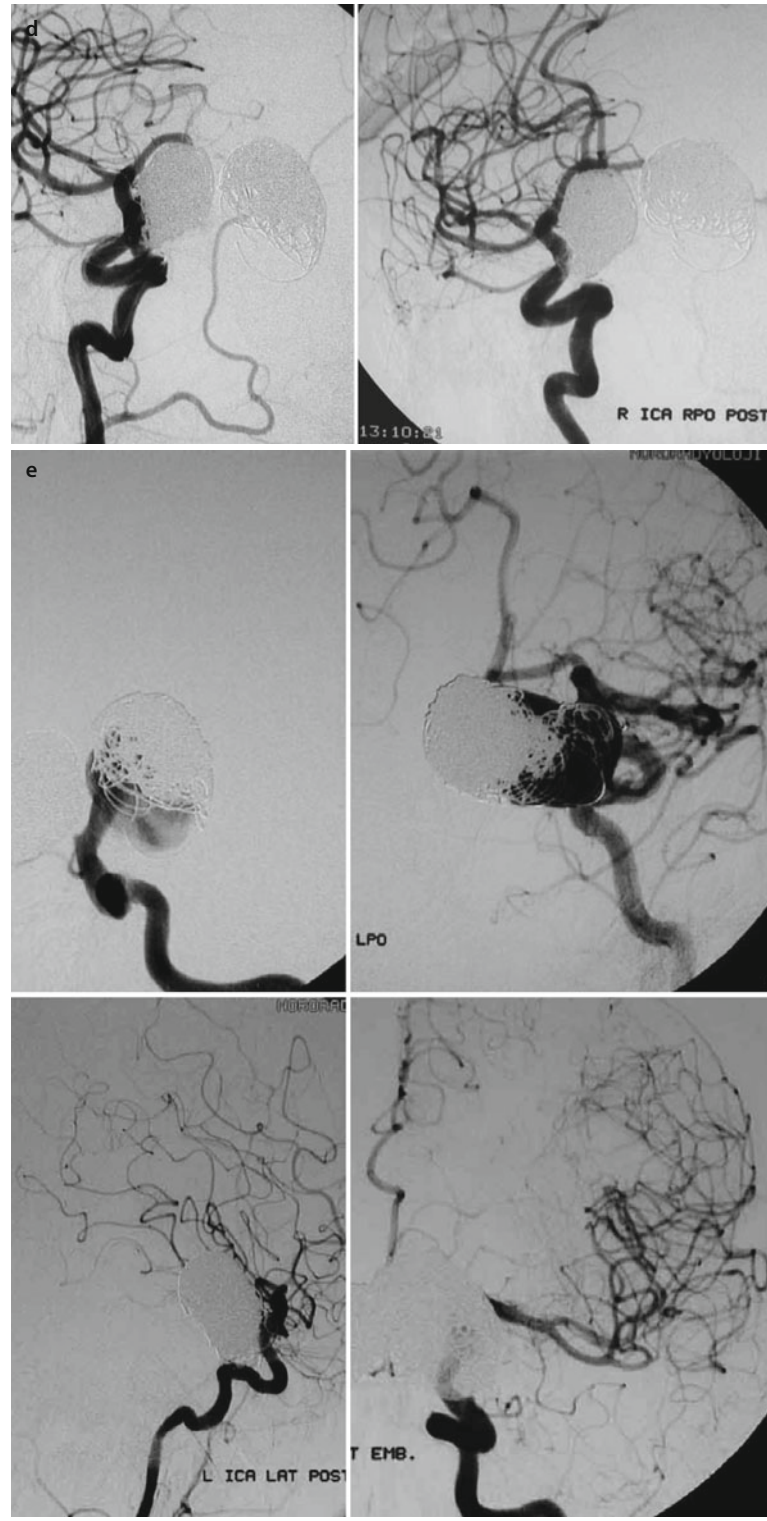

Fig. 15.1 (continued) (**d, e**) Both the supraclinoid aneurysms were treated with Onyx 500 HD® embolization using balloon remodeling

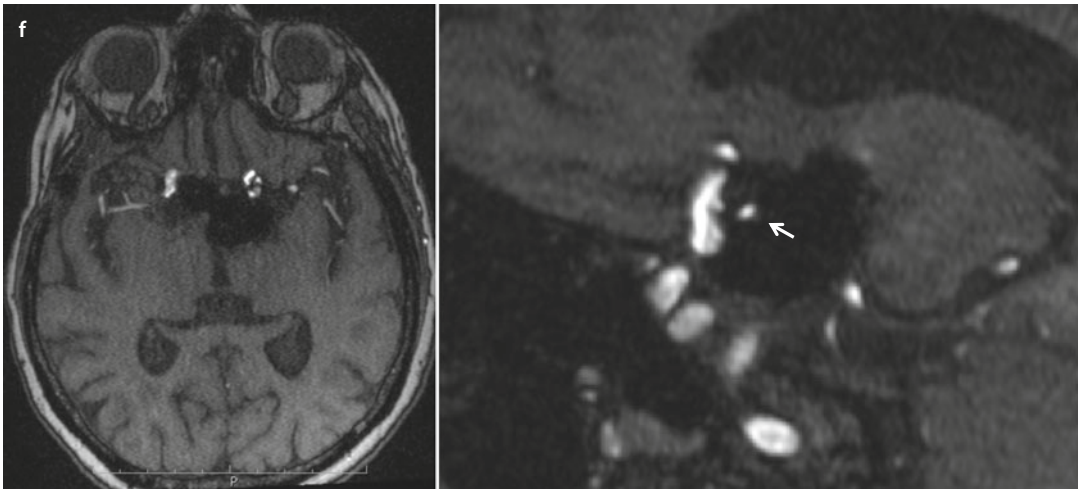

Fig. 15.1 (continued) (**f**) After 13 years, repeat MRA shows a small recanalization (*arrow*) with stable aneurysmal occlusion

Case 16

N. Kocer, *Giant Intracranial Aneurysms*, DOI 10.1007/978-3-319-41788-2_16

"True" PCoM Aneurysms

Keywords: PCoM aneurysm, True PCoM aneurysm, Dissecting aneurysm

Types of PCoM Aneurysms
PCoM aneurysms can be divided into four groups based on their location:

(a) Junctional aneurysms between ICA and PCoM
(b) Aneurysms arising from the PCoM itself ("true PCoM aneurysms")
(c) Posterior wall ICA aneurysm in close relation to but not arising from the PCoM itself
(d) Junctional aneurysms between PCoM and PCA

True PCoM aneurysms arise from PCoM with aneurysmal neck limited to PCoM. True PCoM aneurysms constitute 0.1–2.8 % of all cerebral aneurysms and 4.3–13 % of all PCoM aneurysms [1].

Embryology and Anatomy of PCoM
The origin of PCoMs marks the division of embryonic ICA into cranial and caudal rami. The cranial ramus gives rise to prominent anterior cerebral and anterior choroidal arteries. The caudal ramus forms the PCoMs, the P1 segment of PCAs, and the upper basilar system distal to the origin of trigeminal artery [2]. The PCoMs are of four different varieties, namely, hypoplastic, adult, fetal, and transitional. The risk of development of aneurysms is higher in the hypoplastic, fetal, and transitional varieties compared to the adult PCoM configuration [1]. PCoM gives rise to a number of perforating arteries (4–12, average 7), diameter 0.1–0.6 mm, from its superior and lateral surfaces. These branches penetrate the tuber cinereum and premammillary part of the floor of the third ventricle, posterior perforated substance and interpeduncular fossa, optic tract, pituitary stalk, and optic chaisma. These branches supply the posterior hypothalamus, ventral thalamus, anterior one-third of optic tract, posterior limb of internal capsule, and subthalamus.

Premammillary Artery (PMA)
The largest and most constant perforating artery from PCoM in the premamillary region is PMA or anterior thalamo-perforating artery or thalamo-tuberal artery that is seen in 80 % of individuals. There are four large studies that describe the PMA and its course in brain autopsy studies [3–6]. PMA enters the floor of the third ventricle between the optic tract anteriorly and mammillary bodies posteriorly [6, 7]. In a series of 50 brain autopsies, PMA was commonly seen from middle one-third (50 %) followed by anterior one-third (17 %) and posterior one-third (13 %) of PCoM. In another study, the PMA was most commonly seen from the middle one-third of PCoM (approximately 60 %) in both adult and hypoplastic PCoMs. In the fetal configuration, PMA was predominantly seen from the anterior one-third (41.7 %) of PCoM and has a high rate (50 %) of duplicated PMA origin. The PMA rarely arises from posterior one-third of PCoM in all three configurations [4]. PMA supplies the anterior and lateral thalamus and hypothalamus (see Case 2) [6]. Furthermore, the perforators arising from PCoM and P1 segment of PCA complement each other in supplying the same territory. Occlusion of PMA causes a characteristic neurological syndrome of acute contralateral motor weakness, changes in superficial modalities of sensation, and neuropsychological dysfunction such as apathy, lack of spontaneity, disorientation, and language and memory disturbances [1, 4].

True PCoM Aneurysms
In 1951, Poppen et al. treated two "true PCoM" aneurysms. They were depicted by schematic representation only [8]. *In a study at our institution of true PCoM aneurysms, we found all the five cases to be dissecting in nature. This was discerned based on their morphology (focal arterial wall abnormalities), retention of contrast media on DSA, perforator infarction, or mural thrombus. All the aneurysms were treated with parent vessel occlusion. In a single patient, the aneurysm was treated by additional flow diversion using balloon expandable coronary stent (see* Case 2*). Perforator infarction at presentation is a relatively common feature of true PCoM aneurysms. The infarction commonly involves the anterior thalamic nucleus, ventral thalamic nucleus, and the posterior limb of internal capsule. Therefore, isolated infarctions involving the thalamus should always raise a possibility of PCoM dissections/aneurysms* [1].

References

1. Kocak B, Tureci E, Kizilkilic O, Islak C, Kocer N (2013) Dissecting aneurysms of posterior communicating artery itself: anatomical, diagnostic, clinical, and therapeutical considerations. Neuroradiology 55(9):1103–1112. doi:10.1007/s00234-013-1212-3
2. Lasjaunias P, Berenstein A, Brugge KG (2001) Intradural arteries. In: Clinical vascular anatomy and variations. Springer, Berlin/Heidelberg, pp 479–629. doi:10.1007/978-3-662-10172-8_6
3. Gibo H, Marinkovic S, Brigante L (2001) The microsurgical anatomy of the premamillary artery. J Clin Neurosci Off J Neurosurg Soc Australasia 8(3):256–260. doi:10.1054/jocn.2000.0822
4. Gabrovsky S, Laleva M, Gabrovsky N (2010) The premamillary artery – a microanatomical study. Acta Neurochir 152(12):2183–2189. doi:10.1007/s00701-010-0763-x
5. Pedroza A, Dujovny M, Cabezudo-Artero J, Umansky F, Berman SK, Diaz FG, Ausman JI, Mirchandani G (1987) Microanatomy of the premamillary artery. Acta Neurochir 86(1–2):50–55
6. Saeki N, Rhoton AL, Jr. (1977) Microsurgical anatomy of the upper basilar artery and the posterior circle of Willis. J Neurosurg 46(5):563–578. doi:10.3171/jns.1977.46.5.0563
7. Rhoton AL, Jr. (2002) The supratentorial arteries. Neurosurgery 51(4 Suppl):S53–120
8. He W, Gandhi CD, Quinn J, Karimi R, Prestigiacomo CJ (2011) True aneurysms of the posterior communicating artery: a systematic review and meta-analysis of individual patient data. World Neurosurg 75(1):64–72; discussion 49. doi:10.1016/j.wneu.2010.09.012

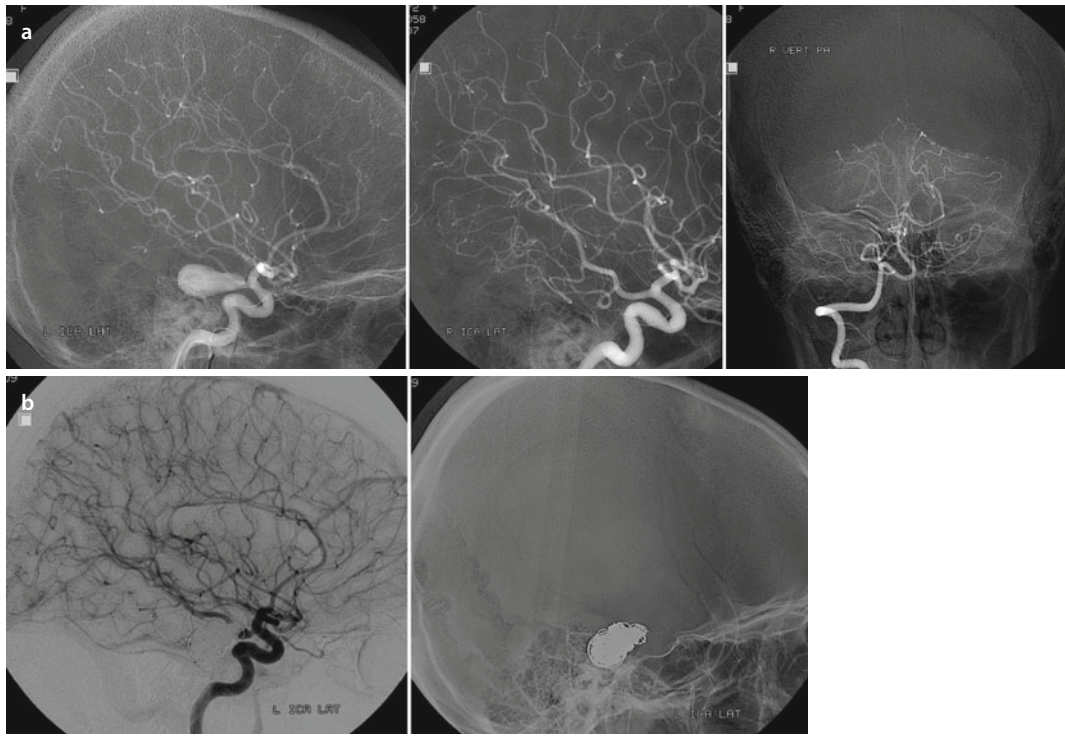

Fig. 16.1 A 37-year-old lady presented with headaches. Cross-sectional imaging reveals an unruptured PCoM GIA. (**a**) Cerebral DSA reveals a 28 × 30 mm-sized GIA of the left PCoM. The aneurysm is arising from the proximal segment of the PCoM artery itself and is not junctional in nature. The patient had bilateral fetal type PCAs with vertebral angiogram not opacifying the PCAs. (**b**) On November 2007, the aneurysm was coiled with occlusion of the neck of the aneurysm with detachable coils. Control angiograms at 2-year and 7-year intervals show persistent and stable aneurysmal occlusion with distal normal perfusion of the PCA territory

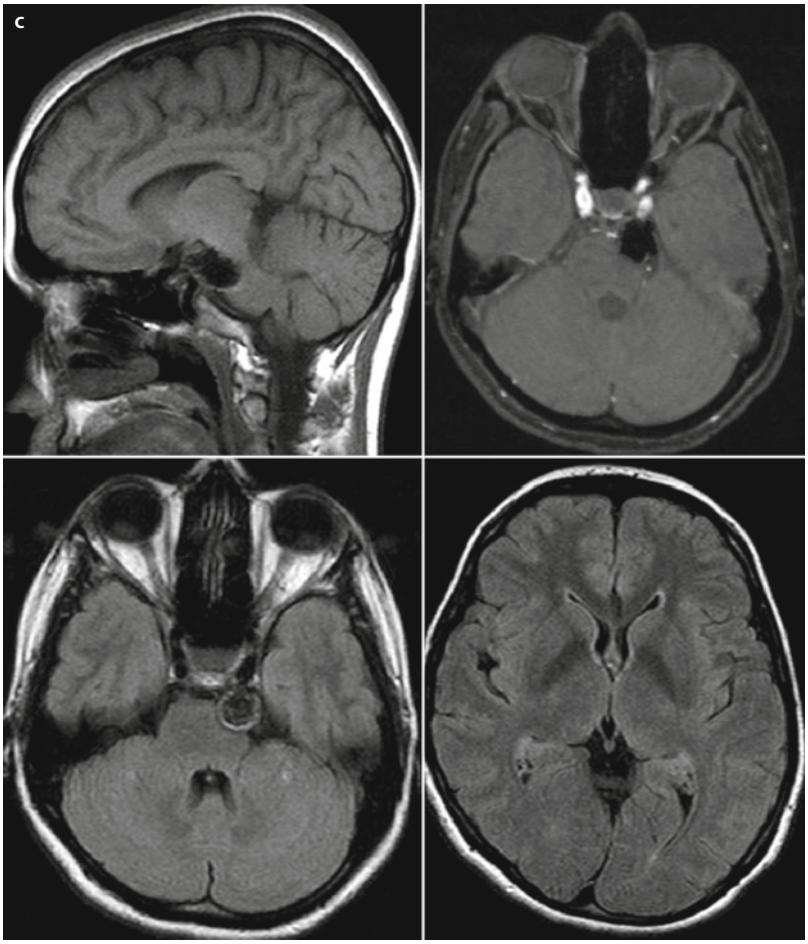

Fig. 16.1 (continued) (**c**) Follow-up, MRI with MRA 9 years later reveals the coiled PCoM GIA in the perimesencephalic cistern with mild residual brainstem compression and no parenchymal abnormality

Case 17

N. Kocer, *Giant Intracranial Aneurysms*, DOI 10.1007/978-3-319-41788-2_17

Endosaccular Occlusion of GIAs with Coils

Keywords: Giant aneurysm, Endosaccular coiling, Recanalization and retreatment

Parent Vessel Occlusion with Coils
Coils (unassisted, balloon assisted, and stent assisted) can be used for PVO and endosaccular occlusion of GIAs. A review comparing the endovascular treatment options of GIAs in 2006 revealed that PVO using coils/balloons with or without bypass had the most encouraging results, with 81 % initial occlusion rate and an extremely low (1 %) recanalization rate. The mortality of PVO in GIAs is 7 % with a morbidity of 17 % [1].

Balloon-Assisted and Unassisted Endosaccular Coiling of GIAs
In the same review, GIAs treated by endosaccular coils (unassisted and balloon assisted) with an intent to preserve parent artery have the worse outcomes compared to other strategies. The overall complete occlusion rate was 43 %, with 9 % mortality and 24 % major neurological morbidity. The recanalization rate was 55 %. This high recanalization rate is because it is difficult or even impossible in most cases to anatomically reconstruct large segmental parent artery defects with randomly distributed strands of coils. Almost invariably there are numerous small gaps that allow blood flow through the interstices of coil mass and the aneurysmal neck. Furthermore, even with the use of new-generation platinum coils in concert with stents, the best achievable packing density ranges between 20 and 40 %. Thus, the major portion of coiled aneurysms is filled by soft intra-aneurysmal thrombus rather than firm coils [1, 2]. Furthermore, endosaccular coiling of large and GIAs over a 5–10-year interval have sudden and unexpected rapid reopening and regrowth with aneurysmal rupture and increased mass effect. This is particularly common in partially thrombosed bifurcation aneurysms [3]. GIAs also have a high prevalence of intraluminal thrombus [4, 5]. This is in accordance with the classic studies by German and Black et al. According to these studies, when the ratio of intra-aneurysmal volume to area of orifice exceeds 25:1, thrombosis is likely to occur. Thus, the coils tend to migrate and compact in this intra-saccular thrombus with high recanalization rates [5]. Additionally, in GIAs, coils don't address the underlying arterial wall disease [1].

Stent-Assisted Endosaccular Coiling of GIAs
The concomitant use of stent and coils in the management of GIAs results in a lower recanalization rate of approximately 20 %. However, multiple treatment sessions with their attendant risks are still a necessity [6]. The review of 2006 for GIAs found no cases (0 %) with complete angiographic occlusion for aneurysms treated with stent-assisted coiling [1]. A recent large retrospective database of stented aneurysms revealed recanalization rate of 53.6 % in the 12 GIAs that were treated by stent-assisted coiling [7].

Comparison of Different Endosaccular Coiling Strategies
A subgroup analysis of GIAs treated with coils (including PVO, unassisted, balloon assisted, and stent assisted), in a large single center retrospective study in 2014, found the rate of complications to be 9.4 %, a recurrence rate of 52 %, and a retreatment rate of 47.6 %. The study also found higher recurrence and retreatment rates in a descending order with unassisted coiling vs. balloon-assisted coiling vs. stent-assisted coiling vs. PVO (i.e., 44 % and 37.2 % vs. 40 % and 40 % vs. 32.5 % and 26 % vs. 18.2 % and 9.2 %, respectively). Recoiling of recanalized large and GIAs (>10 mm) in this study was associated with a low complication rate of 5 % and no mortality. Other studies have shown similar low rates of morbidity in patients treated with recoiling [8].

Recurrence and Recanalization in Endosaccular Coiling of GIAs
The risk of recurrence in large and giant aneurysms (>10 mm) was 54.5 % after the first recoiling and 53.3 % after the second recoiling, proving that aneurysm recurrence remains the main problem in endosaccular coiling procedures [8]. A similar study in 2003 found recanalization rate of 59.1 % for GIAs with rates of approximately 40 % even in the initially completely occluded cases. In this study of 73 GIAs, only 26 % of patients had complete initial occlusion that improved to 40 % in the later part of the study. In this study, 12 patients had delayed aneurysm rupture on follow-up. Of these, ten patients had large or giant aneurysms [9]. This implies a near complete lack of improvement in occlusion and recanalization of GIAs treated by endosaccular techniques over the last 10 years. The authors felt that further improvement in GIA therapy warrants the use of adjunctive therapeutic techniques or devices [8].

References

1. Parkinson RJ, Eddleman CS, Batjer HH, Bendok BR (2006) Giant intracranial aneurysms: endovascular challenges. Neurosurgery 59(5 Suppl 3):S103–S112; discussion S103-113. doi:10.1227/01.neu.0000237410.32115.c9
2. Fiorella D, Lylyk P, Szikora I, Kelly ME, Albuquerque FC, McDougall CG, Nelson PK (2009) Curative cerebrovascular reconstruction with the Pipeline embolization device: the emergence of definitive endovascular therapy for intracranial aneurysms. J Neurointerv Surg 1(1):56–65. doi:10.1136/jnis.2009.000083
3. van Rooij WJ, Sluzewski M (2009) Endovascular treatment of large and giant aneurysms. AJNR Am J Neuroradiol 30(1):12–18. doi:10.3174/ajnr.A1267
4. Whittle IR, Dorsch NW, Besser M (1982) Spontaneous thrombosis in giant intracranial aneurysms. J Neurol Neurosurg Psychiatry 45(11):1040–1047
5. Gonzalez NR, Duckwiler G, Jahan R, Murayama Y, Vinuela F (2008) Challenges in the endovascular treatment of giant intracranial aneurysms. Neurosurgery 62(6 Suppl 3):1324–1335. doi:10.1227/01.neu.0000333797.59585.c0
6. Cekirge HS, Saatci I, Ozturk MH, Cil B, Arat A, Mawad M, Ergungor F, Belen D, Er U, Turk S, Bavbek M, Sekerci Z, Beskonakli E, Ozcan OE, Ozgen T (2006) Late angiographic and clinical follow-up results of 100 consecutive aneurysms treated with Onyx reconstruction: largest single-center experience. Neuroradiology 48(2):113–126. doi:10.1007/s00234-005-0007-6
7. Fiorella D, Albuquerque FC, Woo H, Rasmussen PA, Masaryk TJ, McDougall CG (2010) Neuroform stent assisted aneurysm treatment: evolving treatment strategies, complications and results of long term follow-up. J Neurointerv Surg 2(1):16–22. doi:10.1136/jnis.2009.000521
8. Chalouhi N, Tjoumakaris S, Gonzalez LF, Dumont AS, Starke RM, Hasan D, Wu C, Singhal S, Moukarzel LA, Rosenwasser R, Jabbour P (2014) Coiling of large and giant aneurysms: complications and long-term results of 334 cases. AJNR Am J Neuroradiol 35(3):546–552. doi:10.3174/ajnr.A3696
9. Wehman JC, Hanel RA, Levy EI, Hopkins LN (2006) Giant cerebral aneurysms: endovascular challenges. Neurosurgery 59(5 Suppl 3):S125–S138; discussion S123–S113. doi:10.1227/01.neu.0000237330.11482.90

Regrowth: Sidewall Versus Bifurcation Saccular GIAs (Cases 17 and 20)

Keywords: Sidewall aneurysms, Bifurcation aneurysms, Regrowth

Morphological Types of GIAs

The recanalization observed in ruptured aneurysms (including small, large, very large, and GIAs) is the major drawback of endosaccular coiling and has a prevalence between 4.7 and 33.6 %. The commonest locations with aneurysm recurrence are the basilar top (39.4 %), PCoM (37.2 %), and ACoM (25 %). A number of morphological factors were found to be associated with aneurysm recurrence at these locations [1]. There are two major morphological types of saccular GIAs: sidewall and bifurcation aneurysms [2]. Sidewall aneurysms originate from only one parent artery or from the origin of a branch that is much smaller than the parent artery (<one-fifth the parent artery diameter). Bifurcation aneurysms are located at major bifurcations in the cerebral vasculature [3].

Computational Flow Studies in Sidewall Versus Bifurcation Saccular GIAs

Hassan et al. were the first to classify aneurysms into distinct categories based on the data derived from computational flow dynamic studies that was correlated with intraoperative observation and cerebral angiography. The authors demonstrated high shear wall stress and consequent bleb formation and rupture sites that could be anywhere within a sidewall aneurysm but usually occurred at the aneurysmal inflow zone/dome. They also showed a shift in the shear stress and bleb formation away from aneurysmal wall to dome with increasing angulation of parent artery for sidewall aneurysms. Similarly they demonstrated that sidewall aneurysms with branching vessel usually ruptured at the inflow zone located at the aneurysmal side. In contrast, bifurcation aneurysms usually ruptured at their domes, but the exact site was highly dependent on the direction of the parent artery [4].

Morphological and Hemodynamic Characteristics of GIAs

A retrospective study has shown that the mean size of ruptured intracranial aneurysms is 7.76 mm, whereas the mean size in the combined group of both ruptured and unruptured aneurysms is 6.45 mm. Therefore, it is well known that the mean size of ruptured aneurysms is still less than the 10 mm critical size proposed in the International Study of Unruptured Intracranial Aneurysms (ISUIA) trial. The study of the morphological and hemodynamic aspects of intracranial aneurysms by the authors revealed that the size criterion is valid for sidewall aneurysms but not for bifurcation aneurysms [3].

It has been speculated that the coil packing density necessary to achieve aneurysmal flow stagnation is dependent on its size, type, and geometry. Aneurysmal coiling causes stagnation of blood flow and subsequent aneurysmal clotting. A stagnant volume ratio (SVR) is the ratio of the stagnant blood volume to total aneurysmal volume. The SVR tends to reach 100 % when the packing density is close to 60 %. However, in clinical practice, packing densities of 20–30 % is considered sufficient to obtain stable aneurysmal occlusion. This corresponds to an SVR of 60 % in sidewall aneurysms irrespective of the aneurysm angle. In contrast, to attain a similar SVR in bifurcation aneurysms with greater angulation, the packing density has to be higher. Thus, relatively low packing densities achieve flow stagnation within sidewall aneurysms irrespective of their angulation, but bifurcation aneurysms require higher packing densities especially when they are angled. Furthermore, in bifurcation aneurysms, the efficacy of coiling is not always the same even when the same amount of coils is used for differently angled aneurysms [5].

Hemodynamic Models of GIAs

Hemodynamic models of sidewall aneurysms mostly reveal three distinct flow zones: inflow zone at distal neck, outflow zone at proximal neck, and central area of slow flow. Flow velocities and shear stress are higher in inflow zone. Computer modeling and radiological and pathological studies have shown that saccular aneurysms grow from this inflow zone. Thus posttreatment residual necks are more likely to cause recanalization in sidewall aneurysms.

In contrast, bifurcation aneurysms have a more complex and variable hemodynamic behavior. They have variable inflow zones and higher central velocities that decrease the chances of spontaneous aneurysmal thrombosis. The inflow zone of bifurcation aneurysms depends on the geometry of the lesion and the size of parent and daughter arteries. The blood flow enters at the distal inflow zone if adjacent to a dominant outflow branch with the outflow at the nondominant branch. The blood flow enters at the central portion of the aneurysm if the outflow branches are relatively symmetrical. These intricate features of bifurcation aneurysms adversely affect the technical success of endovascular coiling, as there is an increased rate of coil compaction, redistribution, and dislodgement [2].

References

1. Songsaeng D, Geibprasert S, ter Brugge KG, Willinsky R, Tymianski M, Krings T (2011) Impact of individual intracranial arterial aneurysm morphology on initial obliteration and recurrence rates of endovascular treatments: a multivariate analysis. J Neurosurg 114(4):994–1002. doi:10.3171/2010.8.JNS10241
2. Gonzalez NR, Duckwiler G, Jahan R, Murayama Y, Vinuela F (2008) Challenges in the endovascular treatment of giant intracranial aneurysms. Neurosurgery 62(6 Suppl 3):1324–1335. doi:10.1227/01.neu.0000333797.59585.c0
3. Baharoglu MI, Lauric A, Gao BL, Malek AM (2012) Identification of a dichotomy in morphological predictors of rupture status between sidewall- and bifurcation-type intracranial aneurysms. J Neurosurg 116(4):871–881. doi:10.3171/2011.11.jns11311
4. Hassan T, Timofeev EV, Saito T, Shimizu H, Ezura M, Matsumoto Y, Takayama K, Tominaga T, Takahashi A (2005) A proposed parent vessel geometry-based categorization of saccular intracranial aneurysms: computational flow dynamics analysis of the risk factors for lesion rupture. J Neurosurg 103(4):662–680. doi:10.3171/jns.2005.103.4.0662
5. Otani T, Nakamura M, Fujinaka T, Hirata M, Kuroda J, Shibano K, Wada S (2013) Computational fluid dynamics of blood flow in coil-embolized aneurysms: effect of packing density on flow stagnation in an idealized geometry. Med Biol Eng Comput 51(8):901–910. doi:10.1007/s11517-013-1062-5

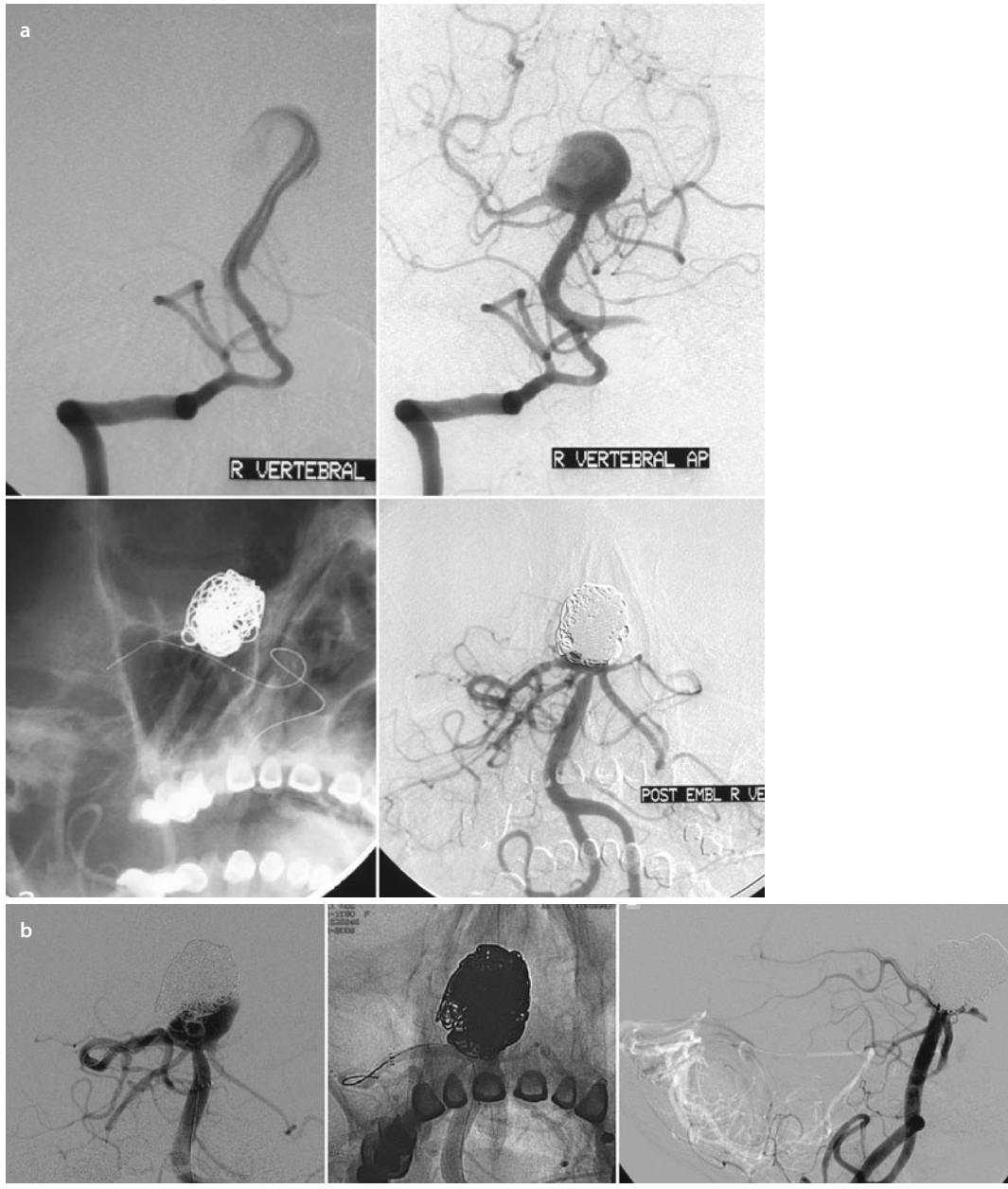

Fig. 17.1 A 56-year-old lady presented with headaches and diplopia. (**a**) Radiological examination revealed an unruptured basilar top GIA incorporating the origins of bilateral PCAs and SCAs. On May 2006, the patient was treated with balloon-assisted coiling of the aneurysm. A transverse *balloon remodeling technique* was used with the balloon navigated across the left PCoM and inflated horizontally at the basilar tip to create a neck. Postprocedural DSA reveals complete occlusion of the aneurysm. (**b**) On a 2-month follow-up radiological examination, the patient had aneurysmal regrowth. On July 2006, the second treatment was done using an Enterprise® (Cordis, Miami Lakes, FL) 4 × 20 mm stent by "stent-assisted coiling" of aneurysm with total aneurysmal occlusion

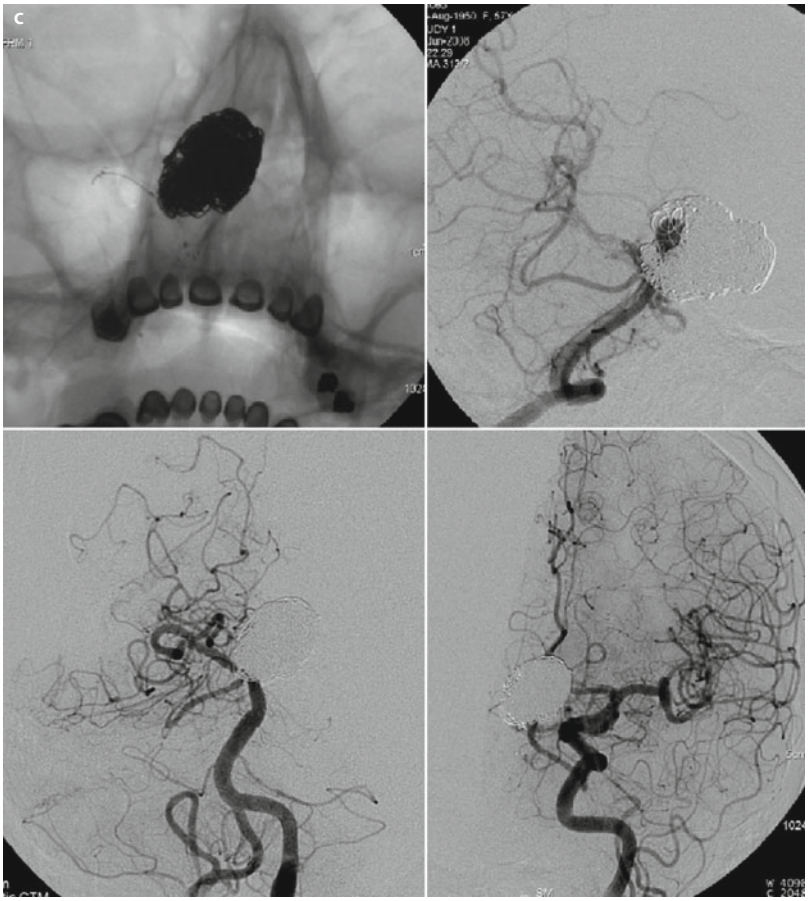

Fig. 17.1 (continued) (**c**) On a 2-year follow-up angiogram after the second treatment, further aneurysmal regrowth is seen. On June 2008, the patient was re-treated with balloon-remodeled coiling of the aneurysmal regrowth and intentional occlusion of left PCA origin. This was done to convert a bifurcation aneurysm to a sidewall aneurysm as the PCoM was adequate to supply the distal left PCA territory

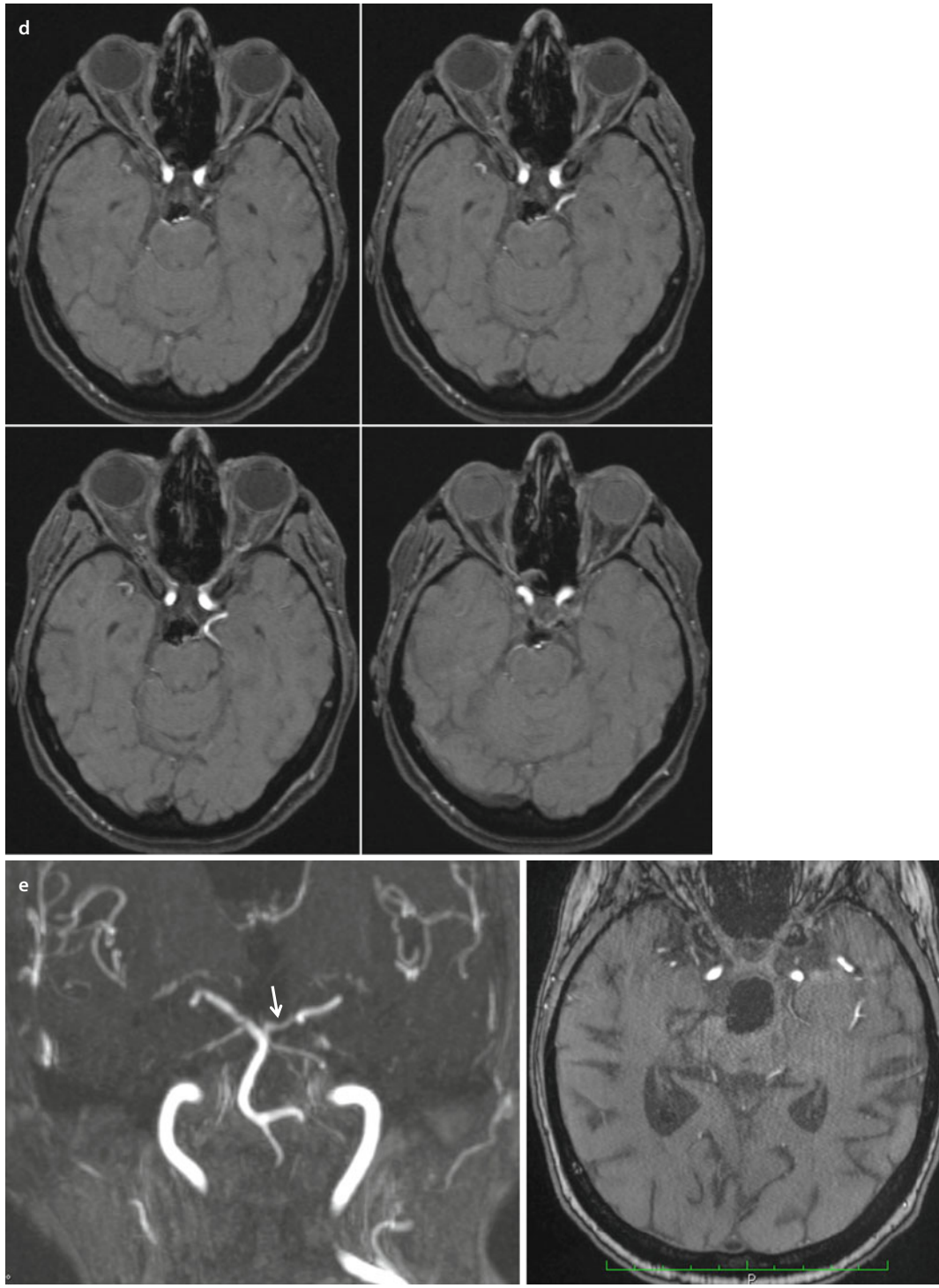

Fig. 17.1 (continued) (**d**, **e**) Follow-up MRI with TOF MRA one and a half years and CE-MRA 8 years after the third treatment shows remodeling of the aneurysmal segment with no further opacification of aneurysm. There are no parenchymal lesions in the brainstem, diencephalon, and left occipital lobe. However, there is reopening of the previously occluded left PCA origin (*arrow*)

Case 18

N. Kocer, *Giant Intracranial Aneurysms*, DOI 10.1007/978-3-319-41788-2_18

Buddy Wire Technique in Bifurcation Aneurysms [1]

Keywords: Bifurcation aneurysm, Y-stenting, Buddy wire technique

Aim of Buddy Wire Technique in Bifurcation Aneurysms

The buddy wire technique was designed to facilitate cannulation and deployment of the second stent in Y-stenting of distal bifurcation aneurysms with difficult bifurcation angles.

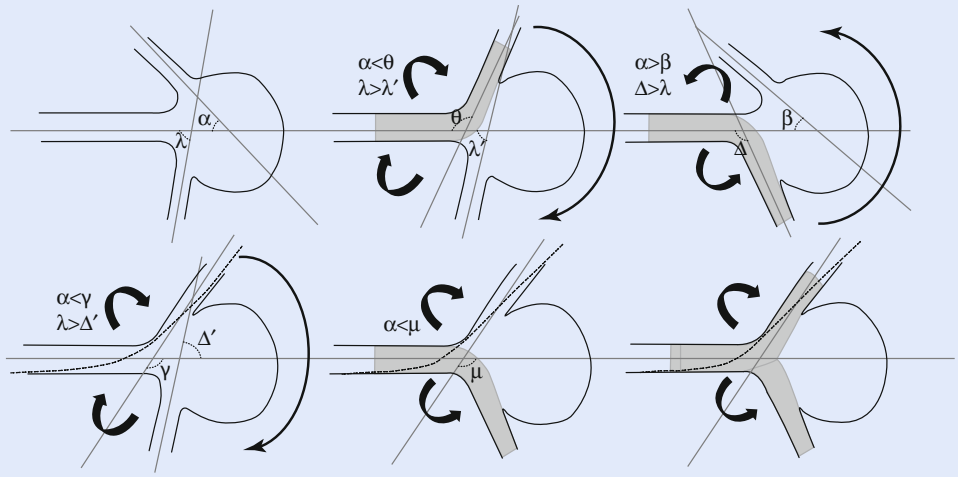

Technical Description

The first illustration depicts the MCA and its bifurcation angles. The second illustration shows the changed angulation if the first stent was deployed into upper division. The angulation of upper division would increase from acute to obtuse, and the angulation of lower division would become more acute due to clockwise rotation of MCA bifurcation. The third illustration depicts the changed circumstances if the first stent was deployed into lower division. This would cause the lower right-angled branching to change to an obtuse angle, whereas the upper division would become more acute due to anticlockwise rotation of MCA bifurcation.

The lower panel images depict the utility of a buddy wire. The initial use of a buddy wire in upper division, prior to stent deployment, would change the angulation of the upper division to an obtuse angle. This facilitates MCA bifurcation Y-stenting by a technically feasible deployment of the first stent in the lower division followed by deployment of the second stent in upper division.

Reference

1. Islak C, Kizilkilic O, Kocak B, Saglam M, Yildiz B, Kocer N (2014) Use of buddy wire to facilitate Y-configured stent placement in middle cerebral artery bifurcation aneurysms with daughter branches arising from the sac: a technical note. Neurosurgery 10(Suppl 1):E167–E171; discussion E171. doi:10.1227/neu.0000000000000130

Y-Stenting in Bifurcation Aneurysms

Keywords: Bifurcation aneurysm, Y-stenting, Flow remodeling, Angular remodeling

Why Y-Stenting?

Stent-assisted coiling is an established treatment strategy for wide-neck aneurysms. However, in cases with unfavorable arterial anatomy and very wide-neck bifurcation aneurysms, it has limited efficacy. Balloon-assisted coiling is an alternative option but may not be suitable for complex aneurysms [1]. Hemodynamic studies show bifurcation aneurysms to have a complex and variable hemodynamic behavior. They are also more prone to coil compaction, redistribution, and dislodgment compared to sidewall aneurysms [2]. Bifurcation aneurysms treated using flow diverters often have suboptimal results with persistent aneurysmal opacification and uncertainty (in-stent stenosis/occlusion) regarding the covered branches [1].

Y-Stenting Techniques

Y-stent-assisted coiling (also known as Y-stenting) is a useful technique for bifurcation aneurysms. Chow et al. first described Y-stenting in 2004 [1]. There are three well-described Y-stenting techniques: crossing Y-, kissing Y-, and non-overlapping Y-stenting [3, 4]. The most commonly used Y-stenting technique is crossing Y-stent, as hemodynamic studies have shown the technique to be associated with the greatest reduction in velocity and shear wall stress [4].

Y-stenting provides simultaneous scaffolding of the aneurysmal neck and protection of distal arterial branches. Y-stenting decreases the risk of coil prolapse and PVO associated with coiling or single stent-coiling techniques. It also enables coiling of very wide-neck and complex aneurysms that are otherwise not amenable to other endovascular techniques [5, 6].

Hemodynamic Study in Y-Stenting

An in vitro hemodynamic study using digital particle velocimetry of Y-stenting revealed a decrease in velocity of jet entering the aneurysm by 11 %. Also, there was a significant decrease in shear stress during diastole with increased duration of reduction in shear wall stresses and vorticity. The decrease in shear stress was prominent at the end of cardiac cycle and was more than 40 % compared to controls [7]. This effect is also known as "flow remodeling."

A recent study on Y-stenting has also shown an "angular remodeling" effect in bifurcation aneurysms. Y-stenting causes straightening of bifurcation and narrows the effective aneurysmal neck. It causes a statistically significant distal shift in the flow impingement zone of bifurcation aneurysms. Both the aforementioned effects promote progressive aneurysmal thrombosis and occlusion of bifurcation aneurysms that are treated by Y-stenting [1, 4].

Flow Diversion in Y-Stenting

A case series in 2011 showed that Y-stenting alone without coiling was sufficient to occlude small bifurcation aneurysms. This was due to the aforementioned hemodynamic effects of Y-stenting. However, the bifurcation GIAs in the series continued to have residual filling [8]. This suggests that the flow-diversion effect of Y-stenting alone was insufficient to occlude giant bifurcation aneurysms.

Initial clinical studies of Y-stenting were done using stents with open cell design [9]. With the availability of closed cell stents, studies showed a decrease in recanalization and retreatment rates. Therefore, at present close cell stents are preferred in Y-stenting [10].

Limitations of Y-Stenting

Y-stenting also has its own limitations, namely, although the distal branches are well protected in Y-stenting, perforators arising from the bifurcation itself may not be fully protected especially if the 3D aneurysmal shape is complex and the coils herniate outside the stent construct [11]. The major concern when using two closed cell stents in Y-stenting is the navigation through the first deployed stent. This is difficult to accomplish compared to open cell stents. Also, the second stent is narrowed along its passage through the first stent; this may increase the risk of thromboembolism, cause impingement, and decrease the long-term patency of the stented segment [12]. However, studies have not shown any significant increase in thromboembolic events with Y-stenting using two closed cell stents when compared to stent-assisted coiling [1, 13].

Y-Stenting in MCA Aneurysms

Sani et al. were the first to demonstrate the successful use of Y-stenting in MCA bifurcation aneurysms [14]. Since then, a number of large studies have demonstrated its use in MCA bifurcation aneurysms with acceptable morbidity and mortality rates [6, 15, 16]. On review of patients with bifurcation GIAs treated with Y-stenting in large case series (>10 patients), data regarding recanalization was available in a single series. In this series, GIAs had a recanalization rate of 40 % (2/5 GIAs) after initial complete occlusion [1, 13].

References

1. Limbucci N, Renieri L, Nappini S, Consoli A, Rosi A, Mangiafico S (2016) Y-stent assisted coiling of bifurcation aneurysms with enterprise stent: long-term follow-up. J Neurointerv Surg 8(2):158–162. doi:10.1136/neurintsurg-2014-011483
2. Gonzalez NR, Duckwiler G, Jahan R, Murayama Y, Vinuela F (2008) Challenges in the endovascular treatment of giant intracranial aneurysms. Neurosurgery 62(6 Suppl 3):1324–1335. doi:10.1227/01.neu.0000333797.59585.c0
3. Zhao KJ, Yang PF, Huang QH, Li Q, Zhao WY, Liu JM, Hong B (2012) Y-configuration stent placement (crossing and kissing) for endovascular treatment of wide-neck cerebral aneurysms located at 4 different bifurcation sites. AJNR Am J Neuroradiol 33(7):1310–1316. doi:10.3174/ajnr.A2961
4. Saglam M, Kizilkilic O, Anagnostakou V, Yildiz B, Kocer N, Islak C (2015) Geometrical characteristics after Y-stenting of the basilar bifurcation. Diagn Interv Radiol 21(6):483–487. doi:10.5152/dir.2015.14523
5. Heller RS, Rahal JP, Malek AM (2014) Y-Stent embolization technique for intracranial bifurcation aneurysms. Clin Neurosci Off J Neurosurg Soc Australasia 21(8):1368–1372. doi:10.1016/j.jocn.2013.11.028
6. Bartolini B, Blanc R, Pistocchi S, Redjem H, Piotin M (2014) "Y" and "X" stent-assisted coiling of complex and wide-neck intracranial bifurcation aneurysms. AJNR Am J Neuroradiol 35(11):2153–2158. doi:10.3174/ajnr.A4060
7. Canton G, Levy DI, Lasheras JC (2005) Hemodynamic changes due to stent placement in bifurcating intracranial aneurysms. J Neurosurg 103(1):146–155. doi:10.3171/jns.2005.103.1.0146
8. Cekirge HS, Yavuz K, Geyik S, Saatci I (2011) A novel "Y" stent flow diversion technique for the endovascular treatment of bifurcation aneurysms without endosaccular coiling. AJNR Am J Neuroradiol 32(7):1262–1268. doi:10.3174/ajnr.A2475
9. Fargen KM, Hoh BL, Welch BG, Pride GL, Lanzino G, Boulos AS, Carpenter JS, Rai A, Veznedaroglu E, Ringer A, Rodriguez-Mercado R, Kan P, Siddiqui A, Levy EI, Mocco J (2012) Long-term results of enterprise stent-assisted coiling of cerebral aneurysms. Neurosurgery 71(2):239–244; discussion 244. doi:10.1227/NEU.0b013e3182571953
10. Chalouhi N, Jabbour P, Singhal S, Drueding R, Starke RM, Dalyai RT, Tjoumakaris S, Gonzalez LF, Dumont AS, Rosenwasser R, Randazzo CG (2013) Stent-assisted coiling of intracranial aneurysms: predictors of complications, recanalization, and outcome in 508 cases. Stroke J Cerebral Circ 44(5):1348–1353. doi:10.1161/strokeaha.111.000641
11. Wehman JC, Hanel RA, Levy EI, Hopkins LN (2006) Giant cerebral aneurysms: endovascular challenges. Neurosurgery 59(5 Suppl 3):S125–S138; discussion S123–S123. doi:10.1227/01.neu.0000237330.11482.90
12. Jeon P, Kim BM, Kim DJ, Kim DI, Park KY (2014) Y-configuration double-stent-assisted coiling using two closed-cell stents for wide-neck basilar tip aneurysms. Acta Neurochir 156(9):1677–1686. doi:10.1007/s00701-014-2163-0
13. Yavuz K, Geyik S, Cekirge S, Saatci I (2013) Double stent-assisted coil embolization treatment for bifurcation aneurysms: immediate treatment results and long-term angiographic outcome. AJNR Am J Neuroradiol 34(9):1778–1784. doi:10.3174/ajnr.A3464
14. Sani S, Lopes DK (2005) Treatment of a middle cerebral artery bifurcation aneurysm using a double neuroform stent "Y" configuration and coil embolization: technical case report. Neurosurgery 57(1 Suppl):E209; discussion E209
15. Suzuki S, Tateshima S, Jahan R, Duckwiler GR, Murayama Y, Gonzalez NR, Vinuela F (2009) Endovascular treatment of middle cerebral artery aneurysms with detachable coils: angiographic and clinical outcomes in 115 consecutive patients. Neurosurgery 64(5):876–888; discussion 888–889. doi:10.1227/01.neu.0000343534.05655.37
16. Johnson AK, Heiferman DM, Lopes DK (2013) Stent-assisted embolization of 100 middle cerebral artery aneurysms. Journal of neurosurgery 118(5):950–955. doi:10.3171/2013.1.jns121298

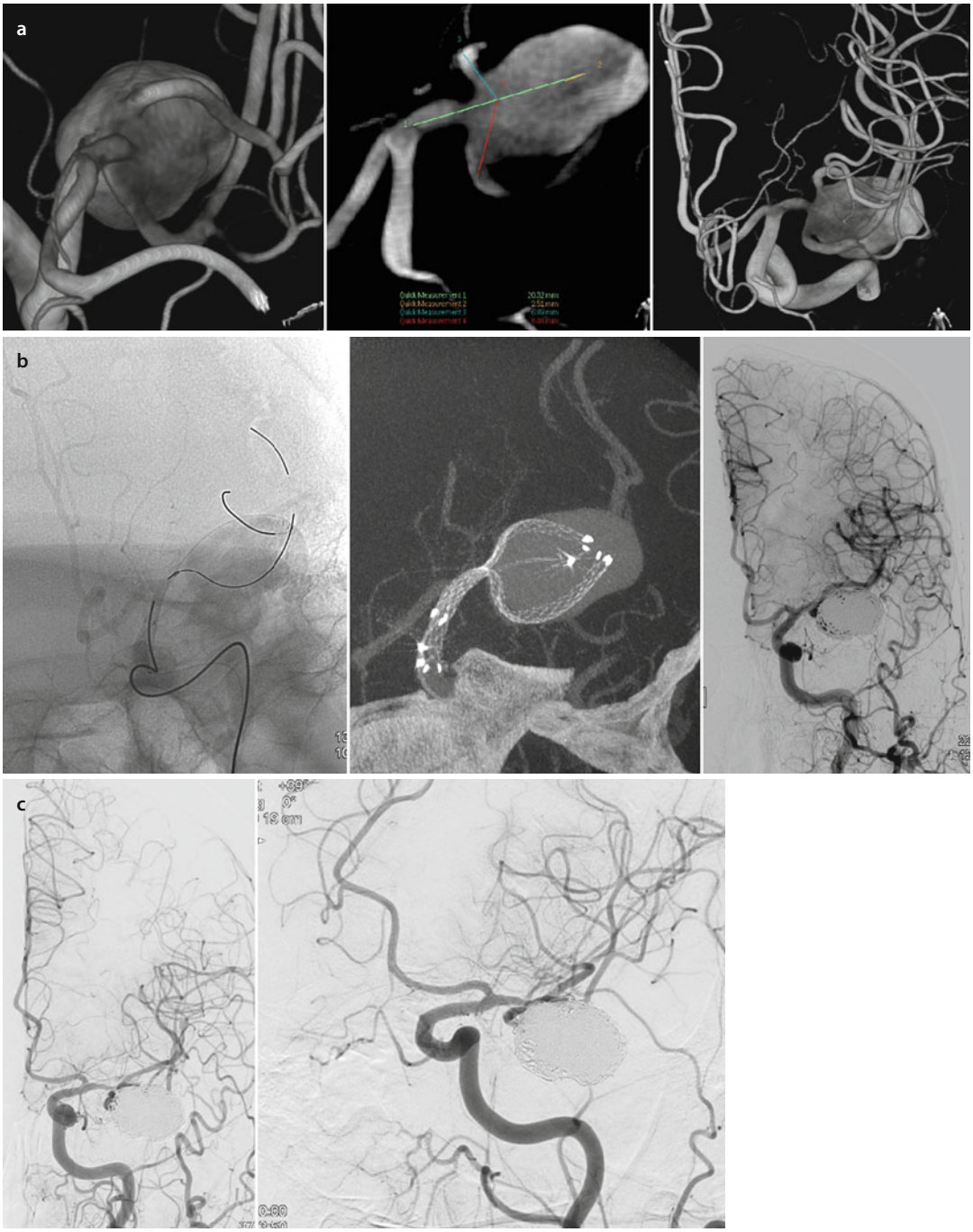

Fig. 18.1 A 60-year-old man planned for cardiac surgery presented with headaches. (**a**) Cerebral DSA reveals a 25 × 17 mm-sized left MCA bifurcation GIA. The aneurysm involves the origin and proximal portions of both the upper and lower divisions of MCA. The upper division arises at an acute angle (57°), whereas the lower division arises at a right angle (90°). (**b**) A buddy wire was navigated into the upper division to change the acute angle to an obtuse angle. Subsequently, the stent delivery system was navigated into the lower division. After deployment of the stent in the lower division, another stent was deployed in the upper division across the bifurcation aneurysm. Post-stenting; VASO CT® images reveal Y-stent configuration and the final changed angle of MCA bifurcation. Immediate post-stenting and coiling images reveal near-complete occlusion of MCA bifurcation aneurysm. (**c**) On 2-year follow-up, there was mild neck recanalization but otherwise stable aneurysm occlusion

Case 19

N. Kocer, *Giant Intracranial Aneurysms*, DOI 10.1007/978-3-319-41788-2_19

Metal Artifact Reduction in Flat Panel Detector CT (FDCT)

Keywords: Flat panel detector CT, Metal artifact, MAR algorithm

Why FDCT?

Flow diverter stents are designed to be highly flexible, low profile with excellent trackability. This enables their use in tortuous and challenging intracranial anatomy. The designing of FDs limits the amount of radiopacity that can be incorporated into FDs. Hence intraprocedural and postprocedural visualization of FDs by conventional radiography are inadequate. To overcome this drawback, FDCT with its better resolution and improved cone-beam volume CT images (MPR and 3D reconstruction) was developed [1].

FDCT Versus MDCT

In comparison to multi-detector CT (MDCT), FDCT has superior spatial resolution and is advantageous for imaging intracranial vessels, especially calcified plaques, stents, and aneurysms [2]. The isotropic voxel size of FDCT is <0.15 mm^3 [3]. FDCT has a similar contrast resolution for high-contrast structures but a clinically negligible inferior resolution for low-contrast structures compared to MDCT. The radiation dose for the head is lower in FDCT compared to MDCT. However, the image noise is approximately 55–71 % higher than MDCT. CT number uniformity and accuracy are also worse with FDCT compared to MDCT [2].

Types and Uses of FDCT

FDCT has been used for intraoperative monitoring of neuroendovascular procedures. It is useful for visualization and characterization of low-profile and radiopaque intracranial stents. In-stent stenosis, calcified plaque and stent-vessel interface that are not visualized by radiography or DSA can be depicted by FDCT [2].

IAFDCTA is useful to visualize intracranial stents and in simultaneous imaging of stent and parent vessel. Its accuracy has been correlated with DSA and histology in assessing degree of in-stent stenosis following stents and FDs. Its accuracy in assessing the status of PED® apposition to vessel wall has been validated with catheter optical coherence tomography. A study in 2016 showed that the accuracy of a 20 s IVFDCTA was good and not substantially different from IAFDCTA in assessing PED®-paved arteries [2]. It is useful for follow-up imaging in cerebral aneurysms and other vascular diseases [3, 4].

FDCT in Cerebral Aneurysm Therapy

Following aneurysm treatment, both coiling and clipping, there is a 4–18 % incidence of neck remnant. In the International Subarachnoid Aneurysm Trial (ISAT), the incidence of re-bleed on an 18-year follow-up ranges from 0.49 in clipping group to 1.56 in endovascular group per 1000 patient-years [3, 5]. Long-term follow-up has shown regrowth of aneurysm and de novo aneurysm formation in these patients. Cerebral DSA and 3D angiography are considered the "gold standard" in the depiction of aneurysm remnants. MRA, CTA, and more recently IVFDCTA have been used as alternate imaging modalities in follow-up of these patients. IVFDCTA has been shown to have a higher sensitivity and specificity compared to IA DSA when metal artifacts do not degrade the image quality. Additionally, the volumetric dataset of FDCTA enables multiplanar reformations of cerebral parenchyma enabling detection of postoperative changes (like hemorrhage, hygroma etc.) [3]. However, metal artifacts due to beam hardening, scattered radiation, and sampling and noise artifacts remain a problem in the presence of embolization coils. Metal artifacts obscure the diagnostic value of the FDCT ROI in close proximity to coils [2].

Metal Artifact Reduction (MAR) Algorithm in FDCT

In cases of stent-assisted coiling, the high x-ray absorption by coil mass generates streak artifacts that obscure surrounding structures. In the 1980s, Glover and Pelc and Kalender et al. suggested manipulating raw data before reconstruction to reduce metallic artifacts. Various methods to reduce metallic artifacts were proposed including different methods of segmentation and interpolation, dual energy, iterative reconstruction, manipulation of reconstructed CT data, and combination of methods [6]. Prell et al. proposed the first FDCT adequate metal artifact reduction (MAR) algorithm that used a nonlinear interpolation to replace corrupted data and decrease metal artifacts [7]. Prell et al. elaborated on the method by Kalender et al. for FDCT that replaces underexposed pixels in raw projection images rather than sinograms. They also showed that 3D linear interpolation is less prone to introduce new artifacts than a technique that uses fewer dimensions. This resulted in an overall improvement in the visibility of neurovascular implants and surrounding structures [6]. The MAR algorithm can be generated by multipass reconstruction algorithm, variations of linear interpolation proposed by Prell et al., nonlinear interpolation, segmentation-based interpolation, and fusion-based prior image approach [8].

Advantages and Limitations of MAR Algorithm FDCT

The severity of metal artifacts depends on the kind, size, and material of the implants. MAR algorithms have been shown to reduce metal artifacts and improve assessment of aneurysm remnants and vascular structures. It allows assessment of in situ vascular implants and host arteries with 3D spatial information and demonstrates adjacent vascular anatomy, potential clot formation, stent-wall apposition, stent herniation, recanalization, intimal tissue growth, and intimal hyperplasia.

However, MAR does not significantly improve assessment of aneurysm remnants, in a number of cases with large coil packages. For such cases, TOF MR angiography might also be used for follow-up imaging [8]. *In our experience, CE MR angiograms can also be used for visualization of aneurysm remnants in large coil masses*.

Studies have also found that despite significant reduction in blurred regions and secondary artifacts, visualization of liquid embolized structures and its surroundings was not significantly improved by MAR algorithms. Furthermore, imprecise boundary definition induces residual streak artifacts in the newly reconstructed volume with onyx® casts, as they are inhomogeneous structures with varying densities [7, 9]. The post-processing time for MAR algorithm based FDCT was quite long compared to the time required for a normal CT reconstruction [8].

References

1. Kizilkilic O, Kocer N, Metaxas GE, Babic D, Homan R, Islak C (2012) Utility of VasoCT in the treatment of intracranial aneurysm with flow-diverter stents. J Neurosurg 117(1):45–49. doi:10.3171/2012.4.jns111660
2. Yu SC, Lee KT, Lau TW, Wong GK, Pang VK, Chan KY (2016) Intravenous C-arm conebeam CT angiography following long-term flow-diverter implantation: technologic evaluation and preliminary results. AJNR Am J Neuroradiol 37(3):481–486. doi:10.3174/ajnr.A4558
3. Psychogios MN, Wachter D, Mohr A, Schramm P, Frolich AM, Jung K, Rohde V, Knauth M (2011) Feasibility of flat panel angiographic CT after intravenous contrast agent application in the postoperative evaluation of patients with clipped aneurysms. AJNR Am J Neuroradiol 32(10):1956–1962. doi:10.3174/ajnr.A2611
4. Doerfler A, Golitz P, Engelhorn T, Kloska S, Struffert T (2015) Flat-panel computed tomography (DYNA-CT) in neuroradiology. From high-resolution imaging of implants to one-stop-shopping for acute stroke. Clin Neuroradiol 25(Suppl 2):291–297. doi:10.1007/s00062-015-0423-x
5. Molyneux AJ, Birks J, Clarke A, Sneade M, Kerr RS (2015) The durability of endovascular coiling versus neurosurgical clipping of ruptured cerebral aneurysms: 18 year follow-up of the UK cohort of the International Subarachnoid Aneurysm Trial (ISAT). Lancet (London, England) 385(9969):691–697. doi:10.1016/s0140-6736(14)60975-2
6. van der Bom IM, Hou SY, Puri AS, Spilberg G, Ruijters D, van de Haar P, Carelsen B, Vedantham S, Gounis MJ, Wakhloo AK (2013) Reduction of coil mass artifacts in high-resolution flat detector conebeam CT of cerebral stent-assisted coiling. AJNR Am J Neuroradiol 34(11):2163–2170. doi:10.3174/ajnr.A3561
7. Stidd DA, Theessen H, Deng Y, Li Y, Scholz B, Rohkohl C, Jhaveri MD, Moftakhar R, Chen M, Lopes DK (2014) Evaluation of a metal artifacts reduction algorithm applied to postinterventional flat panel detector CT imaging. AJNR Am J Neuroradiol 35(11):2164–2169. doi:10.3174/ajnr.A4079
8. Pjontek R, Onenkoprulu B, Scholz B, Kyriakou Y, Schubert GA, Nikoubashman O, Othman A, Wiesmann M, Brockmann MA (2015) Metal artifact reduction for flat panel detector intravenous CT angiography in patients with intracranial metallic implants after endovascular and surgical treatment. J Neurointerv Surg. doi:10.1136/neurintsurg-2015-011787
9. Hung SC, Wu CC, Lin CJ, Guo WY, Luo CB, Chang FC, Chang CY (2014) Artifact reduction of different metallic implants in flat detector C-arm CT. AJNR Am J Neuroradiol 35(7):1288–1292. doi:10.3174/ajnr.A3851

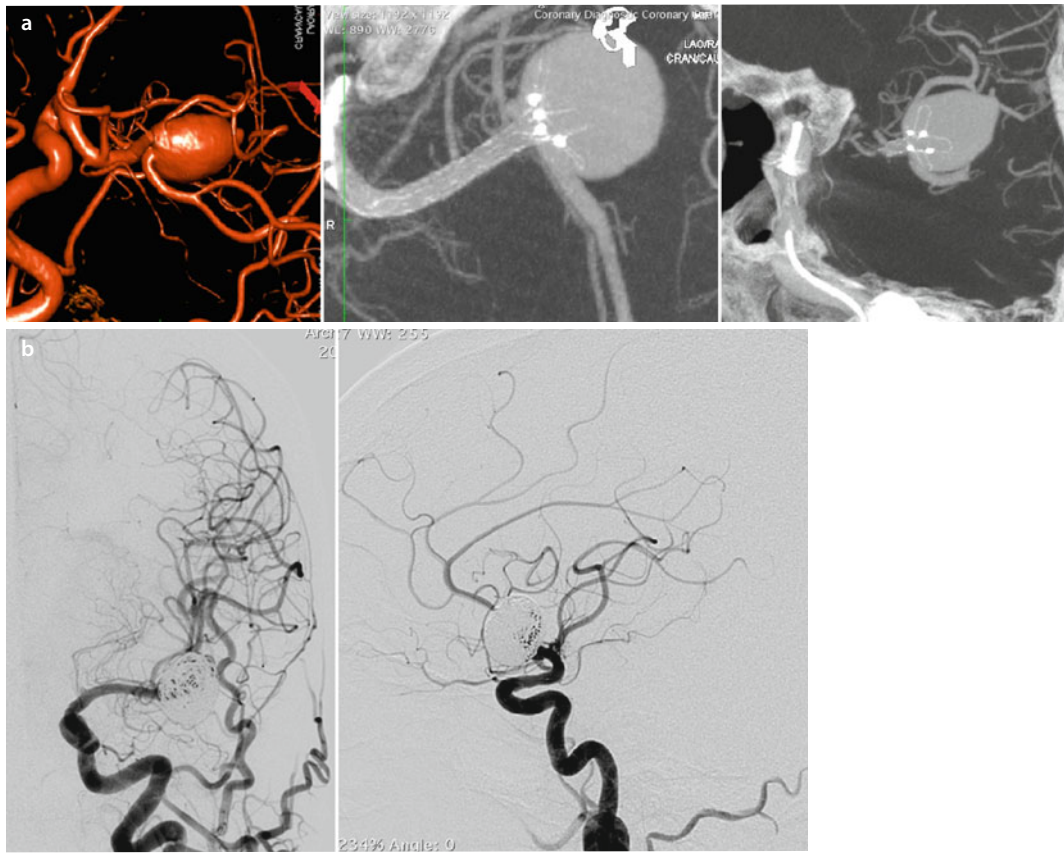

Fig. 19.1 A 56-year-old right-handed woman presented in 1 December 2013 with an unruptured ACoM and left MCA GIA. (**a**) 3D and IAFDCTA (DYNA CTA®) reveal the MCA aneurysm incorporating both the upper and lower divisions of MCA. The initial course of the upper division is acutely angulated with a tight hairpin bend in its proximal segment. A pCONus® (Phenox GmbH, Bochum, Germany) bifurcation device was deployed to protect the origins of both the upper and lower divisions of MCA. (**b**) The MCA aneurysm was then coiled with a near-total occlusion. The ACoM aneurysm was also treated with Y-stenting and coiling

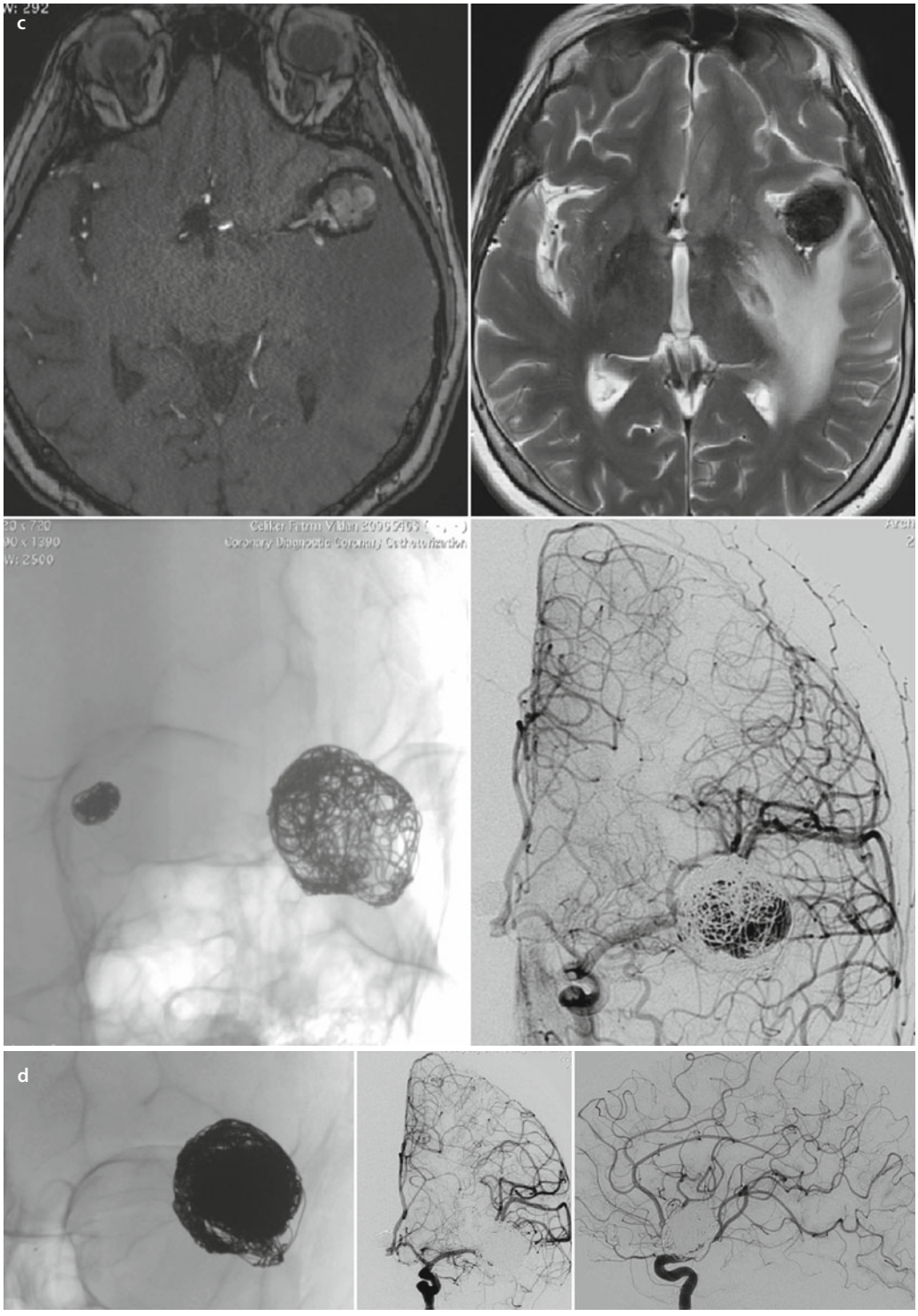

Fig. 19.1 (continued) (**c**) After 10 months, MRI and cerebral DSA reveal enlargement of the entire MCA aneurysm with coil compaction to its periphery. There is massive peri-aneurysmal vasogenic edema probably due to its pulsatility effect. (**d**) On October 2014, the patient was re-treated with coiling of the regrowth followed by a 2.75 × 20 mm-sized PED® FD that was deployed starting from the lower branch of MCA and extending telescopically through the pCONus® (Phenox GmbH, Bochum, Germany) device into the M1 segment

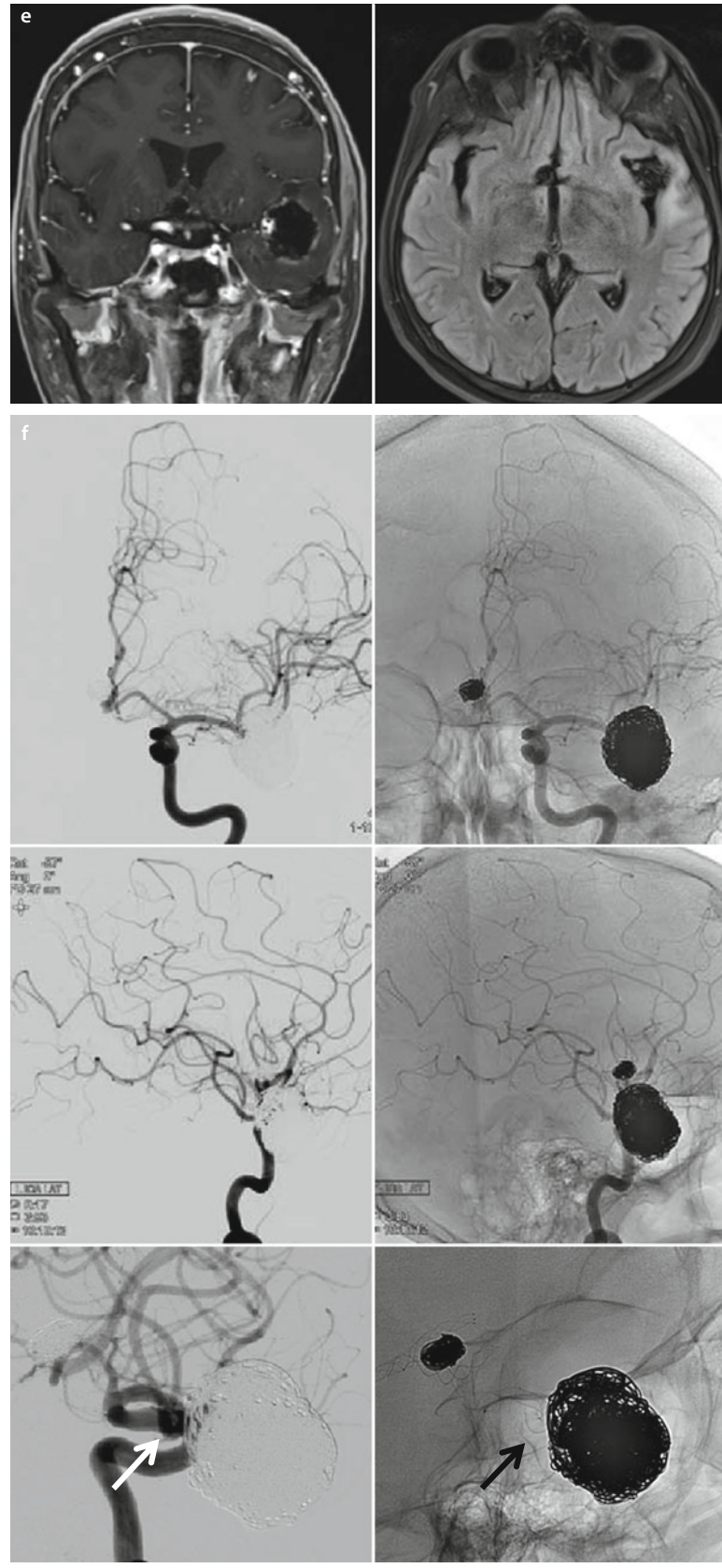

Fig. 19.1 (continued) (**e**) At 1-month follow-up after the second treatment, MRI FLAIR and postcontrast T1W coronal images reveal resolution of the vasogenic edema with a small residual aneurysmal neck filling. (**f**) At 1.5 years after the second treatment, DSA shows total occlusion of the aneurysm with patent lower MCA branch which is stented with PED® (*arrow*) and upper MCA branch

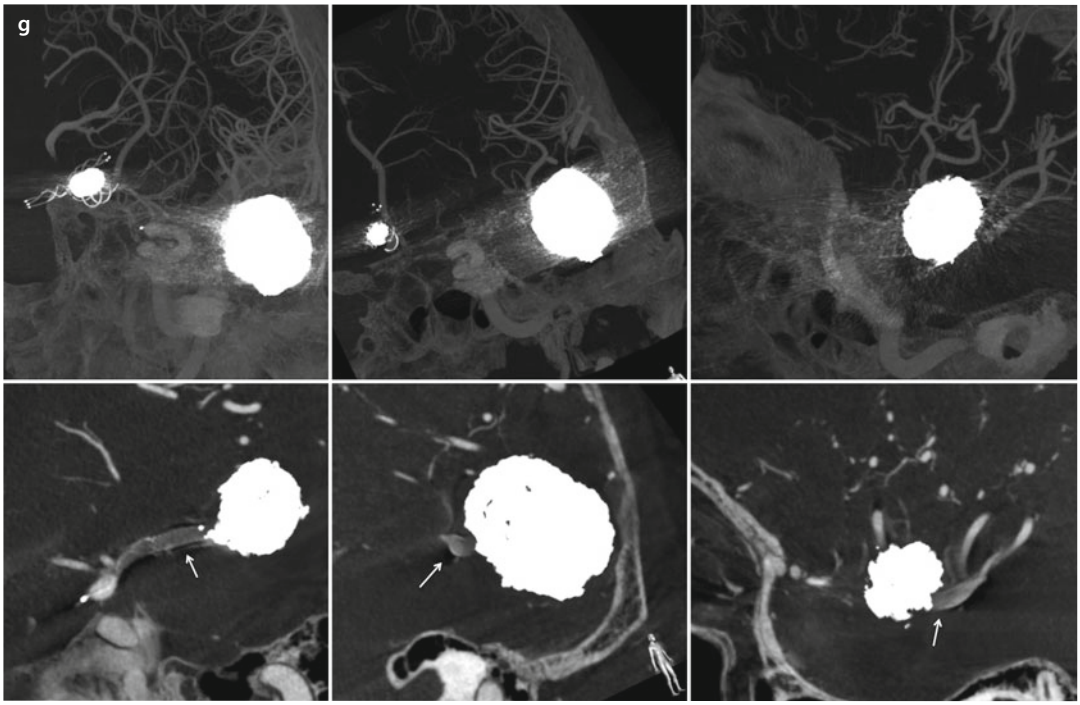

Fig. 19.1 (continued) (**g**) IA VASO CT® Image Panel. Upper row: M1, MCA bifurcation, and M2 segments are hidden by metal artifact from the coils, pCONus® (Phenox GmbH, Bochum, Germany) and PED® devices. Lower row: Post-FDCT metal artifact reduction (MAR) algorithm images reveal the formerly non-visualized M1 segment, proximal lower trunk, and distal lower trunk of MCA that are stented with PED® (*arrow*)

Case 20

N. Kocer, *Giant Intracranial Aneurysms*, DOI 10.1007/978-3-319-41788-2_20

Stent-Assisted Onyx Embolization

Keywords: Giant aneurysm, Onyx embolization, Stent assisted

Stent with Onyx Technique

The original technique of GIA treatment by Onyx 500HD® consisted of DMSO compatible balloon inflation across the aneurysmal neck with a confirmatory seal test followed by intermittent deflation during GIA occlusion [1]. However, the first three patients with GIAs, treated by balloon remodeled onyx® embolization had recanalization. This prompted the authors to reconstruct the aneurysm bearing dysplastic arterial wall with a BMS [2,3]. The first instance was serendipitous when the sealing balloon partially prolapsed into aneurysm during seal test. This prompted the authors to use a BMS across the aneurysmal neck. The balloon of BMS was previously tested for DMSO and Onyx® compatibility. Therefore, after deployment of the stent across aneurysmal neck, the same balloon was used to perform a seal test and inject Onyx® [2].

Advantages and Disadvantages of Stent-Assisted Onyx Embolization

There are a few studies that describe combined use of BMS and onyx® in the treatment of GIAs. In a small series of 11 patients with GIAs, there was residual filling of the GIA in two patients, one of which subsequently occluded on the 6-month follow-up angiogram. In this small series, there were 2 major procedural complications; one patient had parent artery dissection due to balloon over-inflation followed by a fatal ICH. The second patient had a watershed ischemic infarct due to prolonged balloon inflation [2,4]. In another series, on subgroup analysis of 25 patients treated with balloon expandable stent and onyx combination, there was 4% recanalization at 3 to 6 month follow up and one patient died (4%) due to stent related dissection and delayed aneurysm rupture. An additional four patients with GIAs could not be treated in this select group, as the stent could not be navigated across the aneurysmal neck [2]. There is also an ever-present risk of onyx® migration into the parent artery and distal embolization during its use in aneurysmal occlusion [4]. An experimental study using Onyx HD 500® with adjunctive devices (stents, coils, balloons both proximally and across aneurysmal neck) has shown intractable migration of onyx into parent artery irrespective of the adjunctive device (Migration rate 9%-33%). However, the study did show a lower rate of onyx migration when used with stents compared to other techniques [5].

Self-Expanding Stents and Onyx®

In a study of 46 patients with 47 aneurysms treated with onyx 500 HD®, the authors' encountered onyx cast instability in 4 patients (9%). There were two types of instability: en-mass movement of the entire onyx® cast and a pulsating onyx® tail in the parent artery. This prompted the authors to use self-expanding stents to stabilize the cast and prevent cast dislodgement and distal embolization.

The authors used stent remodeling of Onyx HD 500® in patients with GIAs, aneurysms with very wide necks, recanalised aneurysms, balloon prolapse into aneurysmal sac during seal test and in shallow, wide necked aneurysms. This was done to stabilize the onyx® cast [6].

References

1. Cekirge HS, Saatci I, Ozturk MH, Cil B, Arat A, Mawad M, Ergungor F, Belen D, Er U, Turk S, Bavbek M, Sekerci Z, Beskonakli E, Ozcan OE, Ozgen T (2006) Late angiographic and clinical follow-up results of 100 consecutive aneurysms treated with Onyx reconstruction: largest single-center experience. Neuroradiology 48(2):113–126. doi:10.1007/s00234-005-0007-6
2. Mawad ME, Cekirge S, Ciceri E, Saatci I (2002) Endovascular treatment of giant and large intracranial aneurysms by using a combination of stent placement and liquid polymer injection. Journal of Neurosurgery 96(3):474–482. doi:10.3171/jns.2002.96.3.0474
3. Murayama Y, Vinuela F, Tateshima S, Vinuela F Jr., Akiba Y (2000) Endovascular treatment of experimental aneurysms by use of a combination of liquid embolic agents and protective devices. AJNR American journal of neuroradiology 21(9):1726–1735
4. Simon SD, Lopes DK, Mericle RA (2010) Use of intracranial stenting to secure unstable liquid embolic casts in wide-neck sidewall intracranial aneurysms. Neurosurgery 66(3 Suppl Operative):92–97; discussion 97–98. doi:10.1227/01.neu.0000350983.03348.06
5. van Rooij WJ, Sluzewski M (2009) Endovascular treatment of large and giant aneurysms. AJNR American Journal of Neuroradiology 30(1):12–18. doi:10.3174/ajnr.A1267
6. Weber W, Siekmann R, Kis B, Kuehne D (2005) Treatment and follow-up of 22 unruptured wide-necked intracranial aneurysms of the internal carotid artery with Onyx HD 500. AJNR American Journal of Neuroradiology 26(8):1909–1915

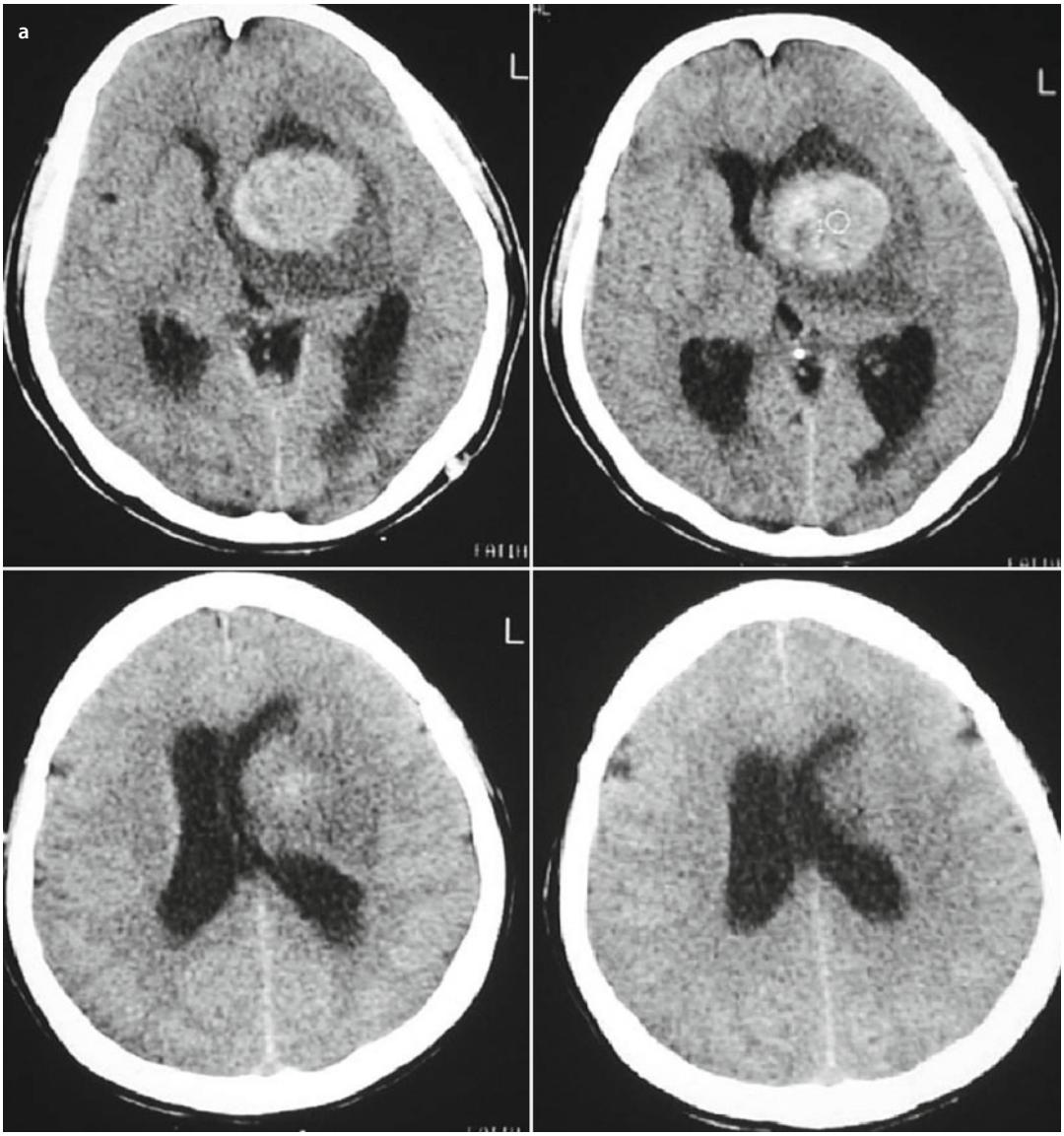

Fig. 20.1 A 51-year-old lady admitted with decreased sensorium. The patient was comatose on examination. (**a**) CECT reveals a 34 × 26 mm-sized unruptured partially thrombosed GIA embedded in the diencephalon with peri-aneurysmal vasogenic edema compressing the left lateral ventricle

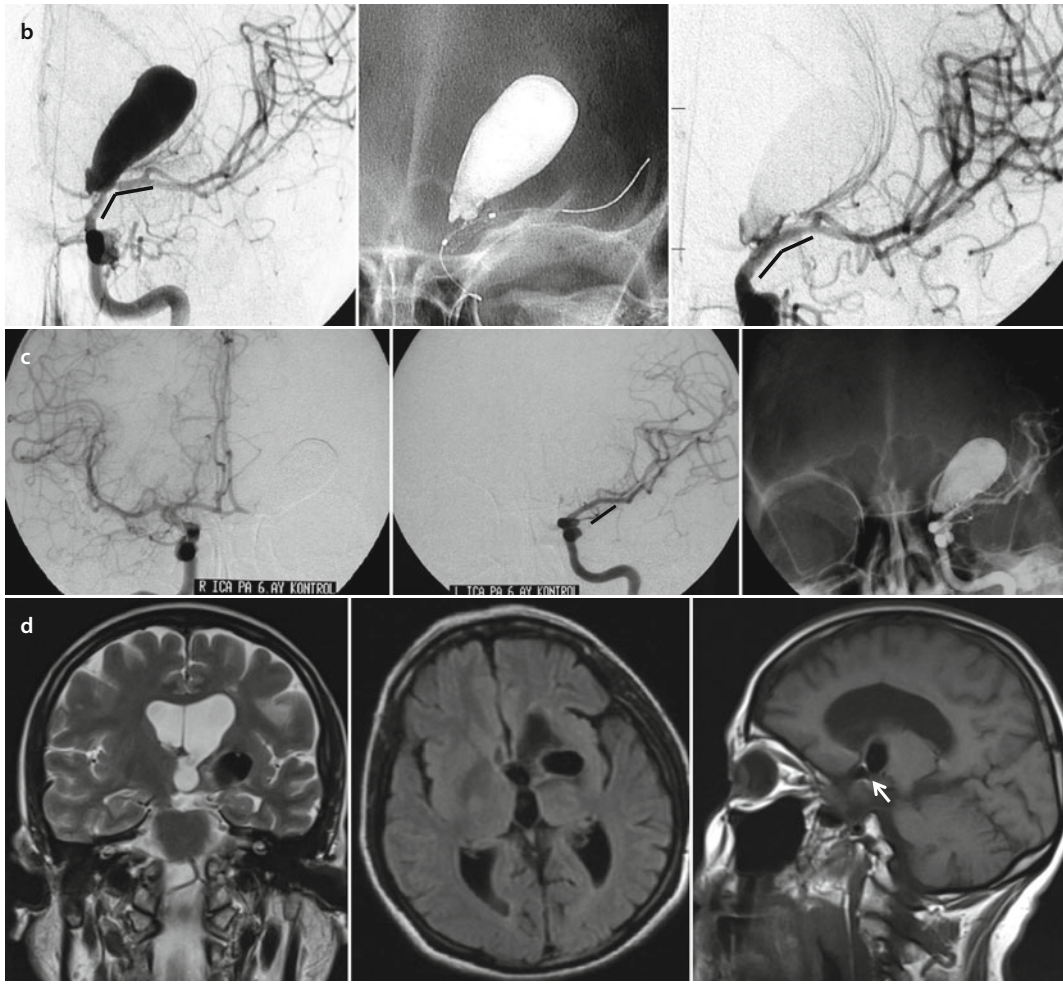

Fig. 20.1 (continued) (**b**) Cerebral DSA AP view reveals a 31 × 14 mm-sized luminal filling of ICA bifurcation GIA with the ACA arising from the aneurysmal neck. There is displacement of the lateral lenticulostriate arteries and ACA. Also note the ICA to MCA angulation. On February 2001, the aneurysm was occluded using Onyx 500 HD® with a coronary BMS (AV 670; Medtronics, Santa Rosa, CA, USA) 2.5 × 9 mm deployed at the ICA termination covering the ACA origin with flow diversion of ICA flow into MCA. There is minimal residual filling of the aneurysmal neck. The rigid coronary BMS intentionally changed the angulation of ICA bifurcation *(the lines depict the carotid bifurcation angulation)*. This in effect resulted in filling of the left ACA by flow reversal from the ACoM. This was done as the aneurysmal neck incorporated the A1 segment of left ACA. Posttreatment DSA and fluoroscopic images show a changed ICA bifurcation angulation and hemodynamic conversion of a terminal bifurcation aneurysm to a sidewall aneurysm. The left ACA is opacified from the opposite ICA. (**c**) On a 6-month and 1-year control angiograms, there is stable aneurysmal occlusion, patent stented segment, and left ACA filling through ACoM via flow reversal. (**d**) A posttreatment patient made gradual but full recovery over a period of 1 month. On 13-year follow-up, MRI reveals stable aneurysmal occlusion, decreased mass effect, and no peri-aneurysmal gliosis. Also, note that the onyx does not produce any imaging artifact on FLAIR, T2W, and T1W images. *Arrow* depicts artifact due to the coronary stent

Case 21

N. Kocer, *Giant Intracranial Aneurysms*, DOI 10.1007/978-3-319-41788-2_21

Spontaneous Thrombosis in GIAs

Keywords: Spontaneous thrombosis, Giant aneurysms

Introduction and Types of Spontaneous GIA Thrombosis

Spontaneous thrombosis in GIAs is either partial or total [1]. Though the incidence of partial spontaneous thrombosis in GIAs is as high as 60 %, total spontaneous thrombosis is uncommon [2]. Lyell first described this phenomenon incidentally during necropsy in a patient who had died of head injuries [1]. GIAs have a high prevalence of intraluminal thrombus [1, 3]. In contrast, spontaneous thrombosis in non-giant unruptured aneurysms is rare [4]. This is in accordance with the classic studies by German and Black et al. They demonstrated that intra-aneurysmal blood velocity is inversely related to the aneurysmal volume and aneurysmal blood flow is related to its orifice [1]. Thus when the ratio of intra-aneurysmal volume to area of orifice exceeds 25:1, thrombosis is likely to occur [3]. The partially or completely thrombosed GIAs are considered unstable and dynamic disease that may grow, recanalize, bleed, compress, or cause thromboembolic events [4].

Imaging Features of Spontaneous GIA Thrombosis

The CT imaging features in spontaneous thrombosis include mixed high-density attenuation in the aneurysmal lumen, the presence of "target sign," curvilinear aneurysmal wall calcification, and peripheral ring enhancement of the aneurysmal wall. The "target sign" may be absent in cases with complete aneurysmal thrombosis or when the patent lumen is below the resolution of the CT scan [1]. Pre-contrast MRI shows "onion skin" appearance of different signal intensities in thrombosed GIAs. On T2-weighted images, peri-aneurysmal edema is frequently associated with thrombosed GIAs. The presence of either a smaller luminal flow void or luminal enhancement on postcontrast T1 images is highly sensitive and specific for intra-aneurysmal thrombosis [2]. The angiographic features suggestive of intra-aneurysmal thrombosis include irregularity and asymmetrical aneurysmal lumen, progressive decrease in the size of the aneurysmal lumen, and significant disparity in the aneurysmal size on comparison between cross-sectional imaging and angiograms [1].

Clinical Features of Spontaneous GIA Thrombosis and Their Evolution

The commonest clinical presentation is a progressive mass effect from the aneurysm including headaches, neurological deficit, seizures, etc. It was believed that thrombosed GIA provides a skeletal lattice that protects against subarachnoid hemorrhage. However, large case series of GIAs revealed a similar rate of subarachnoid hemorrhage (40 % versus 48 %) in thrombosed and non-thrombosed GIAs, respectively. In a study of 12 cases of spontaneous thrombosis in GIAs, subarachnoid hemorrhage was seen in 42 % of patients [1]. There are a few reported cases of thrombosed GIAs with occlusion of the parent artery. However, this phenomenon appears to be extremely rare and has been described in GIAs of the ICA (most commonly), MCA, and PCA [1, 5]. Furthermore, there is a case of spontaneous complete thrombosis of a MCA GIA that evolved into a serpentine GIA over a period of 1 year. Thrombosed GIAs can also cause distal thromboembolism and present with neurological deficits. However, the rates vary from 5 to 59 % in various studies [1].

References

1. Whittle IR, Dorsch NW, Besser M (1982) Spontaneous thrombosis in giant intracranial aneurysms. J Neurol Neurosurg Psychiatry 45(11):1040–1047
2. de Aguiar GB, Pagotto MV, Conti ML, Veiga JC (2016) Spontaneous thrombosis of giant intracranial aneurysm and posterior cerebral artery followed by also spontaneous recanalization. Surg Neurol Int 7:15. doi:10.4103/2152-7806.175898
3. Gonzalez NR, Duckwiler G, Jahan R, Murayama Y, Vinuela F (2008) Challenges in the endovascular treatment of giant intracranial aneurysms. Neurosurgery 62(6 Suppl 3):1324–1335. doi:10.1227/01.neu.0000333797.59585.c0
4. Cohen JE, Itshayek E, Gomori JM, Grigoriadis S, Raphaeli G, Spektor S, Rajz G (2007) Spontaneous thrombosis of cerebral aneurysms presenting with ischemic stroke. J Neurol Sci 254(1–2):95–98. doi:10.1016/j.jns.2006.12.008
5. Sato K, Fujiwara S, Yoshimoto T, Onuma T (1990) Two cases of spontaneous internal carotid artery occlusion due to giant intracranial carotid artery aneurysm. Stroke J Cereb Circ 21(10):1506–1509

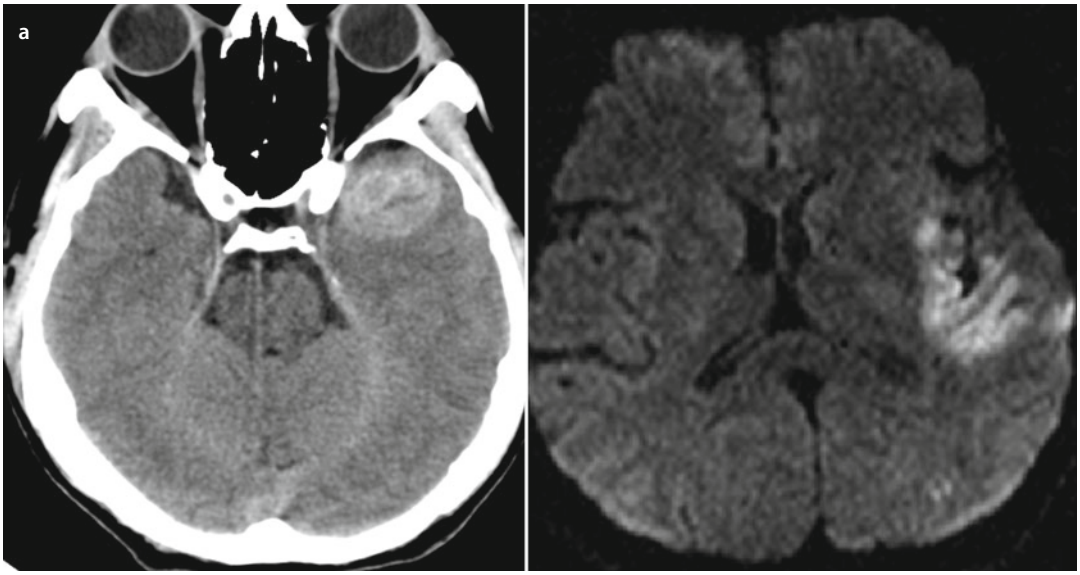

Fig. 21.1 A 49-year-old woman presented with left-sided severe headache. (**a**) NECT on the day of presentation shows a large hyperdense well-defined spherical lesion in the left temporal fossa. DWI shows acute ischemic infarct involving the left MCA territory in peri-insular region

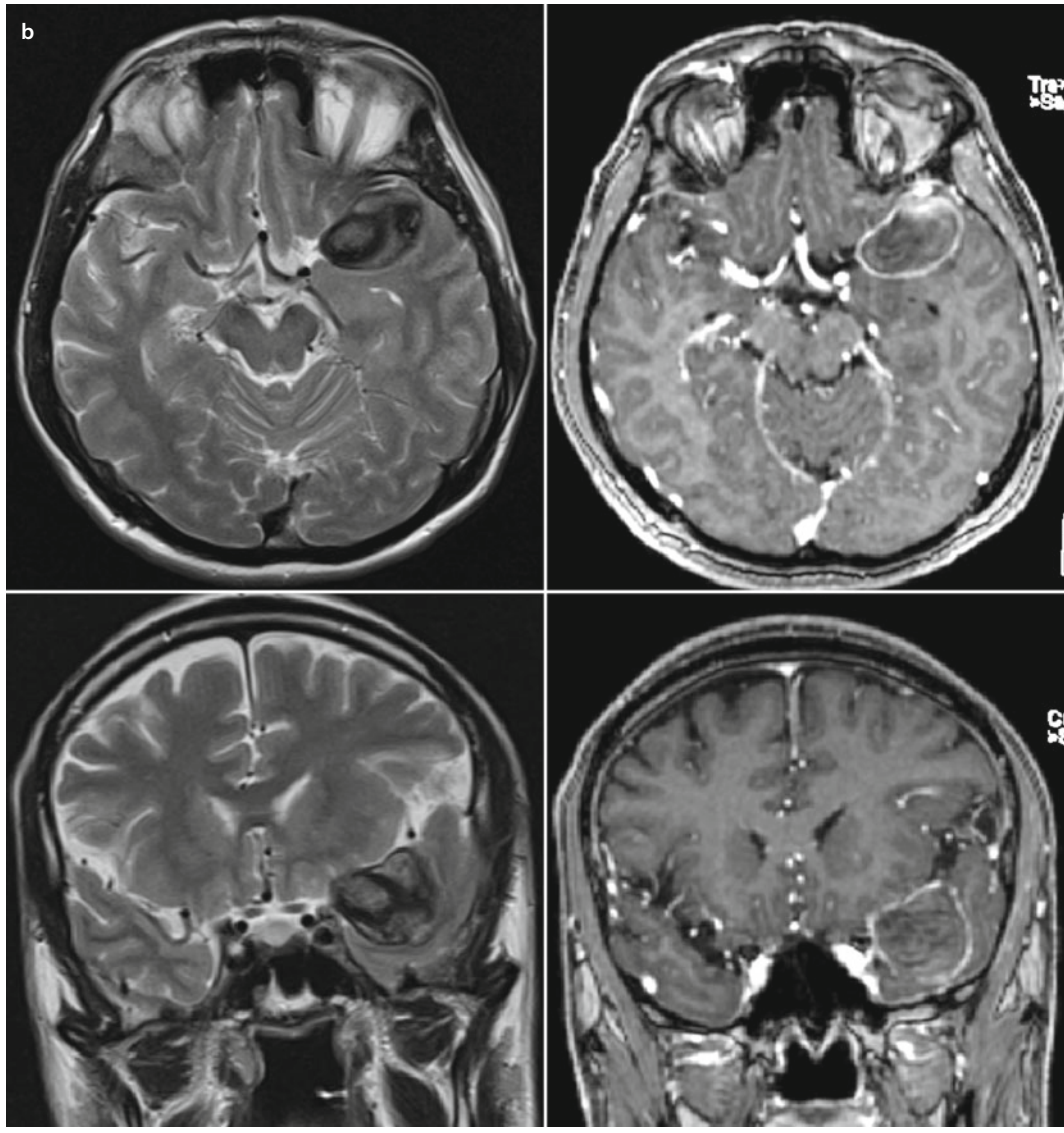

Fig. 21.1 (continued) (**b**) T2W and postcontrast T1W axial and coronal images reveal a large 3 × 2 cm-sized, well-defined, spherical hematoma with an onion skin appearance in the proximal left Sylvian fissure with flattening of adjacent sulci and broadening of gyri due to cerebral edema. There is enhancement of the aneurysmal wall

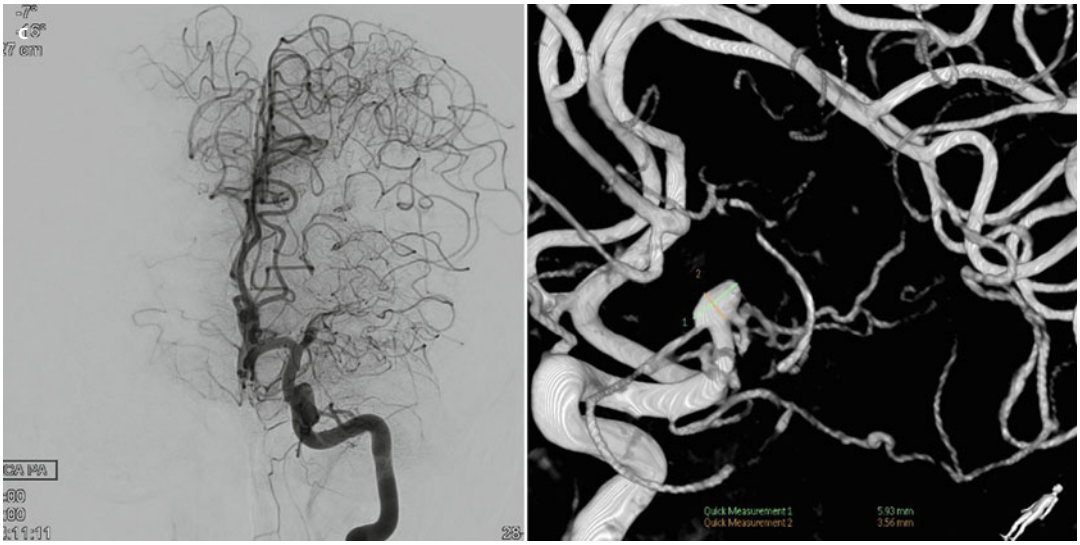

Fig. 21.1 (continued) (**c**) Cerebral DSA AP and 3D-LAO views reveal a small 5 × 3 mm-sized residual filling of proximal left M1 thrombosed GIA. The left M1 segment is occluded. There is extensive leptomeningeal collaterals arising from left ACA with retrograde opacification of distal left MCA branches

Case 22

N. Kocer, *Giant Intracranial Aneurysms*, DOI 10.1007/978-3-319-41788-2_22

Prophylactic Decompression in Basilar Fusiform Aneurysms

Keywords: Basilar fusiform aneurysms, Flow diverters, Prophylactic decompression

Basilar Artery: Anatomy, Clinical Presentation, and Risk of Unruptured Aneurysms

The basilar artery ascends in the prepontine cistern along the anterior surface of pons. The basilar artery and its branches are seen in close relationship with a number of cranial nerves. The third cranial nerve exits the mesencephalon between the PCA and SCA. Lateral to the third CN is the fourth cranial nerve that pierces tentorial dura in this region. The SCA is in close relation to the fifth cranial nerve, and the distal AICA is associated with eighth cranial nerve. A large number of aneurysms in the posterior circulation are detected incidentally and are asymptomatic [1]. Non-saccular aneurysms of the vertebrobasilar system may present with ischemic stroke, compressive symptoms (brainstem compression, hydrocephalus, and cranial nerve palsies), and hemorrhage [2]. The natural history of posterior circulation aneurysm is not well understood. In the ISUIA trial for unruptured aneurysms, the posterior circulation aneurysms had a 2.6–50 % risk of rupture over a 5-year period depending on their size [1].

Fusiform Aneurysms

Wells in 1922 described the first basilar artery fusiform aneurysm on surgical exploration of a patient with sixth, seventh, and eighth cranial nerve paresis and obstructive hydrocephalus. Fusiform aneurysms are strongly correlated with hypertension, tobacco smoking, and Fabry disease [2]. In the largest study of natural history of non-saccular vertebrobasilar aneurysms, nearly 71–75 % of transitional aneurysms (dolichoectasia with superimposed fusiform dilatation) and fusiform aneurysms with compressive symptoms at presentation enlarged over the follow-up period [2]. Patients with compressive symptoms at presentation had aneurysmal cross-sectional enlargement at the rate 1.3 mm per year [2].

Basilar Trunk Aneurysms

These aneurysms constitute less than 1 % of all intracranial aneurysms. Dissecting aneurysms are more common than saccular aneurysms in the basilar trunk. Dissecting and fusiform basilar trunk aneurysms are associated with a high rate of morbidity and with 2-year survival rates of only 20 % [1].

Why Are Vertebrobasilar Aneurysms High Risk?

In the study on natural history of non-saccular vertebrobasilar aneurysms, 40 % of patients died with a median survival of only 7.8 years. The presence of transitional aneurysms, fusiform aneurysms, and basilar artery aneurysms was associated with a progressively increased risk of death [3]. The commonest cause of death in vertebrobasilar aneurysms was due to cerebral infarction (26 %) followed by progressive compression (17 %) and subarachnoid hemorrhage (12 %). Of the 35 patients who presented with compressive symptoms, 77 % had mild or no disability, 23 % had moderate disability, and no (0 %) patient had severe disability or was dead at presentation. At 1-year follow-up, the degree of mild, moderate and severe disability and mortality had increased to 46, 25, 7, and 18 % and had further worsened at 5 years to 18, 18, 7, and 43 %, respectively. Nearly half the patients (43 %) with compressive symptoms at presentation had further progression [3]. The 5-year mortality of growing aneurysms was 56.5 % versus 3.7 % for aneurysms that were not growing [2].

Flow Diverters in the Posterior Fossa and Progressive Mass Effect

Data regarding the use of FDs in basilar fusiform aneurysms is sparse. A meta-analysis on FDs in posterior circulation in 2016 revealed significantly higher mortality rates in patients with giant basilar aneurysms. The study also found the rates of perforator infarction to be 7 %, postoperative SAH 3 %, and intra-parenchymal hemorrhage 4 % in posterior circulation. The higher rate of perforator infarction (14–25 %) accounts for the high mortality rates in giant basilar aneurysms [4]. In a literature review of FDs in posterior circulation, the authors concluded that the worse outcomes were seen in basilar fusiform aneurysms with preexisting mass effect [5]. A few authors have reported progressive increase or persistent mass effect leading to death or poor outcome (mRS 4–5) following FDs in fusiform vertebrobasilar aneurysms [6–8]. It has been suggested by authors of a retrospective study that in a pre-procedural, pre-antiplatelet therapy, CSF flow diversion like the third ventriculostomy may be helpful to prevent progressive mass effect in this subgroup aneurysms [9].

Prophylactic Decompression and Its Role in Fusiform Basilar Aneurysms

It is our experience that a prophylactic occipital bone craniectomy and C1 vertebral posterior laminectomy combined with a ventriculo-peritoneal shunt in the same sitting protects patients with basilar fusiform aneurysms from both hemorrhagic complications of rupture of a progressively thrombotic basilar aneurysm and thrombotic complications due to cessation of anticoagulant therapy to perform a surgical decompression.

With this management strategy in place, we were able to successfully treat four consecutive patients without any mortality. All patients had an mRS of 0 at 6-month follow-up. The strategy was discovered serendipitously, when a patient with a giant fusiform aneurysm while, awaiting treatment, developed sudden onset cardiorespiratory dysfunction due to its compressive effects. After a successful cardiopulmonary resuscitation, the patient underwent an emergency decompressive craniectomy and VP shunt placement. Following surgery, the patient recovered completely and had a successful and uneventful FD therapy for his aneurysm.

It is well known that thrombosis of aneurysmal sac can worsen mass effect. This mass effect can worsen compression on the brainstem, cranial nerve, and CSF pathways in posterior fossa. Thus the critical brainstem structures that are already under compression due to a fusiform basilar aneurysm cannot accommodate any drastic and sudden increase in aneurysmal volume within the rigid and restricted space of posterior fossa. To avoid this particular scenario, a preemptive decompression avoids the life-threatening risk of intracranial hemorrhage associated with an emergency decompressive surgery in a patient on antiplatelets and anticoagulants. At the same time, a prophylactic decompression avoids the risk associated with halting these medications prior to surgery that would further worsen the aneurysmal mass effect and cause acute FD occlusion.

However, the treatment strategy is not without its associated risks. As was speculated in our study, there is a theoretical risk that prophylactic decompression may increase the risk of aneurysmal growth and rupture due to decreased intracranial pressure and tamponade effect [10].

References

1. Marlin ES, Ikeda DS, Shaw A, Powers CJ, Sauvageau E (2014) Endovascular treatment of basilar aneurysms. Neurosurg Clin N Am 25(3):485–495. doi:10.1016/j.nec.2014.04.007
2. Serrone JC, Gozal YM, Grossman AW, Andaluz N, Abruzzo T, Zuccarello M, Ringer A (2014) Vertebrobasilar fusiform aneurysms. Neurosurg Clin N Am 25(3):471–484. doi:10.1016/j.nec.2014.04.006
3. Flemming KD, Wiebers DO, Brown RD, Jr., Link MJ, Huston J, 3rd, McClelland RL, Christianson TJ (2005) The natural history of radiographically defined vertebrobasilar nonsaccular intracranial aneurysms. Cerebrovasc Dis 20(4):270–279. doi:10.1159/000087710
4. Wang CB, Shi WW, Zhang GX, Lu HC, Ma J (2016) Flow diverter treatment of posterior circulation aneurysms. A meta-analysis. Neuroradiology. doi:10.1007/s00234-016-1649-2
5. Toth G, Bain M, Hussain MS, Moskowitz S, Masaryk T, Rasmussen P, Hui F (2015) Posterior circulation flow diversion: a single-center experience and literature review. J Neurointerv Surgery 7(8):574–583. doi:10.1136/neurintsurg-2014-011281
6. Siddiqui AH, Abla AA, Kan P, Dumont TM, Jahshan S, Britz GW, Hopkins LN, Levy EI (2012) Panacea or problem: flow diverters in the treatment of symptomatic large or giant fusiform vertebrobasilar aneurysms. J Neurosurg 116(6):1258–1266. doi:10.3171/2012.2.jns111942
7. Ertl L, Holtmannspotter M, Patzig M, Bruckmann H, Fesl G (2014) Use of flow-diverting devices in fusiform vertebrobasilar giant aneurysms: a report on periprocedural course and long-term follow-up. AJNR Am J Neuroradiol 35(7):1346–1352. doi:10.3174/ajnr.A3859
8. Meckel S, McAuliffe W, Fiorella D, Taschner CA, Phatouros C, Phillips TJ, Vasak P, Schumacher M, Klisch J (2013) Endovascular treatment of complex aneurysms at the vertebrobasilar junction with flow-diverting stents: initial experience. Neurosurgery 73(3):386–394. doi:10.1227/01.neu.0000431472.71913.07
9. O'Kelly CJ, Spears J, Chow M, Wong J, Boulton M, Weill A, Willinsky RA, Kelly M, Marotta TR (2013) Canadian experience with the pipeline embolization device for repair of unruptured intracranial aneurysms. AJNR Am J Neuroradiol 34(2):381–387. doi:10.3174/ajnr.A3224
10. Kizilkilic O, Kayadibi Y, Sanus GZ, Kocer N, Islak C (2014) Combined endovascular and surgical treatment of fusiform aneurysms of the basilar artery: technical note. Acta Neurochir 156(1):53–61. doi:10.1007/s00701-013-1913-8

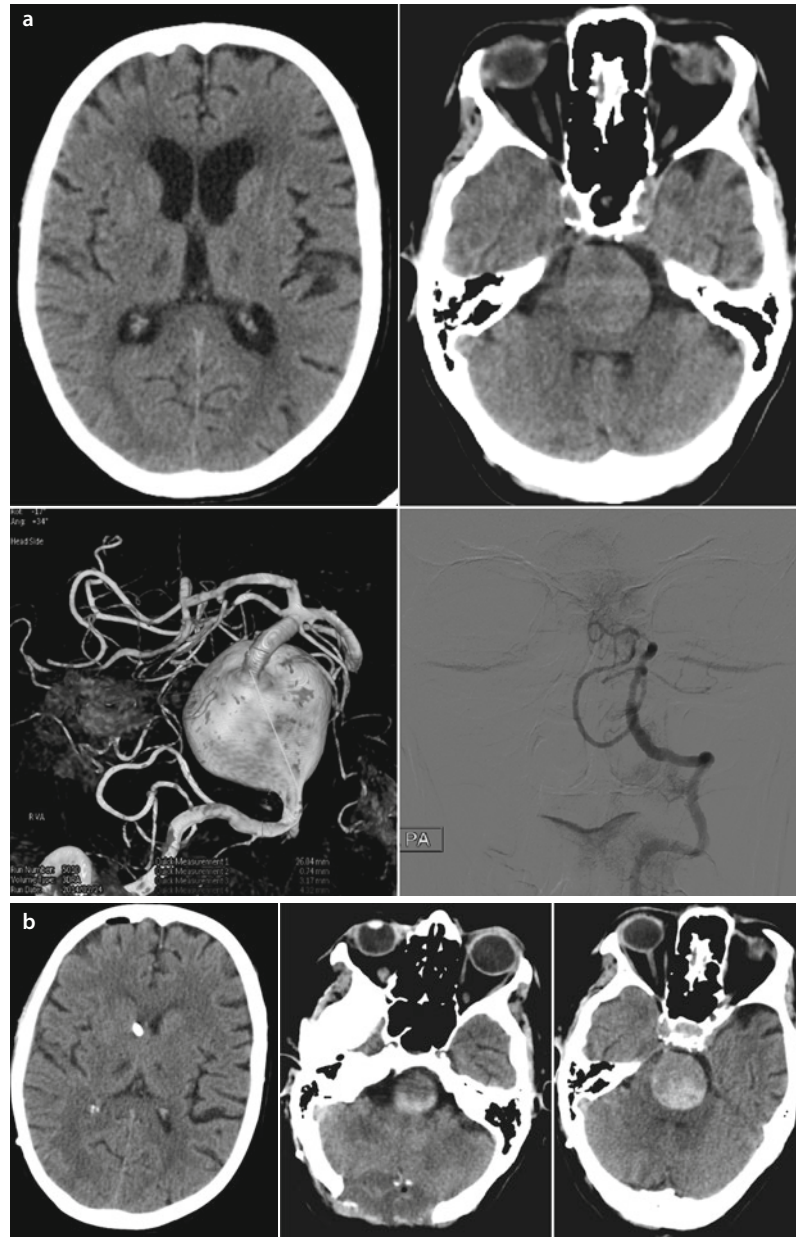

Fig. 22.1 A 57-year-old lady presented with features of brainstem compression. (**a**) On February 2014, NECT and cerebral DSA reveal a 36 × 29 mm-sized mid-basilar, fusiform GIA aneurysm causing brainstem compression and obstructive hydrocephalus. There is no intra-aneurysmal thrombosis or wall calcification. As part of the overall treatment strategy, the patient underwent posterior fossa decompressive craniectomy and ventriculo-peritoneal shunt placement. This was done prophylactically to reduce the increasing mass effect due to a thrombosing basilar aneurysm posttreatment and to avoid bleeding complications in a post-FD patient on antiplatelets and anticoagulants. (**b**) On the second day, postsurgery, the patient had increasing headaches. NECT showed crescentic hyperdensity within the aneurysm that was suggestive of intramural hemorrhage/ intra-aneurysmal thrombosis

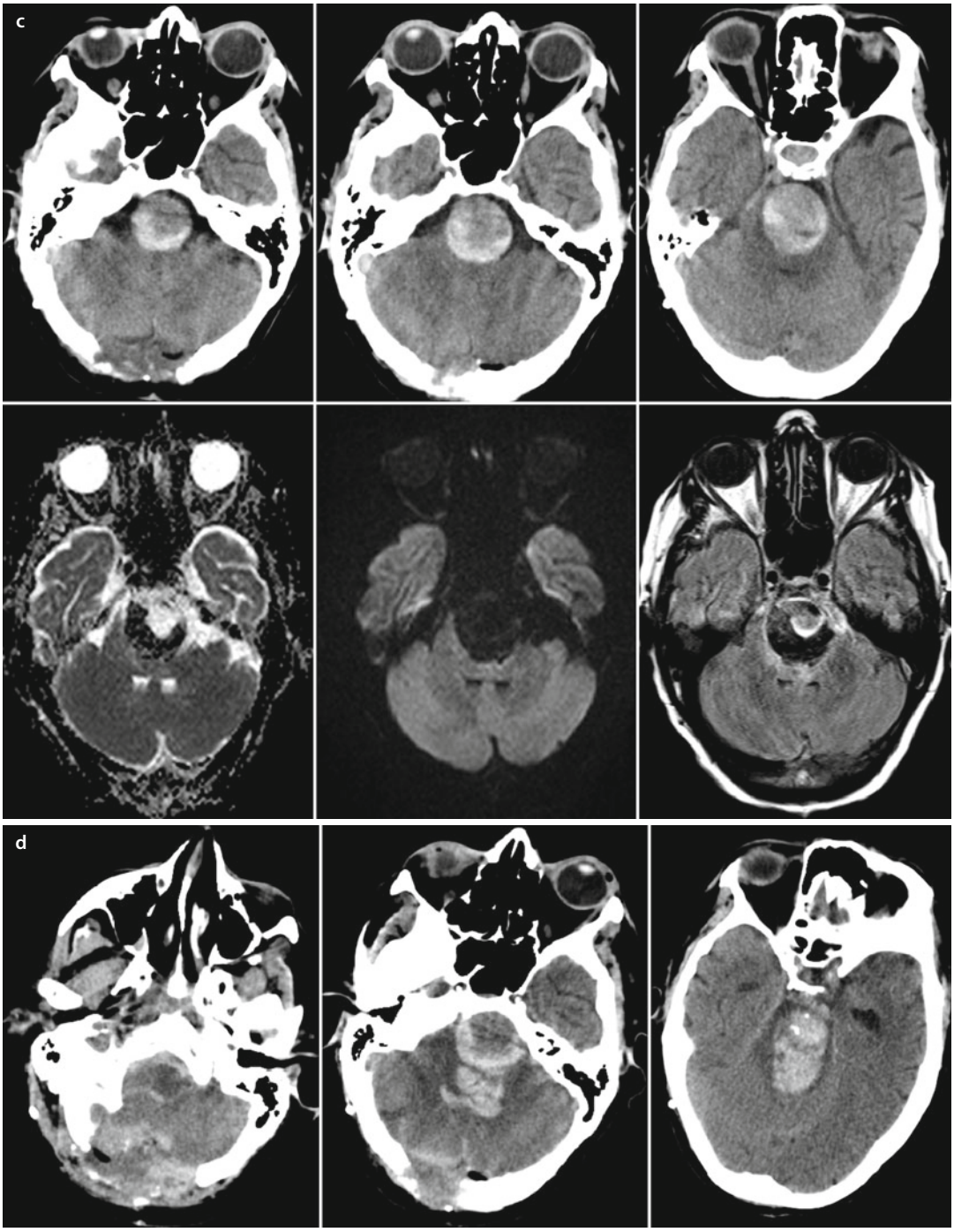

Fig. 22.1 (continued) (**c**) Within the next 24 h, NECT and MRI images reveal a progressive increase in the size of basilar GIA, intra-aneurysmal signal intensity changes, compression of the adjacent brainstem, and vasogenic edema. Note the patient was not on any antiplatelets or anticoagulants during this period. (**d**) Within the next 48 h, the patient became comatose with rupture of basilar GIA.

Case 23

N. Kocer, *Giant Intracranial Aneurysms*, DOI 10.1007/978-3-319-41788-2_23

23

Persistent Trigeminal Artery (PTA)

Keywords: Persistent trigeminal artery, Classification, Cavernous aneurysm

Trigeminal Artery: Embryology and Anatomy

Quain et al. in 1844 first described the PTA in an autopsy case. The first angiographic demonstration was by Sutton in 1950 [1]. Trigeminal artery is the most rostral and the most commonly persistent embryological carotid-basilar anastomosis in adults. The trigeminal artery is first seen in the embryo at 4 mm stage and regresses completely by 7–12 mm stage [2]. The trigeminal artery in the embryo at 2–3 mm stage supplies the primordial hindbrain channel that eventually forms both the longitudinal neural arteries (the future basilar artery) and hindbrain veins. In the 4–5 mm stage, the trigeminal artery supplies the cranial end of both the neural arteries until they involute with formation of PCoMs [3]. It courses along the trigeminal nerve and passes through cavernous sinus. It connects the cavernous segment of ICA to the basilar artery (between the origins of SCAs and AICAs) [2]. The trigeminal artery arises from the C5 cavernous segment as described by Debrun et al. [4]. It involutes in adults and commonly leaves the dorsal meningeal artery as its only remnant [1].

Classification of Persistent Trigeminal Artery

PTA has an incidence of 0.1–0.6 % in large-scale series [5]. Saltzman and Wollschlaeger classified PTAs into three types based on their angiographic anatomy. In Saltzman type 1, the basilar artery proximal to PTA is hypoplastic with absent PCoMs, and the posterior circulation is dependent on the flow from PTA. In Saltzman type 2, PCAs receive blood supply from PCoMs and the basilar artery from one of the vertebral arteries. The PTA is not essential to supply posterior circulation. In Saltzman type 3, also known as PTA variant, the trigeminal artery joins one of the three cerebellar arteries [1].

PTA is also classified into medial/sphenoidal type and a lateral/petrosal type depending on its relation to the sella turcica. Both the medial and the lateral varieties occur with an equal frequency. The medial PTA runs directly posterior from ICA through or over the sella turcica and exits through a dural opening close to the clivus. The lateral PTA runs adjacent to sella and exits through a dural opening inferior to petroclinoid ligament. This variation into either the medial or lateral PTA has an embryological basis [6]. The PTAs in adults have been found to give rise to pontine-perforating branches and supply the trigeminal ganglion (lateral PTA) or persist as dorsal meningeal artery, inferior hypophyseal artery, etc. (medial PTA) [3].

Persistent Trigeminal Artery: Pathology

The PTA can be divided into proximal, middle, and distal one-third from its origin from the ICA to its basilar termination. The proximal two-thirds of PTA is in cavernous sinus and the distal one-third courses through subarachnoid space. Injury or tear in its proximal one-third causes CCFs, in its middle one-third causes trigeminal cavernous fistulas, whereas injury in its distal one-third results in subarachnoid hemorrhage or aneurysms [7]. The PTA can be sacrificed in Saltzman type 2, with a minimal risk of posterior circulation infarction. However, in case of a Saltzman type 1, the PTA must be preserved [7]. An argument could be made that PTA must be preserved irrespective of its particular type, as PTA occlusion has been associated with pontine and midbrain infarcts [8]. PTA is associated with vascular diseases in 25 % of patients. The vascular diseases described in association with PTA include arteriovenous malformations, moyamoya disease, aneurysms, hemangiomas of the head and neck, carotico-cavernous fistulas, Sturge-Weber syndrome, aortic arch anomalies, trigeminal neuralgia, posterior circulation insufficiency, abducens and other cranial nerve palsies, etc. Aneurysms are seen in 14 % of patients with PTA, whereas aneurysms involving the PTA itself are seen in 2 % [9].

References

1. Meckel S, Spittau B, McAuliffe W (2013) The persistent trigeminal artery: development, imaging anatomy, variants, and associated vascular pathologies. Neuroradiology 55(1):5–16. doi:10.1007/s00234-011-0995-3
2. Lasjaunias P, Berenstein A, Brugge KG (2001) The skull base and extradural arteries. In: Clinical vascular anatomy and variations. Springer, Berlin/Heidelberg, pp 387–477. doi:10.1007/978-3-662-10172-8_5
3. Suttner N, Mura J, Tedeschi H, Ferreira MA, Wen HT, de Oliveira E, Rhoton AL, Jr. (2000) Persistent trigeminal artery: a unique anatomic specimen – analysis and therapeutic implications. Neurosurgery 47(2):428–433; discussion 433–434
4. Debrun G, Lacour P, Vinuela F, Fox A, Drake CG, Caron JP (1981) Treatment of 54 traumatic carotid-cavernous fistulas. J Neurosurg 55(5):678–692. doi:10.3171/jns.1981.55.5.0678

5. O'Uchi E, O'Uchi T (2010) Persistent primitive trigeminal arteries (PTA) and its variant (PTAV): analysis of 103 cases detected in 16,415 cases of MRA over 3 years. Neuroradiology 52(12):1111–1119. doi:10.1007/s00234-010-0669-6
6. Salas E, Ziyal IM, Sekhar LN, Wright DC (1998) Persistent trigeminal artery: an anatomic study. Neurosurgery 43(3):557–561; discussion 561–562
7. Geibprasert S, Jiarakongmun P, Krings T, Pongpech S (2008) Trigeminal fistula treated by combined transvenous and transarterial embolisation. Acta Neurochir 150(6):583–588. doi:10.1007/s00701-008-1496-3
8. Gaughen JR, Starke RM, Durst CR, Evans AJ, Jensen ME (2014) Persistent trigeminal artery: in situ thrombosis and associated perforating vessel infarction. J Clin Neurosci Off J Neurosurg Soc Australasia 21(6):1075–1077. doi:10.1016/j.jocn.2013.10.016
9. Caldemeyer KS, Carrico JB, Mathews VP (1998) The radiology and embryology of anomalous arteries of the head and neck. AJR Am J Roentgenol 170(1):197–203. doi:10.2214/ajr.170.1.9423632

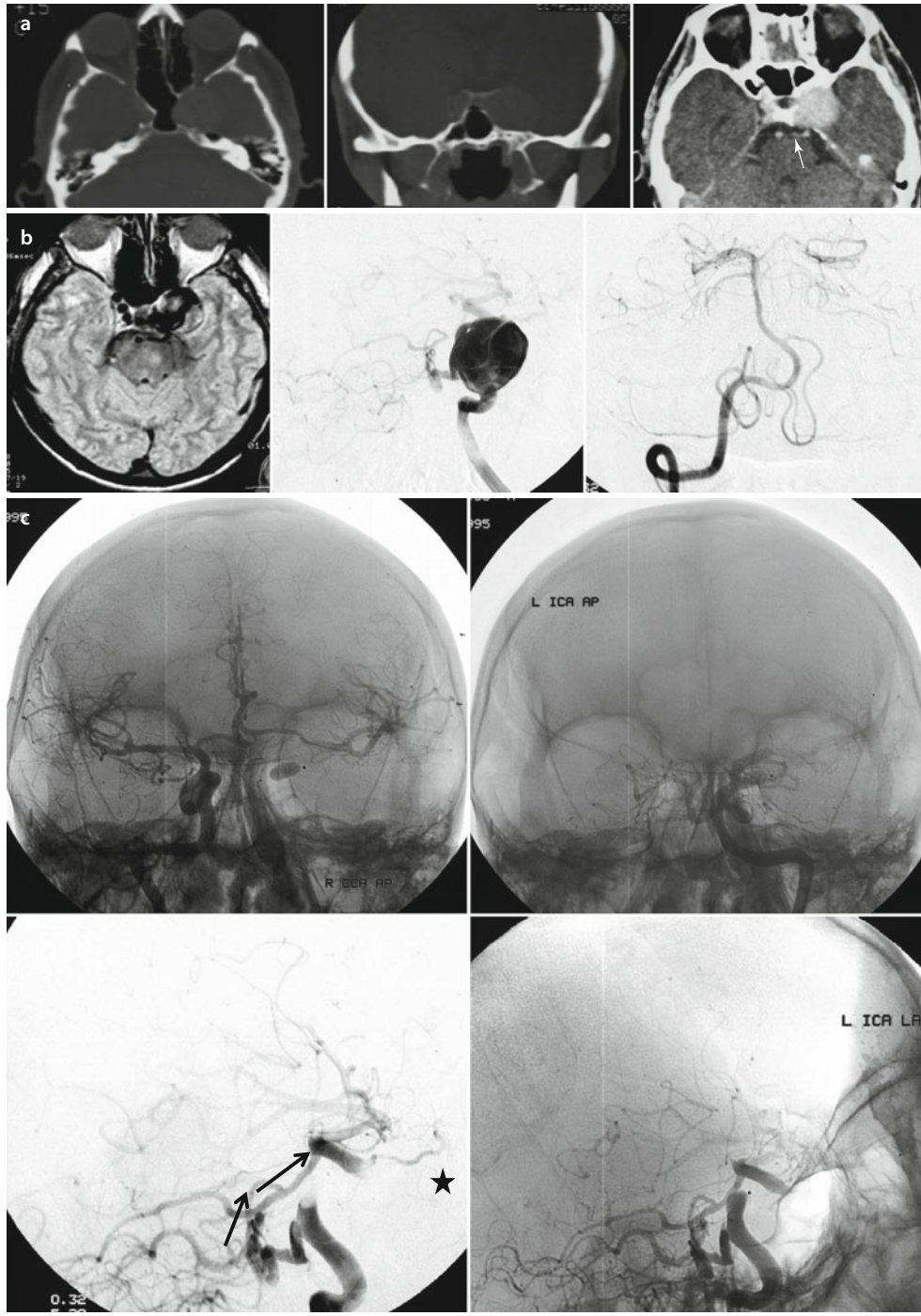

Fig. 23.1 A 62-year-old man presented with headaches and ophthalmoplegia. (**a**) NECT and CECT images reveal a giant cavernous aneurysm remodeling and scalloping the adjacent sphenoid bone. Also, note on CECT, there is an artery connecting ICA with basilar artery (*arrow*). (**b**) On January 1995, MRI and cerebral DSA reveal a 30 × 28 mm-sized, giant left cavernous aneurysm. A persistent trigeminal artery (PTA) is seen connecting the cavernous ICA to basilar artery. The left vertebral artery is absent and the vertebro-basilar system is hypoplastic. (**c**) A balloon occlusion test was well tolerated, and the patient was treated with PVO using a detachable balloon deployed just above the trigeminal artery in the ICA. Immediate postprocedural ICA angiogram reveals opacification of the posterior circulation through the PTA. The posterior circulation via PCoM opacifies the left supraclinoid ICA. Note the intact ophthalmic artery (*star*). *Arrows* indicate the direction of blood flow

Case 24

N. Kocer, *Giant Intracranial Aneurysms*, DOI 10.1007/978-3-319-41788-2_24

Bypass Surgery for Aneurysms

24

Keywords: Giant aneurysm, Bypass surgery, Parent vessel occlusion

Bypass Surgery and Its Role in GIAs

Yasargil and Donaghy in 1967 introduced the technique of intracranial bypass surgery as a treatment strategy for prevention of stroke in patients with intracranial carotid occlusion [1]. Extracranial to intracranial bypass surgery is considered when arterial occlusion of parent artery or one of its major branches is necessary for treatment of GIAs [2].

Indications for Bypass Surgery

The two main indications for bypass surgery are (a) flow augmentation and (b) flow replacement.

Flow augmentation is considered when blood flow is at borderline. The blood flow is sufficient to maintain neuronal viability, though there is a threat of infarction. Moyamoya disease and intra-arterial occlusive disease are typical examples.

Flow replacement is indicated when an artery contributing to or arising from the circle of Willis needs to be sacrificed in the management of complex vascular pathology and head and neck/skull base tumors [2, 3].

Types of Bypass

There are two types of bypasses, namely, low flow and high flow. The decision to use low flow versus high flow is dependent on the anticipated cerebral blood flow needed and the availability of a supply source [3].

Low-flow bypasses may be considered with STA or occipital arteries. They typically deliver a blood flow of 25–30 ml/min with a capacity to dilate and increase flow overtime. Low-flow bypasses are generally inadequate if a large parent artery is sacrificed (like ICA or vertebral artery) unless there is another collateral source of blood supply. Thus the STA is usually anastomosed to the M3 segment of MCA where the demand for blood volume is low [4].

High-flow bypasses can be radial artery graft (RAG) or saphenous vein graft (SVG) [4].

Rationale for Bypass Surgery

The rationale for bypass surgery is hemodynamic security. Both proximal parent vessel occlusion and trapping are well-established treatment modalities for GIAs and complex aneurysms. This is because a diminished intra-aneurysmal pressure promotes thrombosis [1, 5]. In a study on GIAs, more than 95 % of aneurysms demonstrated aneurysmal obliteration after proximal Hunterian ligation [5].

The cooperative study on IC aneurysms and SAH reported that parent artery ligation caused ischemic deficits in 33 % of ruptured and 12 % of unruptured aneurysms [6]. Balloon test occlusion (BTO) was described to identify this subgroup of patients at risk of ischemic deficits after parent artery occlusion.

However, there are several drawbacks in this strategy of selecting patients for PVO by BTO. These include (a) risk of complications associated with BTO itself, (b) ischemic deficits occur in patients who tolerate BTO and subsequently undergo PVO, and (c) there is a small but definitive risk of de novo aneurysm formation following PVO [5].

Historically, surgical carotid occlusion, even when graded, for aneurysm treatment results in cerebral infarction in up to 40 % of patients. The overall complication rate of BTO ranges from 0–8 % [3]. The risk in patients who undergo PVO after a successful BTO is 1.5–4.8 % permanent morbidity and 10–12 % continuing transient ischemic attacks. There is also an overall risk of delayed ischemia of around 10 % [3]. This has prompted two separate therapeutic strategies, namely, universal approach with authors recommending bypass in all patients planned for parent vessel occlusion and selective approach with authors recommending bypass in patients who fail BTO [2].

Drawbacks and Risks Associated with Bypass

There is no class 1 clinical evidence to support the use of high-flow bypass. Both the EC-IC bypass study and Carotid Occlusion Surgery Study (COSS) published unfavorable results for bypass surgery [2]. In a systematic review of 2008 that examined the role of bypass in anterior circulation aneurysms, the patients' neurological status had improved in 74 %, had worsened in 25 %, and was unchanged in 9 %. The perioperative (within 30 days) risk of cerebral or retinal deficits was 2 % (including fatal events). After 30 days, there was major stroke in 4 % and minor stroke in 1 % of patients. There was an overall stroke rate of 1.6 % and recurrent major stroke of 1.1 % per year [5].

The long-term patency of grafts that are supposed to last a lifetime has also been questioned. The overall graft patency rate in the review was 93 % at a median follow-up of 39 months with a 2.3 % failure rate per year after the first year [5].

ELANA/SELANA Technique in Bypass Surgery

In recent years, the excimer laser-assisted non-occlusive anastomosis (ELANA)/sutureless ELANA (SELANA) technique has been described in high-flow bypass surgery. Prof. Tulleken pioneered this technique. The ELANA technique enables anastomosis without temporarily occluding the recipient artery, thus decreasing the risk of cerebral ischemia. However, the technique requires technical expertise and quality control measures, as the failure rate to create an anastomosis is high. Furthermore, initial results, though encouraging, have not reported a reduced stroke risk compared to conventional bypass [3]. In a study of 64 patients treated by ELANA technique in 2012, 77 and 25 % of patients treated for anterior and posterior circulation lesions, respectively, had a favorable outcome. However, the mortality rate was 12 % and 63 %, in the anterior and posterior circulation regions, respectively. There was a failure to perform the anastomosis in a total of eight patients [7].

References

1. Gonzalez NR, Duckwiler G, Jahan R, Murayama Y, Vinuela F (2008) Challenges in the endovascular treatment of giant intracranial aneurysms. Neurosurgery 62(6 Suppl 3):1324–1335. doi:10.1227/01.neu.0000333797.59585.c0
2. Sia SF, Morgan MK (2013) High flow extracranial-to-intracranial brain bypass surgery. J Clin Neurosci Off J Neurosurg Soc Australasia 20(1):1–5. doi:10.1016/j.jocn.2012.05.007
3. Patel HC, Kirkpatrick PJ (2009) High flow extracranial to intracranial vascular bypass procedure for giant aneurysms: indications, surgical technique, complications and outcome. In: Advances and technical standards in neurosurgery. Springer, Vienna. pp 61–83. doi:10.1007/978-3-211-78741-0_3
4. Mohit AA, Sekhar LN, Natarajan SK, Britz GW, Ghodke B (2007) High-flow bypass grafts in the management of complex intracranial aneurysms. Neurosurgery 60(2 Suppl 1):ONS105–ONS122; discussion ONS122–ONS123. doi:10.1227/01.neu.0000249243.25429.ee
5. Schaller B (2008) Extracranial-intracranial bypass to reduce the risk of ischemic stroke in intracranial aneurysms of the anterior cerebral circulation: a systematic review. J Stroke Cerebrovasc Dis Off J Nat Stroke Assoc 17(5):287–298. doi:10.1016/j.jstrokecerebrovasdis.2008.03.010
6. Vilela MD, Newell DW (2008) Superficial temporal artery to middle cerebral artery bypass: past, present, and future. Neurosurg Focus 24(2):E2. doi:10.3171/foc/2008/24/2/e2
7. Vajkoczy P, Korja M, Czabanka M, Schneider UC, Reinert M, Lehecka M, Schmiedek P, Hernesniemi J, Kivipelto L (2012) Experience in using the excimer laser-assisted nonocclusive anastomosis nonocclusive bypass technique for high-flow revascularization: Mannheim-Helsinki series of 64 patients. Neurosurgery 70(1):49–54; discussion 54–55. doi:10.1227/NEU.0b013e31822cb979

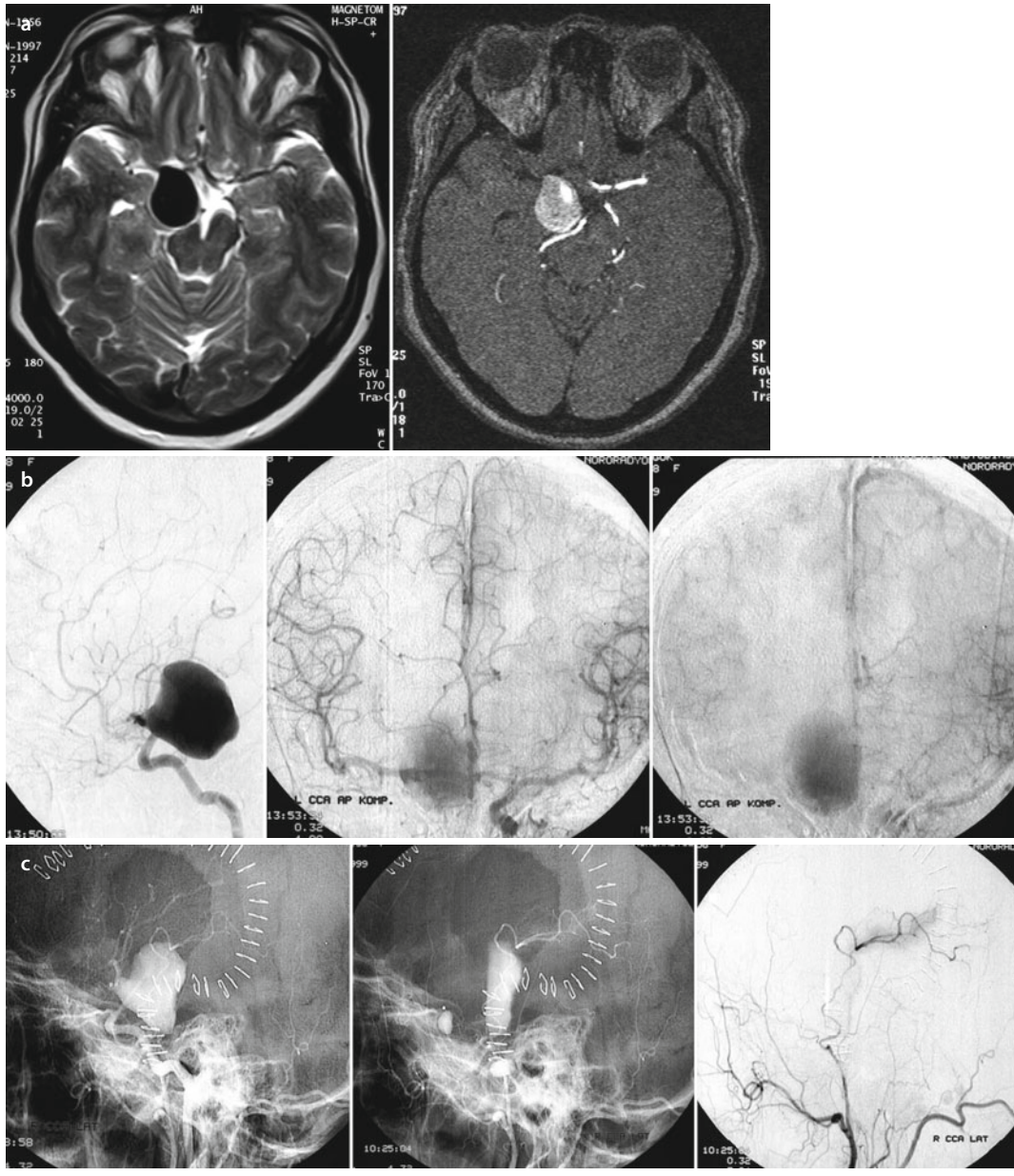

Fig. 24.1 A 41-year-old lady presented with headaches. (**a**) MRI T2W axial and MRA images reveal a very large 23 × 15 mm-sized supraclinoid unruptured ICA aneurysm compressing the medial temporal lobe and mesencephalon. (**b**) On March 1999, the patient presented with acute SAH. Cerebral DSA shows further enlargement of the supraclinoid ICA aneurysm (GIA) with inadequate cross-circulation across the ACoM (venous delay more than 2 s). (**c**) After a STA-MCA bypass, a balloon occlusion test was done. The patient tolerated the occlusion well and was treated with parent vessel occlusion using detachable balloons deployed in cavernous and petrous segments of ICA

Case 25

N. Kocer, *Giant Intracranial Aneurysms*, DOI 10.1007/978-3-319-41788-2_25

Flow Reversal in Posterior Circulation

Keywords: Vertebrobasilar junctional aneurysm, Flow reversal, Parent vessel occlusion

What is Flow Reversal?

The literature describing flow reversal is scanty. This is mainly because most of the papers combine the results of flow reversal and parent vessel occlusion without further differentiation. Flow reversal consists of intentional occlusion of the parent artery proximal to the aneurysm after ensuring adequate flow in parent artery distal to the occlusion. The reversed flow in the artery ensures a significant decrease in hemodynamic stress and persistent perfusion of the parent artery, perforators, and side branches. The reduction in blood flow within the aneurysm provides an opportunity for the diseased vessel to thrombose gradually [1–3]. Bryne et al. first elucidated the technique of flow reversal and its clinical importance. They described the technique in a patient with a basilar GFA. After ensuring bilateral large PCoMs, the authors performed serial BTO in both the vertebral arteries, followed by coiling and occluding them proximal to PICA origin (flow reversal). Follow-up MRI at 4 months showed a decreased aneurysmal mass effect on brainstem [4].

Vertebrobasilar Aneurysms

Flow reversal technique is of particular importance in the treatment of complex vertebrobasilar aneurysms [5]. The treatment of fusiform vertebrobasilar aneurysms began in 1960s and was best described by Charles Drake. The treatment strategy consisted of flow reduction in cases with inadequate collaterals, flow reversal in cases with adequate collaterals, and trapping with mural hematoma decompression in cases with acute mass effect. Patients had good/excellent outcome when treated with flow reversal/flow reduction by single vertebral artery occlusion or tourniquet-induced stenosis in 63 %, flow reversal with bilateral vertebral occlusion in 74 %, and trapping with decompression in 71 % of patients [6].

In a study describing deliberate PVO of basilar or vertebral arteries for the treatment of unclippable aneurysms, the critical role of PCoM and its size was elucidated. The study found the tolerance to proximal basilar artery or vertebral artery occlusion increased with the presence of large (>1 mm) PCoMs. Patients with at least one large PCoM had a 6.7 % incidence of brainstem ischemia compared to 43 % in patients with bilateral small (<1 mm) PCoMs. Additionally, the outcomes were excellent in 83 % with at least one large PCoM compared to 57 % with two small PCoMs [6, 7]. Occlusion of vertebral artery proximal to aneurysms involving the vertebral artery also constitutes flow reversal with filling from the contralateral vertebral artery or PCoMs if the contralateral vertebral artery is hypoplastic [7]. Also in patients with poor collaterals, a distal bypass followed by PVO ensures adequate flow reversal [3, 6].

How Is Flow Reversal Different from PVO Alone?

Flow reversal is a well-established treatment strategy to induce partial or complete aneurysmal thrombosis. However, PVO alone may cause immediate or delayed cerebral ischemia due to progressive thrombosis of parent artery or perforators or decreased blood flow in the parent artery with resultant infarction. The resultant complications cause transient neurological deficits in 5–31 % and permanent deficits in 0–18 % of individuals with PVO of vertebral or basilar arteries. Augmenting the blood flow distal to the site of occlusion can prevent ischemia. This can be achieved by either a flow reversal technique by ensuring a retrograde flow in the occluded parent artery through adequate native collaterals or by performing a distal bypass [3–5].

Flow reversal may be considered in giant or surgical/endovascular failed basilar top aneurysms, blister aneurysms, dissecting aneurysms involving the PICA, AICA or ASA, when the dissected segment is too narrow or too risky to cross and in aneurysms with involvement of the vertebrobasilar junction. It should also be considered in cases where stable coil mass is unlikely, for example, pseudoaneurysms, fusiform aneurysms in the posterior circulation, etc. [8, 9].

Outcome of Patients with Flow Reversal in Posterior Circulation

In a study of ten patients with vertebrobasilar aneurysms, the authors started with flow reversal after occlusion of a single vertebral artery. If the aneurysm did not regress on follow-up, the contralateral vertebral artery was also occluded ensuring additional flow reversal. The group had 80 % angiographic cure and 90 % of patients had improvement or normalization of their clinical examination [6].

Caveats of Flow Reversal in Posterior Circulation

(a) Flow reversal is better suited in patients with significant aneurysmal thrombosis and collateral recruitment to their brainstem territories [5].
(b) Prior assessment of PCoM size by Allcock Test (vertebral angiography with carotid compression) is essential [4]. The presence of at least one large (>1 mm) PCoM enables favorable outcomes [6].
(c) In flow reversal, vertebral occlusion should be performed proximal to PICA origin to prevent brainstem infarction from perforator occlusion [4].*It is our belief that the sump effect created by the PICA ensures adequate flow reversal in the distal vertebral and basilar artery*.
(d) The point of occlusion must be as close as possible to the aneurysm to achieve maximum effect [6].
(e) A recent study in 2014 showed that the vertebral artery can be safely occluded in its cervical segment in all cases, without a prior BTO, as flow reversal is always seen in the occluded vertebral artery up to the PICA [10].
(f) Dissecting aneurysms of the vertebral artery involving PICA origin is associated with the highest rate of recurrence and consequent disastrous rebleeding among vertebrobasilar aneurysms treated by flow reversal [11].

References

1. Amin-Hanjani S, Ogilvy CS, Buonanno FS, Choi IS, Metz LN (1997) Treatment of dissecting basilar artery aneurysm by flow reversal. Acta Neurochir 139(1):44–51
2. Hoh BL, Putman CM, Budzik RF, Carter BS, Ogilvy CS (2001) Combined surgical and endovascular techniques of flow alteration to treat fusiform and complex wide-necked intracranial aneurysms that are unsuitable for clipping or coil embolization. J Neurosurg 95(1):24–35. doi:10.3171/jns.2001.95.1.0024
3. Kalani MY, Zabramski JM, Nakaji P, Spetzler RF (2013) Bypass and flow reduction for complex basilar and vertebrobasilar junction aneurysms. Neurosurgery 72(5):763–775; discussion 775–776. doi:10.1227/NEU.0b013e3182870703
4. Boardman P, Byrne JV (1998) Giant fusiform basilar artery aneurysm: endovascular treatment by flow reversal in the basilar artery. Br J Radiol 71(843):332–325. doi:10.1259/bjr.71.843.9616247
5. Kalani MY, Zabramski JM, Nakaji P, Spetzler RF (2014) Twenty-year follow-up of flow reversal and revascularization for a giant serpentine basilar artery aneurysm. Neurosurgery (10 Suppl 3):E493–E497; discussion E497. doi:10.1227/NEU.0000000000000438
6. Serrone JC, Gozal YM, Grossman AW, Andaluz N, Abruzzo T, Zuccarello M, Ringer A (2014) Vertebrobasilar fusiform aneurysms. Neurosurg Clin N Am 25(3):471–484. doi:10.1016/j.nec.2014.04.006
7. Steinberg GK, Drake CG, Peerless SJ (1993) Deliberate basilar or vertebral artery occlusion in the treatment of intracranial aneurysms. Immediate results and long-term outcome in 201 patients. J Neurosurg 79(2):161–173. doi:10.3171/jns.1993.79.2.0161
8. Sorteberg A (2014) Balloon occlusion tests and therapeutic vessel occlusions revisited: when, when not, and how. AJNR Am J Neuroradiol 35(5):862–865. doi:10.3174/ajnr.A3852
9. Rabinov JD, Hellinger FR, Morris PP, Ogilvy CS, Putman CM (2003) Endovascular management of vertebrobasilar dissecting aneurysms. AJNR Am J Neuroradiol 24(7):1421–1428
10. Zoarski GH, Seth R (2014) Safety of unilateral endovascular occlusion of the cervical segment of the vertebral artery without antecedent balloon test occlusion. AJNR Am J Neuroradiol 35(5):856–861. doi:10.3174/ajnr.A3885
11. Kim BM, Shin YS, Kim SH, Suh SH, Ihn YK, Kim DI, Kim DJ, Park SI (2011) Incidence and risk factors of recurrence after endovascular treatment of intracranial vertebrobasilar dissecting aneurysms. Stroke J Cerebral Circ 42(9):2425–2430. doi:10.1161/strokeaha.111.617381

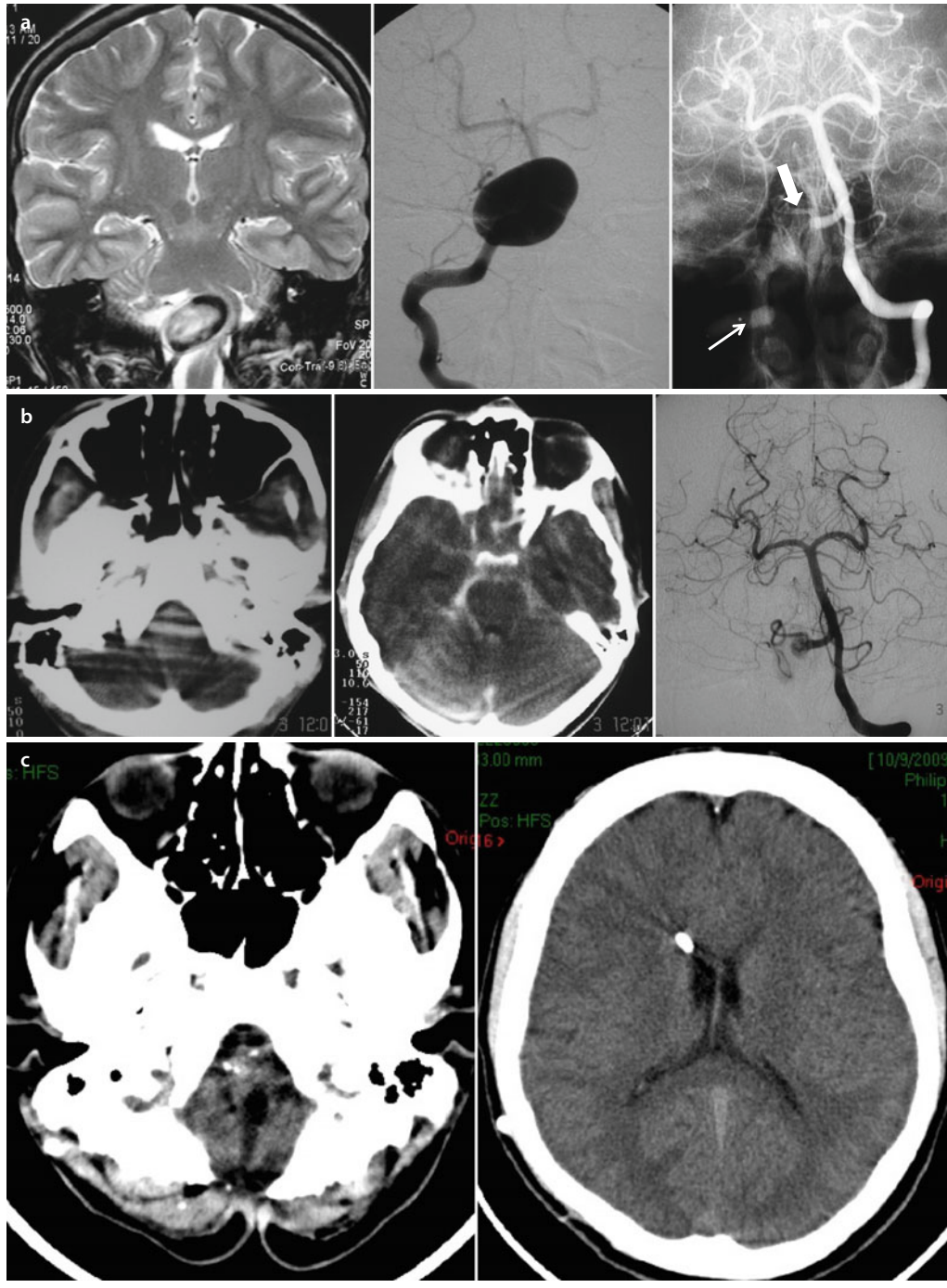

Fig. 25.1 A 17-year-old man presented with clinical features of brainstem compression. (**a**) On February 2004, coronal T2 W MRI and cerebral DSA reveal a 28 × 16 mm-sized right V4 GIA causing brainstem compression. There is no intra-aneurysmal thrombosis. On July 2004, the patient was treated with PVO of the right vertebral artery using detachable balloons (*arrows*). Postprocedural DSA reveals flow reversal in the right vertebral distal V4 segment opacifying PICA that is incorporated into the aneurysm (*block arrow*). (**b**) After a month, the patient presented with acute posterior fossa SAH. Note that the patient was not on any antiplatelets or anticoagulants at the time. Cerebral DSA reveals filling of the PICA and distal portion of the aneurysm via flow reversal from the left vertebral artery. The patient was managed with posterior fossa decompressive craniectomy and ventriculo-peritoneal shunt placement. (**c**) After 5 years, the patient had moderate residual disability

Case 26

N. Kocer, *Giant Intracranial Aneurysms*, DOI 10.1007/978-3-319-41788-2_26

Vasa Vasorum in GIAs

Keywords: Cerebral aneurysm, Vasa vasorum, CT, MRI, Flat panel detector CT angiography

Vasa Vasorum in Intracranial Arteries

The outer layers of major extracranial arteries receive substantial blood flow through vasa vasorum [1]. In young adults, the intracranial arteries are devoid of any demonstrable vasa vasorum. However, with age, the proximal portions of carotid and vertebral arteries develop vasa vasorum [2]. In 1865, Gimbert reported that vasa vasorum in basilar artery was less numerous than the aorta and upper and lower limb arteries. In a study of 30 human autopsy specimens, vasa vasorum was found in the proximal 1–2 cm of all vertebral and internal carotid arteries immediately after dural penetration. Vasa vasorum in distal intracranial arteries (anterior and middle cerebral arteries) is seen only in pathological states such as large thick-walled aneurysm or severe atheromatous plaque [1]. Vasa vasorum has also been described in association with vasculitis and intracranial dissections [3].

Atkinson showed atheromatous intracranial disease has a marked tendency for increased adventitial vasa vasorum. Furthermore, there is increased vasa vasorum with increasing severity of atherosclerosis and increasing age and prior cerebrovascular disease. In an autopsy of 50 cadavers, vasa vasorum was found in the tunica media in six patients. All the six specimens with vasa vasorum in media were accompanied by complicated intramural hemorrhage. Additionally, five out of these six specimens had aneurysms and had died of subarachnoid hemorrhage [1].

Role in Aneurysm Pathogenesis

Katayama et al., in 1991, described a case of completely thrombosed basilar aneurysm that continued to grow and produced intractable mass effect that was relieved after clipping and partial surgical excision of the thrombosed aneurysm. The excised mass showed an onion skin-laminated structure of hemorrhages [4]. Subsequently, several histopathological and radiological studies have shown that hemorrhage in the aneurysmal wall or between old luminal thrombus and aneurysmal wall is common in growing thrombosed GIAs. This prompted a number of authors to hypothesize that sub-adventitial rupture of vasa vasorum was one of the underlying mechanism of enlargement in GIAs. This was subsequently demonstrated in surgically treated GIAs that had an extensive network of vasa vasorum [2]. Studies have also shown an association between partially occluded vasa vasorum with a disrupted IEL and ruptured aneurysms [3]. In a study by Krings et al. of 21 patients with partially thrombosed aneurysms and intramural hemorrhage on cross-sectional imaging, 18 had strongly enhancing walls (presumably due to vasa vasorum and inflammation), and 17 had surrounding vasogenic edema (a manifestation of extraluminal inflammation) [5].

Imaging Features of Vasa Vasorum in Aneurysms

In a study, CT angiography showed wall enhancement of cervical ICA in patients with 70 % or more stenosis that correlated with stroke symptoms. It was speculated that the enhancement depicted vasa vasorum. It has also been suggested that enhancement of the outer rim of CCA and ICA on dynamic CE MRI represents vasa vasorum. It has been shown that the transfer constant (K^{trans}) of gadolinium enhancement in carotid plaques correlates with vasa vasorum density. Thus, adventitial enhancement on CE MRI studies can be used to measure vasa vasorum density and may indicate plaque neovascularity and risk of disruption [3].

Adventitial arterial enhancement (especially in intracranial arteries) on CT and MRI is an indicator of vasa vasorum formation or its disruption. Focal enhancement of aneurysmal wall may also correlate with rupture risk. However, further studies are needed to better understand whether rupture depends on vasa vasorum integrity or its presence alone and its relation with wall enhancement [3].

Therapeutic Strategy in Growing Thrombosed GIAs with Vasa Vasorum

The aforementioned hypothesis has prompted a few authors to speculate that surgical trapping of thrombosed growing GIAs is a better therapeutic option rather than endovascular trapping as the juxtamural and exoluminal vasa vasorum can be completely excluded only by the former treatment [2, 6]. Several alternative theories have also been advanced to explain this growth phenomenon, including hemorrhage from the newly formed capillaries in thrombus and inflammation following activation of 5-lipooxygenase pathway with the excess leukotrienes binding to the endothelium of vasa vasorum causing degradation of media and internal elastic lamina with wall weakening and aneurysmal growth [2].

A recent study in 2013 exploring the relationship between aneurysm dimensions, rupture, flow, and thrombosis involved various swine aneurysm models. In this study, 7 days after clipping, numerous engorged vasa vasorum and thrombosis with hemorrhagic wall transformation and inflammation were seen in both ruptured and unruptured aneurysms. However, rupture was more commonly seen in large/giant aneurysms and in aneurysms with large aspect ratio. The ruptured aneurysms were most often associated with residual blood flow or with a reestablished flow between thrombus and degenerated aneurysmal wall [7].

References

1. Takaba M, Endo S, Kurimoto M, Kuwayama N, Nishijima M, Takaku A (1998) Vasa vasorum of the intracranial arteries. Acta Neurochir 140(5):411–416
2. Krings T, Mandell DM, Kiehl TR, Geibprasert S, Tymianski M, Alvarez H, terBrugge KG, Hans FJ (2011) Intracranial aneurysms: from vessel wall pathology to therapeutic approach. Nat Rev Neurol 7(10):547–559. doi:10.1038/nrneurol.2011.136
3. Portanova A, Hakakian N, Mikulis DJ, Virmani R, Abdalla WM, Wasserman BA (2013) Intracranial vasa vasorum: insights and implications for imaging. Radiology 267(3):667–679. doi:10.1148/radiol.13112310
4. Katayama Y, Tsubokawa T, Miyazaki S, Furuichi M, Hirayama T, Himi K (1991) Growth of totally thrombosed giant aneurysm within the posterior cranial fossa. Diagnostic and therapeutic considerations. Neuroradiology 33(2):168–170
5. Alvarez H (2009) Etiology of giant aneurysms and their treatment. AJNR Am J Neuroradiol 30(1):E8; author reply E9–10. doi:10.3174/ajnr.A1370
6. Dehdashti AR, Thines L, Willinsky RA, Tymianski M (2009) Symptomatic enlargement of an occluded giant carotido-ophthalmic aneurysm after endovascular treatment: the vasa vasorum theory. Acta Neurochir 151(9):1153–1158. doi:10.1007/s00701-009-0270-0
7. Raymond J, Darsaut TE, Kotowski M, Makoyeva A, Gevry G, Berthelet F, Salazkin I (2013) Thrombosis heralding aneurysmal rupture: an exploration of potential mechanisms in a novel giant swine aneurysm model. AJNR Am J Neuroradiol 34(2):346–353. doi:10.3174/ajnr.A3407

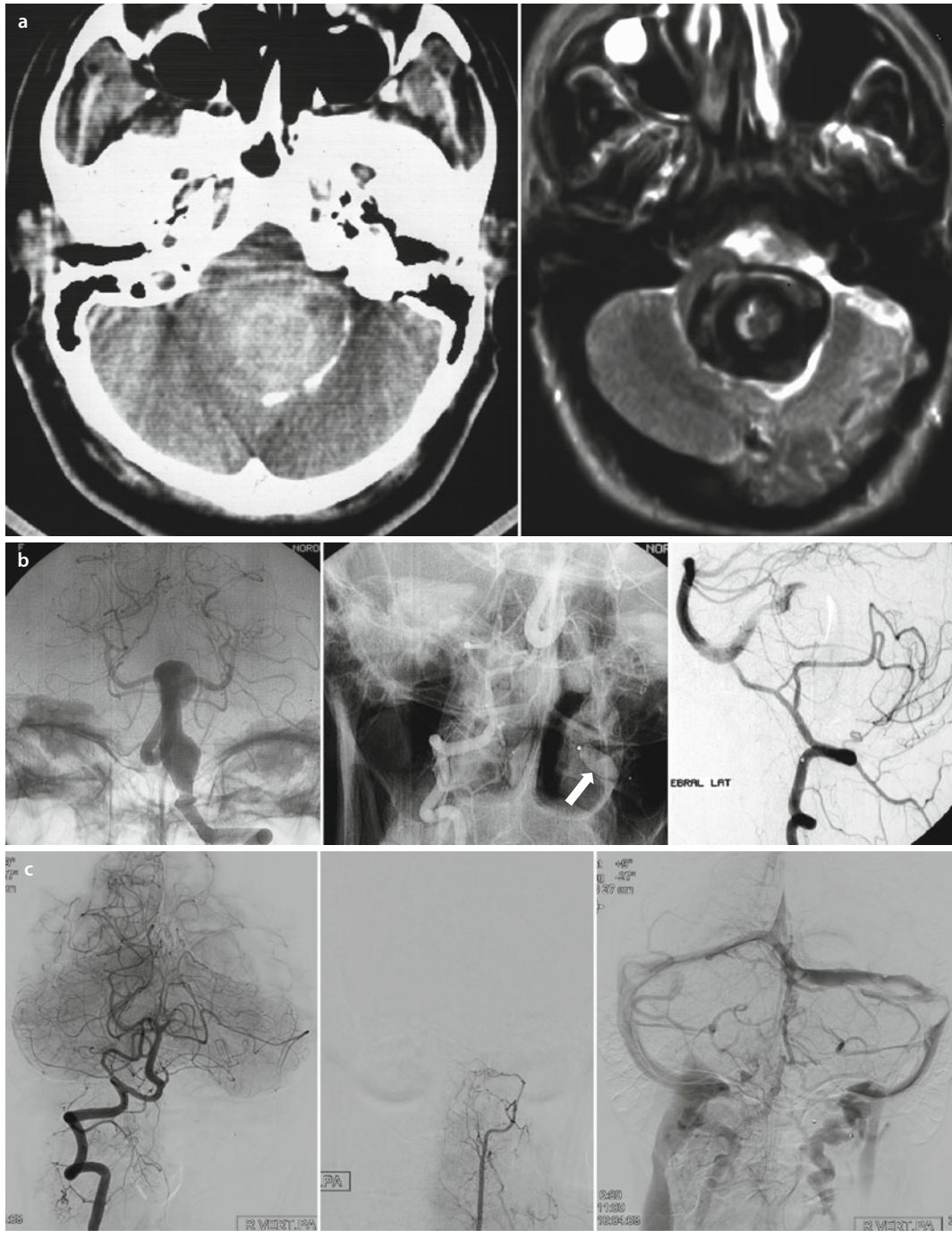

Fig. 26.1 A 33-year-old lady initially presented with headache, nausea, and vertigo. (**a**) Axial NECT and T2-W MRI reveal partially thrombosed and calcified GIA causing brainstem and cerebellar compression. (**b**) Cerebral DSA reveals luminal opacification of a fusiform left V4 vertebral GIA suggestive of underlying dissection. Treatment was done by occlusion of the left vertebral artery using detachable balloons (*arrow*). There was adequate flow reversal with good opacification of the basilar system from the right vertebral artery. (**c**) The patient was asymptomatic for 15 years. After 15 years, the patient presented with recurrent vertigo. Cerebral DSA reveals a stable occlusion of left vertebral artery and its GIA. The left vertebral artery has diminished in caliber, and the right vertebral artery has enlarged

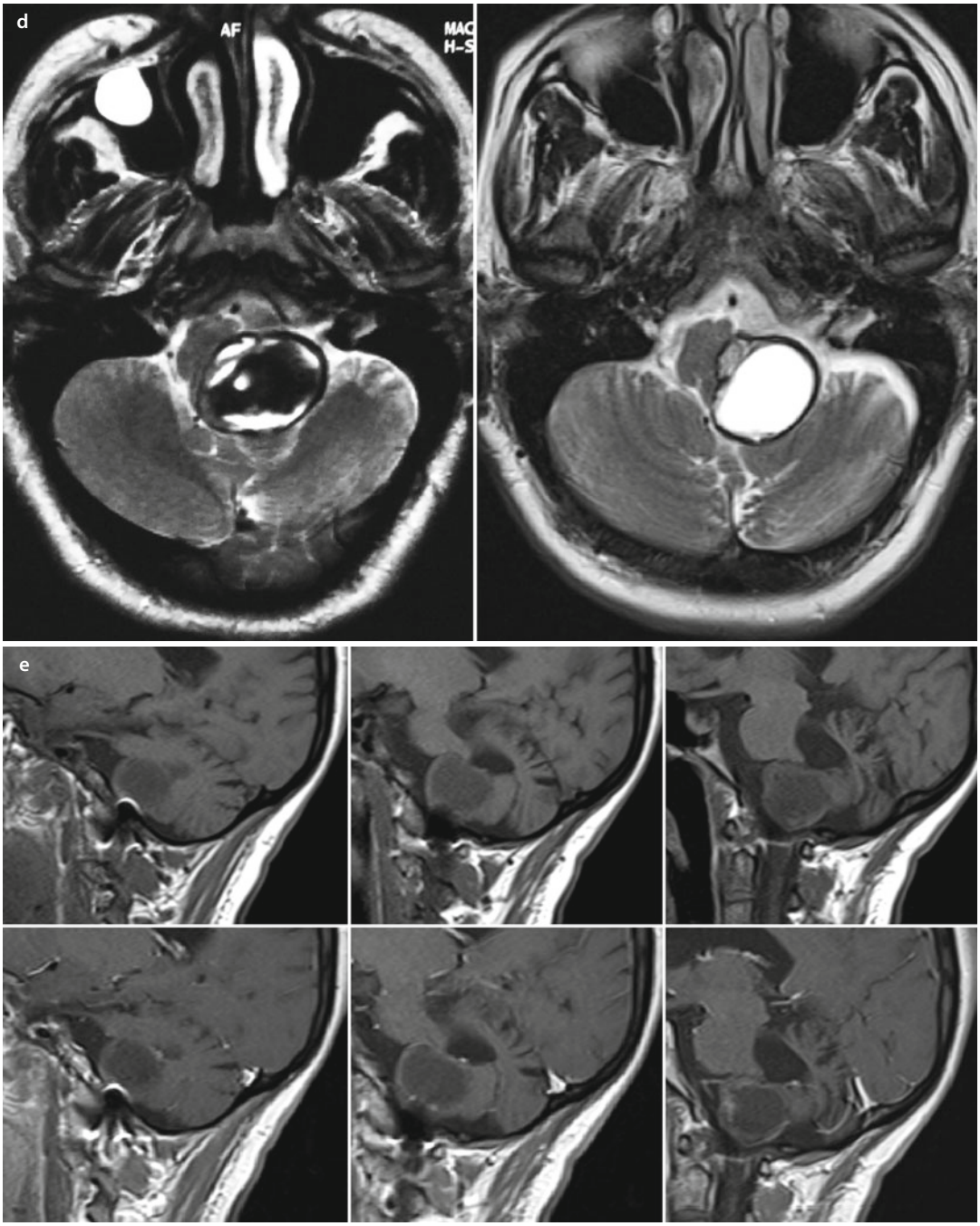

Fig. 26.1 (continued) (**d**) Comparison of T2W axial images at 1 month and 15 years posttreatment reveals progressive aneurysmal shrinkage and signal intensity changes in the thrombosed GIA. (**e**) Pre- and postcontrast T1W MRI images after 15 years reveal mural enhancement of the occluded left vertebral GIA

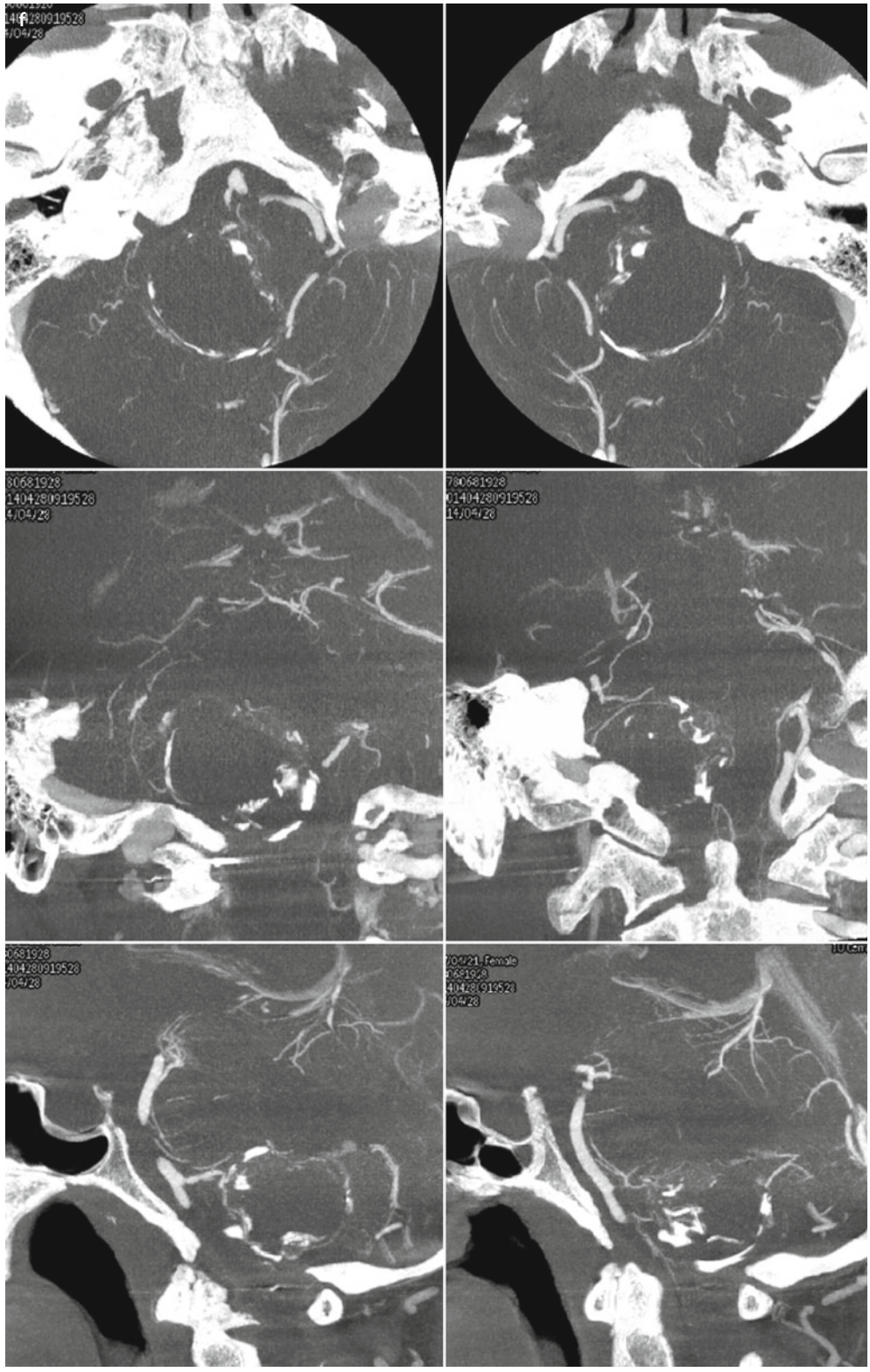

Fig. 26.1 (continued) (**f**) IAFDCTA reveals non-opacification of the left vertebral aneurysmal lumen. There is no or minimal aneurysmal shrinkage over a period of 15 years. However, there is enlarged mural vasculature in the aneurysmal wall possibly due to enlarged vasa vasorum

Service Part

N. Kocer, *Giant Intracranial Aneurysms*, DOI 10.1007/978-3-319-41788-2

Appendix

Case no	Gender	Age	Symptom	Location	Rupture status	Size	Morphology	Treatment date	Tx technique	Imaging	Date
1	F	44	Headache, vomiting and confusion	L VBJ	Ruptured	25 × 24 mm	Fusiform	23.08.2001	AVE S7 3 × 30 mm, 3 × 12 mm JOSTENT	MR	03.08.2001
										DSA	09.08.2001
										DSA	03.09.2001
										DSA	22.01.2002
										DSA	08.09.2003
										MRI, DSA	19.07.2004
										DSA	02.09.2006
										DSA,VasoCT	28.03.2016
2	F	47	Intermittent headaches, memory loss and left anisocoria	L PCoM	Un ruptured	25 × 22 mm	Fusiform	17.10.2000	AVE 2.5 × 9 mm	DSA	06.04.2001
										DSA	10.05.2002
										DSA	15.03.2007
										MR	10.03.2012
3	F	12	Absence seizure	L suprac–linoid ICA	Un ruptured	42 × 36 mm	Fusiform	11.12.2012	LEO (3.5*50, 3.5*35) + SILK (4.0*35, 4*20)	DSA	12.12.2012
										DSA	15.03.2013
										MR	17.06.2013
										MRA	04.06.2014

4	F	32	Headache, ophtalmoplegia	L ICA cavernous	Un ruptured	30 × 27 mm	Sacculo-fusiform	30.05.2013	LEO + SILK	DSA	05.03.2008
										MR	20.05.2013
										DSA	31.05.2013
										CT	10.06.2013
										DSA	01.07.2013
										DSA	09.12.2013
										Vaso CT	26.11.2014
5	M	36	SAH	L MCA M1	Ruptured	35 × 30 mm	Fusiform	12.04.2011	LEO (3.5*50) + SILK (3*30)	CT	26.03.2011
										DSA,CT	13.04.2011
										MR,CT	26.04.2011
										MR,CT	09.05.2011
										DSA	03.06.2011
										MR	08.07.2011
										DSA	13.02.2014
6	M	66	SAH	R MCA M1	Ruptured	25 × 22 mm	Fusiform	2004 year 03.07.2014	Clipping FRED (3.5*40*36)	DSA	03.07.2014
										DSA	08.07.2014
										CT	10.03.2014
										DSA	30.10.2014
										DSA	17.02.2015
										Vaso CT	26.05.2015
										DSA	08.01.2016

(continued)

(continued)

Case no	Gender	Age	Symptom	Location	Rupture status	Size	Morphology	Treatment date	Tx technique	Imaging	Date
7	M	17	SAH	Mid-basilar	Ruptured	26×26 mm	Dissecting	08.09.2013 25.09.2013 02.12.2013	First tx: balloon assisted coiling Second tx: coiling + FRED (4×18×12) Third tx: PED (4×16)	DSA, CTA	07.09.2013
										CT	10.09.2013
										CT	11.09.2013
										MR	17.09.2013
										MR,CT	30.11.2013
										DSA	03.12.2013
										MR	13.12.2013
										MR	07.03.2014
										DSA	13.01.2015
8	F	64	Headache, vision problem	L suprac linoid	Un ruptured	25×19 mm	Sacculo-fusiform	13.08.2013	FRED (4.5*26*20) (4.5*25*18)	DSA	13.08.2013
										MR,CT	15.08.2013
										CT	20.08.2013
										Vaso CT	24.09.2013
										DSA	21.02.2014
										DSA	25.08.2014
										DSA	17.08.2015

9	M	30	Ophtalmopleagia, retrobulbar pain	R petro-cavernous	Unruptured	29 × 29 mm	Sacculo-fusiform	01.03.2011 20.09.2012 05.05.2015 11.05.2016	LEO (4.5*40) + SILK (4*25) SILK (4.5*3.5*30) PIPELINE (4.5*25) PAO	MR	24.05.2010
										Vaso CT	18.05.2011
										CT	02.10.2012
										Vaso CT	04.12.2012
										Vaso CT	06.01.2012
										DSA	09.12.2013
										MR	27.03.2015
										DSA	24.04.2015
										DSA	06.05.2015
										MR	22.05.2015
										Vaso CT	11.08.2015
										MR	03.05.2016
10	F	63	Headache and visual disturbances	L parophtalmic	Unruptured	27 × 23 mm	Sacculo-fusiform	14.08.2013	FRED (4.5*25*18)	DSA	14.08.2013
										MR	15.08.2013
										MR	22.08.2013
										CT	23.08.2013
11	F	47	Headaches and visual disturbances	L paraoph thalmic	Unruptured	27 × 20 mm	Saccular	07.04.2011	SILK (4*25)		06.12.2010
											07.04.2011
											08.04.2011

(continued)

(continued)

Case no	Gender	Age	Symptom	Location	Rupture status	Size	Morphology	Treatment date	Tx technique	Imaging	Date
12	F	34	SAH	L MCA bifurcation	Ruptured	27 × 25 mm	Fusiform	25.03.2014	FRED (3.5*40*36)	CT	3.2014
										DSA	24.03.2014
										DSA	26.03.2014
										CT	27.03.2014
										CT	01.04.2014
										Vaso CT	08.05.2014
										CT	01.07.2014
13	M	32	Headache, vomitted, diaphoresis	R P2-P3 serpentine	Unruptured		Serpentine	26.3.2013	PAO with detachable coils	MR, DSA	18.05.2007
										DSA	26.03.2013
										MR	28.03.2013
										DSA	19.06.2014
14	F	37	Headache	L suprac linoid ICA	Unruptured	31 × 20 m	Sacculo-fusiform	30.05.2002 09.06.2014	Onyx Coil + FRED (3.5*40*36) *Pipeline* (*3.5 × 20*)	MR	17.01.2011
										CT	03.12.2011
										DSA	23.10.2013
										MR	22.10.2014
										DSA	31.10.2014
										DSA	27.10.2015
15	F	55	Progressive visual loss, increased symptom	L supraclinoid ICA	Unruptured	26 × 19 mm	Sacculo-fusiform	01.04.2000 25.12.2001	First tx coil Balloon remodelling onyx	MR	29.03.2000
										DSA	05.04.2000
										MRA	13.02.2002
										DSA	26.06.2002
										MRA	11.06.2010
										MR	20.11.2013

16	F	37	Headache	PcomA	Unruptured	30 × 28 mm	Dissecting	28.11.2007	Coil	CT, DSA	28.12.2007
										DSA	28.12.2007
										MR	19.07.2008
										DSA	16.03.2009
										MR	13.02.2010
										MR	23.05.2012
										DSA	03.04.2014
17	F	56	Headache, diplopia	Basilar top	Unruptured	25 × 22 mm	Sacculo-fusiform	05.05.2006 07.12.2006 09.06.2008	Balloon assisted coiling Stent assisted coiling L PCA occlusion coiling	DSA	08.11.2006
										DSA,VasoCT	23.11.2006
										DSA,VasoCT	07.12.2006
										DSA	08.03.2007
										DSA,VasoCT	08.06.2007
										MR	12.01.2009
										MR	16.03.2012
										MR	15.01.2016
18	M	60	Headache	L MCA bifurcation	Unruptured	25 × 17 mm	Fusiform	15.03.2013	Buddy wire	DSA	20.09.2011
										CT	15.03.2013
										MRI	16.03.2013
										DSA	30.09.2013
										DSA	22.09.2014
										DSA	09.03.2015

(continued)

(continued)

Case no	Gender	Age	Symptom	Location	Rupture status	Size	Morphology	Treatment date	Tx technique	Imaging	Date
19	F	58	Headache	L MCA bifurcation	Unruptured	27 × 21 mm	Sacculo-fusiform	27.12.2013 28.01.2014 22.10.2014	TX PCONUS ACOM ANEVRIZMA TX TX COIL + 2.75 × 20 mm BIPLANE STENT)	MRA	14.10.2014
										MRA	24.11.2014
										MRA	12.02.2015
										VasoCT	20.03.2016
										MRI	20.03.2016
20	F	51	Decreased sensorium	ICA bifurcation	Unruptured	34 × 26 mm	Sacculo-fusiform	13.02.2001	Onyx + AV 670 2.5 × 9 mm	CT	24.01.2001
										DSA	31.08.2001
										DSA	21.03.2002
										DSA	14.02.2006
										MR	30.04.2008
										MR	17.12.2014
21	F	49	Headache	L MCA M1	Unruptured	30 × 20 mm	Thrombosed fusiform		Spontaneous thrombosis	CT	28.07.2015
										MR	28.07.2015
										MR	30.07.2015
										DSA	03.08.2015
22	F	57	Features of brainstem compression	Midbasilar	Unruptured	36 × 29 mm	Fusiform	14.05.2014	Decompressive crainectomy and ventriculo-peritoneal shunt	DSA	24.02.2014
										CT	13.05.2014
										CT	15.05.2014
										CT,MR	17.05.2014
										CT	18.05.2014

23	M	62	Headache, ophtalmoplegia	Cavernous ICA	Unruptured	30 × 28 mm	Sacculo-fusiform	07.02.1995	PAO detachable balloon	CT	04.01.1995
										MR	18.01.1995
										DSA	31.01.1995
										CT	14.02.1995
										MR	18.01.1995
24	F	41	Headache	Supraclinoid	Unruptured	23 × 15 mm	Dissecting	3.1999 19.03.1999	STA-MCA bypass surgery	MR, MRA	15.06.1997
									PAO	DSA	05.03.1999
										CT	19.05.2014
25	M	17	Features of brainstem compression	R VA, V4	Unruptured	28 × 16 mm	Fusiform	29.07.2004	PAO detachable balloon	MR	08.02.2004
										DSA	24.05.2004
										CT	30.08.2004
										DSA	30.08.2004
										CT	10.09.2009
26	F	33	Headache, nausea, vertigo	L VA, V4	Unruptured	39 × 34 mm	Fusiform	12.03.1999	PAO with detachable balloon	CT	02.02.1999
										MRI	09.02.1999
										MRI	07.04.1999
										MRI	10.10.1999
										MRI	14.04.2014
										DSA, VasoCT	28.04.2014

Index